
THE KOCAELI, TURKEY EARTHQUAKE OF 17 AUGUST 1999

A FIELD REPORT BY EEFIT

Dina D'Ayala (editor)

Matthew Free (editor)

Roger Bilham

Paul Doyle

Russ Evans

Paul Greening

Robert May

Alan Stewart

Berrak Teymur

Dale Vince

Earthquake Engineering Field Investigation Team
Institution of Structural Engineers
11 Upper Belgrave St
London SW1X 8BH

Tel: +44(0)207 235 4535

Fax: +44(0)207 235 4294

©EEFIT

February 2003

ISBN 0 901279 283

In memory of Professor Aikut Barka

EEFIT gratefully acknowledges the support of its Corporate Members:

Arup

Gifford

EQE International Ltd

CREA Consultants

Table Of Contents

PREFACE	page VII
The Kocaeli 17 August 1999 earthquake	VII
The EEFIT Mission	VIII
Acknowledgments	IX
List of useful Internet links	IX
1. THE EARTHQUAKE AFFECTED REGION	1
Introduction	1
Seismic hazard of Turkey and the Marmara Sea Region	1
Socio-economic profile of the Marmara Sea Region	3
Socio-economic effects of the Kocaeli earthquake and comparison with past earthquakes	7
Conclusions	13
References	13
2. GEOPHYSICAL ASPECTS AND SEISMOLOGY	15
Basic seismological data	15
Tectonic setting of Turkey	15
Historic earthquakes and surface slip on the Northern Anatolian fault	16
Teleseismic observation of the 17 August 1999 earthquake	17
Surface slip during the 17 August 1999 earthquake	19
Secondary effects	21
References	23
Appendix 2A	25
3. STRONG-MOTION AND MACRO-SEISMIC INTENSITY	27
Introduction	27
Strong Ground Motion Stations	27
Strong Motion Records	28
Measured Ground Motions	29
Response Spectra	33

Measured Ground Motions	29
Response Spectra	33
Factors Influencing the Observed Strong Ground Motions	34
Macroseismic Intensity Distribution	38
Conclusions	44
References	45
Appendix 3A	47
Appendix 3B	52
Appendix 3C	57
4. GEOLOGICAL AND GEOTHECNICAL ASPECTS	81
Introduction	81
Local Ground Conditions	83
Fault rupture	89
Site response	92
Liquefaction	95
Earthquake induced slope instability	99
Earthquake effects on building foundations	100
Earthquake effects on retaining structures	101
Earthquake effects on Earth Embankments	102
Gas Venting	102
References	103
Appendix 4A	104
5. PERFORMANCE OF BUILDINGS	123
Introduction	123
Building codes requirements	124
Performance of residential buildings	128
Typical collapse modes in concrete buildings	133
Geographical and statistical analysis of damage	144
Damage Survey in Izmit	151
Conclusions	153
References	154

6.	PERFORMANCE OF INDUSTRIAL AND COMMERCIAL SITES	155
	Introduction	155
	Damage survey of Industrial estate	155
	Petrochemical plants	161
	Car Plants	165
	Performance of Commercial Buildings	170
	Appendix 6A	173
	Appendix 6B	177
7.	INFRASTRUCTURES AND MARINE FACILITIES	179
	Introduction	179
	Performance of terrestrial infrastructures	179
	Comments	188
	Performance of waterfront structures	188
	Conclusions	195
	References	195

Preface

Dina D'Ayala,
University of Bath

1. The Earthquake

The Izmit earthquake occurred at 00:01:39.80 UTC (3:01 a.m. local time), and its epicentre is located at 40.702° N., 29.987° E, about 11km south-east of the city of Izmit. This location indicates that the earthquake occurred on the northernmost strand of the North Anatolian fault system, originating at a depth of 17 km, and caused right-lateral strike-slip movement on the fault. Field observations indicate that the earthquake produced 126 km of surface rupture associated to right-lateral offsets as large as 5.5 meters. The associated magnitude has been calculated at Mw 7.4 of the Richter scale. This makes it the second most destructive earthquake this century in Turkey.

The incredible amount of destruction caused in the urban centres within the epicentral area and the associated death toll have been widely and extensively broadcast, amounting to more than 16000 fatalities and more than 40000 injured. Almost 600000 people were left homeless and it is estimated that more than 15000 are still missing or unaccounted for. Residential blocks of flats, 4 to 8 storeys high, built of reinforced concrete, in the past 20 to 30 years, were the structures that suffered the highest damage: up to 140000 residential units collapsed or were damaged beyond repair; this, together with the time of occurrence of the earthquake, corresponding to maximum occupancy of these units, explains the high number of casualties. Most of the industries in the epicentral area suffered structural damage and business disruption, epitomised by the collapse of the 115 metre high reinforced concrete heater stack, and the fire of the tank farm at the Tupras oil refinery. The civil engineering infrastructure also suffered substantial disruption. In Aryfie, 40 Km from the epicentre along the fault rupture, a bridge of the highway collapsed, killing 12 people. Water supplies, electricity and telecommunication have been severely affected, with service failures lasting several hours. Total economic loss estimates associated to the Kocaeli earthquake range from £4.0 billion to £24.0 billion, with a cost to the government of up to £3.8 billion, corresponding to a 3.5% reduction in GDP for 1999.

Data on seismic performance of buildings in Turkey had been collected by EEFIT in two other occasions, in 1983 and in 1992. The present earthquake however occurred in an highly industrialised area, in contrast with the previous two. Buildings that have collapsed here were of relatively recent build, mostly successive to the Turkish seismic code of 1975. The code requirements, however had not necessarily been implemented in many of the collapsed structures. The level of destruction and death toll is similar to the Erzincan earthquake of 1939, of similar magnitude, occurred in an eminently undeveloped area with a building stock of mainly vernacular masonry.

The Kocaeli earthquake has highlighted the indissoluble link between safer engineering and its technical implementation, socio-economic policies and territorial and urban planning issues. The high level of reported damage can be ascribed to two factors: a high level of urbanisation in a region of known active faults; a building stock characterised by a wide range of standards of construction due to uneven enforcement of building regulations. This begs the question of why such level of urban development and industrial settlements have been allowed, and whether they were essential to the economic and social growth of the country.

There are in the world a number of major cities developed or developing on or near active fault systems and this is the first earthquake with epicentre in such a scenario, after the 1903 San Francisco earthquake. The damage produced and the socio-economic consequences arisen are of major relevance worldwide.

The level of enforcement of the seismic code and the quality of construction of the residential building stock is again a problem common to most developing countries with large urban agglomerates. Much discussion has taken place on the general and technical media on the low quality of the materials, and lack of proper seismic engineering associated with the Turkish building stock. Indeed from the reconnaissance survey it emerged that many of the collapsed or seriously damaged buildings had been conceived to withstand vertical loads only, without structural connection between parallel frame systems, lack of shearwalls, presence of heavy floor slabs and weak and brittle infill panels. This applies to self constructed housing, but also to sizeable residential, commercial or industrial developments, built by medium size contractors, over the past 20 years, in a situation of booming construction industry and fast rising economic inflation.

It is an issue of general technical education of the people involved in the building industry at all levels, as it is apparent that the shortcoming of these structures are the result of a lack of seismic culture.

Reinforced concrete frame buildings are the most common in urban areas of developing and western countries, notwithstanding the high seismic risk associated with it. Data which can correlate construction detailing and damage are essential for a better development of mitigation and strengthening policies.

Together with the reconstruction and re-housing logistics, strengthening and upgrading policies are perhaps the most crucial issue that the political authority and the technical institutions are faced with in the follow up of such devastating event.

Most buildings have been left either damaged beyond repair or with non apparent structural damage.

Because of the high number of casualties, many buildings have been immediately demolished and many others have been scheduled for demolition. Given the substantial numbers involved, this is neither a simple process nor a painless one, as the cost of rebuilding will be very high. Moreover for the many industrial facilities, and medium-small commercial enterprises, demolition will also mean bankruptcy, as many will not have the necessary capital to start again. Hence there is a technical, but also political problem, of possibly implementing short term repairs of very weak buildings. This is complicated by the lack of technical expertise to carry out appraisal and strengthening work, as admitted by many political and technical officials.

2. The EEFIT Mission to Turkey

EEFIT is an association affiliated to the Institution of Structural Engineers, U.K., formed by professionals and academics, which organises field missions in the immediate aftermath of earthquakes in order to gather data on the performance of structures, foundations, industrial facility, lifelines, etc. EEFIT was founded in 1982 with the aim of reporting to the UK and international engineering communities lessons to be learnt from damaging earthquakes. This work contributes to an improved understanding of structural behaviour under seismic loads and an evaluation of the adequacy of current design practices and regulations.

The Turkish region of the Marmara sea, the most populated and developed of Turkey had been struck by an earthquake of magnitude Mw 7.4 on the night of the 17th of August 1999. EEFIT sent a team of 13 that reached Istanbul on the 6th of September and spent 8 days in the disaster area. The team was composed of structural and geotechnical engineers, a geophysicist and a seismologist, from academy and industry: Dina D'Ayala, University of Bath, team leader; Roger Bilham, University of Colorado at Boulder; Tim Courtney, Ws Atkins, Bristol; Paul Doyle, Babbie Group; Abbas El-Hussaini, University of Westminster; Russ Evans, British Geological Survey; Matthew Free, Ove Arup & Partners, Hong Kong; Paul Greening, University of Bristol; Robert May, Jacobs Gibb; Alan Stewart, Babbie Group; Berrak Teymur, University of Cambridge; Dale Vince, Jacobs Gibb; and Keith Waterhouse, Ws Atkins, Bristol.

In Turkey the team benefited from collaboration and assistance by the following institutions: Bogazici University, Kandilli Observatory, Istanbul Technical University, Middle East Technical University, Kocaeli University, Adapazari University, Tubitak Research Centre, The crisis centre of the prime minister office, Ove Arup Turkey, Owen Williams Turkey.

During the mission the following centres were surveyed from West to East along the ruptured fault lines: on the north shore of the Marmara Sea: Gebze, Derince, Izmit, Adapazari, Düzce; on the south shore of the Marmara sea : Yalova, Deregemendere, Gölcük. Damage to residential buildings was recorded in each centre. In Adapazari, Gölcük and Yalova a few blocks were systematically surveyed. The fault rupture was followed and detailed measurement taken in the area immediately east of Izmit. Further to that a number of strong motion record instruments were inspected and buildings surrounding the instrument were surveyed at Gebze, Tubitak and Arcelik stations; at Izmit Yarimca Petchem station; Adapazari station, and Düzce meteorological station. Hospital facilities were visited and hospital administrators interviewed in Gebze, Izmit, Adapazari, Düzce.

The report presents findings relating to the seismic history and hazard of the region and its socio-economic development in the last fifty years: within this context, the general data on casualties and material damage are discussed and compared with the outcome of other earthquake of similar magnitude worldwide (Chapter 1). The history and mechanics of rupture of the north Anatolian fault have been object of detailed studies in the past fifty years. These are summarised in Chapter 2 and constitute the framework within which the surface faulting caused by the 17 August event and the associated tsunami and other secondary effects are analysed.

The Kocaeli earthquake provided a unique wealth of strong motion records for an earthquake of high magnitude at short distance from the rupturing fault, as at least 6 instruments were sited within 20 km from the fault. The recorded accelerogrammes present peak ground accelerations which are generally smaller than values predicted with empirical

correlations. This can be partly explained by the housing conditions of some of the instruments, as discussed in detail in Chapter 3. This chapter also presents the correlation of the instrumental records with local damage surveys and with macroseismic intensity evaluations.

Ground failure and geotechnical effects were extensively distributed within the epicentral area and were often the trigger of further structural damage. A brief review of the ground conditions in the visited areas of the region, which are relevant to the understanding of the seismic effects observed is reported in Chapter 4. Then the detailed observations carried out with reference to fault rupture, site response, liquefaction or soil failure, and slope instability are discussed for each of the districts visited. Finally the response of geotechnical structures such as building foundations, retaining walls and earth embankments are presented.

The poor soil condition on which many of the collapsed buildings were founded has been identified as concurrent cause of the widespread destruction. The major reason for the poor performance of residential buildings, which caused such a high number of casualties, should not however be considered a shortcoming of the code prescriptions as much as the general poor quality of materials and construction details, and in many cases the total lack of basic seismic provisions. Indeed the enforcement of the existing code remains a major obstacle for life safety. Most of the building stock throughout Turkey, and especially in the Istanbul metropolitan area, has similar characteristics, albeit with lower levels of hazard, according to the macrozonation map, and hence the implications in terms of possible devastation and casualties by future earthquakes are only too evident. Chapter 5 presents a discussion on the 1975 and 1997 seismic codes provisions and compare it with other codes and with an investigation of the constructional process and materials on site. An extensive collection of damage details is then presented with commentary followed by a statistical and geographical analysis of the damage observed in two case study areas in Adapazari and Izmit. The damage to industrial facilities is discussed in chapter 6 while damage to civil engineering structures and port facilities is analysed in chapter 7, which concludes this report.

3. Acknowledgments

EEFIT is grateful to the following for their assistance with this mission and the publication of this report:

The Engineering and Physical Science Research Council, who provided funding to the UK academics of the EEFIT mission under grant GR/N03426

The Guggenheim foundation for sponsoring the participation of R. Bilham

The Babbie Group, WS Atkins, Jacobs Gibb, Ove Arup Hong Kong, the BGS, for sponsoring the participation of their employees

The late Prof. Barka and staff of Kandilli Observatory, and Prof Mustafa Erdik and his team at Bogazici University who provided initial briefing and orientation and transportation facilities; Prof. Karadogan and Prof. Attila Ansal of Istanbul Technical University who provided useful discussion, documentation and access to damaged industrial sites. Prof. Karaesman of METU and his students for the initial contacts and for helping the team with translation and local knowledge during the on site visits.

Ian Smith, Polat Gulkan, David Mallard, Willi Aspinall, Jack Pappin, Edmund Booth, Jochen Schwarz, Zygmunt Lubkowsky for the thorough review and editorial suggestions for this report.

4. List of Useful Internet Links (updated to 15 April 2002)

4.1 Turkish Sites:

- <http://www.deprem.gov.tr/> - General Directorate of Disaster Affairs Earthquake Research Department of Turkey
- <http://www.istanbul.edu.tr/eng/jfm/jeofizik/deprem/indexeng.html> - University of Istanbul, Department of Geophysical Engineering Special Earthquake Page.
- <http://www.koeri.boun.edu.tr/depremmuh/default.htm> - Kandilli Observatory & Earthquake Research Institute, Bogazici University website from which a report in .pdf format can be downloaded.

- <http://193.140.203.16/geophy/ingl/engver1.html> - BU Kandilli Observatory & Earthquake Research Institute, Department of Geophysics Web page
- <http://www.turkishpress.com/> - Turkish Press Review
- <http://mantle.geop.itu.edu.tr/E/main.html> - Istanbul Technical University / Department of Geophysics
- <http://www.metu.edu.tr/home/wwwdmc/main-e.html> Middle East Technical University, Disaster Management Implementation and Research Centre site

4.2 European Sites:

- <http://www.igf.edu.pl/seis/turkey.html> - link to Polish station data
- http://www.gfz-potsdam.de/pb2/pb21/Task_Force/izmit/izmit_text.html - The Izmit Earthquake Mission of the German Task Force for Earthquakes
- [ORFEUS](#) - access to ORFEUS SPYDER[®] data - KNMI / The Netherlands
- http://www.pz.cnr.it/imaaa/turchia/report_e.html National Group for Protection Against Earthquakes (GNDT). Final report in English and Italian
- [BBC news site](#)
- <http://www.arch.oita-u.ac.jp/a-kou/turkey.pdf> Paper on analysis of damage of concrete buildings in Adapazary.

4.3 US and Canada Sites:

- [Access to WILBER](#) - browse seismograms, request SPYDER[®] data
- <http://www.iris.washington.edu/DOCS/turkey.htm> - IRIS Special Event File: Turkey Earthquake and tectonic map with plate motions - submitted by Meredith Nettles, University of Arizona
- [USGS Report](#) - This page feature reports and pictures posted by the USGS reconnaissance team and <http://greenwood.cr.usgs.gov/pub/circulars/c1193/> USGS final report on line in .pdf format
- <http://www.eeri.org/earthquakes/Reconn/Turkey0899/Turkey0899.html> -Earthquake Engineering Research Institute on line relevant newsletter issue
- <http://www.seismo-watch.com/EQS/AB/99/990817.Turkey7.8.html> - SeismoWatch report page
- <http://atlas.geo.cornell.edu/turkey/turkey.html> - Eastern Turkey Seismic Experiment: Lithospheric Structure in an Active Continental Collision Zone / Cornell University
- <http://www.geo.lsa.umich.edu/SeismoObs/STF.html> - Source time functions
- <http://www.okgeosurvey1.gov/level2/ok.grams/T990817.html> - Six seismograms and a particle motion plot / Oklahoma Geological Survey
- <http://www.eng.uottawa.ca/profs/murat/KocaeliEQ.html> On line report on the Kocaeli earthquake
- <http://mceer.buffalo.edu/research/turkeyeq/> University of Buffalo Multidisciplinary Centre for Earthquake Engineering Research, Reconnaissance report on line.
- <http://www.cco.caltech.edu/~ayhan/EQ/KOCAELIEQList.html> Photographic documentation of an eye witness
- <http://www.wje.com/earthqke/newsletr.pdf> Wiss, Janney Elstner Associates Inc, reconnaissance report
- [CNN news reports](#)

1 The Earthquake Affected Region

Roger Bilham,
CIRES and Dept. of Geological Sciences, University of Colorado, Boulder

Dina D'Ayala,
University of Bath

1.1 Introduction

On 17 August 1999, at 03:02 local time, the second largest earthquake of the 20th Century in Turkey struck the northwestern region of the country. The earthquake was generated by the western section of the North Anatolian fault and its epicentre has been located at 40.702N, 29.987 E, on the southeast shore of the Gulf of Izmit, with a focal depth of approximately 17 km. Official estimates associated a magnitude of Mw 7.4 and Ms 7.8 (U.S.G.S. and Kandilli Observatory) to this earthquake known as the Kocaeli earthquake, by the name of the epicentral region, a region highly urbanised and populated. The earthquake caused destruction along a vast portion of the eastern shores of the Marmara Sea and inland east beyond the lake Sapanca and up to Düzce over a surface area of approximately 50000 km². This region on one hand is characterized by the highest seismic hazard of the country and on the other has been affected in the last 20 years by the highest population growth associated with a very fast economic development which sees more than 40% of the national industry and more than 25% of the Turkish population resident here. This situation resulted in a very high number of casualties and injuries, more than 17000 people died and 44000 were injured, an astonishing level of structural failures with more than 140000 residential units either collapsed or beyond repairs, and economic losses estimates ranging from £4.2 billion to £20 billion.

This chapter presents first a comparison between recent seismic hazard studies for the region and the latest national seismic code, to highlight implications on the vulnerability of the building stock, and correlates this with an analysis of the socio-economic dynamics and the development of the construction industry to define the region's exposure to earthquake damage. Within this framework the socio-economic effects of the Kocaeli earthquake are then presented in terms of analysis of fatalities and structural damage and these figures are compared with other destructive earthquakes occurred in Turkey during the 20th Century and with other earthquakes of similar magnitude occurred in the last 20 years worldwide.

1.2 Seismic Hazard of Turkey and the Marmara Sea Region

Catalogues of historical earthquakes are notorious for inaccuracies, repetitions, omissions and exaggerations, and the historical record for Turkey is no exception. The widely available global digital listing of disastrous earthquakes published by NGDC (Dunbar et al., 1992) contains 348 entries for Turkish earthquakes over the past 2500 years (Figure 1.1), some of which are listed two or more times with different coordinates, dates, and fatality statistics. Although source information is provided, no attempt has been made in this catalogue to evaluate data reliability. Sources are frequently secondary works by authors who have similarly merged previous catalogues of earthquakes, repeating or adding errors in earthquake parameters and dates, and sometimes omitting to cite their sources, making it impossible to ascertain data reliability. Mixed with these generally unuseful citations are specific studies that have been undertaken to clarify the details of individual events. However, these more discriminating assessments of individual earthquakes are given equal weight.

Fortunately Turkey and the Middle East have one of the most reliable records of historical earthquakes anywhere in the world thanks to a sequence of studies initiated by N.N. Ambraseys and other authors, who have recognized the perils of earlier compilations and have undertaken the monumental task of compiling a new catalogue based solely on original sources (Ambraseys and Finkel, 1995; Ambraseys and Jackson, 1981). Although a 2500 year history of earthquakes is available for Turkey, the quantity and quality of detail concerning individual events not unexpectedly increases in accuracy towards the present time. Notwithstanding the very real possibility of numerous earthquakes being missing from the current compilations, a clear pattern of earthquake distribution in time and space is evident.

While most earthquakes follow the plate boundaries of Turkey, with a predominance of strike-slip faulting along the North and East Anatolian faults, and dip slip events on the western Aegean margin, severe earthquakes also occur within the Turkish plate. The tectonic details of the motion of the Turkish plate are discussed in Chapter 2, but it is

important to note that the slip along the North Anatolian fault (NAF) appears to occur in sequences with durations of approximately 100 years, followed by long intervals that are relatively inactive. In general, during these periods of quiescence on the North Anatolian fault, a sequence of significant earthquakes occurs along the South Anatolian fault. The magnitudes of strike slip earthquakes along these northern and eastern boundaries are typically much larger than those that occur elsewhere in Turkey (Demirtas et al 1999).

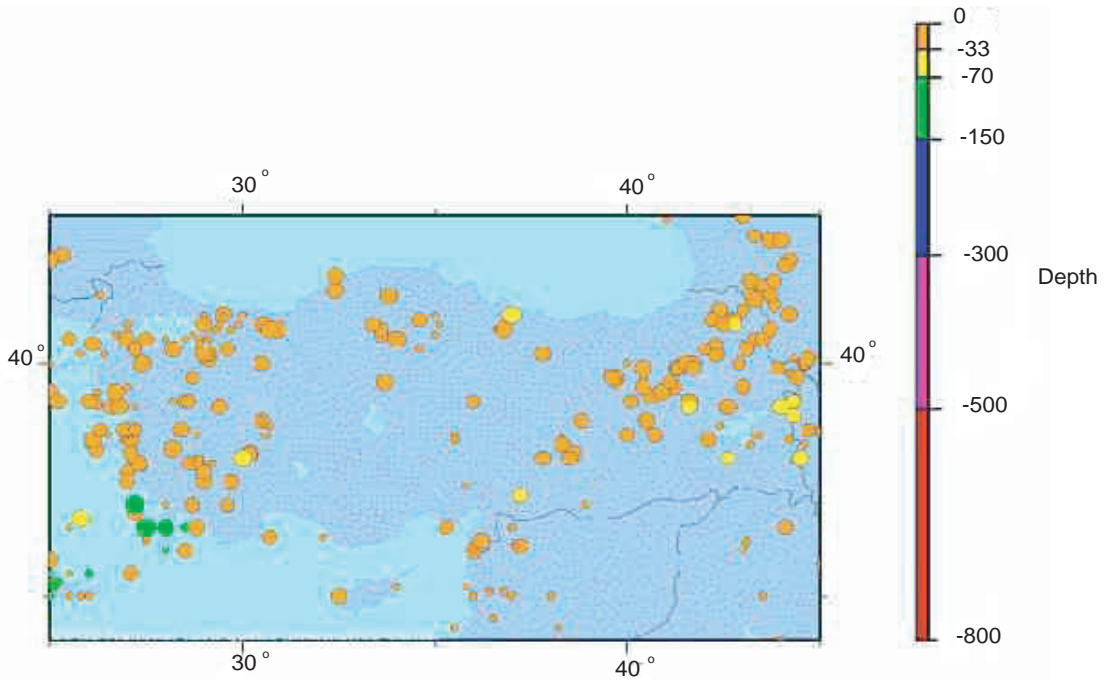


Figure 1.1: Distribution of damaging earthquake epicentres in the Anatolian peninsula (USGS)

A comprehensive study of the seismic hazard of Turkey has recently been completed by Erdik et al. (1999), in connection with the Global Seismic Hazard Assessment Program (GSHAP, Giardini et al. 1993). The work identifies specific seismogenetic areas and quantifies seismic risk based on past seismicity, tectonic setting and attenuation relationships. Thirty-seven seismogenetic zones are identified, with modifications to take into account continuity of probability of occurrence across zone borders. For each of these zones recurrence curves were developed, using an empirical Gutenberg-Richter relationship developed from recorded seismicity and/or from models of fault segmentation.

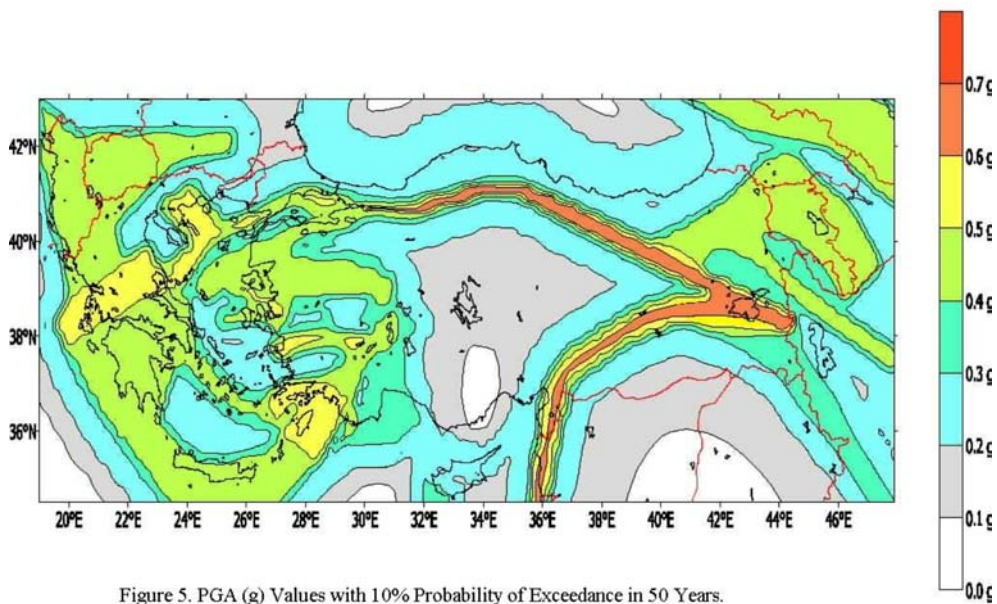


Figure 5. PGA (g) Values with 10% Probability of Exceedance in 50 Years.

Figure 1.2: PGA (g) values with 10% exceedance probability in 50 years (after Erdik et al., 1999)

As part of this study, the horizontal component of Peak Ground Acceleration (PGA) for specified return periods was mapped in terms of iso-horizontal PGA contours associated with a 10% probability of being exceeded in 50 years, and assuming a competent free-field ground with a shear-wave propagation velocity exceeding 700 m/s (Figure 1.2). Of relevance to the present work, the North Anatolian Fault is identified with the highest PGA (0.6 g) for this return period. This peak ground acceleration is based on the assumption of homogeneous consolidated surface materials and on the assumption of invariability of the recurrence model with time. While this last assumption is reasonable for a specified time period, the values for PGA are significantly influenced by the presence of unconsolidated surface materials of appreciable depth, as it will be seen more in detail in the discussion of the strong motion records for the Kocaeli earthquake (Chapter 3).

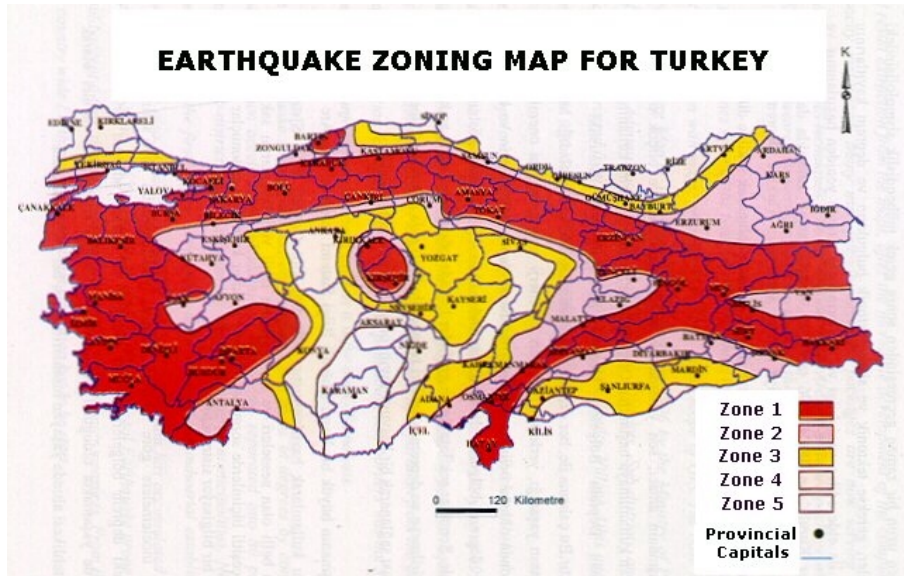


Figure 1.3: Seismic zoning map for Turkey associated with the Turkey National Seismic Code (1998).

Comparison of the predictions of this latest study with the earthquake zonation map developed for the Turkish National Seismic Code (Aydinoglu et al. 1998) (Figure 1.3) yields some interesting observations. The code identifies 5 zones of uniform expected shaking intensity. With the exception of central Turkey, the zone of highest design acceleration, Zone 1, coincides in shape and location with the region enclosed within the 0.4 g contour of Figure 1.2. However for a 50 year design-interval, the code assumes 0.40g as maximum value for this zone, overlooking the narrower strip along the NAF with maximum values of acceleration up to 0.6g in 50 year intervals (see Figure 1.2). It would appear then, that the National Seismic Code base map (Fig 1.3) underestimates the distribution of potential intensities along the North and East Anatolian faults compared to the study undertaken by Erdik et al. (1999). Moreover, because possible amplification effects caused by local site conditions have not been considered in the formulation of Figure 1.2, potential maximum shaking intensities could be further underestimated by the National Code Map. Further observations on the detailed provisions of Turkish seismic codes is contained in Chapter 5, while a detailed discussion of the seismic setting of the North Anatolian fault and the region adjoining the epicentral region of the Kocaeli and Düzce earthquakes is provided in Chapter 2.

1.3 Socio-economic Profile of the Marmara Sea Region

1.3.1 Population Dynamics in Turkey and in the Marmara Sea Region

The annual growth-rate of Turkey's population this century is among the highest of any in Europe. Census statistics available for the period 1927 to 1997 reveal fluctuations in rate from 10%/year to more than 28%/year. Maximum growth occurred during the period 1955-1965 but growth exceeding 20% was sustained between 1950 and 1990. Since then the rate of growth has declined to 15%/year, still several times higher than the European average growth rate. In less than 70 years the Turkish population has quadrupled from 15 million to 63 million (Figure 1.4).

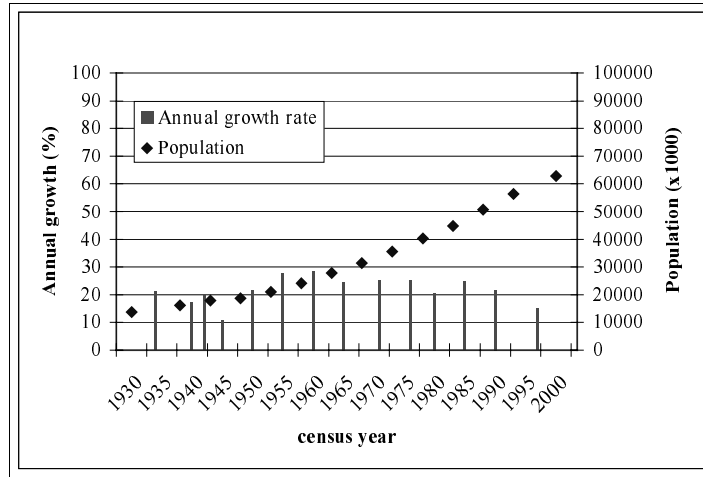


Figure 1.4: Population by Census for the past 70 years.

During this same period there has been a steady migration of population from rural areas to urban centres, a migration that accelerated in 1985 when for the first time the urban share of the population exceeded the rural village population (Figure 1.5). In 1985 a 60%/year rate of urban growth was accompanied by a 10%/year decline in rural population (Figure 1.6). Close to 70% of the total population now live in an urban setting.

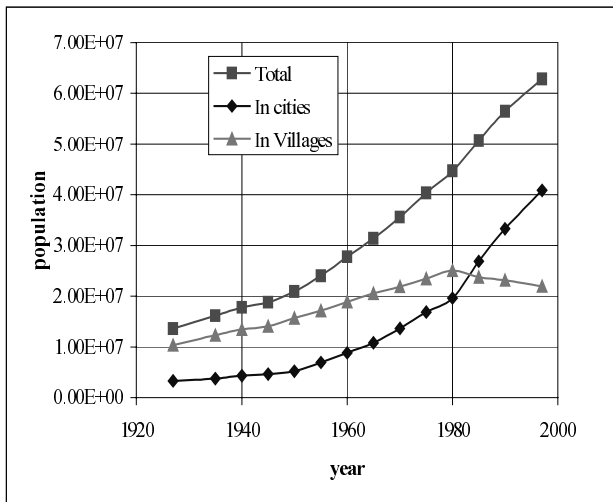


Figure 1.5: Population growth in Turkey in urban and country areas

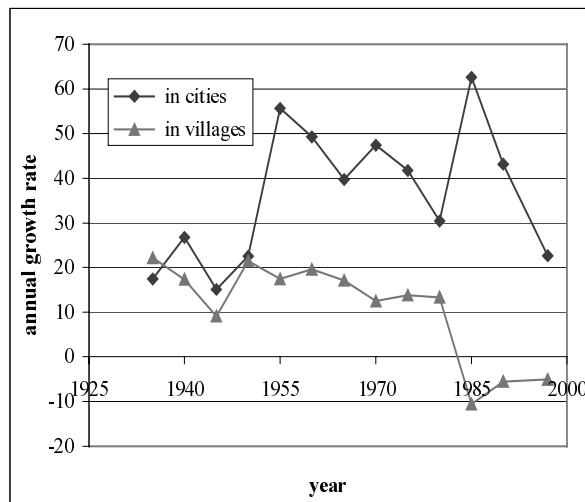


Figure 1.6: Variation in quinquennial growth rate for population in cities and villages in Turkey

Since 1980 the population growth in cities has exceeded the national growth rate, fuelled partly by migration from villages to cities, as it is evident from the decline in rural population since 1980. The increase in population over the last 40 years has increased the mean population density from 36 people/km² in 1960 to 81 people/km² in 1997.

In the past 20 years the most pronounced demographic growth in Turkey has occurred in the Marmara Sea region, which includes the capital, Istanbul, and which was most affected by the earthquake. As recently as 1980 the population of this region was distributed equally between urban centres and rural communities. By 1990 its rural population was outnumbered 2:1. By 1997 urban dwellers outnumbered rural dwellers by a factor of 3, a ratio that continues to increase driven by an urban growth rate exceeding the National average.

By 1997 the 1990 urban population of the Marmara Sea region had grown by 21.74%, compared to the 11.32% National average in the same period (Figure 1.7). The districts of fastest growth within the region were Kocaeli and Istanbul, followed by Yalova and Bursa. These districts are recognized as hosting the recent rapid industrial transformation of Turkey. The percentage population growth of this region is one of the highest in the world.

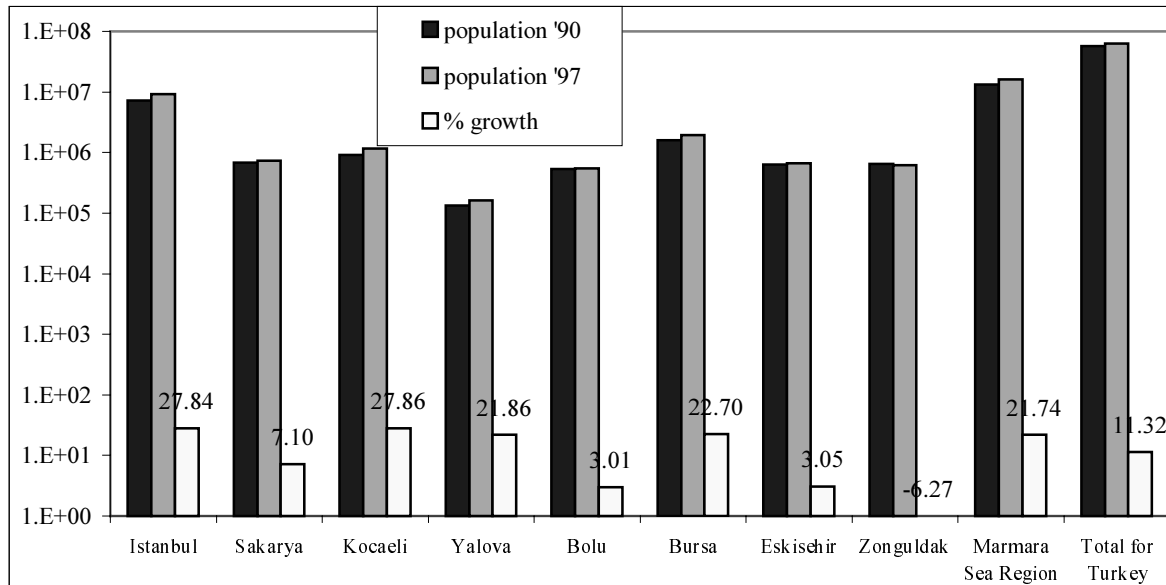


Figure 1.7: Population and percentage growth 1990-1997 for the districts of the Marmara Sea Region affected by the earthquake

1.3.2 The construction industry

The growth in population and its concentration largely within urban areas has resulted in an unprecedented expansion in the regional construction industry. This has required not only substantial changes in building methodologies, but also in the way that new construction is financed.

Changing trends in construction methods can be established from 5-yearly reports of new construction starts available for the period 1965-1997¹, plotted on a logarithmic scale in the diagram of Figure 1.8.

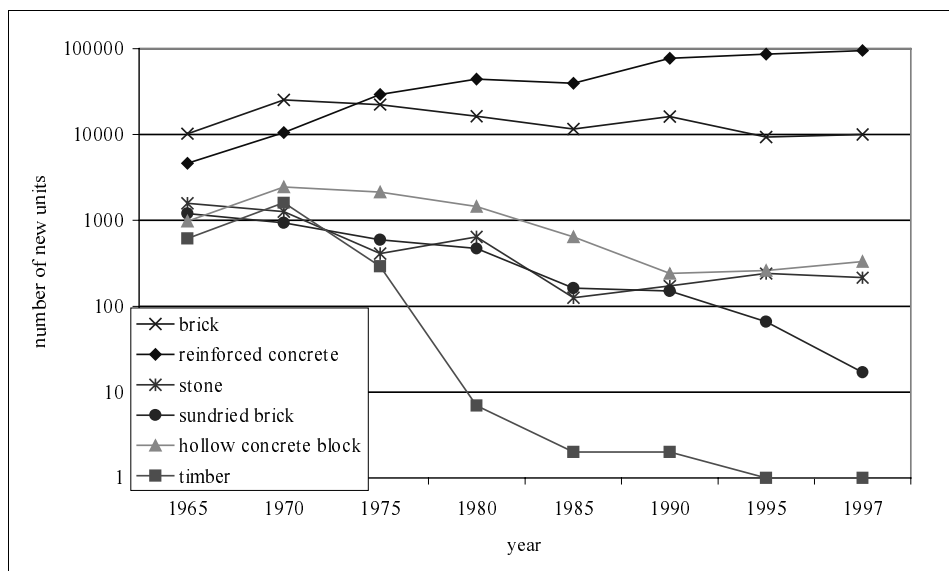


Figure 1.8: New constructions 1965-1997 classified by structural method (note log scale).

A steady increase in reinforced concrete is accompanied by a corresponding decline in traditional construction methods such as timber structures, stone masonry and sun dried bricks. It will be noticed that the largest decline,

¹ Bayinderilik web site, September 1999, data from national Census

evident in Figure 1.8, is the number of new timber structures. These have traditionally been the most resistant to seismic shaking. A 20-fold increase in new concrete structures occurs between 1965 and 1997.

The change in construction method is accompanied by an increase in the number of households per dwelling unit. A sharp rise in the number of households in apartment blocks occurred in the period 1965-1980, followed by a steady growth of these and single household houses (Figure 1.9). In urban centres 8-30 people per dwelling are now quite common. Data for the year 1997-1998 suggest a possible increasing trend in the number of single dwelling, and a substantial increase in the construction of public and religious buildings. This changing pattern is presumably attributable to the recent decline in annual rate of population increase and to the effort of providing urban infrastructures to the new mushrooming neighbours (Figure 1.6).

Although a high population density per dwelling unit is recognized as a major factor in increasing the potential vulnerability of local populations to seismic hazards (Coburn and Spence 1992), the introduction of modern construction methods since 1965 should in principle have resulted in improved resistance to seismic hazards. In particular, post-1975 construction in Turkey should intrinsically be less vulnerable to damage from earthquakes, since it was in this year that a modern seismic-resistant building code was introduced. In later chapters we shall discuss possible reasons for the apparent failure of 1975-1999 constructions to resist damage from earthquake shaking in 1999.

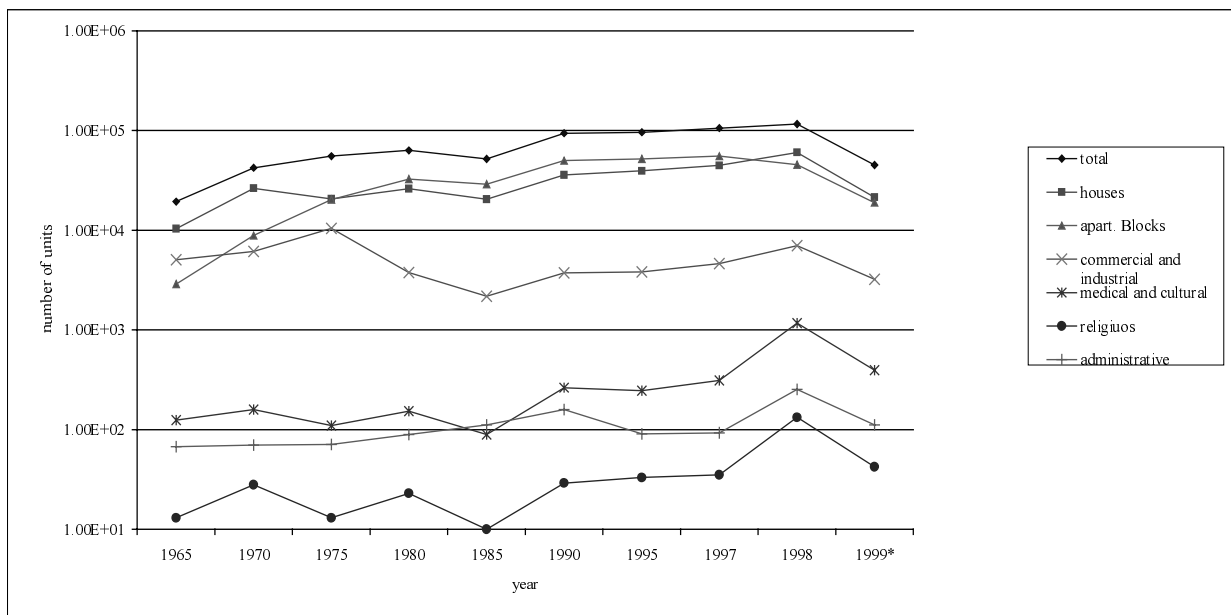


Figure 1.9: New construction classified by use in the period 1965-1998. Year 1999 data account for first quarter only.

In order to finance the tenfold expansion of the residential construction industry between 1967 and 1997, increasing recourse has been made to “co-operatives”. These are associations of single buyers that secure sufficient funds to buy land for construction, and then contract a builder to construct one or more apartment blocks upon it. In this way the cost of land acquisition and construction is shared among many, who are also usually the future occupants of the dwellings. Because the availability of cash is limited and borrowing is kept to a minimum, very often the contractor is paid in kind, by building additional units whose subsequent sale is used as payment to the contractor. As shown by the indicators plotted in Figure 1.10 this form of finance has become increasingly popular, the percentage of total buildings being realised in this way moving from 4.4% in 1967 to 31% in 1992.

Moreover as the cost of land suitable for new construction has increased, the number of dwellings per building has increased from less than 2 units per building in 1967 to 8 and 9 units per building in 1976 and 1986, respectively. In the last decade, however, the number declined to 5 units per building. The dimensions of the units show little variation in size averaging 100 m² per unit during the period, despite an exponential growth in their resale value in the period 1976 to 1992.

This perceived absence of diversity in the dimensions of dwelling units was noted during the EEFIT mission. Most structural units were based on a regular structural grid of planar concrete frames spaced at 4-5 m intervals.

Variations within individual modules are accommodated by means of cantilevered balconies and in the layout of internal partitions.

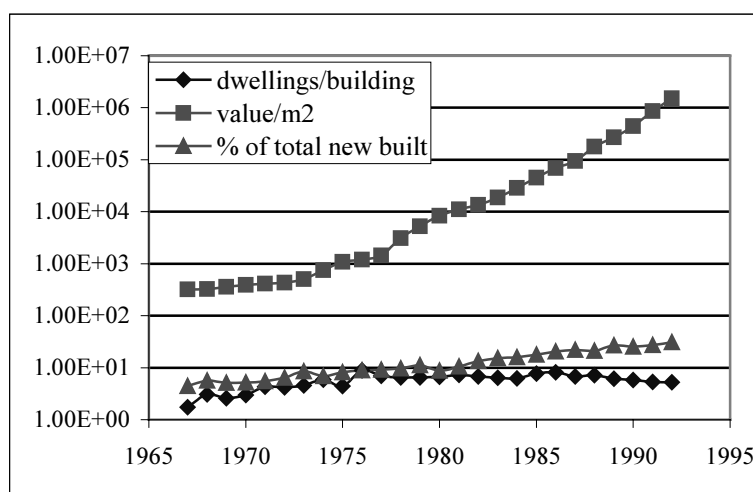


Figure 1.10: Statistics for co-operative financed residential buildings in Turkey.

1.4 Socio-economic Effects of the Kocaeli Earthquake and Comparison with Past Earthquakes

1.4.1 Post seismic damage, fatalities, injured, missing and economic losses.

Figures released on 10 October 1999 by the Prime Ministry of Turkey Disaster Relief Office² indicated that the Izmit earthquakes resulted in 17,439 fatalities, 43,953 injuries and 600,000 people needing re-housing. Among the population an often repeated assertion was that at least another 16,000 people were missing, but no official estimate of those missing has been offered.

In Table 1.1 the official figures in terms of heavy, medium and light damage to residential and commercial units are summarised. Units are in terms of households and commercial outlets rather than buildings.

Table 1.1: Official count of damage to residential and commercial units

High Damage		Medium Damage		Light Damage	
Residential	Commercial	Residential	Commercial	Residential	Commercial
66441	10901	67242	9927	80160	9712

Temporary shelters were initially in the form of cloth-walled tents, and there was some discontent at the fact that these were usually inadequate to accommodate an average Turkish family of 5 to 6 members. The country was not equipped to face such a huge demand of temporary accommodation, made worse by the bad weather that shortly followed the main shock. Starting from the second week of September 1999 prefabricated unit camps were delivered, and their distribution by district, at 10th October 1999, in terms of planned and allocated centres is summarised in Table 1.2.

On 17 August 2000, one year after the earthquake, the official death toll was 17,840 but there remained no reliable tally of the number of missing or unaccounted for. Two reasons for the possible lack of information about the

² Web site: <http://www.die.gov.tr>

number missing are given: survivors may have left the area permanently following the main shock to join families in other parts of Turkey, and in some cases entire families may have been lost with no one to indicate those missing. Authorities indicate that 88% of the badly damaged structures have been demolished but that more than 1100 are still standing. Thousands of moderately damaged structures remain uninhabitable. More than 42000 new houses under construction are scheduled for completion before the spring of 2001. Nearly 150000 people are still living in prefabricated huts, and more than 30000 still live in tents.

Table 1.2: Distribution of prefabricated temporary shelters by district at 10/10/ 1999

District	Number of residential units	Residential Centres	Centres already allocated
Kocaelý	15210	17	9
Sakarya	5510	3	3
Yalova	5150	5	3
Bolu	456	1	
Total	26326	26	15

1.4.2 Analysis of fatality data for Turkey

The earthquake of Kocaeli, shortly after followed by another destructive earthquake in Düzce on 12th November 1999, represented a major shock to the Turkish nation in terms of destruction and loss of lives. The high death toll has been ascribed (Bilham, 1988; 1995) to trends in urbanisation that have occurred this century, and to the resulting increased vulnerability of global communities, as shown in the previous section. In this context, the Turkish earthquakes of 1999 represent a paradigm of possible damage scenarios that may occur in other industrialised regions with similar population density and non-engineered building stock. As such these disastrous events can be viewed as part of a global trend that may be repeated many times in the next century. In the following paragraphs the Izmit earthquake is ranked against similar destructive earthquakes world-wide and against the seismic activity in Turkey in the last two centuries.

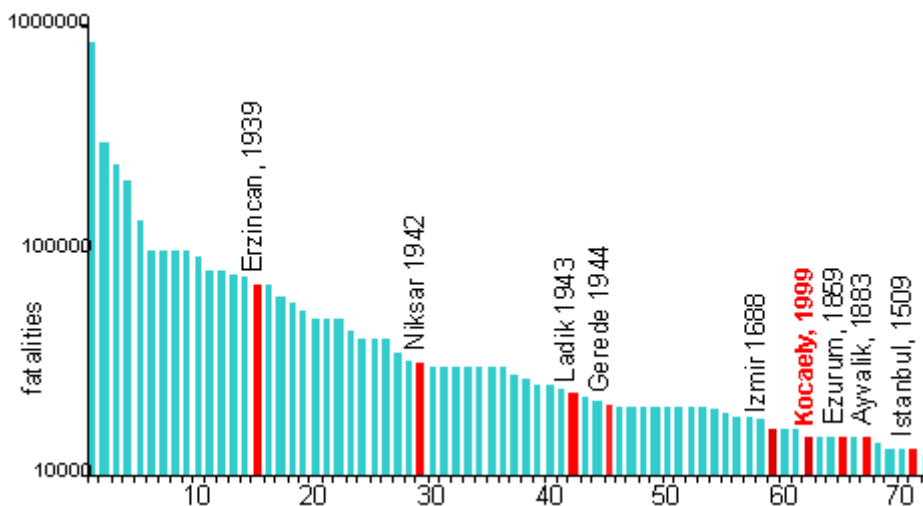


Figure 1.11: Ranking of destructive earthquakes world-wide by loss of life. Turkish earthquakes (labelled) account for 12% of all disasters in this figure, and though the loss of life in 1999 exceeded 17000, it ranks 62nd in the catalogue.

In the following analysis for the period 1500 to the present we exclude duplicate entries in the NGDC global catalogue of significant earthquakes (Dunbar et al. 1992) and earthquakes with fewer than 13000 fatalities. Fatality

accounts for all Turkish earthquakes since 1900 have been revised with data from Ambraseys and Finkel (1995), and Ambraseys and Jackson, (1981), and are used exclusively in the subsequent analysis of smaller events.

A histogram ranking the most disastrous earthquakes since 1500 shows that nine (12.5%) of these events occurred in Turkey, and five (7%) occurred this century. The worst Turkish earthquake is one that occurred in 1939 claiming 74,800 lives and ranking 15th on the global histogram of Figure 1.11. The 1999 event is the sixth most fatal earthquake in Turkey and the fourth worst fatality event to occur on the Anatolian fault. The North Anatolian fault has claimed more than 147,000 lives this century.

Figure 1.12 shows the cumulative loss of life from all Turkish events in the last two millennia. Although fatality counts are unreliable especially prior to 1500, the total loss of life from earthquakes exceeds 1.1 million. Apparent changes in gradient reflect demographic changes as well as variations in reporting. The occurrence of large events near population centres is responsible for the large steps in the graph.

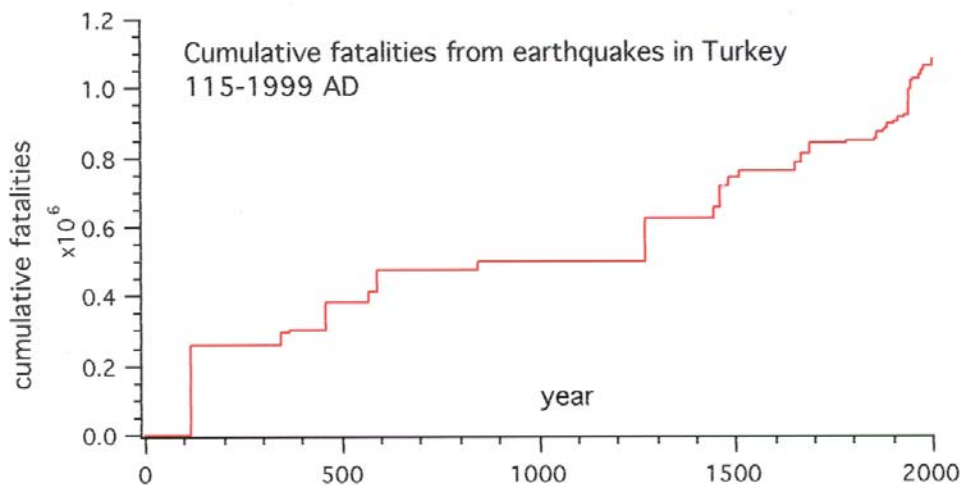


Figure 1.12: Cumulative fatalities form earthquake in Turkey in the last two millennia

The timing and fatality count of disastrous Turkish events since 1800 are shown in Figure 1.13. More than twelve earthquakes with a fatality-count exceeding 4000 have occurred, and 6 of these occurred this century, concentrated in clusters with a return period of approximately 30 years. The total loss of life in this interval is approximately 300,000. Two features are particularly evident in Figure 1.13: the 1940's loss of life from faulting along the North Anatolian fault, in 3 closely spaced events totalling more than 12,000 deaths, and the recent over 20 years interval in which comparatively few earthquake fatalities have occurred. Indeed since 1980 there have been several destructive earthquakes but loss of life has been less than 100 in each case.

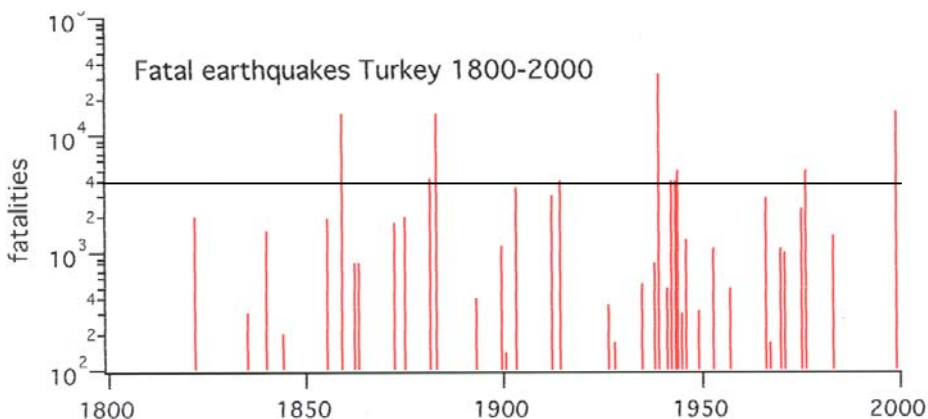


Figure 1.13: Distribution of fatal earthquakes in Turkey in the last 200 years.

The Izmit event has occurred at a time when the Turkish population at 63 million is larger than ever before but when there has not been a catastrophic sequence for more than 40 years, nor any major loss of life for 20 years, despite

several major earthquakes with magnitudes similar to the recent event. The transient low fatality rate in the past 20 years suggest that this may have led to complacency among the earthquake hazard community. However, this is clearly not an appropriate conclusion for it is during this period of time that a comprehensive earthquake resistant code was implemented in Turkey.

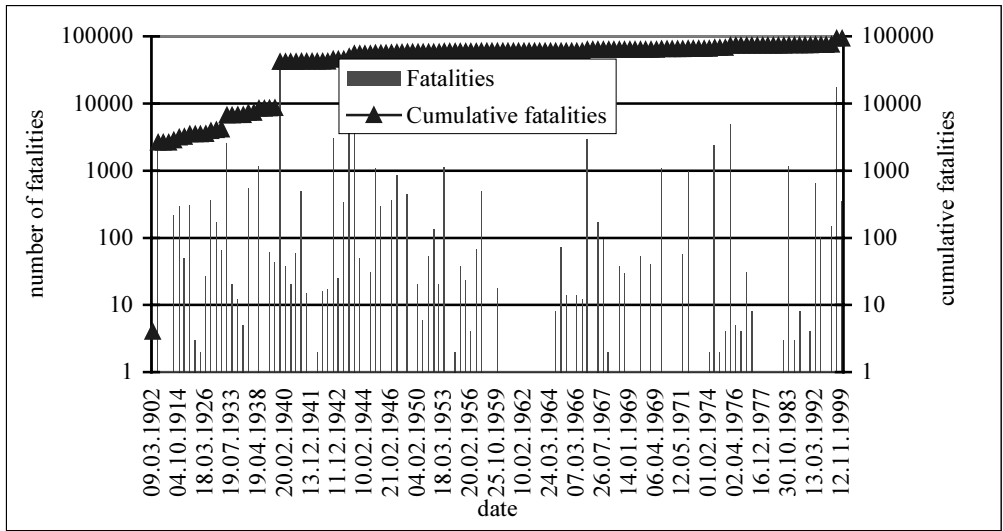


Figure 1.14: Number of fatalities by earthquake, and their cumulative contribution for the period 1900-1999. Note that the time scale is non-linear.

In order to better appreciate this last point a more detailed analysis is presented for $M > 4$ events in the last 100 years. The database used was prepared by Bađćy et al. (1999), and corrected on the basis of the more reliable catalogues discussed in previous sections. We are using this database because contains information not only on fatalities and magnitude but also on injured, heavy damaged households, and an estimated MSK maximum intensity. The data are not complete for every earthquake, and some figures related to fatalities are lower than databases compiled from original source materials. On the basis of this list the total count of fatalities this century, Figure 1.14, is just below 100000, with the Kocaeli earthquake second worst after the 1939 Erzincan earthquake.

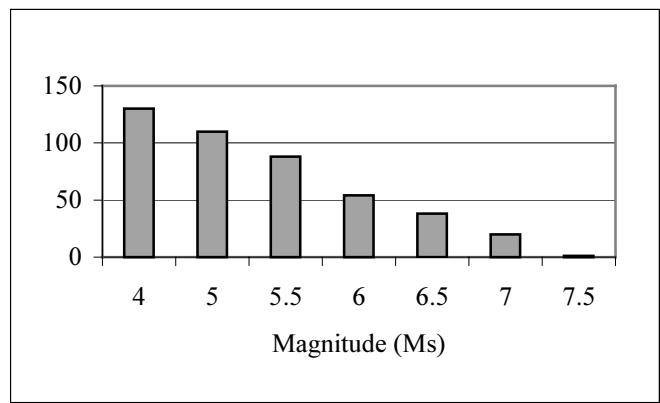


Figure 1.15: Cumulative number vs magnitude distribution of Turkish earthquakes, 1900-1999

One hundred and thirty destructive earthquakes have occurred this century with $M_s > 4$, of which 55 are $M_s > 6$ (Figure 1.15). Only one, however, exceeded the magnitude of the Kocaeli earthquake, the 1939 Erzincan earthquake of $M_s = 7.8$. The 1939 event is associated with the highest fatality count and largest number of damaged dwellings (see Figure 1.16). Figure 1.16 shows the distribution of fatalities as function of earthquake magnitude, and an exponential regression curve with a correlation factor $R^2=0.33$. The relatively low correlation is due to the fact that the fatality count is a function of numerous variables including population density, building vulnerability, local amplification effects, in addition to earthquake magnitude. Perhaps not unexpectedly better correlation is obtained between fatalities and damaged households as shown in Figure 1.17, with a correlation coefficient $R^2= 0.94$. The

data for the two parameters were available for 127 of the 130-recorded earthquakes. A value of 0 fatality was assigned to the few cases for which data were unavailable. The scatter for moderate earthquakes is larger because for these events a larger proportion of fatalities are not directly attributable to structural collapse. For the correlation to be manifest for a data set with duration of 100 years suggests that the building stock has not improved substantially, and hence the lethality ratio (Coburn and Spence, 1992) has not been reduced, despite recent changes in construction methods (see Figure 1.8).

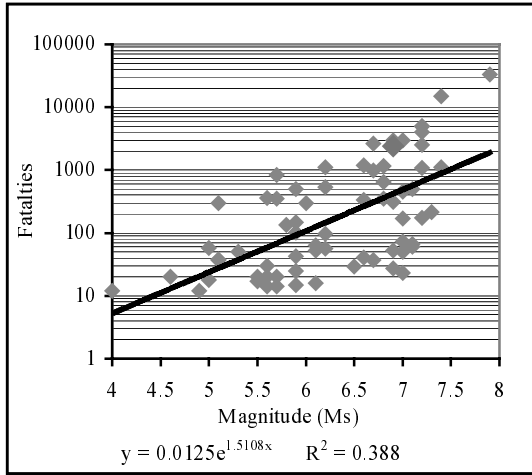


Figure 1.16: Distribution of fatalities as function of earthquake magnitude Ms

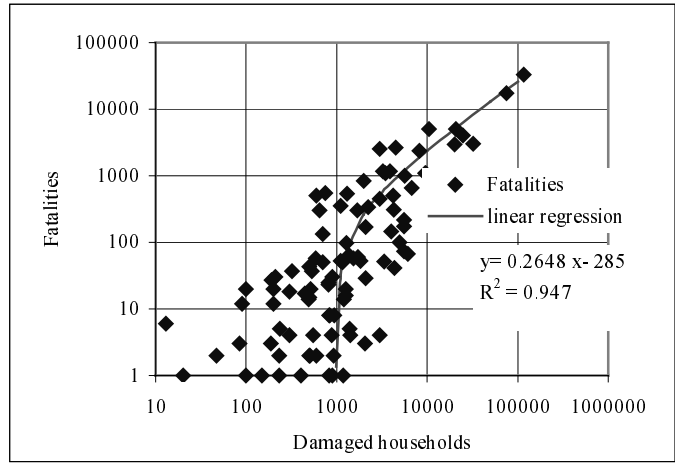


Figure 1.17: Correlation between damaged households and fatalities

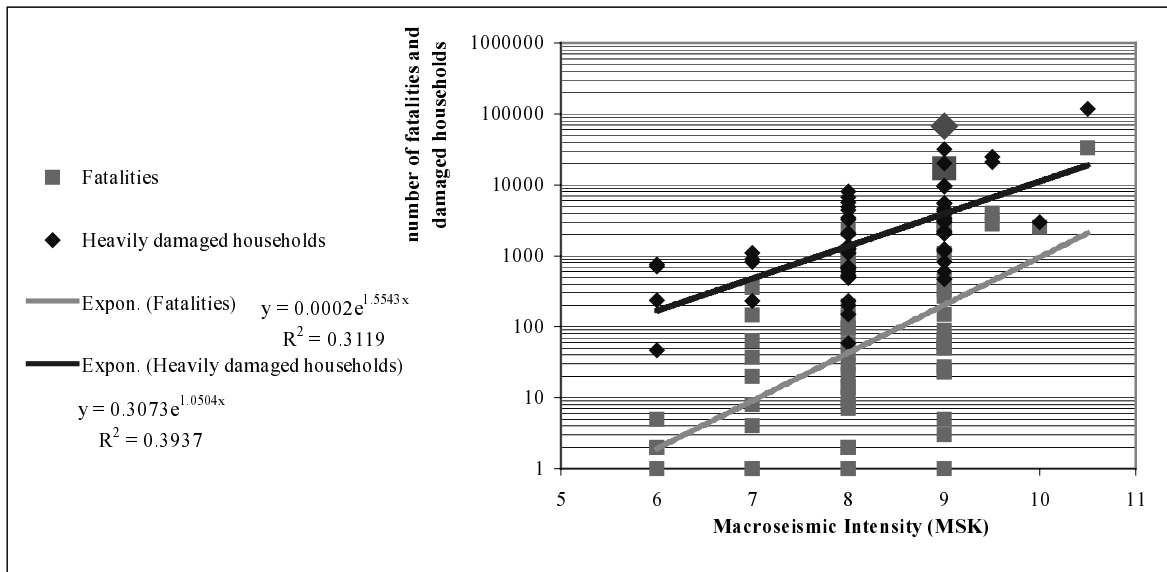


Figure 1.18: Distribution of damaged households and fatalities by intensity. Symbols representative of the Kocaeli earthquake are of greater dimension

Finally the distribution of damage and fatalities as a function of maximum estimated Intensity (Figure 1.18) are examined. The scatter in these graphs is considerable as one might expect since it includes a mix of building vulnerabilities and local amplification effects. However, it shows quite clearly that the Kocaeli event is anomalously high both in its damage and fatality count. The death toll and the structural damage caused by this earthquake are an order of magnitude greater than the regression curve for previous events this century. In the next section the distribution of damage and fatalities at a district level within the epicentral region caused by the Kocaeli event is discussed and compared with data from other recent earthquakes.

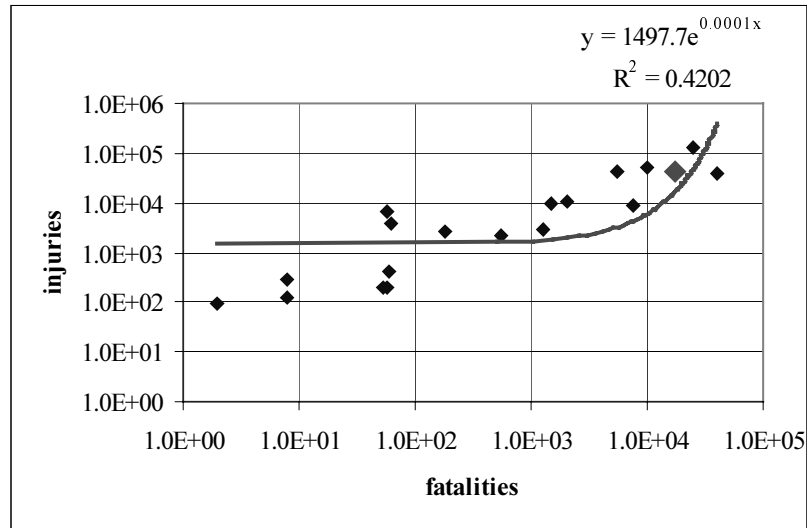


Figure1.19: Correlation between fatalities and injuries in 20 earthquakes worldwide from 1970 to date (Kocaeli event, larger symbol on diagram)

1.4.3 Death toll in this earthquake

The most recent figures available from the Crisis Centre set the total death toll to 18058 (June 2000) while the total accounted injuries has rose to 43953. The total of destroyed, heavy and light damage units, both residential and commercial, is set to 77927, 76768 and 89290, respectively, however the break down by municipality does not reach these totals. In table 1.3 the data by district on damage of households and casualties is presented together with the urban population census of 1997.

Table 1.3: Statistics of damage and casualties for the 17 august 1999 earthquake

City	destroyed	heavy damage	light damage	Deaths	Injuries	Urban Population '97	Deaths/ population	Death/ households
Bolu	3095	4180	3303	264	1163	265052	0.000996	0.024957
Bursa	29	104	401	268	2375	1484838	0.00018	0.501873
Eskýpehýr	76	47	315	86	375	518643	0.000166	0.196347
Istanbul	3073	13339	12455	984	7204	9198809	0.000107	0.034087
Kocaelý	19315	21287	22452	4843	8487	750138	0.014488	0.076807
Gölcük	12310	7789	9299	6025	9960			0.204946
Sakarya	19043	12200	18720	3046	6884	412625	0.007382	0.060965
Yalova	9462	7917	12685	2539	5937	110106	0.023060	0.084453
Zonguldak	0	0	0	3	26	239186	1.25E-05	
Total	66403	66863	79630	18058	42411	12979397	0.00139	0.084821

As already mentioned, the most striking feature of this earthquake is the high death toll. The average ratio of death to injuries is slightly higher than 2/5 with a maximum of 3/5 in Gölcük. The first figure should be compared with 1/7 average ratio for Kobe earthquake (EEFIT 1997) and 1/5 ratio for Chi-Chi Taiwan earthquake (RMS 2000) of comparable magnitude (see Figure 1.19).

Correlation of the death toll data with the latest population census in the urban areas reveal that the death toll reaches values of 0.7 % in Sakarya and 1.4% and 2.2 %, in Kocaeli and Yalova respectively. The Kocaeli figure considers the aggregate deaths in Gölcük and Izmit. These values compare with 0.6%, as the worst death toll in the Kobe earthquake (EEFIT 1997).

Explanation of this high death toll ratio can be found in the time of day of occurrence of the earthquake, while occupancy of the residential buildings was at a maximum, and in the relatively long duration of the shocks, which, according to the latest interpretation of the strong motion records, might have been generated by two closely subsequent ruptures (Aydan et al. 1999).

The total death toll by district has also been correlated with the total damaged households (sum of the 3 categories of damage in Table 1.3). Among the districts in the highest intensity area, Gölcük presents the highest death toll per damage household with 2 in 10, while Sakarya has the lowest with 6 in 100. In the area of low intensity, Bursa district shows a high rate of death to damaged households of 5 in 10. The average total is 8.4 in 100. Data from correlation of fatalities and damaged households worldwide in earthquakes where deaths were caused predominantly by damage of concrete structures show rates varying from 2 in 100 (Philippines 1990) to 2 in 10 (Mexico 1985).

1.5 Conclusions

The Kocaeli earthquake of 17th August 1999 occurred in the region of highest seismic hazard of Turkey, as a result of rupturing of the North Anatolian Fault. It affected a vast region along the shores of the Marmara Sea bringing destruction to the most developed and industrialised part of the country. The major characteristic of this earthquake is the widespread collapse of relatively recently built residential buildings, made of reinforced concrete frame supposedly designed according to seismic code provision. A comparison of the code zonation map with the latest hazard studies highlight a possible underestimate of expected peak ground acceleration for return period of interest to building life span. The analysis of the population dynamics and the economic associated to the development of the modern construction industry in the last forty years in Turkey explains some of the intrinsic vulnerability of the resulting building stock. The consequent death toll, significantly affected by the time of occurrence of the earthquake, is the fifth highest of earthquake history in Turkey only second to the 1939 event this century.

The average ratio of death over population of the entire affected region is 0.14%, but the highest in Yalova reaches 2.2%. The highest ratio of death per household was recorded in Gölcük with 2 in 10, while the average value over the region is 8.4%. These ratios are the highest compared with earthquakes of similar magnitude occurred in urban areas worldwide. The implication for earthquake risk in fast developing countries around the world it is evident and daring. The recent Bhuj earthquake, in India, has confirmed that fast growing industrial-urban community where reinforced concrete construction has replaced traditional buildings forms are extremely vulnerable to destructive earthquakes and will cause large fatality numbers.

1.6 References

- Ambraseys, A. A. and J. A. Jackson,(1981), Earthquake Hazard and Vulnerability in the north eastern Mediterranean: the Corinth earthquake sequence of February-March 1981, *Disasters*, 5(4), 355-368, 1981.
- Ambraseys, N. N. and C. Finkel, The seismicity of Turkey and Adjacent Areas: a historical review, 1500-1800. Istanbul: Mu hit tin Salih EREN, 1995.
- Aydan O., Ulusay R., Hasgur Z. Taskin B., (1999), A site investigation of Kocaeli earthquake of August 17, 1999. Turkish earthquake Foundation, 1999.
- Aydinoglu M.N. et al., (1998), Specification for Structures to be Built in Disaster Areas: Part III-Earthquake Disaster Prevention, Ministry of Public Works and Settlement, Republic of Turkey.*

- Bađcý, G., Yatman, A., Özdemir, S., Altýn ,N.,(1999) Türkiye'de Hasar Yapan Depremler Deprem Arařtırma Bülteni, Sayý 69,113-126
- Bilham, R., (1988) Earthquakes and Urban Development, *Nature(Lond)*, 336,625-626,1988
- Bilham, R., (1995) *Santa Fe Institute Studies in the Sciences of Complexity*, 25,19-31, Addison Wesley , 1995
- Coburn A., Spence R., Earthquake protection, Wiley 1992
- Demirtas R., Yilmaz R.,(1999) Seismotectonics of Turkey. See <http://angora.deprem.gov.tr/jpg/Turkey.htm>
- Dunbar, P. K. , P. A. Lockridge and L. S. Whiteside (1992) Catalogue of Significant Earthquakes 2150 BC to 1991 AD, Including Quantitative Casualties and Damage, *National Geophysical Data Center Report SE49* pp. 320, Sept 1992. 1999 revision.
- EEFIT (1997), The Hyogo-Ken Nanbu (Kobe) earthquake of 17th January 1995, Institution of Structural Engineers, London 1997
- Erdik M., Alpay Biro Y., Onur T. Sesetyan K., Birgoren G., Assessment of earthquake hazard in Turkey and Neighbouring regions, see <http://193.140.203.8/earthqk/gshap.htm>, Bogazici University, Istanbul, 1999.
- Frankel, A., *Bull. Seism. Soc. Am.*, 84,462-465,1994.
- Giardini, D., Basham P., (1993),The global seismic hazard program, *Annali di Geofisica*, Vol. XXXVI. N 3-4, June –July 1993
- Poirier, J.P., and Taher, M.A., 1980, Historical seismicity in the near and Middle East, North Africa, and Spain from Arabic Documents (VIIth - XVIIIth Century): *Bulletin of the Seismological Society of America*, v. 70, no. 6, p. 2185 -2201.
- RMS, (2000), Chi-Chi Taiwan Earthquake, Event Report, 2000 Risk Management solutions, Inc.
- United Nations, (1999), *World Urbanization Prospects*, 1998 revision, United Nations, New York, 1999.

2 Tectonic and Seismological Aspects

Roger Bilham,
CIRES and Dept. of Geological Sciences, University of Colorado, Boulder

Russ Evans,
British Geological Survey

2.1 Basic Seismological Data

On August 17, 1999 at 00:01:40 (UTC) a moment magnitude M_W 7.4 earthquake struck the province of Kocaeli in western Turkey. The earthquake ruptured a 140km segment of the North Anatolian fault between Gölcük and Lake Melen, with a right lateral offset of up to 5.5m and a vertical surface displacement of up to 2.4m. The source mechanism for the earthquake indicates a purely right lateral strike-slip displacement on an east-west trending, near vertical fault plane (Lettis et al, 2000). The official data from the U.S. Geological Survey and Kandilli Observatory include: surface wave magnitude M_S 7.8; body wave magnitude m_b 6.3; moment magnitude M_W 7.4; epicenter, 40.702°N, 29.987°E; depth, 17 km.

Just three months later on November 12, 1999 at 16:57:20 (UTC) a moment magnitude M_W 7.2 earthquake struck the nearby city of Düzce. The earthquake ruptured another 40km segment of the North Anatolian fault at the eastern end of the initial rupture with a right lateral offset of up to 4.5m.

2.2 Tectonic Setting of Turkey

Convergence between the African and Eurasian plates in the eastern Mediterranean results in the westward motion of the Turkish plate on which most of the land area of Turkey lies. The plate is bounded to the north by the 1200-km-long North Anatolian Fault (North Anatolian Fault), and to the south by the Southern Anatolian Fault, which slip in a right-lateral and left-lateral sense respectively. The Black Sea margin of Turkey lies on the stable Eurasian Plate, which displays little seismicity. In contrast, the western margin of Turkey and the floor of the Aegean Sea, including the Marmara Sea region, is an area of active crustal extension characterized by 'normal'-type earthquakes with a substantial vertical slip component. The Izmit earthquake of August 1999 is a strike-slip earthquake at the western end of the northern Anatolian Fault system, near the point where the strike-slip regime gives way to the extensional one (Figure 2.1).

The slip rate on the North Anatolian Fault determines its rate of seismic productivity. This is currently estimated to be 22 ± 7 mm/yr using direct observations from a network of fixed and mobile geodetic GPS receivers whose relative positions have been monitored over the five years to 1999 (Reilinger et al. 1997, Straub et al. 1997). This value is consistent with estimates of plate motion derived from geological considerations and from historical seismicity (Ambraseys & Jackson 2000). The curved form of the Northern Anatolian fault is accounted for by the rotation, as well as westward translation, of the Turkish mini-plate relative to Eurasia. This geometry allows displacement across the fault to be predominantly strike-slip style along its entire length.

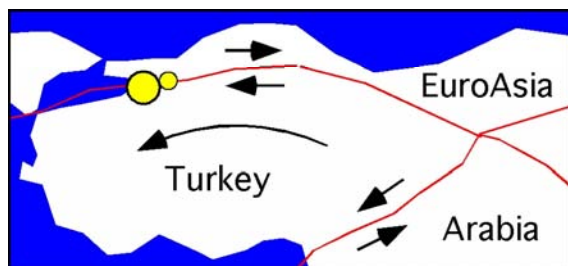


Figure 2.1: Map showing tectonic setting of Turkey. The Arabian plate approaches from the SE at 22 ± 6 mm/year resulting in slip on the N. Anatolian fault of 22 ± 7 mm/year. The sense of slip on the fault systems surrounding Turkey is shown by arrows and the curved arrow indicates the approximate rotation vector of the Turkey Plate. The location of the Kocaeli earthquake is shown by the yellow circle.

2.3 Historic Earthquakes and Surface Slip on the Northern Anatolian Fault

Earthquakes on the Anatolian fault have been documented in various degrees of detail in historical accounts throughout the past 2000 years, and these accounts have been used to construct earthquake catalogues (Ambraseys and Finkel, 1995). Ambraseys (1970) identified the rupture zones of 20th century earthquakes to demonstrate a convincing case that contiguous ruptures overlapped little and progressed sequentially along the entire length of the fault. This is indicated in Figure 2.2 after Stein et al (1997). These data have been supplemented by field studies (Barka 1992, Barka and Eyidogan 1993) and trench excavations (Okumura et al. 1990, 1993; Ikeda et al. 1991) to confirm both recent slip, and slip in historic earthquakes. The slip distribution of most historic earthquakes along the northern Anatolian Fault remains incomplete.

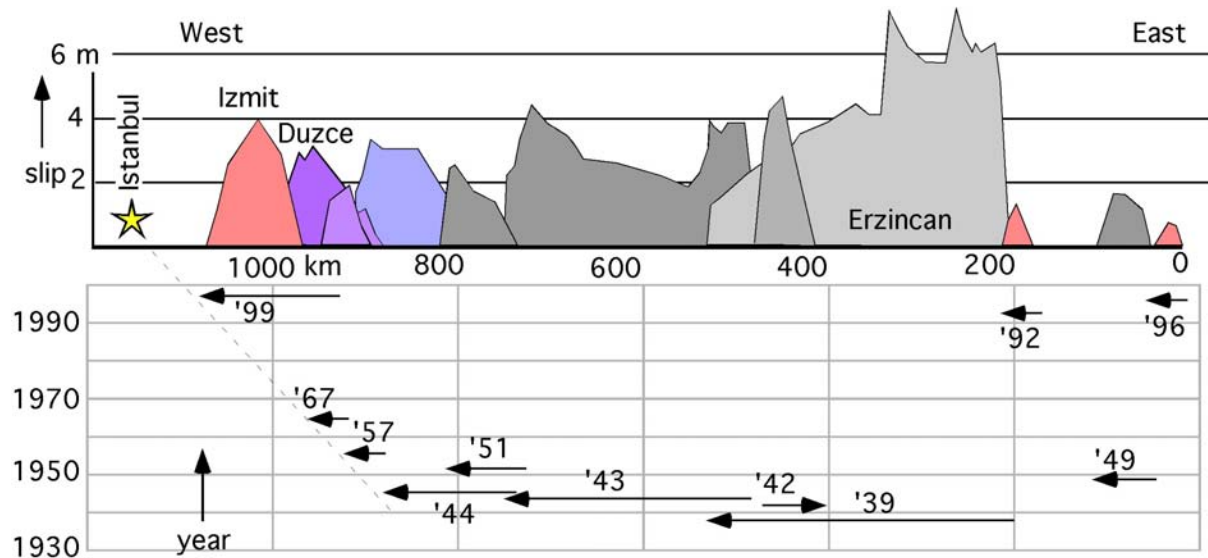


Figure 2.2: The most recent sequence of earthquakes started in 1939 and has propagated westward with occasional exceptions (figure after Stein et al. 1997). The central 640 km of the fault ruptured westward in the five years following 1939. Since 1944 there has been an approximately linear westwards propagation of the western tip of the rupture front of 200 km in 25 years (8 km/yr) which would suggest that the remaining segment of the fault near Istanbul (yellow star at km-1200) will be ready for rupture no later than 2025. Ruptures to the west are documented by Nalbant et al., 1998 and Hubert-Ferrari et al, 1999.

Notwithstanding the incompleteness of slip data collected during the past millennium it is possible to develop a view of the northern Anatolian fault as a system of contiguous segments that occasionally experience *sequences* of earthquakes (Ketin, 1969). Each sequence is hypothesized to permit the entire fault to slip. The 22-24 m of plate motion imposed on the northern Anatolian fault in the past 1000 years appears to have been released in three sequences of earthquakes that propagated along the entire fault at intervals of about 450 years (Figure 2.3). Four such sequences would be necessary if they each released a maximum of 6 m of slip as occurred in the 1939 Erzincan event, suggesting that the amount of slip may sometimes exceed 6 m. Earthquakes that occurred in 1754 and in 1784, at each end of the Anatolian fault (Figure 2.3) may signify the end of a sequence that included the 1668 earthquake, whose rupture was apparently longer than that associated with the 1939 M=7.8 earthquake. Empirical relationships between fault length and maximum slip suggest that the slip in this event might well have been in the range 7-9 m, which would partly or completely eliminate the apparent slip deficit in the past millennium. The observed tendency for the fault to rupture different combinations of contiguous fault segments suggests that co-seismic slip release may be locally somewhat irregular over many centuries.

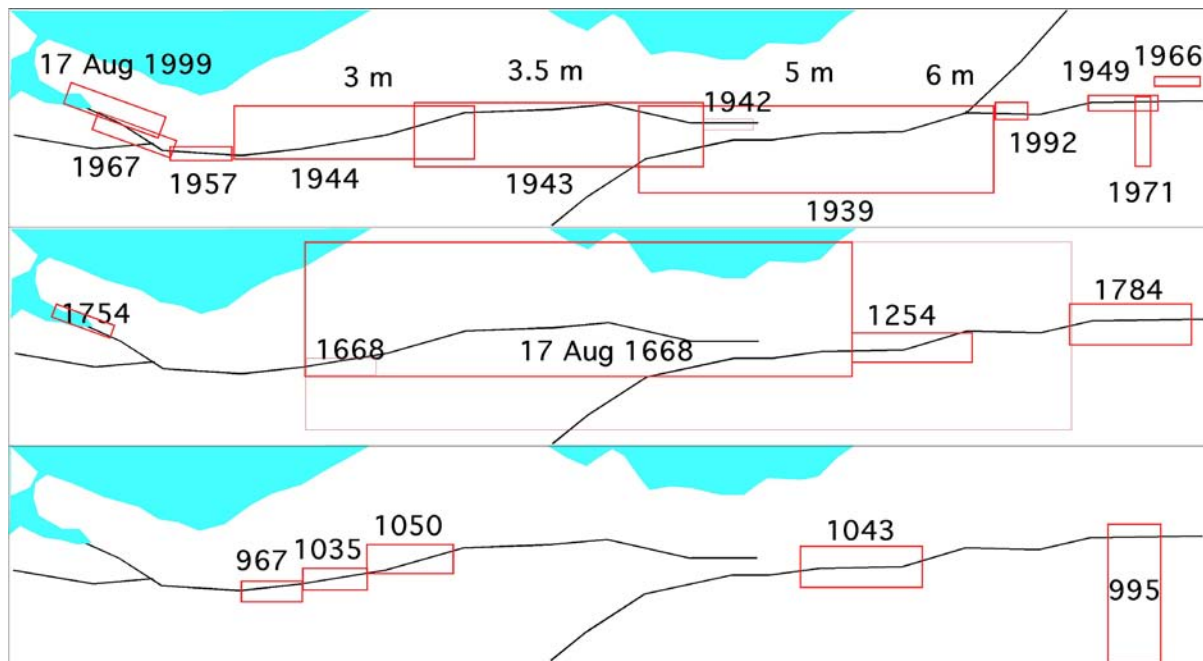


Figure 2.3: Historic ruptures (projection after Stein et al. 1977) with areas of boxes scaled to rupture length, The lower box shows the 967-1043 sequence, the middle box the 1668-1784 sequence. Geological and contemporary GPS measurements suggest that 22m of slip has accumulated on the fault since 937AD, yet if slip in pre-twentieth century events is assumed to be similar to that of the 1939-1999 sequence, only 12-15m is accounted for. Simple scaling laws applied to the August 17 1668 event suggest that it may have been associated with 7 to 9m of slip, thereby accounting for the apparent slip deficit on the fault since 967

Sufficient fault rupture data are available from the past 60 years to permit the stress distribution along the North Anatolian Fault to be analyzed in terms of a series of dislocations that propagate westward, with each successive earthquake modifying the stress field so as to encourage further slip on adjoining segments. The method used in these studies is to take the observed slip distribution in each rupture and to estimate the resulting stress near its ends. These stresses consist of two parts – a shear stress tending to make the fault slip and a dilatational stress that tends to clamp or release a fault depending on its sign (King et al. 1994). The sum of these two component stresses is known as the Coulomb failure stress. Stein et al. (1997) and Nalbant et al. (1998) have shown that during the 1939-1999 sequence of earthquakes on the North Anatolian Fault, most earthquakes gave rise to increased Coulomb failure stress on adjacent segments, which subsequently failed, producing the succeeding earthquake. Both of these studies identified the Izmit/Istanbul region as having a high probability for future rupture. Subsequent to the 1999 earthquake, Hubert-Ferrari et al. (1999) have calculated increased probabilities for rupture closer to Istanbul following the 1999 earthquakes. We note that the western tip of the westerly propagating rupture front (1944-1999) has migrated 200 km west in 25 years (8 km/yr) (Figure 2.2). This (admittedly simplistic) analysis would suggest that the remaining segment of the fault near Istanbul (at km 1200) will be ready for rupture no later than 2025. This is within the window of forecast for rupture indicated by Hubert-Ferrari et al. (1999). Several compilations of articles on the tectonics and seismology of the 1999 earthquakes are now published (USGS, 1999; Barka et al., 2000).

2.4 Teleseismic Observations of the 17 August 1999 Earthquake

The 17 August 1999 earthquake was sufficiently large to be well observed on seismographs throughout the world. These instruments are operated by a wide variety of public and private organizations, and the dissemination and interpretation of the data produced are coordinated by a number of national and international agencies. Two Turkish agencies operate ‘weak-motion’ (continuously-recording) instruments in the Marmara Sea area – Kandilli Observatory and Earthquake Research Institute of Bosphorus University (KOERI), and the Earthquake Research Department of the General Directorate of Disaster Affairs (ERD). Several foreign agencies were operating temporarily-installed seismographic instruments in the general area on 17th August. The locations of all these instruments are shown in Figure 2.4. There is no formal mechanism for co-ordinating the interpretation of the data from these networks. Each agency undertakes its own analysis independently, using such data sources as are available to it.

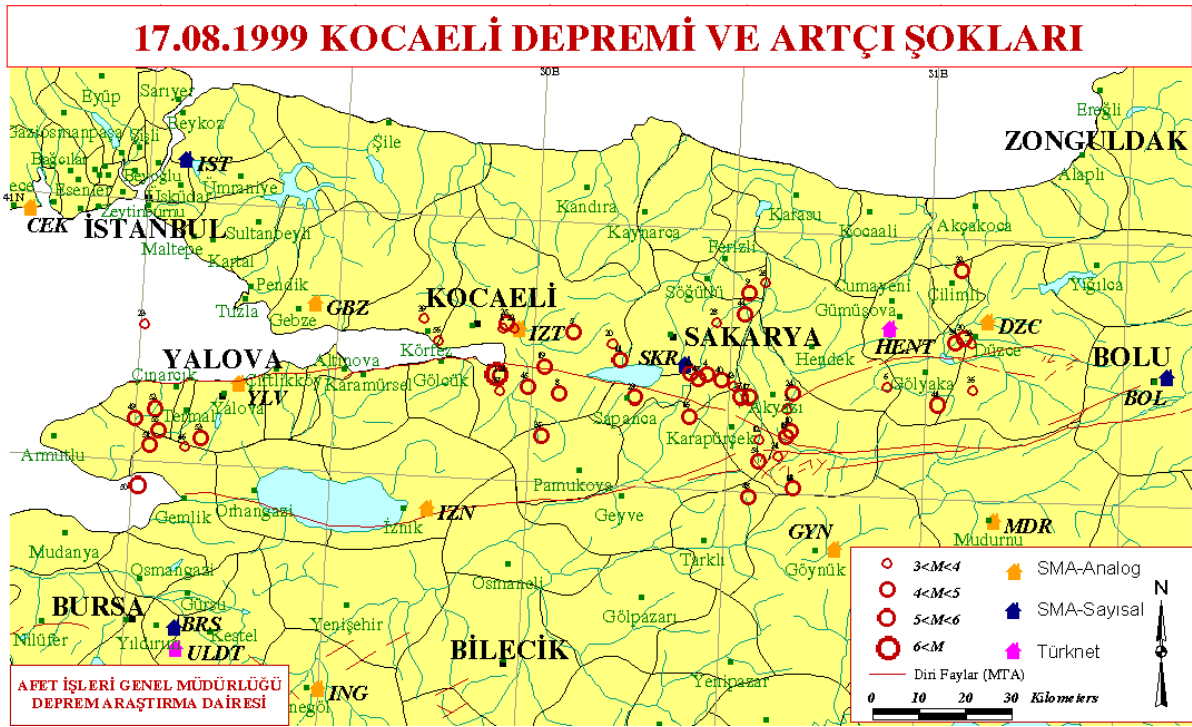


Figure 2.4 Locations of instruments of terrestrial and teleseismic networks and location of aftershocks

In practice, KOERI has established itself as the principal reporting agency for this region. The methods adopted at KOERI have been established over some 25 years, but are designed for responding to the kind of public inquiries that the agency routinely meets. These typically involve earthquakes in the magnitude range M_L 3 to 6, and most larger earthquakes have occurred at some distance from the Marmara Sea. The methods that KOERI have developed are appropriate to this application and to the robust but limited short-period instrumentation available to that institution. A ‘duration magnitude’ M_D is calculated from the recorded traces and is employed as a proxy for ‘Richter local magnitude’ M_L . In practice, few seismological agencies currently determine M_L directly, and proxies of one sort or another are almost universally employed. ‘Duration magnitude’ is simple and robust, but is not widely used, because a large number of constants must be empirically determined and these are valid only within a specific range of magnitudes and distances. The calibrating database on which KOERI’s coefficients are based does not include any large earthquakes in the immediate vicinity of the observing network. As a result, the duration magnitude calculated and announced by KOERI, $M_D=6.8$, proved to be a poor proxy for those measures of magnitude (M_L and M_S) which are typically reported as ‘Richter magnitude’ by the media. This low reported value for the magnitude may have been a factor in the relatively slow response of the Turkish government.

Arguably, the ERD network fared even less well, because the receiving mast for its telemetry system, sited in Adapazari, collapsed during the earthquake, and data from its weak-motion system was only partly recovered when the system was restored to operation.

Because earthquake energy is radiated with varying strength in different directions, determinations of magnitude at individual stations or at distant groups of stations always show a degree of variation, and for that reason, the international co-ordinating agencies try to gather and average determinations from a widely separated sample of stations. In the case of the August 17th earthquake, individual agencies reported unusually wide variations in magnitude. The US Geological Survey (the most widely quoted source of rapidly integrated earthquake information) initially reported a surface-wave magnitude M_S of 7.8. Although this has not been withdrawn, it was superseded within a few days by a ‘moment magnitude’ determination, M_W , of 7.4. Moment magnitude is widely regarded as the most robust available method of measuring the size of an earthquake, because it is not dependent on details of the equipment used to record the event. The USGS M_W value of 7.4 has been universally adopted as the agreed best estimate of the size of the earthquake.

Using recordings from high-quality ‘broadband’ seismic stations worldwide, it is possible to determine the history of slip on the earthquake fault in some detail. Several researchers have conducted the necessary calculations, and various models are available. Of particular interest is the one derived by Pinar of KOERI (Gulen, Pinar et al., 2002), using Kikuchi’s method (Kikuchi and Kanamori, 1991). Pinar’s model shares many characteristics with that of Yagi & Kikuchi (Yagi and Kikuchi, 1999) but the input data extend for a longer time

period and it is therefore believed to model slip at later times somewhat better. It suggests that following the initiation of rupture, maximum slip occurred during the first 20 seconds in the region immediately above the epicentre. Teleseismic observations suggest that the rupture then propagated eastward in a series of subevents, first due east towards Akyazi and then ENE towards Duzce. Between 60 and 100 seconds after the start of rupture, a further series of subevents occurred to the west of the initial rupture point. The major moment release corresponds to a region between Golcuk and lake Sapanca, for which offset slip of 4.1 and 5.3 metres, respectively, are computed with this model, resulting in good agreement with on site observations. The precise geographic locations at which each of these events occurred is tied through this model to the calculated position of the hypocentre – hence the importance of determining this as accurately as possible.

2.5 Surface Slip during the 17 August 1999 Earthquake.

Figure 2.5 shows surface fractures mapped by a USGS team in the several days following the earthquake. Although the EEFIT mission arrived too late (20 days after the rupture) to measure the offsets of roads because these had been repaired and resurfaced, in several cases offsets could be measured precisely from the relative displacements of long walls, fences, river banks or rows of trees crossing the fault (Table 2.1 in Appendix 2A, and Figure 2.5). Time did not permit the entire fault to be visited eastward by the EEFIT members. The rupture consisted of a series of en-echelon fractures mostly in unconsolidated materials. Whereas the central 30 km of the fault slipped 2-4 m the easternmost end of the fault had an average slip of approximately 0.8 m with maximum slip of 1.6 m. This NE trending rupture overlaps the Mudurnu Valley rupture of 1967 (Ambraseys and Zatopec 1969), which ruptured south of the fracture that developed in 1999. A damaging earthquake was previously recorded in the Adapazari region in 1943 (Pamir et al. 1943).

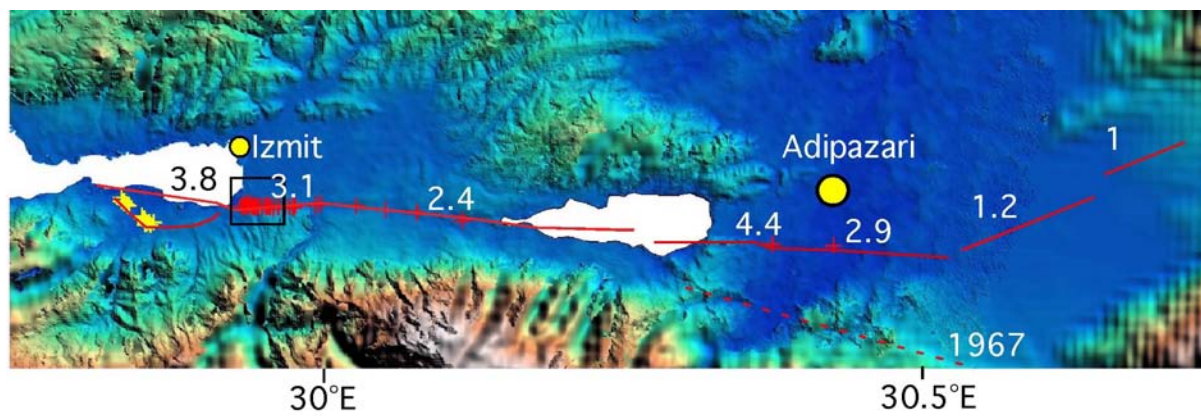


Figure 2.5: 100-km-long ERS1/2 composite SAR image in which gaps caused by steep slopes or heavy vegetation (resulting in incoherence) have been filled with ETOPO30 DTED (by Eric Fielding). Red crosses indicate EEFIT-measured fault offsets located using GPS and taped to 0.1 m accuracy. Yellow crosses indicate measurements across the western margin of a slump scarp that drowned the coast at the SE corner of Izmit Bay near Gölcük (Figure 2.7) The length of the fault inspected by the EEFIT team was 41 km. The total length of the rupture is approximately 100 km. The November 12 Düzce earthquake propagated 40 km eastward from the eastern edge of this map with maximum slip of ≈ 4 m. Black square shows location of Figure 2.6.

The mean slip in the earthquake has been estimated using GPS data to be 2.9m although a more complex distribution of slip is likely to be proposed as more data become available (Reilinger & Burgmann, personal communication 1999). The mean slip observed at surface locations is approximately 3m, with a maximum slip of 4.4m. In Figure 2.5 are shown details of the variation in observed slip as a function of distance over a 12km length of the fault east of Izmit Bay. Overlapping, en echelon, fractures show variable slip along strike and as a result, all observations underestimate the total slip to varying degrees. Intervening segments of the fault are rotated in ways that cannot be estimated without precise geodetic control.

In several locations high voltage power lines cross the fault and these are sufficiently large in scale to permit fault offsets to be measured without errors arising from local deformation near the fault zone. The success of these measurements depends partly on the availability of accurate engineering maps of the original pylon locations; we were unable to determine whether these were available at the time of our field study. At $40^{\circ}43'07''N$, $29^{\circ}58'14''E$ a pylon had been buckled and pulled toward the fault, and the adjacent pylon at $40^{\circ}43'10''N$ and $29^{\circ}58'02''E$ had been pulled and bent in the other direction by a measured 3.3m offset of the

fault. This 290m span crosses the fault at an oblique angle of 20°, implying that the distance between the pylons had been increased by at least 3.1m. The line appeared to be functioning, even though the normally vertical insulator suspension had been pulled close to horizontal toward the fault, and despite the very high stress in the cables, evident from the abnormally low catenary sag in both the span which crossed the fault and in those adjacent.

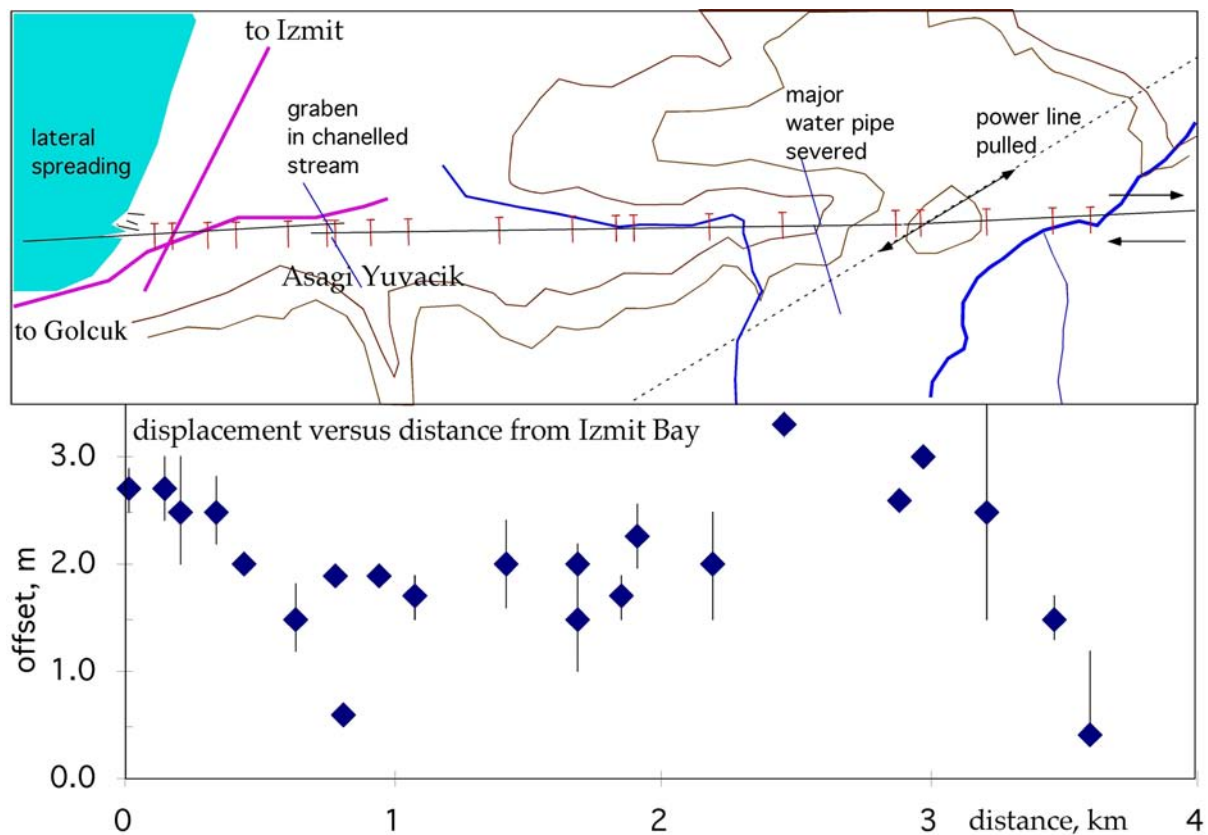


Figure 2.6: Map and slip distribution of rupture offsets for 4 km of the fault near Izmit.

The fault continues an unknown distance beneath Izmit Bay having been recorded to cross the Naval Base at Gölçük; colleagues at Kandilli Observatory measured 2.9m offset at locations within the base, and 2.95m offset at the boundary wall of the base on Amiral Kayacan Caddesi, a civilian street to the west of the base. During the EEFIT field mission, we undertook a careful inspection of the triangular-shaped Hersek peninsula, north of Altinova, but found no evidence for slip (although permission was not granted to enter the small military encampment that occupies the extreme northern end of the peninsula). A 0.6m concrete water pipe, consisting of segmented concrete culvert sections, heads north along the entire peninsula. We observed two leaks in the pipe, but these were not associated with any nearby evidence for offset and were presumably caused by shaking of the low lying ground in the peninsula. Numerous examples of liquefaction were observed together with lateral spreading and mud volcanoes near the west coast of the Peninsula while locals reported the occurrence of a tsunami at the northern tip. One local account indicated a 200-250m recession of the sea followed by a 2m high surge 20m onto land. Evidence for such a surge was located in a preserved sea-weed strand line crossing the road to the pier at on the northern part of the peninsula. A ductile steel submarine LPG pipe crosses the Bay and required a repair near a gate valve at 40°43'26.4"N 29°29'49.8"E . The caretaker on site informed the EEFIT team that the pipe had not fractured, and this was subsequently confirmed with the pipeline operator by colleagues at Kandilli Observatory. This suggests that if the fault has any surface expression this far west of Golcuk, it is associated with a low level (<1 m) of slip. Measurement of the line of this pipe using an inspection "pig" equipped with a gyrocompass might quantify this weak constraint on fault slip.

The EEFIT mission observed small-scale ground rupture apparently associated with local slumping, further east at Aydin. More extensive rupture and "normal faulting" has been reported from the nearby aerodrome (Kalafat, personal communication, 2000) and it has been suggested that these features may be surface faulting directly associated with the 17 August earthquake. At this stage, it is not clear whether these features are directly related to fault slip.

Further analysis of GPS data which has become available since the EEFIT field mission suggests that the fault did experience some slip in the vicinity and to the west of the Hersek peninsula. Reilinger's interim results

(2000, personal communication) yield an average slip at depth in this part of the fault of about 1m. This is not necessarily inconsistent with our field observations.

Synthetic aperture radar (SAR) imagery and GPS measurements constraint the westernmost limit of rupture. These images show a rapidly decaying strainfield to 20 km west of Izmit and a fairly-long wavelength decay in the strain field further west. This suggests that the fault does not extend very much west of 29.6°E

2.6 Secondary Effects -Tsunami, Slumping, Compaction and Liquefaction

In this section some observations made by the EEFIT team about secondary effects are discussed and placed in the context of observations by other groups.

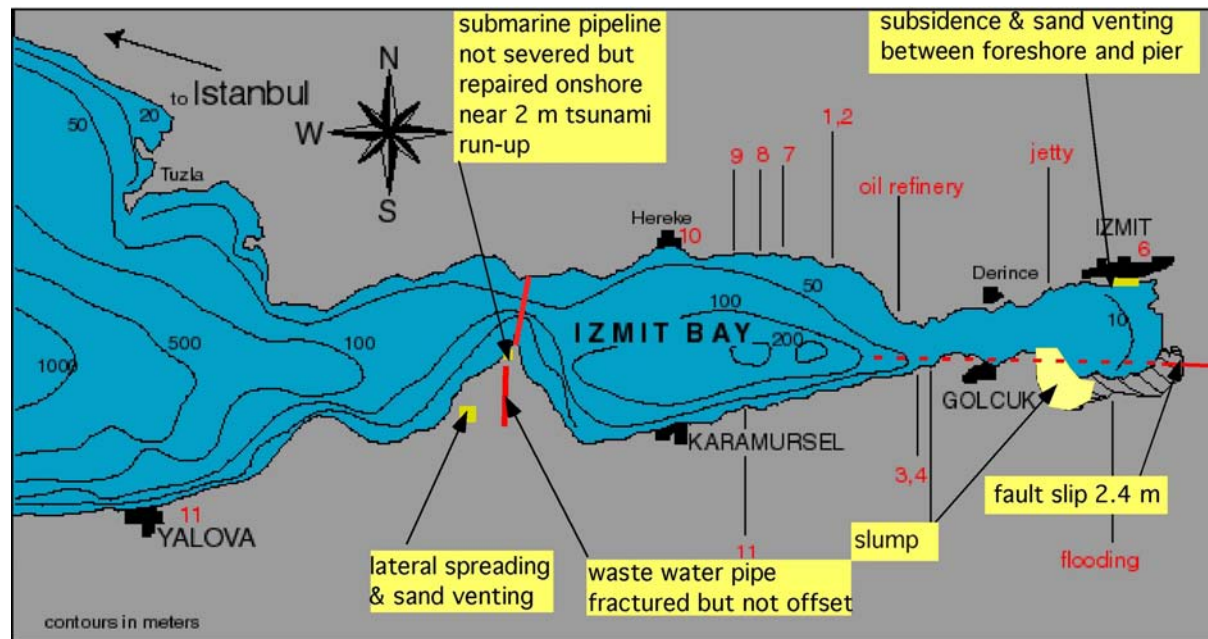


Figure 2.7: Sites around Izmit Bay visited by the USCSB Tsunami team 4 days after the earthquake (red numbering) and by the EEFIT geology team (yellow boxes).)

2.6.1 Tsunami

There are numerous accounts of a tsunami having been generated during the main shock. There are also several anecdotal accounts that the sea was unusually turbulent before the mainshock with waves exceeding a metre in height preventing local fishermen from seeing the shore the previous afternoon. These accounts cannot be verified because there are apparently no tide gauges anywhere in the region, but we did find some evidence for a sea wave having swept about 20m onshore at 29.5E (location 40°43'26.4" N 29°29'49.8"E). The run-up height here was about 2m, judging from the strand-line left by seaweed on the path leading to the jetty. Several contacts reported a ship's captain indicating that the sea retreated 200-250m before rushing inland, but we suspect that these reports refer to a single originating account, possibly placed in widespread circulation through the media, since most of the population was asleep at the time of the earthquake. A ship was driven ashore by the force of the wave near Golcuk, near to where one of the reports of a recession is known to have originated. We were unable to gather direct information on the height of the tsunami elsewhere. (See the USC Santa Barbara Tsunami web page)

2.6.2 Slumping

The eastward 3 m motion of the NE shore and floor of Izmit Bay could have generated the tsunami but it is almost certain that the slump of the SE shore contributed to its generation. Figure 6 is from the University of California, Santa Barbara, (USCSB) tsunami web page, which shows the approximate area of slumping. We measured the western 3.5 km of the slump to have sunk 2m with subsidence reducing eastward short of the area indicated by the USC map (Table 2.2 in Appendix 2A). The USC map is misleading in respect to subsidence at the extreme SE corner of Izmit Bay - and an accurate map of the feature has been published by Lettis et al.

(2000). The surface area of the slump is extensive and shows no fissuring where we could see it exposed. Trees and buildings showed no tilt over most of its surface. This suggests that the slump slip surface is planar or perhaps only weakly curved. Certainly back tilting of the surface of the slump was undetectable without instruments. A possibility exists that the slump represents the surface manifestation of a deep seated pull-apart feature related to a right-stepping offset of the Anatolian fault here.

There is abundant evidence to suggest that the southern edge of the slump was a reactivated feature. Not only were there several indications along its length for a gentle topographic step down to the north in the former ground surface, but we observed it to represent the junction between several cultural features. In one location, for example, it represented a boundary between apple/pear orchard and timber forest. In another it represented the boundary between pasture and orchard. Several houses and a mosque had been constructed on the head of the scarp resulting in their complete destruction. Another house that had been constructed across a secondary scarp north of the mosque tilted during the mainshock only to collapse in a strong aftershock one week later.

2.6.3 Sand venting and liquefaction

The EEFIT team observed these phenomena in two locations around Izmit Bay but no doubt there are many others. Water continued to issue out of saturated ground roughly 1 m above sea level at 40°42'31.9N, 29°28'26.7 E for a day after the earthquake bringing with it sand and silt (0.2-2 mm grain size). Three weeks after the earthquake the soil surface near these vents was still significantly wetter than the surrounding soils. The ground was fissured heavily parallel to a west-facing inlet of the sea with lateral spreading fissures of 12-20 cm width and 20-40 m length abundant. Water and sand had vented through some of these fissures widening them and channeling flow toward the sea in places. An empty 10m wide, 8m deep heavily reinforced cylinder (1m wall thickness at surface) under construction for waste water processing had apparently been extruded about 20 cm at this location. Sand venting had occurred around its edges.

Sand venting also occurred, although less extensively, in the NE corner of Izmit Bay between the former shoreline and a concrete pile pier. Lateral spreading was evident at the eastern approach in this presumed fill zone (40°45'35" N, 29°55'57" E) associated with maximum subsidence of about 1.5 m. Subsidence of less than 30cm with sand venting was present on 10-20 m long fissures some 200m to the west (at 40°45'37" N, 29°55'18"E). The subsidence had affected the shoreline road support soils in this region with sand vented through pavement cracks. A large concrete structure crossing beneath the road had not suffered this subsidence presumably indicating that its effects are not deeply seated. The result was that the road, though not itself ruptured had a ramp and vertical step of 20-30 cm on each side of the concrete substructure, necessitating the traffic to slow considerably in its vicinity.

Lateral spreading was observed to be associated with the surface fissures evident in many places in Adapazari. According to a local observer in one location a 4 storey concrete dwelling tilted into a fissure in the several minutes following the mainshock. The cracks at this location consisted of two north-south open fissures separated by approximately 10 m with two parallel compression features in the road surface approximately 20 m on each side of these tension gashes. Water had evidently been ejected from the fissure though not in any great quantity and without silt or sand. The water table was less than 1 m below the surface when we visited. It is hypothesized that the fractures acted as strain concentration features with opening and closing displacements pounding their edges to cause the observed compression fractures (Figure 2.8).

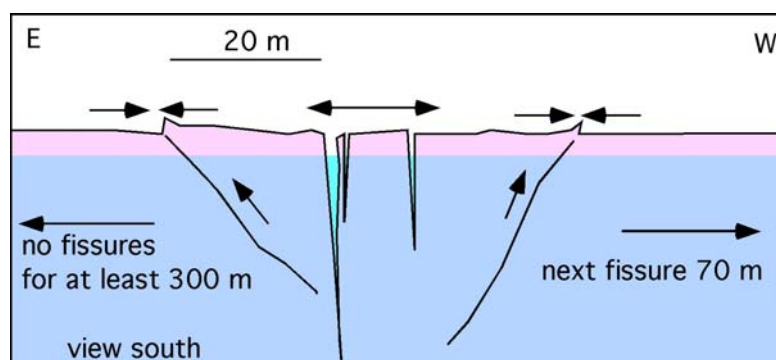


Figure 2.8: Inferred cross-section through fissure approximately 1 km north of Adapazari Railway Station. The fissure shows compression fractures near edges of the tension fissures suggestive of pounding of the tension gashes during strong ground shaking. The water table is within 1 m of the surface.

Fracture spacing to the west of the fracture was irregular but averaged 70-100 m for a distance of 500 m. Beyond this distance and to the other side of this lateral spreading feature we found no evidence for fractures, and although they are repeated in other parts of the city, we were unable to map their distribution in the time available to the EEFIT mission. A similar large fissure was found in a cooking oil factory to the NE of the previously described fissure. At this location the water table was again within 1m of the surface although it was reported to have dropped by ~50 cm in the week preceding our visit. There was clear evidence for sand venting through parts of this fissure. Factory buildings were severely tilted indicating a loss of shear strength in the soils underlying the structures and slabs in the compound.

2.6.4 Earthquake lights

Several accounts of a luminous red glow in the sky were reported in the newspapers. The association of a luminous glow in the night-time sky at the time of an earthquake is not a new phenomenon and though common is rarely recorded instrumentally (Derr, 1973; Johnston, 1991). There is considerable dispute about the origin of these lights. Some attribute the phenomenon to piezoelectric discharge caused by coseismic stressing, while others link it to the emission of charged ions by gas venting from the earth's surface. In the 1999 Izmit earthquake the phenomenon was apparently recorded by surveillance cameras at the BP oil refinery and shown several times on television. Although we have not seen it we were told that this footage is available from local TV channels (ATV and Kanal D). The lights apparently glow for a 1-2 seconds before shaking commences at the camera suggesting that they may record coseismic phenomena near the remote rupture that precedes the arrival of seismic waves.

2.7 References

Ambraseys, N. N. and A. Zatopek, The Mudurnu Valley, west Anatolia earthquake of 22 July 1967, *Bull. Seism. Soc. Am.*, 59, 521-589, 1969.

Ambraseys, N. N. and C. Finkel, Long-term seismicity of Istanbul and of the Marmara Sea region, *Terra Nova*, 3, 527-539, 1991.

Ambraseys, N. N. and C. Finkel, The Anatolian earthquake of 17 August 1668, In . W. H. K. Lee, H. Meyers, and K. Shimisaki, (Eds), *Historical Seismograms and earthquakes of the world (173-180)* New York, Academic Press, 1988.

Ambraseys, N. N. and C. Finkel, The seismicity of Turkey and Adjacent Areas: a historical review, 1500-1800. Istanbul: Muhittin Salih EREN, 1995.

Ambraseys, N. N., Some characteristics of the North Anatolian Fault Zone, *Tectonophysics*, 9, 143-165 (1970)

Ambraseys, N. N., Value of Historical Records of Earthquakes, *Nature*, 232, 375, 1971.

Barka, A. A. and Eyidogan, The Erzincan earthquake of 13 march 1992 in eastern Turkey, *Terra Nova*, 5, 190-194, 1993.

Barka, A. A., Slip distribution along the north Anatolian Fault associated with the large earthquakes of the period 1939-1967, *Bull. Seismol. Soc. Am.*, 86, 1238-1254, 1996.

Barka, A. A., The North Anatolian Fault Zone, *Ann. Tectonicae. Suppl. VI*, 164-195, 1992.

Barka, A., O. Kozaci, S. Akyuz, E. Altunel, ed *The 1999 Izmit and Duzce earthquakes: Preliminary results.* Istanbul Technical University 2000. pp 349.

Derr, J. Earthquake sounds, *Bull. Seism. Soc. Am.*, 63, 2177-2187 (1973).

Gulen, L., A. Pinar, D. Kalafat, N. Ozel, G. Horasan, M. Yilmazer, A. M. Isikara, Surface fault breaks, aftershock distribution, and rupture process of the 17 August Izmit, Turkey, *Earthquake, Bull. Seism. Soc. Am.*, 92, pp. 230-244, 2002

Hubert-Ferrari, A., A. Barka, S. S. Nalbant, E. Jacques, B. Meyer, R. Armijo, P. Tapponier, and G. C. P. King, Seismic Hazard in the Sea of Marmara following the 17 August 1999 earthquake, submitted to *Nature* Aug 1999.

Johnston, A. C., Light from seismic waves, *Nature(Lond)* 354, 361, 1991

- Ketin, I, On the strike-slip movement of North Anatolia (in German), *Bull. Miner. Res. Explor. Inst. Turkey*, 72, 1-28, 1969.
- King, G.C. P., R. S. Stein, and J. Lin., Static stress changes and the triggering of earthquakes, *Bull. Seism. Soc. Am.*, 84, 935-953, 1944 .
- Kikuchi, M., and H. Kanamori, Inversion of complex body waves-III, *Bull. Seismol. Soc. Am.*, 81, 2335, 1991.
- Lettis, W., J. Bachhuber, A. Barka, W. Witter and C. Brankman, Surface Fault Rupture and Segmentation during the Kocaeli Earthquake in Barka, A., O. Kozaci, S. Akyuz, E. Altunel, ed The 1999 Izmit and Duzce earthquakes: Preliminary results. Istanbul Technical University 2000. pp 349.
- Lettis, W., J. Bachhuber, A. Barka, C. Brankman, P. Sommerville and R. Witter, 1999 Kocaeli, Turkey Reconnaissance Report, Chapter 1- Geology and Seismology, Earthquake Spectra, Supplement A to Volume 16, December 2000.
- Nalbant, S. S. A. Hubert, and G. C. P. King, Stress Coupling between earthquakes in Northwest Turkey and the north Aegean Sea, *J. Geophys Res.*, 103, 24469-24486, 1998.
- Okumura, K., T Yoshioka, I. Kucsu, H. Kayanne, and Y. Suzuki [1990] Activity of the North Anatolian Fault during these two Millennia on the Surface Faults of 1944 Earthquake Based on Trenching and Microtopographic Studies. *EOS*, vol. 71, no. 43 supplement, p.1560.
- Okumura, K., T. Yoshioka, I. Kucsu, T. Nakamura, and Y. Suzuki [1993] Recent Surface Faulting Along the North Anatolian Fault East of Erzincan Basin, Turkey--a Trenching Survey. *EOS*, vol. 74, no. 43 supplement, p.545.
- Okumura, K., T. Yoshoka and I. Kucsu [1993] Surface Faulting on the North Anatolian Fault in these two Millennia. U.S. Geological Survey Open-file Report, 94-568, 143-144.
- Pamir, H., F. Baykal, and I. Ketin, A Geological report on the Adapazari Hendek earthquake (20.06.1943) Report Earthquake Research Institute, Ankara, Turkey (in Turkish). 1943.
- Reilinger, R. E., S. C. McClusky, M. B. Oral, R. W. King, M. N. Toksoz, A. A. Barka, I. Kinik, O. Lenk., and I. Sanli, Global Positioning System measurements of the present day crustal movements in the Arabia-Africa-Eurasia plate collision zone, *J. Geophys. Res.*, 102, 9983-9999, 1997.
- Stein, R. S. A. A. Barka, and J. H. Dieterich, Progressive failure on the North Anatolian fault since 1939 by earthquake stress triggering, *Geophys. J. Int*, 128, 594-604, 1997.
- Straub, C., H. G. Khale, and C. Schindler, GPS and geological estimates of tectonic activity in the Marmara Sea area. *J. Geophys. Res.*, 102, 28587-27601, 1997.
- U. S. Geological Survey Implications for Earthquake Risk Reduction in the United States from the Kocaeli, Turkey, Earthquake of August 17, 1999. US GS Survey Circular 1193, 1999.
- Yagi, Y. and M. Kikuchi, Source rupture process of the Kocaeli, Turkey, earthquake of August 17, 1999, obtained by joint inversion of near-field data and teleseismic data, *Geophysical Research Letters*

APPENDIX 2A

Table 2.1 Offsets measured 10-12 Sept during EEFIT mission (sub-areal exposure of fault only).

slip,m	± m	lat. N	long. E	Feature at GPS position ±30 m.
2.7	0.2	40.7211	29.9372	edge of Bay. Oblique concrete path offset
2.7	0.3	40.7208	29.9386	road repair on Izmit road fixed c. 2 Sept. No afterslip 12 Sept
2.5	0.5	40.7233	29.9406	workshop cut by fault
2.5	0.3	40.7211	29.9411	road repair on road going east. No afterslip 12 Sept
2.0	0.1	40.7214	29.9425	average of both edges of offset wall
1.5	0.3	40.7219	29.945	masonry shed cut by fault and rotated
1.9	0.1	40.7211	29.9464	N. offset culvert (river edge) with step up downstream of 50 cm
0.6	0.1	40.7203	29.9464	S offset culvert (river edge) with water fall into sag graben
1.9	0.1	40.7206	29.9481	two E. perimeter walls of destroyed school
1.7	0.2	40.7211	29.95	3 tree alignments offset by fault
2.0	0.4	40.7208	29.9539	trace lost near culvert by road repairs.
2.0	0.2	40.7211	29.9572	offset fence
1.5	0.5	40.7217	29.9575	ditch with pipes offset
1.7	0.2	40.7211	29.9592	fence posts offset and fault bearing 279-270
2.3	0.3	40.7206	29.9597	moletrack fence offset
2.0	0.5	40.7206	29.9631	offsets stream and large trees. Poor estimate.
3.3	0.1	40.7208	29.9664	offset barbed wire fence with cows
2.6	0.1	40.7214	29.9717	offset masonry wall next to house with nice man and his children
3.0	0.1	40.7208	29.9725	offset cast concrete wall in front of row of collapsed 5 storey buildings.
2.5	1	40.7211	29.9756	offset in curved barbed wire fence
1.5	0.2	40.7214	29.9786	offset grassy wheel track in mud
0.4	0.8	40.7219	29.9806	Two small offsets and waterfall in stream fronting forested hill
1.8	0.2	40.7231	29.9972	offset in trees lineaments shown to us by villagers. (near bridge)
1.2	0.2	40.7236	30.0008	road near woodyard
2.0	0.2	40.7236	30.0308	offset in steep bank of stream covered with brambles
2.9	0.1	40.7211	30.0547	average of 6 tree offsets (encountered Potsdam group)
1.8	0.1	40.7206	30.0806	house slab offset near drain
2.0	0.5	40.7164	30.1186	timber mill wall
2.0	0.5	40.7081	30.3742	bridge parapet offset on motorway
2.0	0.5	40.7081	30.4239	Toyota plant entrance

Table 2.2 Locations of head of slump in SE corner of Izmit Bay

#	North lat	East long	offset m	km	m
1	40.72369	29.8375	2	0.40635	1
2	40.72136	29.8377	2	0.50976	1
3	40.72106	29.8383	1.5	0.57444	1.5
4	40.72147	29.84	1	0.69781	2
5	40.71986	29.8403	2	0.7835	2
6	40.71942	29.8419	2	0.9298	2
7	40.71917	29.8433	2	1.05957	2
8	40.71864	29.8437	2	1.1094	2
9	40.71206	29.8546	2	2.26336	2
10	40.71111	29.8551	1.7	2.34267	1.7
11	40.71033	29.8574	2	2.56399	2
12	40.70894	29.8582	1	2.68309	1
13	40.70722	29.8583	1.5	2.75906	1.5
14	40.70878	29.8585	1.5	2.71711	1.5
15	40.70736	29.8595	1.5	2.85346	1.5
16	40.70861	29.8611	0.5	2.93875	0.5
17	40.70694	29.8622	0.7	3.09372	0.7
18	40.70883	29.865	0.5	3.2524	0.5

3 Strong-Motion and Macro-Seismic Intensity

Matthew Free,
Ove Arup & Partners Hong Kong Ltd

Dina D'Ayala,
Bath University

3.1 Introduction

During the 17 August 1999 Kocaeli earthquake, strong ground shaking caused widespread damage and destruction; more than 18,000 structures were destroyed, more than 17,000 thousand people lost their lives in collapsed buildings and over 600,000 people were made homeless.

Given the notorious activity of the North Anatolian Fault a relatively large number of ground motion arrays and station had been installed along its length and strong ground motions were recorded at a relatively large number of sites around the region by several organisations. This chapter provides a summary of the strong-motion data, describes the locations at which the strong motion recordings were made and provides a brief discussion of some of the characteristics of the strong-motion records. The last section of this chapter presents a discussion on the correlation between the records and macroseismic effects to neighbouring structures.

3.2 Strong Ground Motion Stations

The major network of strong motion instruments in the region is the National Strong Motion Network (NSMN) operated by the Earthquake Research Department, Directorate for Disaster Affairs of the Ministry of Public Works and Settlement (ERD) with 22 stations in Istanbul and the Aegean Region, while smaller networks are operated by four other institutions:

- Kandilli Observatory and Earthquake Research Institute (KOERI), 14 instruments.
- Istanbul Technical University (ITU).
- Public Water Works (DSI).
- Middle East Technical University (METU).

A summary of the known details of the stations is provided in Table 3A.1 in Appendix 3A.

Figure 3.1 shows the location of some of these instruments. Of the total number of instrument six were placed in the vicinity of the rupture caused by the Kocaeli earthquake, and two in the epicentral area. Detailed information with regard to the ground conditions of most stations has not been documented at this stage although a number of researchers have summarised their field observations (Anderson *et al.*, 2000; Beyen *et al.*, 2000).

Members of EEFIT visited five of the strong-motion stations in the region. The visits included photographing and describing the instrument housing, checking the instrument type and orientation, making an assessment of the ground conditions or other relevant features and checking the location of the instrument using a hand-held global positioning system (GPS) receiver. The information obtained from these visits was summarised on Strong-Motion Instrument Summary Sheets (see Appendix 3B). Data on damage for the buildings in the immediate vicinity of the instruments and in nearby urban settlements was also collected with an aim to correlate macroseismic observation with instrumental records; this is reported in section 3.7.2 and Table 3.3. While no detailed information on the ground conditions at the strong-motion stations was available an assessment of the ground conditions was made based on reference to geological maps and a site walk-over carried out by the geologist members of the team.

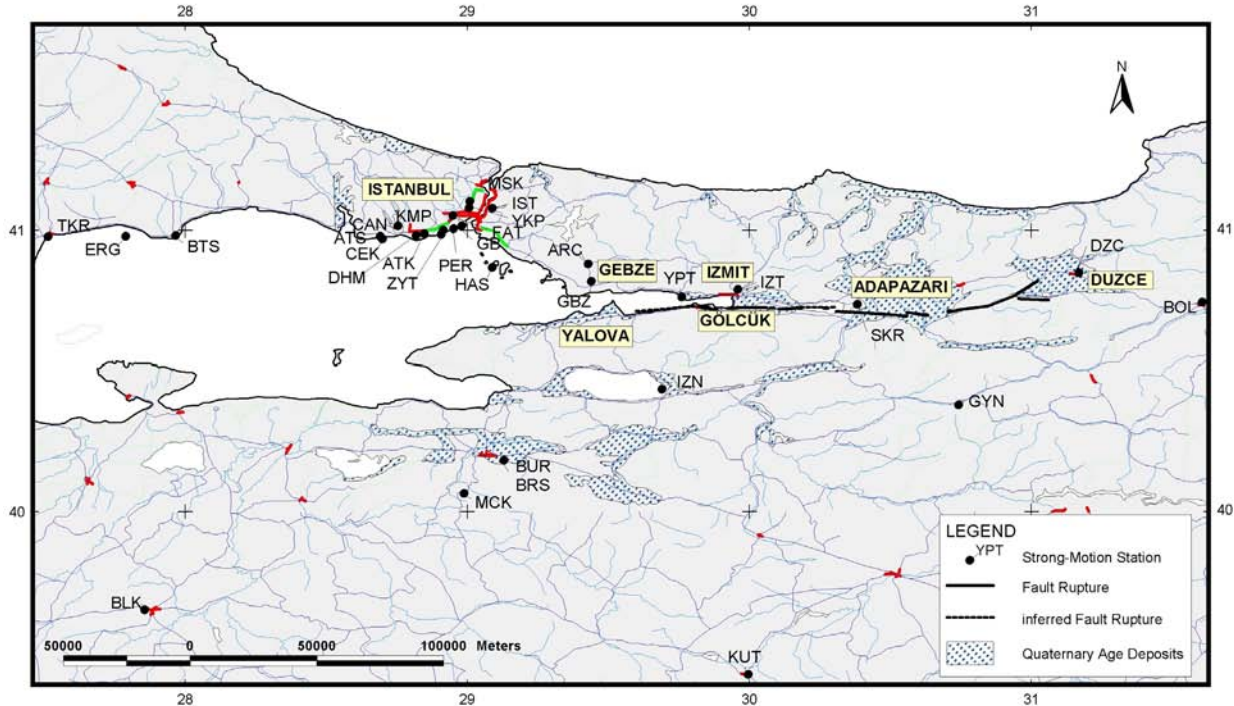


Figure 3.1: Location of the instrumentation and peak ground acceleration recorded. Indicative fault rupture line

The major finding of these inspections can be summarised as follows:

- Of the five instruments visited three, Gebze (GBZ), Adapazari (SKR) and Duzce (DZC), belong to the General directorate for Disaster Affairs, while Arcelik (ARC) and Yarimca (YPT) are operated by Bogazici University. The instruments are either SMA-1 or GRS-16 types;
- Only the SKR station in Adapazari is regarded as truly free field as it was not located within a major building being sheltered by a small hut. This station is located on the side of a hill with a shallow thickness of soil over rock. The ground conditions are rather different to those found in the city centre.
- The YPT station was the closest to the estimated epicentre in Golcuk. The instrument is located on a raised level ground floor of a three storey office block within the Yarimca Petkim plant compound. It is possible that the accelerogram recorded here has been considerably influenced by the structural response to the earthquake of the host building. It was also noted at the time of the visit to the station that the instrument was not oriented N-S but approximately 330° in the longitudinal direction.
- The other three instruments were hosted either in lower ground floor or ground floor of differing size buildings. The building and foundation may have affected these records where ground conditions are relatively soft.

3.3 Strong Ground Motion Records

A total of 38 strong motion records of ground response were obtained during the 17 August 1999 Kocaeli earthquake. Of the 38 ground response records, 24 were obtained by the Earthquake Research Department of the General Directorate of Disaster Affairs (ERD), 10 were obtained by Kandilli Observatory and Earthquake Research Institute (KOERI) and 4 were obtained by Istanbul Technical University (ITU). The acceleration records (longitudinal, transverse and vertical) from 36 strong-motion stations that recorded at least one component (longitudinal, transverse or vertical) are provided in Appendix 3A table 3A.2.

In addition to the main shock records, immediately after the 17 August earthquake, teams from the United States, Germany, France and Japan deployed portable instruments to record aftershocks in and around damaged towns and the epicentral region. Some of the aftershock data has been used to derive spectral attenuation laws (Lang et al. 2000). Furthermore three sets of structural response records were obtained from the 17 August 1999 earthquake. KOERI obtained records from the structural response arrays at the Suleymaniye Mosque and Aya Sofya Museum in Istanbul. Information on these arrays is described by Birgoren and Golyilmaz (1999). It is also understood that METU obtained records from an instrumented six-storey building in Gerece. Celebi et al. (1999) reported that DSI did not obtain any records from its dams within the earthquake region.

3.4 Measured Ground Motions

3.4.1 Peak horizontal acceleration

The distribution of peak horizontal accelerations in the earthquake region is plotted in Figure 3.2. The trace of the fault surface rupture is also shown to illustrate the relative distance of the recordings to the fault. A number of the stations, although distant from the epicentre that is located near the town of Gölcük, are relatively close to the rupture. This map clearly illustrates the importance of calculating source to site distance in terms of the distance to the surface projection of the fault rather than epicentral distance for large magnitude events where the fault length is significant.

The largest recorded peak acceleration during the main shock of 17 August 1999 was 0.41 g recorded at approximately 3.5 km from the fault at Sakarya (SKR) station in the east-west (fault-parallel) direction. The north-south component of this station was not recorded due to an instrument malfunction. Other stations with high horizontal accelerations were Düzce (DZC) = 0.37g, Yarımca (YPT) = 0.32g, Gebze (GBZ) = 0.27g, Ambarlı Power Plant (ATS) = 0.25g and İzmit (IZT) = 0.23g. The stations SKR, DZC, YPT, GBZ and IZT are all located close to the fault. The ATS station is located 100km east of the epicentre and over 50 km east of the eastern end of the fault. Celebi et al. (1999), have pointed out that these were probably not the largest ground acceleration values that actually occurred. The number of recordings in the very near field, i.e. close to the fault rupture, is relatively few. During the 12 November 1999 aftershock ($M_s = 7.2$), a peak horizontal acceleration of 0.8 g was recorded at Bolu in the very near field (Celebi et al., 1999). However, it should be noted that the higher ground motions recorded during the 12 November 1999 aftershock may also be attributed to the particular characteristics of the rupture, e.g. stress drop.

The recorded peak horizontal accelerations are plotted versus distance to the surface projection of the fault rupture in Figures 3.3 and 3.4. The recorded values are compared with the published attenuation relationships often used for the region, i.e. relationships for California (Boore et al. 1993) and for Europe (Ambraseys et al. 1995) respectively. The attenuation relationships of Boore et al. (1993) have been determined for three site classes: Class A are rock sites with average shear wave velocity $>760\text{m/s}$; Class B are stiff soil sites with average $V_s = 360\text{m/s}$ to 760m/s ; and Class C are soft soil sites with average $V_s < 360\text{m/s}$. The Boore et al. (1993) relationships also differentiate between style of faulting: reverse slip and strike-slip, and the strike-slip fault option has been selected. The attenuation relationship curves for strike-slip faulting for Class A rock sites and Class C soft soil sites are plotted on Figure 3.3. Also shown on Figure 3.3 are the known peak horizontal acceleration values (values below 0.01g are not shown). These have been divided into rock, soil and unknown ground in accordance with the information available on the ground conditions. It should be noted that a number of the ground response records were recorded in the basements or ground levels of buildings with more than two stories and these data points do not meet the selection criteria specified by Boore et al. (1993) when deriving their attenuation relationships. In addition, the attenuation relationship curves plotted are for the random horizontal component while the recorded values shown are the larger of the two horizontal values. However, it can be seen that the Boore et al. (1993) attenuation relationships provide a good fit to the data both in the near and far field.

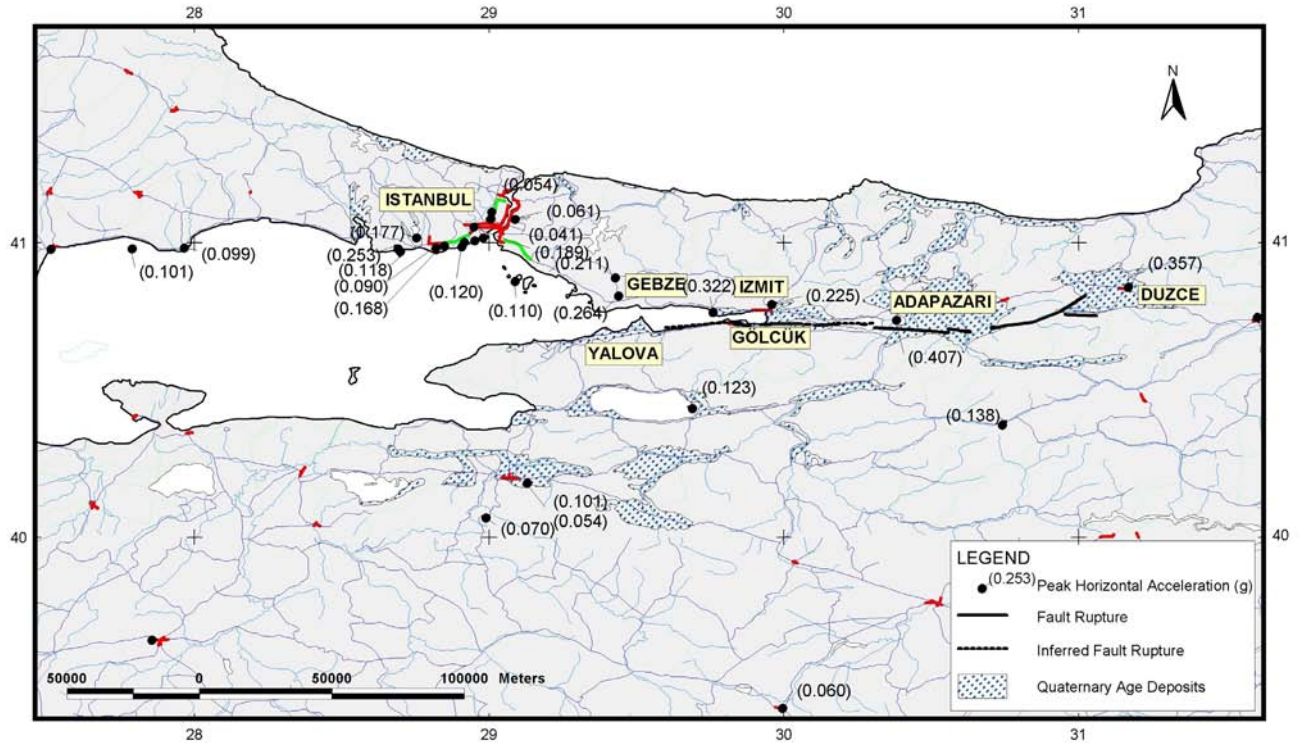


Figure 3.2: Distribution of peak horizontal acceleration in earthquake region. For station names refer to Figure 3.1. (Location of fault rupture from Lettis et al. 2000. Location of Quaternary Age Deposits from Emre et al. 1998.).

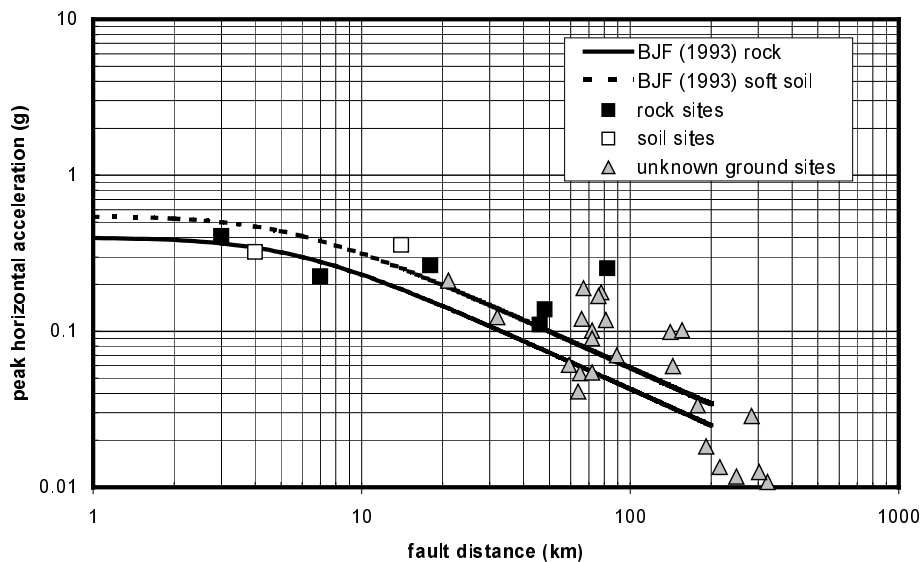


Figure 3.3: Plot of peak horizontal acceleration versus fault distance. Also shown are attenuation relationship curves of Boore et al. (1993) for rock (solid line) and soft soil (dashed line) for a magnitude $M_w = 7.4$.

The attenuation relationships of Ambraseys et al. (1995) have also been determined for three site classes: rock sites; stiff soil sites; and soft soil sites using the same shear wave velocity ranges as Boore et al. (1993). The Ambraseys et al. (1995) relationships do not differentiate between types of faulting. The attenuation relationship curves for rock sites and soft soil sites with magnitude $M_s = 7.8$ are plotted on Figure 3.4, together with all the

known peak horizontal acceleration values. The Ambraseys et al. (1995) relationships show a good fit to the data at distances greater than 30 km but are above the data at distances less than 10 km.

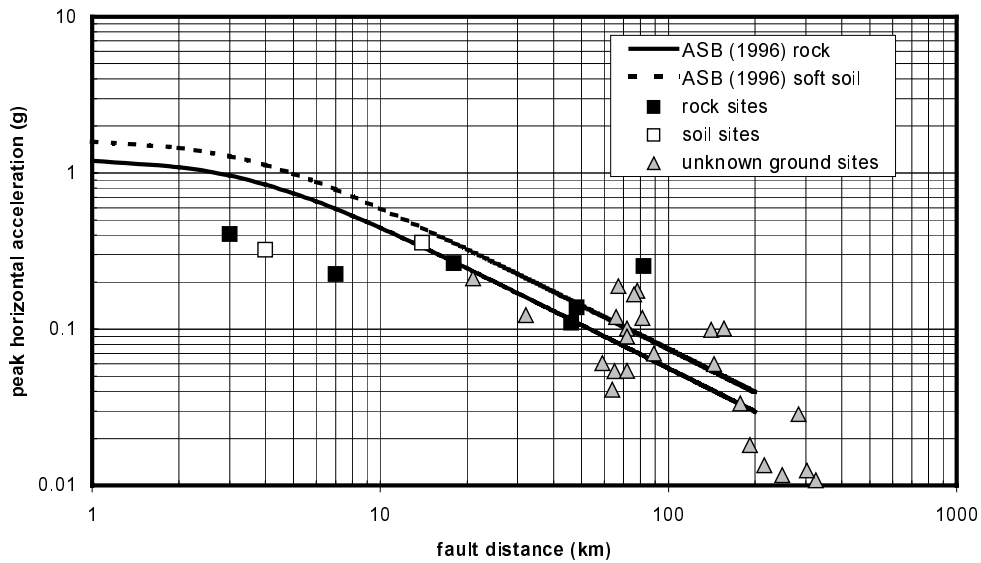


Figure 3.4: Plot of peak horizontal acceleration versus fault distance. Also shown are attenuation relationship curves of Ambraseys et al. (1995) for rock (solid line) and soft soil (dashed line) for a magnitude $M_S = 7.8$.

3.4.2 Peak vertical acceleration

The distribution of peak vertical accelerations in the earthquake region is plotted in Figure 3.5. The largest recorded peak vertical acceleration recorded during the 17 August 1999 earthquake was 0.48g at Düzce station (DZC). Significant vertical peak accelerations were also recorded at Sakarya (SKR) = 0.259g and Yarimca (YPT) = 0.242g.

The recorded peak vertical accelerations are plotted versus distance to the surface projection of the fault rupture in Figures 3.6. The recorded values are compared with the published attenuation relationships for peak vertical acceleration used for Europe (Ambraseys and Simpson, 1995). The attenuation relationships of Ambraseys and Simpson (1995) have been determined for three site classes: rock sites; stiff soil sites; and soft soil sites using the same shear wave velocity ranges as for the peak horizontal accelerations and do not differentiate between type of faulting. The attenuation relationship curves for rock sites and soft soil sites with magnitude $M_S = 7.8$ are plotted on Figure 3.6. The relationships show a very good fit to the peak vertical acceleration data.

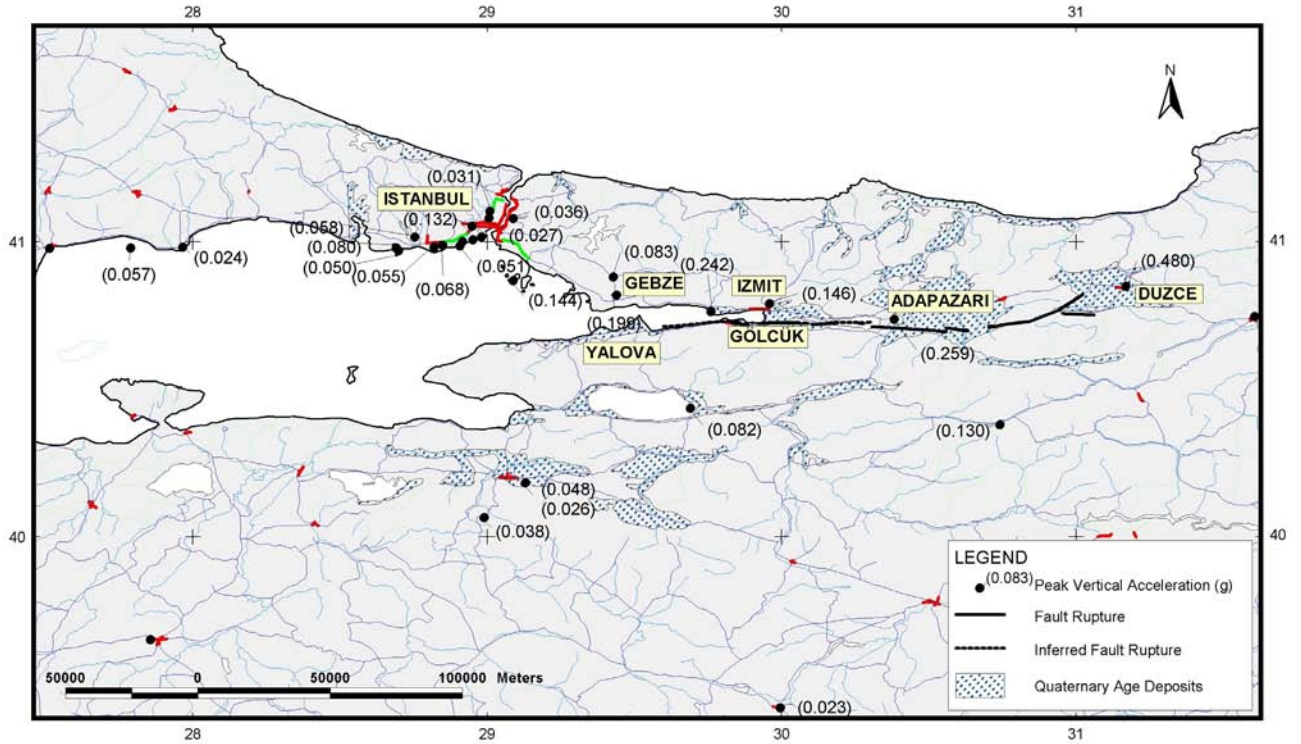


Figure 3.5: Distribution of peak vertical acceleration in earthquake region. For station names refer to Figure 3.1. (Location of fault rupture from Lettis et al. 2000. Location of Quaternary Age Deposits from Emre et al. 1998.).

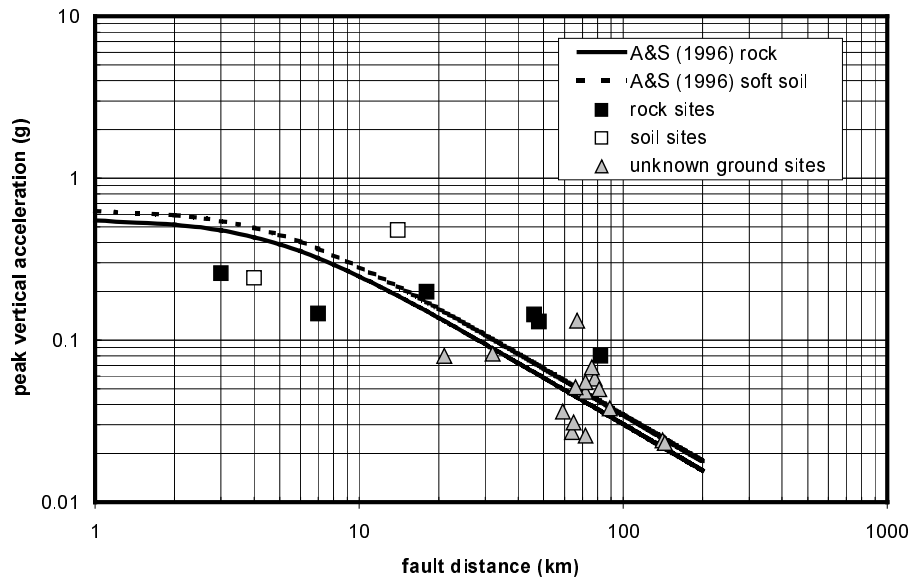


Figure 3.6: Plot of peak vertical acceleration versus fault distance. Also shown are attenuation relationship curves of Ambraseys and Simpson (1995) for rock and soft soil for a magnitude $M_S = 7.8$.

3.4.3 Significant duration of the main shock

Figure 3.7 provides a comparative measure of the significant duration of the ground shaking at selected locations and a quantity representative of the total energy released during the main shock. This is calculated from the accelerogram digital records as the cumulative sum of the square of the accelerations (Trifunac and Brady 1975). For each station the East-West component of the horizontal acceleration is considered. It is assumed that a common origin of times applies to the recorded accelerograms. In Figure 3.7, the time differences between the points at which the curves rise sharply from the horizontal axis can be interpreted as a measure of the locations of the instruments relative to each other along the direction of propagation of the seismic wavefront. At Yarimca (YPT), 75% of the energy is released in about 9 seconds and the effective shaking associated with the main shock lasted about 12 seconds, while 20% of the total energy released is associated with the second recorded peak occurred about 30 seconds after the first. Düzce record was shorter than others with only about 25 seconds of significant readings. The significant shaking occurred here within a very short time of about 3 seconds during which 83% of the total energy was released. At Adapazari (SKR), 84% of the energy is released in about 6 seconds and for these two records a second contribution is not clearly identifiable. For the Izmit record the effective shaking occurred over a longer period of 14 seconds with an associated 83% of the total energy released while the second event, clearly identifiable contributed 13%. Arcelik (ARC) and Gebze (GBZ) have very similar record in terms of total energy released, while the time gap between the two of approximately 3 seconds relates to the greater distance of Arcelik from the fault. .

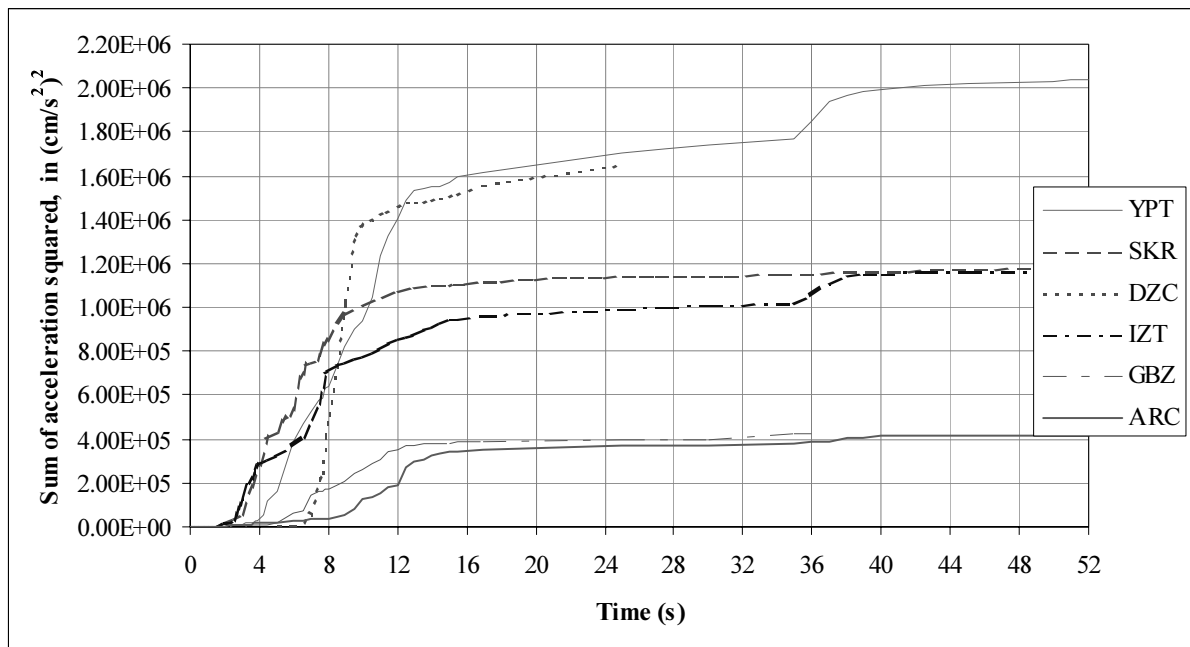


Fig. 3.7: Measure of the significant duration of shaking for the horizontal component of acceleration

3.5 Response Spectra

The pseudo acceleration response spectra (5% damping) of the time histories are shown in Appendix 3b. Those for four stations, Yarimca (YPT), Izmit (IZT), Sakarya (SYK) and Duzce (DZC) are shown in Figure 3.8 (from Beyen *et al.* 2000). All are near field stations that recorded significant peak accelerations. The Yarimca and Duzce stations are located on deep weak soil deposits while the Izmit and Sakarya stations are located on rock or have a thin layer of stiff soil over rock. Also shown on Figure 3.8 for comparison is the Turkish Seismic Design Code (1997) for Seismic Zone 1 and Site Class Z4 (deep soft soil). It can be seen that the design spectra forms a suitably conservative envelope to all the response spectra except for the Duzce response spectrum in the 0.2 to 0.4 second period range and the Yarimca response spectrum in the less than 0.2 second period range. It can also be seen that the soil sites (YPT and DZC) have significantly higher spectral amplitudes in the longer period range than the rock sites (IZT and SKR). Further comparisons between inelastic spectra and the code provision are presented in Chapter 5.

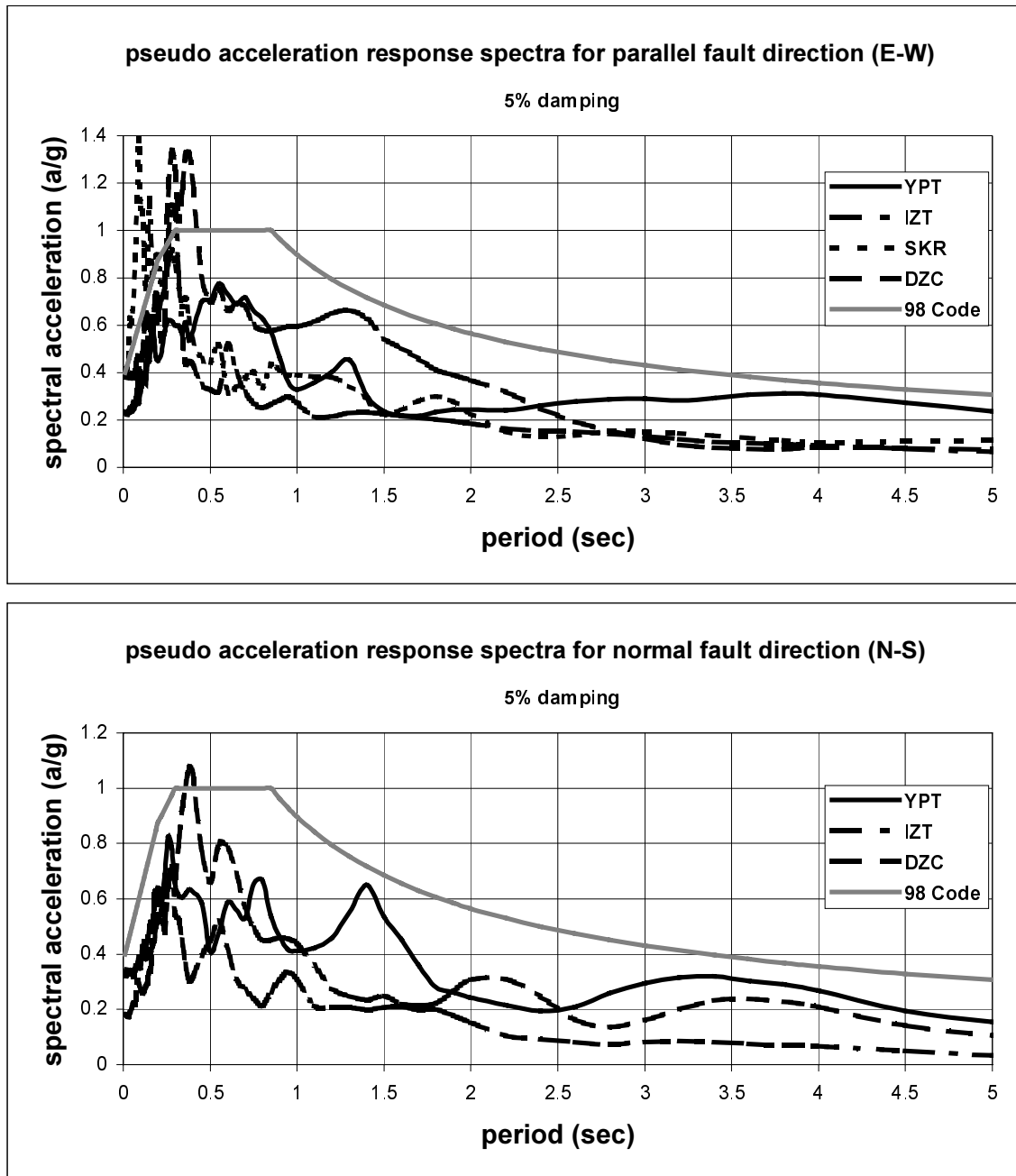


Figure 3.8: Pseudo-acceleration response spectra for the Yarimca Petkim (YPT), Izmit (IZT), Sakarya (SKR) and Duzce (DZC) horizontal acceleration components in the fault-parallel (E-W) and fault-normal (N-S) directions. Also shown is the Turkish Seismic Design Code (1998) design spectra for Sesismic Zone 1 and Local Site Class 4 (deep soft soil).

3.6 Factors Influencing the Observed Strong Ground Motions

3.6.1 Fault directivity effects

Somerville *et al.* (1997) have investigated the effect of rupture directivity on ground motion. They have found that the propagation of a rupture towards a site at a velocity that is almost as large as the shear velocity causes most of the seismic energy from the rupture to arrive in a single large pulse of motion. Evidence for this effect has also been reported by Heaton (1982) for the San Fernando 1971 earthquake, Wald and Heaton (1994) for the Landers 1992 earthquake and Wald *et al.* (1996) for the Northridge earthquake. The North Anatolian Fault Zone

is tectonically very similar to the San Andreas Fault Zone and as such a similar directivity effect can be expected. The causative fault zone, the North Anatolian Fault Zone (NAFZ), is a right lateral strike slip fault. The segments of the NAFZ that ruptured during the Kocaeli event are almost purely strike-slip with the exception of a 2km to 3km pull-apart zone at Golcuk that resulted in oblique normal – strike slip offset. The fault rupture is interpreted to have propagated bi-directionally from an epicentre near Golcuk. (Anderson *et al.* 2000). A number of the strong-motion stations are located in close proximity to the fault and a number of these records may be interpreted as showing fault directivity effect characteristics.

Figure 3.9 shows the acceleration records, and the calculated velocities and displacements from two near-field stations, Yarimca (YPT) and Izmit (IZT) . The three stations show the pulse like velocity records and step-like displacement records that are often associated with near-field motions from strike-slip earthquakes (Safak *et al.* 2000). In addition, the fault parallel (East-West) velocity records show the pronounced pulses in velocity and step in displacement that may be associated with the permanent offset on the fault. Further study is required to investigate these issues.

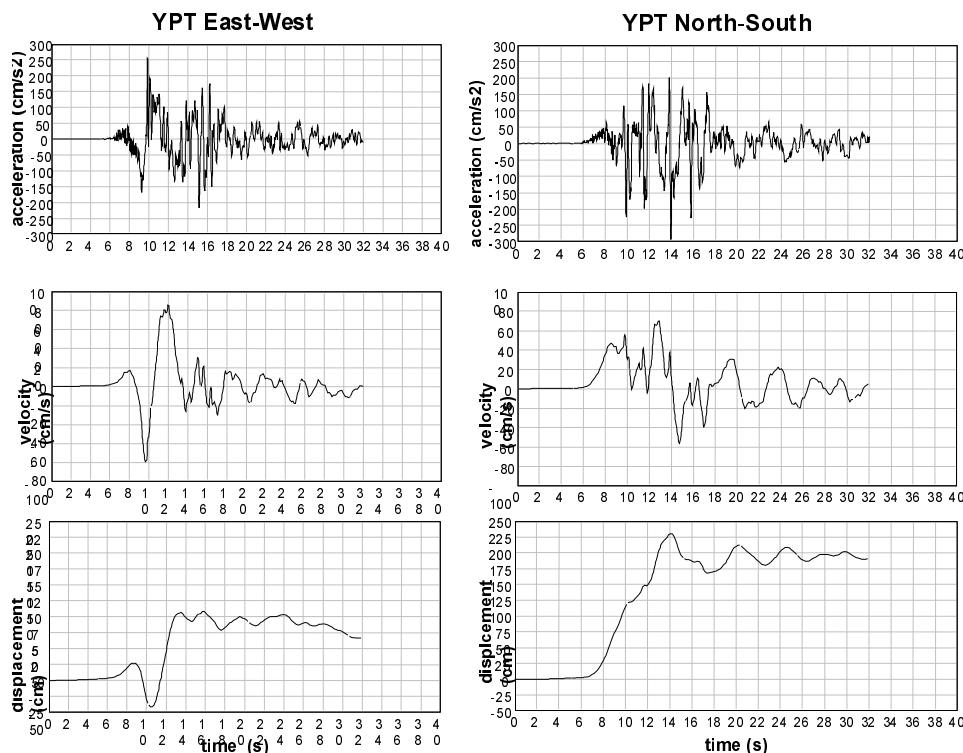


Figure 3.9a: Time histories of recorded acceleration (cm/s^2) and calculated velocity (cm/s) and displacement (cm) for the Yarimca Petkim Station (YPT) showing the pulse-like velocities and step-like displacements that are typical of near-field motions (from Safak *et al.* 1999).

The Düzce station is located approximately 12 km to the east of the eastern segment of the August 17 fault. This segment of the fault ruptured from west to east and as such the Düzce station is in the forward directivity region. The Düzce record has a relatively short duration when compared to other records at similar distance to the fault such as the Yarimca, Izmit and Sakarya stations. In addition, the response spectral amplitudes of the Düzce record are larger than those from the other three near-field records. The western segment (Gölcük toward Yalova) of the August 17 fault ruptured from east to west. It has therefore been speculated that directivity effects may have contributed to the unusually severe damage in cities west of the fault rupture, such as Yalova and Cinarcik. However, Anderson *et al.* (2000) have rightly emphasised that other important factors such as the site conditions and basin effects in these areas requires more detailed assessment before the severe damage can be attributed to fault directivity effects.

A number of the acceleration records reveal two distinct earthquake pulses. The Yarimca (YPT) record shows a second event approximately 33 seconds after the mainshock (see Figure 3.10). Similar secondary pulses are evident on the Izmit (IZT), Gebze (GBZ) and Arcelik (ARC) records (see Appendix 3B). Anderson *et al.* (2000) suggest that this pulse represents an early aftershock.

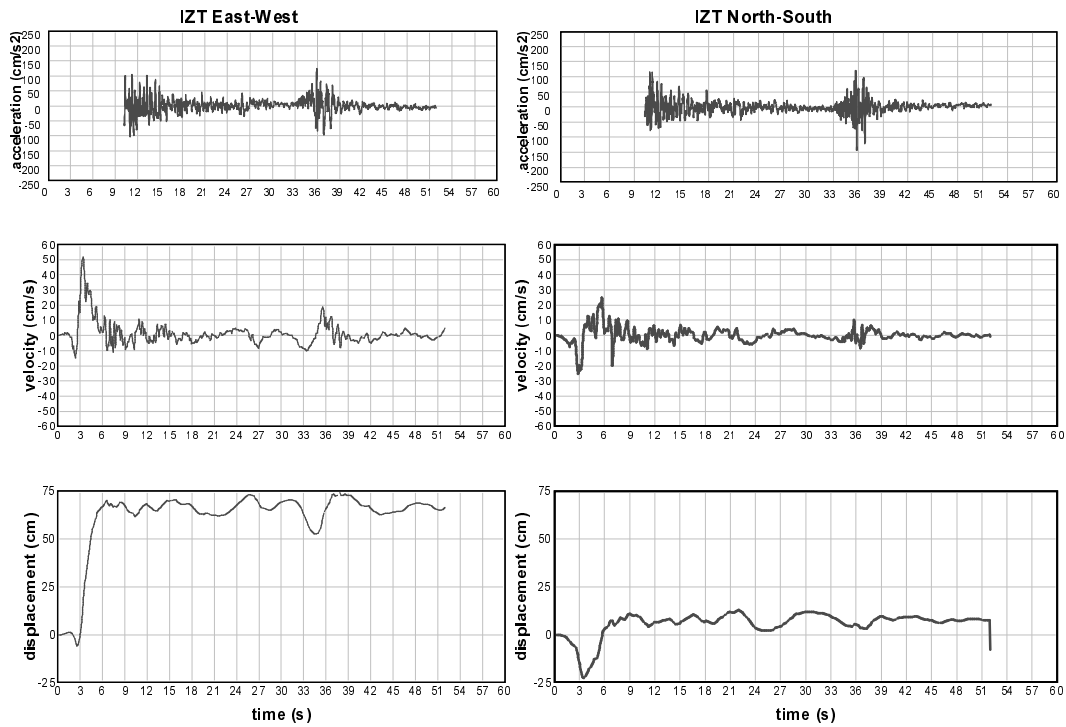


Figure 3.9b: Time histories of recorded acceleration (cm/s^2) and calculated velocity (cm/s) and displacement (cm) for the Izmit Station (IZT) showing the pulse-like velocities and step-like displacements that are typical of near-field motions (from Safak et al. 1999).

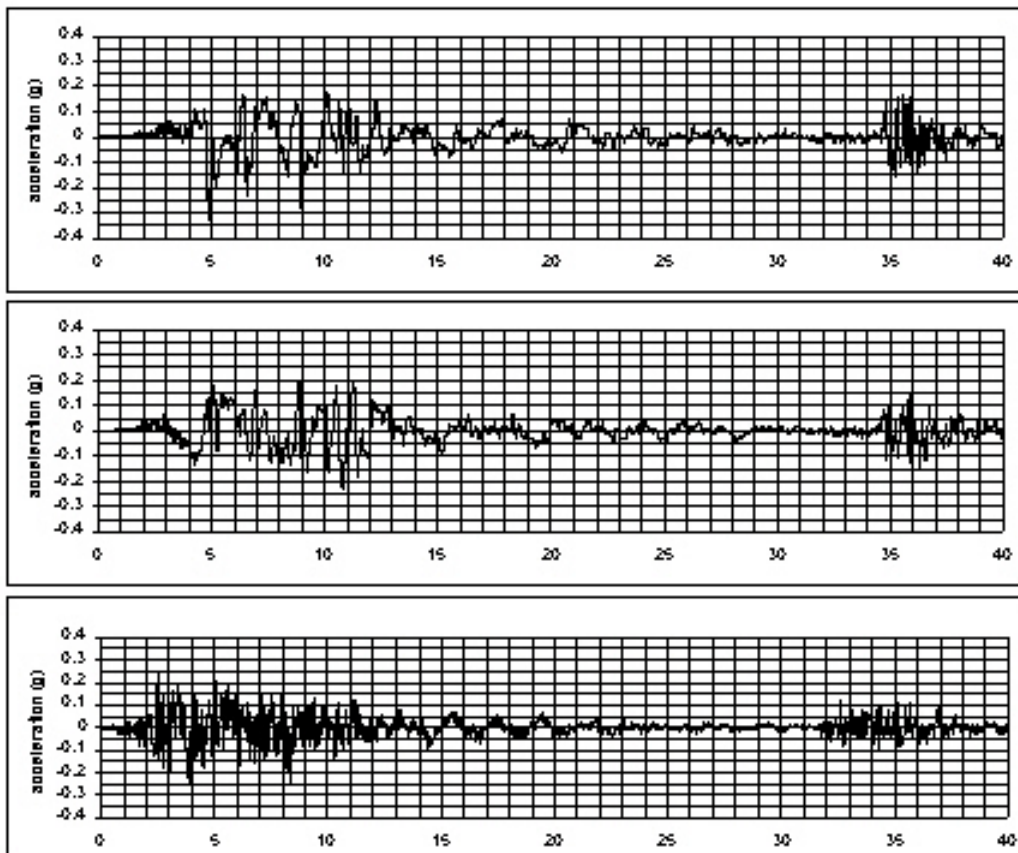


Figure 3.10: Strong-motion record from Yarimca Petkim (YPT) station: acceleration (g) versus time (s). Top: horizontal component, N-S direction; middle: horizontal component, E-W direction, bottom: vertical component. Note secondary pulse of shaking at 35 s. on horizontal records and at 30 s. on vertical record

3.6.2 Regional geology (Basin) effects

Over geological time, the right stepping en-echelon structures of the NAFZ have resulted in the formation of fault bounded, elongated, “pull-apart” basins (see Figure 4.1). These basins form a number of the dominant topographic features in the region; the Marmara Sea, Izmit Bay, Sakaraya Lake and Iznik Lake. Seismic waves may have been trapped and amplified within these elongated “pull-apart” sedimentary basins due to the waves being reflected at basin boundaries and being effectively channelled along strike. The centres of Adapazari, Golcuk, Yalova and Duzce all fall within these basins. This channelling may also have contributed to the significant shaking felt in Avcilar, a suburb located west of Istanbul Airport, which is located approximately 80km away along strike from the main-shock seismic source zone, at the north-eastern end of the Marmara Sea basin.

3.6.3 Local site effects

Following the 17 August 1999 earthquake, a number of teams established strong-motion instruments in the epicentral region. Aftershock studies provide a unique opportunity to understand how the ground conditions influenced the characteristics of the ground-motion as monitoring points can be established at selected locations where ground conditions are known. The USGS, in collaboration with KOERI, deployed 16 digital instruments to assess local site effects. The preliminary results of these studies at Adapazari, Avcilar, Dilovasi and Korfez have been presented by Safak *et al.* (2000). Safak *et al.* (2000) report that a network of 11 stations for aftershock monitoring was set up in and around Adapazari. Adapazari is located within a sedimentary basin underlain by thick soft soil deposits. The city suffered severe damage, which has been interpreted to be induced by site amplification and liquefaction. Six stations were established within Adapazari City, three stations at the Toyota Factory, one station at Hendek, and one station at Gebes Village. Safak *et al.* (2000) report the analysis of results from two stations for nine aftershocks with magnitude ($M = 3.6$ to 5.8). One of the stations, IMAR, is located on rock adjacent to the Sakarya station (SKR). The other station, HASTANE, is located within Adapazari on soft soil. The recorded horizontal accelerations at the two stations during the 31 August 1999 ($M=5.2$) and 13 September 1999 ($M=5.8$) aftershocks are shown in Figure 3.11.

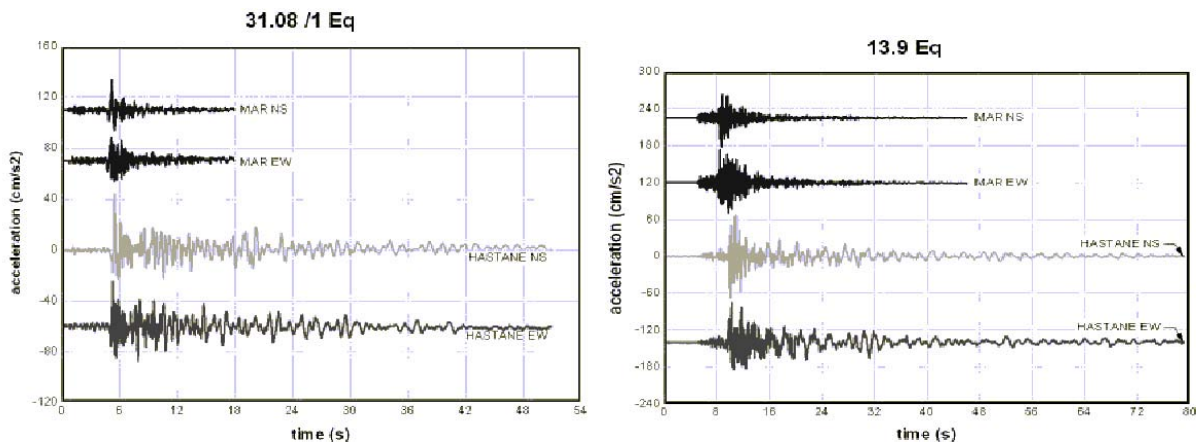


Figure 3.11: Horizontal acceleration time histories recorded at IMAR station (rock) and HASTANE station (soil) during the 31 August 1999 ($M_w = 5.2$) and 13 September 1999 ($M_w = 5.8$) aftershocks. Note the increase in amplitude and duration and shift in frequency content of the records recorded on soil (from Safak *et al.* 1999).

The effect of the ground conditions on the peak amplitude, frequency content and duration is clear. The soil/rock spectral ratio for all nine aftershocks for both horizontal directions is shown in Figure 3.12. A site amplification factor of about 10 can be seen in the frequency band of 1 to 4 Hz. It should be noted that for larger amplitude ground motions the amplification factor will be less due to damping in the soft soils and at very high amplitudes the soil damping may induce a reduction in amplitude.

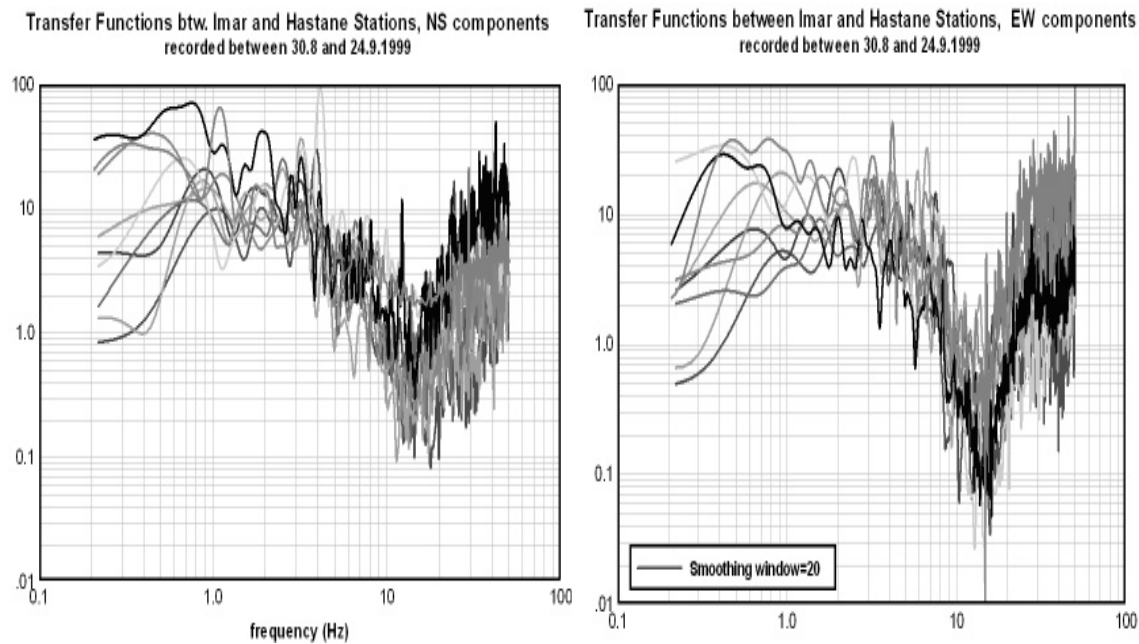


Figure 3.12: Soil-to-rock spectral ratio versus frequency (Hz) for horizontal motions from nine aftershocks recorded at the IMAR (rock) and HASTANE (soil) stations (from Safak et al. 1999).

3.6.4 Station location effects

A number of the strong-motion stations are located at the basement level of relatively large structures (e.g. the Gebze Tubitak Marmara Arastirma Merkezi station). In addition, in some cases the instruments are located within relatively flexible structure (e.g. the Yarimca station). Under these circumstances the recorded motions may have been influenced by the response of the structure. The effects of soil-structure interaction on strong-motion accelerograms have been discussed by Luco *et al.* (1990) and more recently by Stewart *et al.* (1999a,b). The assessment of the effect of soil-structure-interaction (SSI) on strong-motion records is a complex issue and is not considered to be within the scope of this report. The reader is directed to the references noted above and recent discussions by Trifunac (2000) for further information.

3.7 Macroseismic Intensity distribution

It has been pointed out in numerous occasions in this work and in other reports on the Kocaeli earthquake, that this event has shocked the community for its high level of damage. This has been attributed to the combination of the rapid development of heavily urbanised areas, the poor standard of construction quality, the proximity of the fault and the “poor” soils on which some of the urban centres have been developed. The following section provides a discussion of the distribution of macroseismic intensity in the region, a comparison between strong motion records and damage surveys and finally a comparison of intensity distribution and damage as recorded for the 1992 Erzincan earthquake.

3.7.1 Comparison of isoseismal maps

In the first week after the earthquake an EERI team led by Dr. Andrew Coburn visited the affected area and surveyed more than 2200 residential buildings in Izmit, Gölcük, Adapazari and Yalova and in some of the smaller centres along the north and south shore of the Marmara Sea. Note that the survey did not include Düzce. On the basis of this survey each building was attributed a damage category based on a six points scale summarised in table 3.1. On the basis of the cumulative damage distribution, a first isoseismal map was produced based on MMI intensity scale (RMS, 2000) and is reproduced here in Figure 3.13. Ground shaking of Intensity MMI VII (corresponding to moderate damage) occurred over a region of approximately 200*100 km with major axis along the North Anatolian Fault. Moreover two separate areas of level IX were identified, one

extending for about 15 km east of the epicentre and for a narrow band of a couple of kilometres westward from Gölcük to Yalova, and a second one from the western shore of Lake Sapanca just to the east of Adapazari city centre. This level of intensity corresponds to most building being seriously damaged or collapsed.

Table 3.1: Damage levels for concrete structures, used in the RMS and EEFIT surveys

D0	Undamaged: no apparent damage visible on the exterior of the structure
D1	Slight damage: Infill panels damaged
D2	Moderate damage: Cracks less than 10mm wide in the structure
D3	Heavy damage: Heavy damage to structural members, loss of concrete
D4	Partial destruction: Complete collapse of an individual structural member
D5	Total collapse: Failure of structural members sufficient to allow collapse of roof or slab

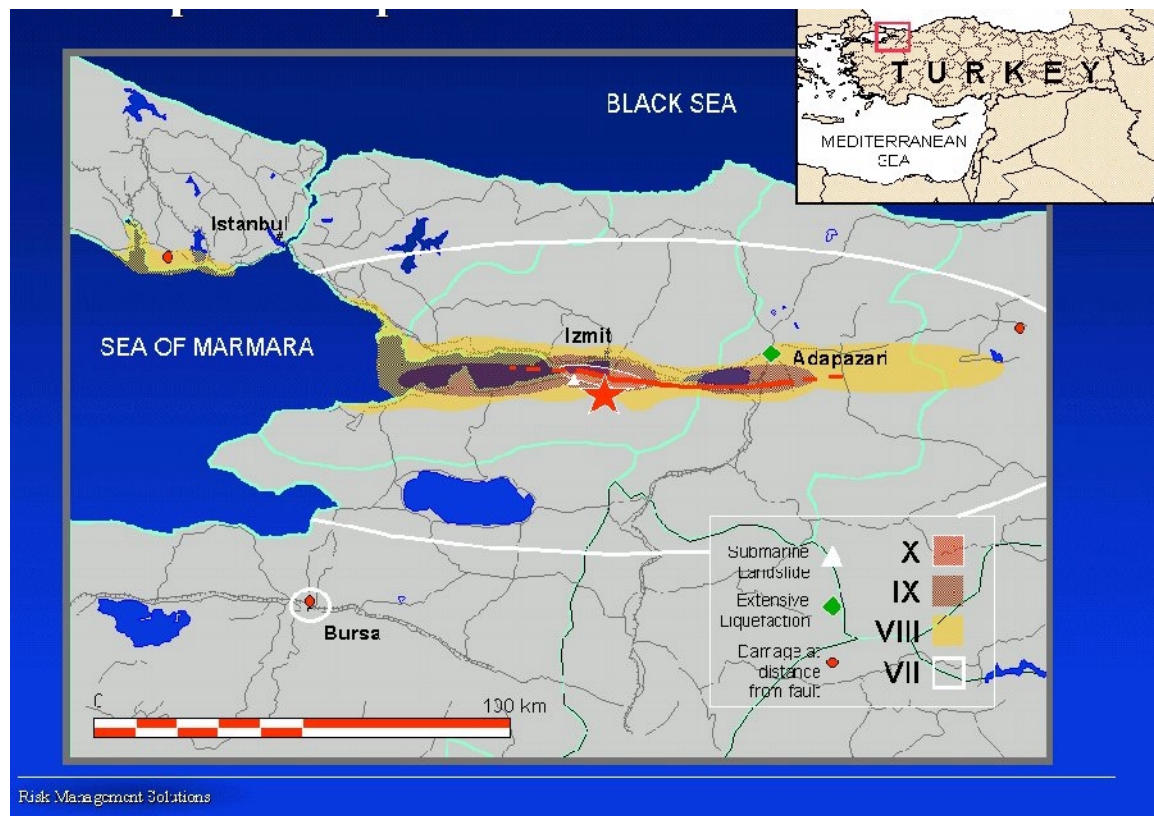


Figure 3.13: Macroseismic intensity map produced by RMS

Comparison of this map with the geological map shown in Figure 4.2 in the next chapter shows clearly the correspondence between high level intensities with the distribution of recent (Quaternary age) superficial soils. The distribution of these soils is discussed in Chapter 4 and their effect on the measured strong-motion is discussed earlier in this Chapter. Where the geological formations are older and typically rock, the intensity is reduced by approximately one degree. The Intensity X region, according to RMS intensity map, is defined by an elliptical area of length 20 km and width 4 km centred on the epicentre and crossed longitudinally by the fault.

A first estimate of the isoseismal map was also produced by the Earthquake Research Department of the General Directorate of Disaster Affairs, in Ankara, based on their official damage survey (see Figure 3.14). No explicit reference to the Intensity scale used is made. The map shows two larger areas of Intensity X, roughly

corresponding to the two regions of Intensity IX of the previous estimate. An isoseismal contour of Intensity IX extends for the entire length of the fault rupture from Düzce to Yalova reaching the suburb of Avcılar north west of Istanbul and the north shore of the Iznik Lake on the south. A rather large Intensity VII region includes Zonguldak in the north and Bursa in the south west.

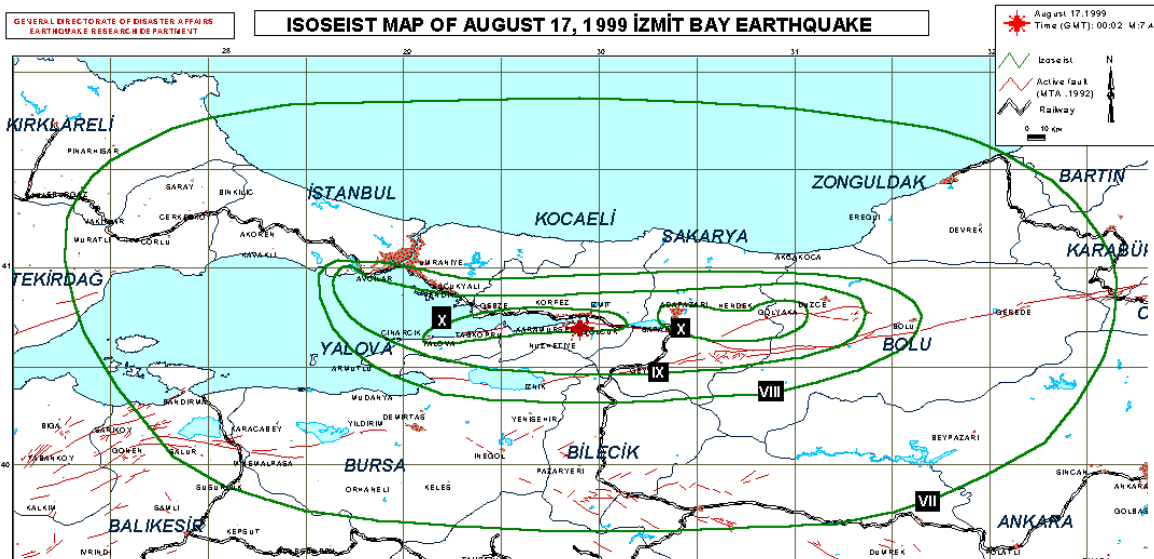


Figure 3.14: Macroseismic intensity map produced by ERD, General Directorate of Disaster Affairs

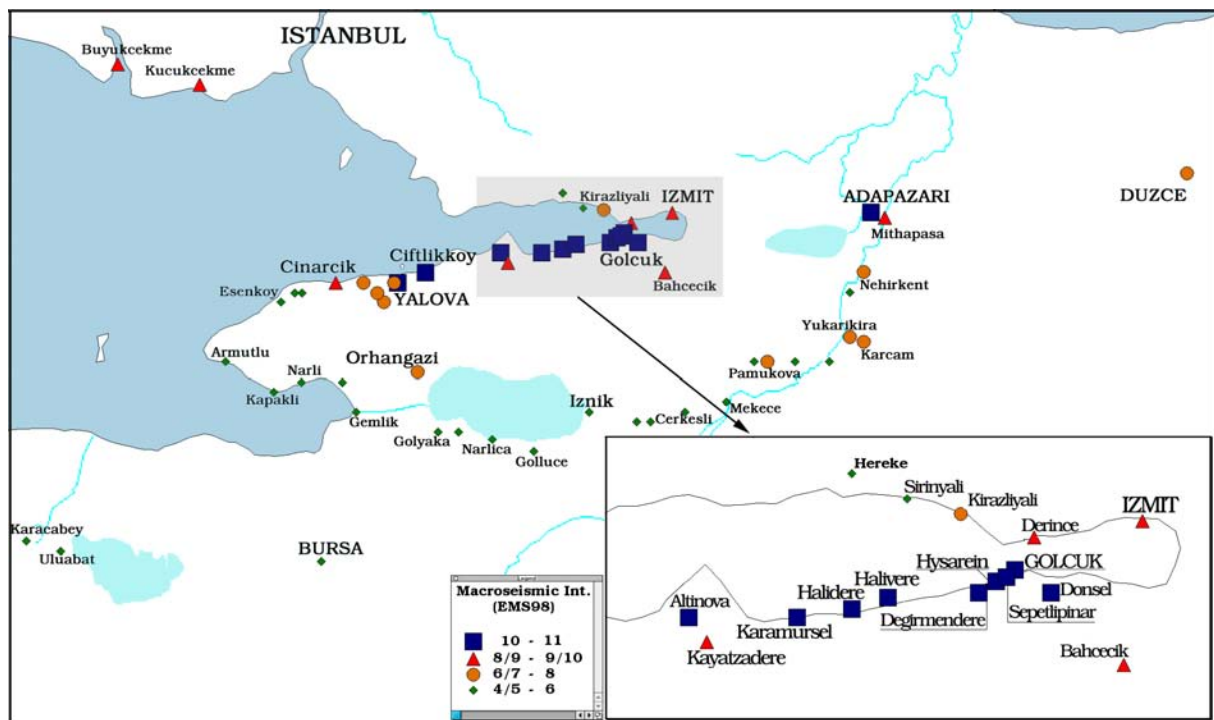
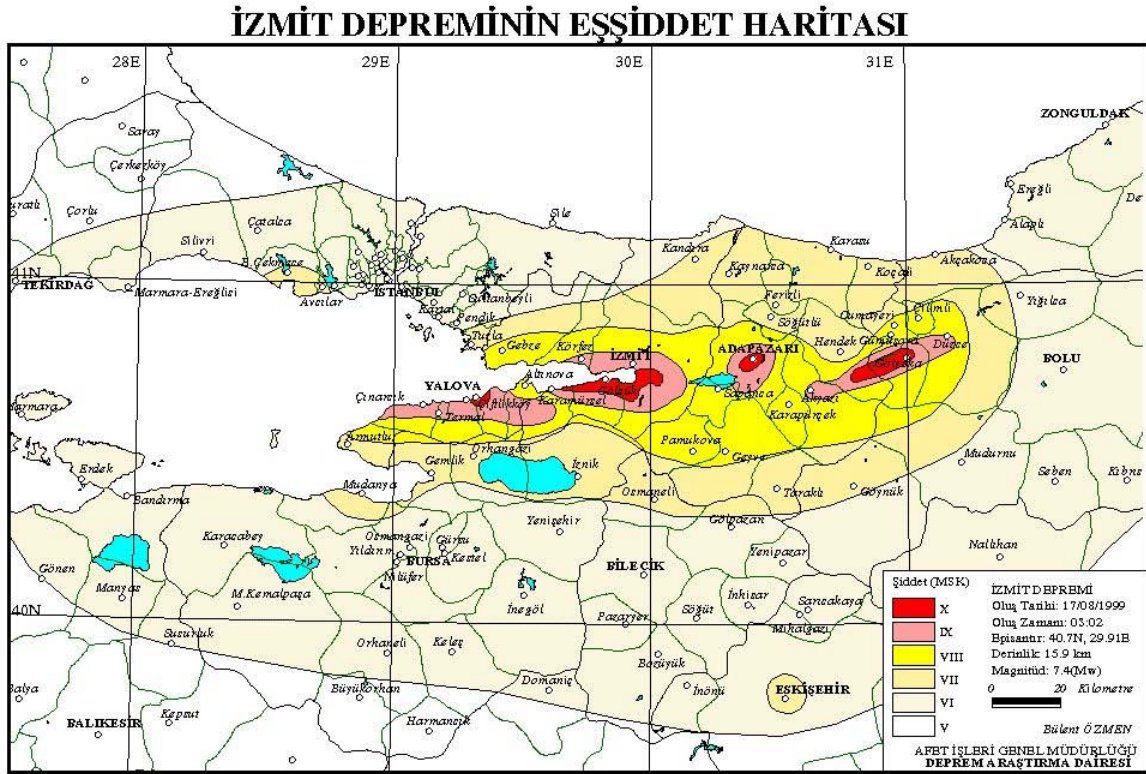


Figure 3.15: Distribution of intensity based on ems98 scale produced by GNDT, Italy.

A different approach was followed by the Italian team of the GNDT (GNDT website 1999) that limited its estimate to the attribution of an Intensity level to the urban centres visited, rather than applying these to geographical regions (see Figure 3.15). The scale used is the EMS 98. On the basis of this Gölçük, Dergimendere and Adapazari were attributed an intensity between X and XI, Yalova and the other centres on the south coast of the Izmit bay were attributed intensity level between VIII and X, Izmit IX, and Düzce VIII. An equivalent isoseismal contour VI can be identified, running from the Marmara Sea coast along the south shore of

the Iznik Lake, and north east towards Adapazari, delimiting the region subjected to damaging shaking. This zonation failed to consider the localised but relatively high damage observed in Bursa while Zonguldak was not visited.

On the basis of the completed official damage data collection an isoseismal map was then produced by the Turkish National Disaster Relief Centre using the MSK scale (see Figure 3.16). According to this map areas of level X are identified in Düzce and Yalova together with Golcuk and Adapazari and compared with the RMS these extend farther away from the fault. The intensity level VIII isoseismal contour extends beyond Düzce in the east and some 20 km west of Yalova, with a maximum extension north south of 30 km in the proximity of Adapazari. Interestingly Avcilar is assigned intensity VII and Bursa intensity VI.



Şekil 3 : İzmit depreminin eşiddet haritası

Figure 3.16: MSK intensity map produced by the Turkish National Disaster Relief Centre.

Comparison of the different maps is made somewhat difficult by the use of different Intensity scales. Assuming substantial equivalence for the MSK and EMS98 scales for intensities 8 to 10, then there is good agreement between the GNDT map and the Turkish National Disaster Relief Centre (TNDRC) map. Substantial differences are identified in the area around Düzce, where a level X is assigned by (TNDRC) and a level VIII by GNDT; and in the fact that the Iznik Lake is within isoseismal curve VII for TNDRC and VI for EMS98. However the possible correlation between a MSK VII and EMS 98 VI level is clearly outlined in Grünthal (1998).

3.7.2 Correlation of strong motion records with damage surveys and isoseismal distribution

It is possible to estimate areas of isoseismal intensity rather than from the damage distribution, by correlation with peak ground acceleration. The actual areas of isoseismal distribution for an earthquake of Magnitude $M_s = 7.8$ and focal depth 17 Km, using Ambraseys (1995) PGA attenuation relationship for European earthquakes together with the conversion proposed for PGA to MSK Intensity, are summarised in table 3.2 for isoseismal 7, 8 9 and 10. Ellipses of these areas centred on the Iznik epicentre, with an axis ratio of 5 and major axis oriented along the Gölçük-Düzce direction, are superimposed in Figure. 3.17 together with the prevalent level of damage surveyed in the closest city to each of the strong motion records available along the fault (see Table 3.3). It can be noted that there is a substantial good agreement between the isoseismal curves and the surveyed damage, except for the severe localised damage in Adapazari, as it will be further discussed in Chapter 5.

Table 3.2: Expected areas within MSK isoseismals

MSK intensity	Area (km ²)
X	80
IX	1018
VIII	5026
VII	20000

In order to explore a correlation between the damage observed and the ground shaking recorded at the instrument, the EEFIT team also carried out surveys of the buildings in the vicinity of the instruments. The damage levels recorded were then compared with the peak ground acceleration recorded and with damage surveys carried out in the nearest town centre to the instrument. A summary of the results obtained is presented in Table 3.3

The number of buildings that could be surveyed in the immediate vicinity of each instrument depended on its location and on the access policy of the hosting institution. Only in the case of Düzce is the station less than a kilometre from the city centre. In this case, for the buildings along the road where the Düzce Meteorological Institute is situated, there was very little apparent damage. However, on the main road, some 150 m to the south, a set of 5 buildings constituting a recent residential development show ground and lower ground floor failure and damage up to level D4. The most common level of damage along the main road leading west to the city centre of Düzce was D3 with consistent occurrence of D4.

Table 3.3: Comparison of damage surveys near to instruments and in nearby towns with PGA's recorded values

Instrument	PGA (max Hor.) (g)	Survey in the immediate vicinity			Survey in nearby town		
		Number of buildings	Prevalent Damage level	Intensity	Town	Prevalent Damage level	Intensity
YPT	0.322	10	D2	VII	Derince	D4	VIII-IX
SKR	0.41	20	D3	VIII	Adapazari	D4-D5	IX-X
DZC	0.38	25	D2	VII	Düzce	D3-D4	VIII
ARC	0.26	10	D1	VI	Gebze	D2-D3	VII
GBZ	0.25	5	D1	VI	Gebze	D2-D3	VII

A similar scenario was observed in Derince, in which a few complete failures were also observed, increasing in quantity moving away from the instrument and towards the shoreline. Images of Adapazari destruction in the city centre are all too familiar and any possible correlation is highly impaired by the substantial difference in soil conditions between the city and the instrument location. The apparent reduced level of damage at the immediate vicinity of the instrument in respect to the damage observed in the urban centre, is however common to all locations

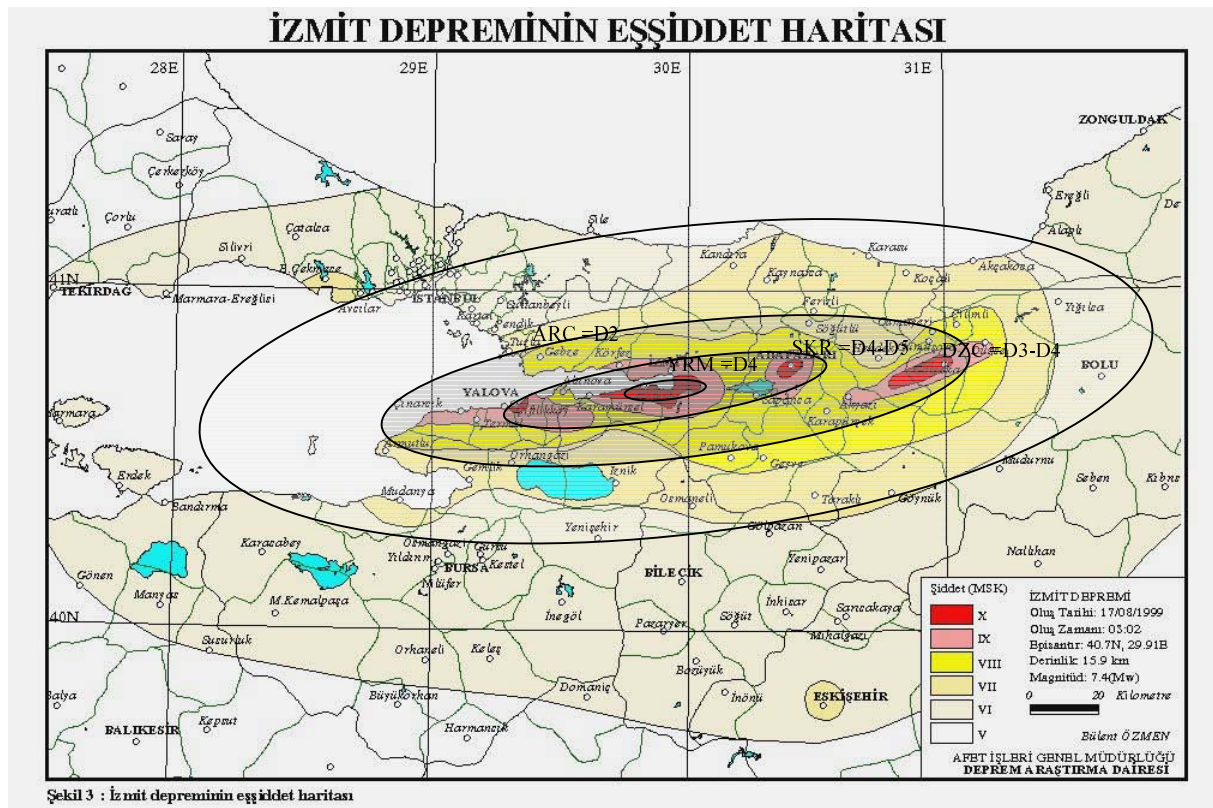


Figure 3.17 Comparison of calculated isoseismal and surveyed levels of damage according to MSK scale for degrees 10 to 7

EMS98 attempts to improve the precision in the assignment of intensities by separating vulnerability and damage, and adopting a statistical approach for both categories (Grünthal 1998). The definition of an intensity degree is correlated with the assumption that certain types of buildings of known vulnerability¹ will be damaged to a certain extent. Typically, for instance, if most unreinforced masonry buildings have experienced damage level D3 and a few D4 and few reinforced concrete buildings have experienced level D3, it can be said that the area has been affected with an intensity VIII (for damage levels see Table 3.1). Clearly the judgement is all the more reliable, as more types of buildings of known vulnerability are present in the area under consideration. In quantifying the vulnerability of a differentiated building stock however two factors should be considered besides the identification of structural types: the historical improvement of vernacular forms of construction towards aseismic typologies as a result of direct experience, and the necessity of the whole construction process to be engineered in order to ensure the aseismicity of modern forms of construction.

A problem raised by the Kocaeli earthquake is that on the basis of typological surveys only, the great majority of the building stock belongs to one type, reinforced concrete frame with infill panels. The assignment of vulnerability classes for this type of buildings spans over a wide range depending on the level of seismic provision and earthquake resistant design compliance (Grünthal 1998), which however is rather difficult to assess from simple external inspection of the building. Assuming that the great majority of these buildings were designed according to the 1975 Turkish seismic requirements, then they would have had low to moderate seismic provisions. Accordingly they would have been assigned to vulnerability classes C to D of the EMS98 vulnerability table, with C being the most likely class. Earlier concrete structures or structures that were substandard could have been assigned vulnerability class B or C, with C being the most likely.

The evidence of this earthquake shows that in many cases buildings assumed to belong to a lower vulnerability class, such as 1 to 3 storey masonry or timber buildings, experienced less damage than the 4 to 6 storey concrete frames. This would then lead to the assumption that either the intensity would be VII to VIII based on the first

¹ EMS 98 identifies 6 classes of vulnerability A to F, A being the most vulnerable and F the least. It also assigns a most probable class and a possible range to each type of structure. See Grünthal 1998 for more details.

estimate, or IX to X if the damage to concrete frames is taken as representative of the shaking, and if these are assumed to belong to class C or D of vulnerability.

One other problem is the fact that the damage distribution was far from homogeneous within relatively small geographical areas for the same type of building. Indeed in many localities along the same road buildings belonging to the same typology were standing undamaged next to completely destroyed ones and in proportions that made it difficult to identify an intensity level (for instance the absence of intermediate level of damage: many D1, many D4-D5, but few D2 and D3). The damage distribution may be partly explained by the distribution of the local ground conditions, which are in general largely unknown. Although EMS 98 explicitly states that ground conditions should be taken into account from the point of view of the damage caused, it is not actually included in the vulnerability classes, i.e. it is not stated that a 4 storey concrete frame with superficial foundation on soft soil is actually more vulnerable than the same structure with continuous rafter foundation on competent soil or on piles. Hence again the difficulty in correlating distribution of damage with the correct intensity level.

3.7.3 Comparison with Erzincan 1992 earthquake

It is worth comparing the Kocaeli earthquake with the damage distribution of the Erzincan 1992 event (EEFIT 1993), at the eastern end of the North Anatolian fault. Although this event had lower magnitude but higher peak ground epicentral acceleration than the Kocaeli event, the geomorphologic characteristics of Erzincan City and Adapazari are rather similar. In that case, a survey in the vicinity of the only instrument present in Erzincan was carried out and it showed the same trend identified in the present case: the discrepancy between the level of damage at the instrument site and in the city centre could be ascribed to two principal factors:

- difference of soil condition between the location of the instrument and its surroundings and the main centre of the city where most of the damage was concentrated;
- lower rise buildings, 2 to 3 storey high in the vicinity of the instrument in comparison with the majority of buildings having 4 storeys or more in the city centre.

In Erzincan the official number of total collapses amounted to less than 10% of the buildings, while in the Kocaeli earthquake this is at least 15 to 20% of the total, with higher peaks in Golcuk and Adapazari. The Erzincan 1992 earthquake was to a certain extent considered anomalous from other Turkish earthquakes for its relatively low rate of damage, and this was ascribed to the rather substantial focal depth of the event (27 Km), as opposed to 17 km in the case of Kocaeli earthquake.

3.8 Conclusions

A relative large number of strong motion records are available for the Kocaeli earthquake, although only two instruments were located in the immediate vicinity of the epicentre. The reliability of the records obtained has been discussed with reference to the location of the instruments, and particularly the fact that only one of the strong motion records (Adapazari) can be considered as real free-field. This influences the results of any correlation with existing attenuation laws. Moreover it appears difficult to reconcile the high levels of damage observed with some of the peak ground acceleration records available.

The significant number of strong-motion records has provided valuable information for engineers to consider when planning the rebuilding of areas damaged during the earthquake. However, strong-motion stations were not located in sufficient density to record ground motions in a number of key areas such as near to the fault rupture, near to the epicentre, within the areas where the greatest damage to buildings was recorded (e.g. Golcuk and Adapazari). It is important to increase the number of strong-motion stations in urban areas and in areas with a range of well-defined ground conditions. It would also be useful to establish an array across the NAFZ in an area with a high probability for a future event.

A number of the characteristics of the strong-motion records are consistent with concept of fault directivity focusing of the ground motion in the near-field although further work is required before this conclusion can be made with confidence. Somerville *et al.* (1997) have proposed a technique for inclusion of directivity effects within seismic hazard analysis. Inclusion of these effects in future seismic hazard analyses of the region would

be beneficial, although it should be noted that the location of a site relative to individual future earthquakes will remain unknown. Detailed information on the ground conditions at the strong-motion stations is unknown at this stage. Priority should be given to compiling this information while the earthquake engineering community's research effort is concentrated on the recent earthquake events in the area.

The distribution of damage in the region identifies at least two areas of EMS Intensity X, one around the epicentre and one in the town of Adapazari. The influence of soil and foundation characteristics on the level of vulnerability of particular structural types and the consequent possible influence on the attribution of Intensity level have been discussed. The observed Intensity levels compare well with expected intensity derived from attenuation laws except for the noted anomaly of Adapazari.

3.9 References

- Ambraseys, N.N. (1995), The estimation of earthquakes ground motions in Europe, in A. Elnashai (ed.) *European Seismic Design Practice in Europe*, Balkema, Rotterdam.
- Ambraseys, N.N., K.A. Simpson and J.J. Bommer (1995). Prediction of horizontal response spectra in Europe, *Earthquake Engineering & Structural Dynamics*, vol. 25, 371-400.
- Ambraseys, N.N. and K.A. Simpson (1995). Prediction of vertical response spectra in Europe, *Earthquake Engineering & Structural Dynamics*, *ESEE Research Report No. 95/1*, July 1995, ESEE Group, Imperial College, University of London, UK.
- Anderson, J.G., H. Sucuoglu, A. Erberik, T. Yilmaz, E. Inan, E. Durukal, M. Erdik, R. Anooshehpour, J. Brune, and S-D. Ni (2000). Strong ground motions from the Kocawli and Duzce, Turkey, earthquakes, and possible implications for seismic hazard analysis (in press).
- Aydinoglu, M.N. (1997). Specification for structures to be built in disaster areas, Part III – Earthquake disaster prevention (Chapter 5 – 13), English Translation. Ministry of Public Works and Settlement, Government of Republic of Turkey.
- Aydan O., Ulusay R., Hasgur Z. Taskin B., (1999), A site investigation of Kocaeli earthquake of August 17, 1999. Turkish earthquake Foundation, 1999.
- Birgoren and Goyilmaz (1999). Kandilli Observatory and Earthquake Institute (KOERI), [<http://193.140.203.8/earthqk/earthqk.html>]
- Boore, D.M., W.B. Joyner and T.E. Fumal (1993). Estimation of response spectra and peak accelerations from western North American earthquakes: An interim report Part 2, U.S. Geol. Surv. Open-File Rep. 94-127, 40p.
- Boore, D.M., W.B. Joyner and T.E. Fumal (1994). Estimation of response spectra and peak accelerations from western North American earthquakes: An interim report, U.S. Geol. Surv. Open-File Rep. 93-509, 72p.
- Celebi, M., S. Toprak and T. Holzer (1999). Strong-motion, site effects and hazard issues in rebuilding Turkey: in light of the 17 August, 1999 earthquake and its aftershocks (in press).
- EEFIT (1993), The Erzincan , Turkey earthquake of 13 March 1992, The Institution of Structural Engineers, 1993.
- Grunthal G., Ed., (1998), European Macroseismic Scale 1998, Cahiers du centre europeen de Geodynamique et de Seismologie, Vol. 15, Conseil de L'Europe.
- Heaton, T.H. (1982). The 1971 San Fernando earthquake; a double event? *Bull. Seis. Soc. Am.*, Vol. 72, 2,037-2,062.
- Lettis, W., J. Bachhuber, A. Barka, R. Witter, and C. Brankman (2000). Surface fault rupture and segmentation during the Kocaeli earthquake (in press).
- Luco, J.E. M.D. Trifunac, and H.L. Wong. (1987). On the apparent change in dynamic behaviour of a nine story reinforced concrete building, *Bull. Seis. Soc. Am.*, Vol. 77, no. 6, 1961-1873.
- RMS, (2000). Event Report, Kocaeli, Turkey Earthquake, Risk Management Solutions Inc. 2000

- Safak, E., M. Erdik, K. Beyen, D.Carver, E. Cranswick, M. Celebi, E. Durukal, M, Erdik, T. Holzer, M. Meremonte, C. Mueller, O. Ozel, E. Safak, and S. Toprak (2000). Recorded mainshock and aftershock motions (in press).
- Somerville, P.G., N.F. Smith, R.W. Graves, and N.A. Abrahamson (1997). Modification of empirical strong ground motion attenuation relations to include the amplitude and duration effects of rupture directivity, *Seismological Research Letters*, Vol. 68, no. 1, 199-222.
- Stewart, J.P., G.L. Fenves and R.B. Seed (1999a). Seismic soil-structure interaction in buildings. I: Analytical methods, *Jn of Geotech and Geoenviron Eng.*, Vol. 125, no.1.
- Stewart, J.P., R.B. Seed G.L. and Fenves (1999a). Seismic soil-structure interaction in buildings. II: Empirical methods, *Jn of Geotech and Geoenviron Eng.*, vol. 125, no.1.
- Trifunac, M.D. (2000). Discussion, Seismic soil-structure interaction in buildings. I: Analytical methods, Seismic soil-structure interaction in buildings. II: Empirical methods, *Jn of Geotech and Geoenviron Eng.*, Vol. 126, no.7.
- Trifunac, M.D., Brady, A.G. (1975). A study on the duration of strong earthquake ground motion> *Bullettin of the seismological society of America* 65, pp. 581-626.
- USGS (2000). Implications for earthquake risk reduction in the United States from the Kocaeli, Turkey, Earthquake of August 17, 1999, *U.S. Geological Survey Circular 1193* (Sci. Ed. T.Holzer).
- Wald, D.J., T.H. Heaton, and K.W. Hudnut (1996). The slip history of the 1994 Northridge, California earthquake determined from strong motion, teleseismic, GPS and levelling data, *Bull. Seis. Soc. Am.*, Vol. 86, S49-S70.

APPENDIX 3A

Table 3A.1: Strong-Motion Stations in Istanbul and the Aegean Region

Instruments Operated by the Earthquake Research Department of the General Directorate of Disaster Affairs (ERD)

Station Name	Abbreviation	Coordinates	Elevation	Instrument Type	Housing	Ground Conditions
Adapazari (Sakarya)*	SKR	40.737N 30.384E		GSR-16	1 storey building with dimensions 16m x 6m of fibreboard on wood frame construction with corrugated iron roof. Concrete slab on grade on west side of building but elevated approx. 1m on east side.	Topography is sloping to south at 10° to 20°. Building at south end of cut platform probably on shallow fill. Cut is in limestone or calcareous mudstone.
Afyon Bayındırlık ve İskan Müdürlüğü	AFY	38.792N 30.561E	Unknown	SM-2	Office of Ministry of Settlement	unknown
Aydın Hayvan Hastanesi	AYD	37.837N 27.838E	Unknown	GSR-16	Veterinary School	unknown
Balıkesir Huzur Evi	BLK	39.650N 27.860E	unknown	GSR-16	Rest Home	unknown
Bolu Bayındırlık ve İskan Müdürlüğü					Office of Ministry of Settlement	
Bornova Ziraat Fakültesi Dekanlığı (İzmir)	BRN	38.455N 27.229E	unknown	GSR-16	9 Eylül University Faculty of Agriculture	unknown
Bursa Sivil Savunma Müdürlüğü	BRS	40.183N 29.131E	unknown	GSR-16	Office of Civil Defense	unknown
Canakkale Meteoroloji İstasyonu	CNK	40.142N 26.402E	unknown	GSR-16	Meteorological Observatory	unknown
Cekmece Nükleer Santral Binası (İstanbul)	CEK	40.970N 28.700E	unknown	SMA-1	Nuclear Plant	unknown
Düzce*	DZC	40.850N 31.170E	unknown	SMA-1	Meteorological Observatory 1.5 storey reinforced concrete building with masonry infill. 15m x 12m dimensions. Slab on grade or slightly raised on fill platform.	Topography is flat alluvial plane/basin. Underlain by undifferentiated alluvium (Quaternary).
Eregli Kaymakamlık Binası (Tekirdağ)	ERG	40.980N 27.790E	unknown	SMA-1	District Governor Building	unknown
Gebze Tubitak Marmara Araştırma Merkezi*		40°47.25'N 29°26.90'E	unknown	SMA-1	Basement of 4 storey reinforced concrete building with masonry infill. Building dimensions 15m x 20m.	Topography is rolling hills with buildings on cut and fill platforms. Foundation appears to be basement slab excavated to weathered rock through 2-4m of soil.
Goynuk (Bolu)		40.381N	unknown	SMA-1	State Hospital	Topography is flat

		30.743E			Irregular building 1-5 stories, approx. 50m x 50m. Instrument in 1 storey section 10m x 16m. Instrument located on pedestal on grade, building floor slab on grade cut away around instrument. ²	alluvial valley/basin. Underlain by undifferentiated alluvium (Quaternary).
Istanbul Bayindirlik ve Iskan Mudurlugu	IST	41.080N 29.090	unknown	GSR-16	Office of Ministry of Settlement	unknown
Izmit Meteoroloji Istasyonu	IZT	40.790N 29.960E	unknown	SMA-1	Meteorological Observatory	unknown
Izmit Karayolları Sefligi	IZN	40.440N 29.750E	unknown	SMA-1	Office of Highway Works	unknown
Kutahya Sivil Savunma Mudurlugu	KUT	39.419N 29.997E	unknown	GSR-16	Office of Civil Defense	unknown
Manisa Bayindirlik Binasi	MNS	38.580N 27.450E	unknown	SM-2	Office of Ministry of Settlement	unknown
Tekirdag Hukümet Konagi	TKR	40.979N 27.515E	unknown	GSR-16	Office of Ministry of Settlement	unknown
Tokat DSI Misafirhanesi	TKT	40.328N 36.554E	unknown	GSR-16	Guest House of Government Water Works	unknown
Tosya Meteoroloji Mudurlugu	TOS	41.013N 34.037E	unknown	GSR-16	Meteorological Observatory	unknown
Usak Meteoroloji Istasyonu	USK	38.671N 29.404E	unknown	GSR-16	Meteorological Observatory	unknown

Instruments Operated by Bogazici University, Kandilli Observatory

Station Name	Abbreviation	Coordinates	Elevation	Instrument	Housing	Ground Conditions
Aksaray?	PER					
Ambarlic Thermic Power Plant	ATS					Hard rock
Asian Cimento?	DAR					
Bursa Tofas Factory	BUR	40.183N 29.131E	unknown			unknown
Botas Gas Terminal?	BTS (BOT)					
Cekmece Nuclear Research Centre	CNA	39.650N 27.860E	unknown			unknown
Fatih Mosque Complex	FAT	40.980N 27.790E	unknown			unknown
Gebze Arcelik Factory	ARC	40.142N 26.402E	unknown	GSR-16	Arcelik Factory Sound Laboratory. Reinforced concrete frame with masonry infill.	Topography is gently rolling hills on elevated plateau. Building on cut platform.
Heybeliada Hospital, Princes Islands	HAS	40.970N 28.700E	unknown			Hard rock Paleozoic age sandstone, mudstone and shale.
Kocamustafapasa Tomb, Istanbul	KMP	38.455N 27.229E	unknown			unknown
Sirkeci?	GB					

Yapi Kredi Plaza, Levent Istanbul	YKP	37.837N 27.838E	unknown			unknown
Yarimca Petkim*	YPT	38.792N 30.561E	unknown	GSR-16	3 storey reinforced concrete building with masonry infill, building dimensions 40m x 12m. Floor slab is slightly above grade.	Flat to very gently south sloping topography on coastal plain river delta. Underlain by Quaternary deposits (clay/silt/sand). Building constructed on cut and fill platform. Height of fill at front approx. 1m .
Yesilkoy Airport	DHM					

Instruments Operated by Istanbul Technical University

Station Name	Abbreviation	Coordinates	Elevation	Instrument	Housing	Ground Conditions
Atakoy	ATK	40.989N 28.849E	unknown			unknown
Mecidiyekoy	MSK	41.104N 29.010E	unknown			unknown
Maslak	MCK	41.065N 28.990E	unknown			unknown
Zeytinburnu	ZYT	40.986N 28.908E	unknown			unknown

* Stations visited by EEFIT

Table 3A.2 Strong-Motion Records 17 August 1999 Kocaeli Earthquake**Instruments Operated by Bogazici University, Kandilli Observatory (KOERI)**

Station Name	Abbreviation	Fault Distance (km)	PGA L (mG)	PGA T (mG)	PGA V (mG)	Ground Conditions
Ambarlic Thermic Power Plant	ATS	82	180.	252.6	80.1	soft soil
Arcelik Factory, Gebze	ARC	20	211.4	133	83.3	stiff soil
Bursa Tofas Factory	BUR	72	100.9	100	48.2	soft soil
Botas Gas Terminal?	BTS (BOT)	141	98.9	87.	23.6	stiff soil
Cekmece Nuclear Research Centre	CNA	78	132	177.3	57.7	stiff soil
Fatih Mosque Complex	FAT	67	162	189.4	131.7	soft soil
Heybeliada Hospital, Princes Islands	HAS	46	110.2	142.	143.5	rock
Yapi Kredi Plaza, Levent Istanbul	YKP	64	36.	41.1	27.1	rock
Yarimca Petkim	YPT	4 (2.6 ²)	262.	298.	241.9	soft soil ²
Hava Alani Yesilkoy Airport	DHM	72	84.	90.2	55.1	stiff soil

Instruments Operated by Istanbul Technical University (ITU)

Station Name	Abbreviation	Fault Distance (km)	PGA L (mG)	PGA T (mG)	PGA V (mG)	Ground Conditions
Atakoy	ATK	76	103	168	68	stiff soil
Mecidiyekoy	MCD	65	54	70	38	shallow stiff soil
Maslak	MSK	89	54	38	31	rock
Zeytinburnu	ZYT	66	120	109	51	stiff soil

Instruments Operated by the Earthquake Research Department of the General Directorate of Disaster Affairs (ERD)

Station Name	Abbreviation	Fault Distance (km)	PGA L (mG)	PGA T (mG)	PGA V (mG)	Ground Conditions
Adapazari (Sakarya)	SKR	3 (3.1 ²)	407.	-	259	Rock (1-3m soil)
Afyon Bayindirlik ve Iskan Mudurlugu	AFY	215	13.5	15	5	unknown
Aydin Hayvan Hastanesi	AYD	353	5.9	5.2	3.3	unknown
Balikesir Huzur Evi	BLK	192	17.8	18.2	7.6	unknown

Bolu Bayindirlik ve Iskan Mudurlugu		48				
Bornova Ziraat Fakultesi Dekanligi (Izmir)	BRN	325	9.9	10.8	3.3	unknown
Bursa Sivil Savunma Mudurlugu	BRS	72	45.8	54.3	25.7	stiff soil
Canakkale Meteoroloji Istasyonu	CNK	283	24.6	28.6	7.9	unknown
Cekmece Nukleer Santral Binasi (Istanbul)	CEK	81	89.6	118	49.8	unknown
Duzce	DZC	14 (12.7 ²)	356.5	305.8	480.0	soft soil ²
Eregli Kaymakalik Binasi (Tekirdag)	ERG	156	91.4	101.4	57	unknown
Gebze Tubitak Marmara Arastirma Merkezi		18 (5-30 ²)	144.	266.	196.	rock ²
Goynuk (Bolu)		37 (35.49 ²)	117.8	137.7	129.9	rock ²
Istanbul Bayindirlik ve Iskan Mudurlugu	IST	59	42.7	60.7	36.2	stiff soil
Izmit Meteoroloji Istasyonu	IZT	7 (4.8 ²)	224.9	171.2	146.4	rock ²
Izmit Karayollari Sefligi	IZN	32 (31.8 ²)	123.3	91.8	82.3	soft soil
Kutahya Sivil Savunma Mudurlugu	KUT	144	50	59.7	23.2	soft soil
Manisa Bayindirlik Binasi	MNS	302	12.5	6.5	4.5	unknown
Tekirdag Hukumet Konagi	TKR	178	32.2	33.5	10.2	unknown
Tokat DSI Misafirhanesi	TKT	465	0.8	1.2	0.4	unknown
Tosya Meteoroloji Mudurlugu	TOS	248	11.7	8.9	4.4	unknown
Usak Meteoroloji Istasyonu	USK	227	8.9	7.2	3.4	unknown


fault distance = distance to fault rupture

fault rupture alignment from Lettis et al. (2000)

² = distance values from Anderson *et al.* (2000)

APPENDIX 3B: DESCRIPTIONS OF 5 STRONG MOTION SITES VISITED

Station Name: Gebze	Abbreviation: GBZ
Co-ordinates: N 40.820 E 29.440	Elevation: unknown
Instrument Type: SMA-1	Instrument Orientation: L = N - S T = E -W
Station Address: Tubitak Marmara Arastirma Merkezi, Gebze	
Station Owner: Earthquake Research Department of General Directorate Affairs	
Instrument Location Details: Basement floor of 4 storey reinforced concrete structure. Instrument located near outside wall, beneath staircase adjacent to single storey covered walkway.	
	
Station Topography: Cut and fill benched slope at top of 5 degree slope.	
Regional Geology: Tubitak Marmara Research Centre is located on a hill composed of meta-sedimentary and metamorphic rocks (quartzite, limestone and schist) (Paleozoic Age?). Cut and fill platforms have been formed for the research centre buildings. It is understood that the fill is sourced from recent alluvium deposits.	
Station Ground Conditions: Rock. Details unknown.	

Station Name: Arcelik	Abbreviation: ARC
Co-ordinates: N 40. - E 29. -	Elevation: unknown
Instrument Type: GSR - 16	Instrument Orientation: L = E - W T = N - S
Station Address: Arcelik Acoustic Laboratory Building, Arcelik Factory, Gebze	
Station Owner: Bogazici University	
Instrument Location Details: Basement floor of 1.5 story, 12m x 12m x 6m, reinforced concrete frame with brick infill structure. Instrument located near exterior strip footing on blinding layer between interior strip foundations of structure, 4 m below base isolated acoustic laboratory room (10m x 10m x 3m).	
	
(9/9/99)	
Station Topography: Cut and fill slope benched on less than 5 degree slope. Structure within cut.	
Regional Geology: The Arcelik Facility is located in a shallow valley within a plateau composed of meta-sedimentary and metamorphic rocks (quartzite, limestone and schist) (Devonian Age?). Cut and fill platforms have been formed for the facility buildings.	
Station Ground Conditions: Details unknown.	

Station Name: Yarimca Petkim	Abbreviation: YPT
Co-ordinates: N 40.45.51 E 29.45.35.7	Elevation: 13mPD
Instrument Type: GSR-16	Instrument Orientation: L = E -W T = N - S
Station Address: Petkim Administration Building, Yarimca	
Station Owner: Bogazici University	
Instrument Location Details: Elevated ground floor of 3 story reinforced concrete structure. Instrument located near outside wall. Ground floor elevated 1.0m to 1.5m.	
	
(9/9/99)	
Station Topography: Gentle slope down to flat coastal plain. Administration block is located on a cut and fill platform.	
Regional Geology: Yarimca is located near the fault boundary between the old meta-sedimentary and metamorphic rocs (Silurian Age?) and coastal Quaternary deposits.	
Station Ground Conditions: Soil. Details unknown.	

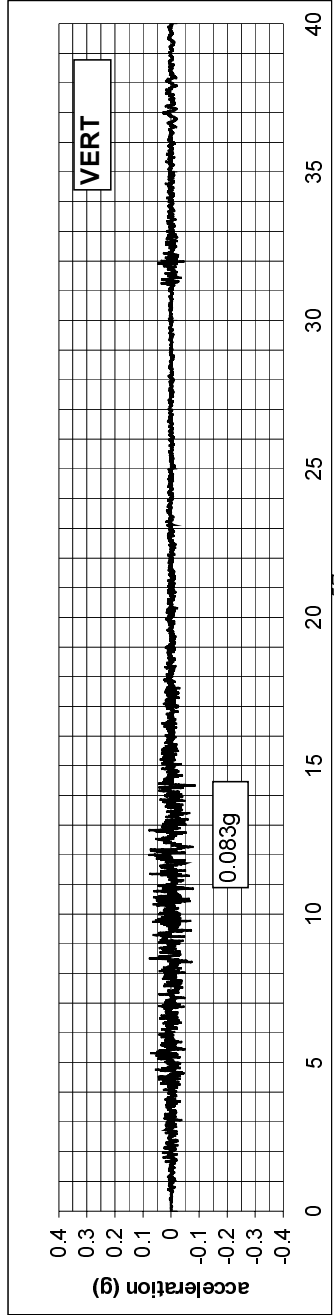
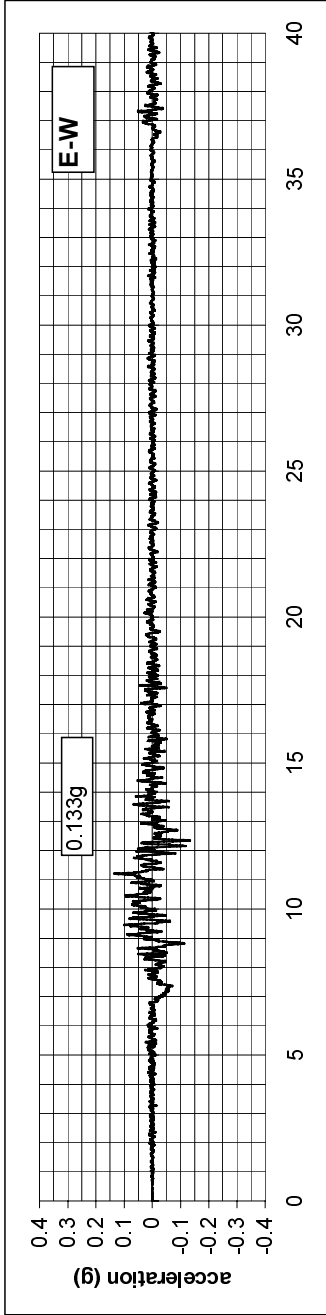
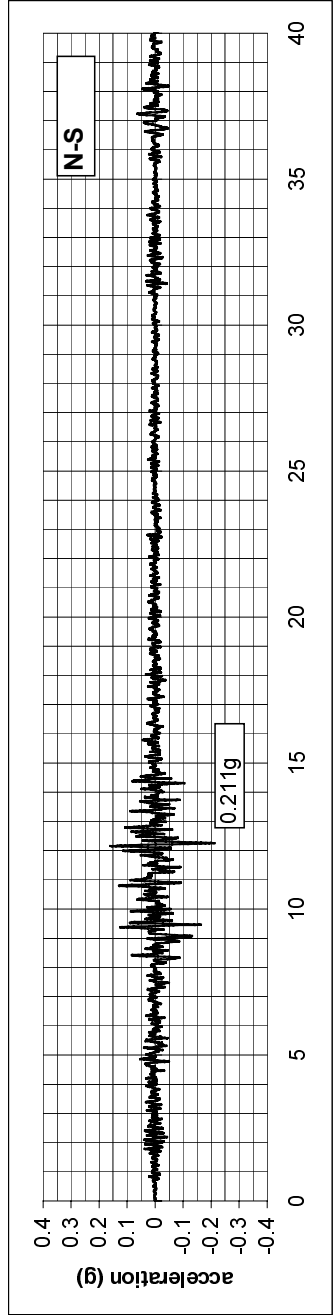
Station Name: Sakarya (Adapazari)	Abbreviation: SKR
Co-ordinates: N 40.737 E 30.384	Elevation: unknown
Instrument Type: GSR - 16	Instrument Orientation: L = 170 - 350 T = 80 - 260
Station Address: Office of Ministry of Development	
Station Owner: Earthquake Research Department of General Directorate of Disaster Affairs	
Instrument Location Details: Ground floor of single story, 13m x 5m x 3.5m, wood frame structure. Instrument located on 0.6m x 0.6m x 0.35m pedestal on grade.	
	
(9/9/99)	
Station Topography: The station is located on a south facing approximately 10 degree slope on a hill on the northern side of Adapazari. The housing structure is located at the edge of a 30m wide cut platform bench at 40m to 50m above the Adapazari plain level.	
Regional Geology: The hill is composed of meta-sedimentary and metamorphic rocks (sandstone, mudstone, schist)(Devonian Age?).	
Station Ground Conditions: Rock. Details unknown.	

Station Name: Düzce	Abbreviation: DZC
Co-ordinates: N 40.850 E 31.170	Elevation: unknown
Instrument Type: SMA-1	Instrument Orientation: L = 80 - 260 T = 170 - 350
Station Address: Duzce Meteorological Observatory	
Station Owner: Earthquake Research Department of General Directorate of Disaster Affairs	
Instrument Location Details: Ground floor of 1.5 story reinforced concrete structure. Instrument in front room near outside wall.	
	
12/9/99	
Station Topography: Flat	
Regional Geology: Duzce plain is located within a graben infilled by recent, predominantly alluvium, deposits comprising alternating clays, sands and gravels to a depth of 70mbgl. The ground water level is 2 to 7mbgl.	
Station Ground Conditions: Soil. Details unknown.	

APPENDIX 3C: STRONG GROUND MOTIONS RECORDS AND RESPONSE SPECTRA

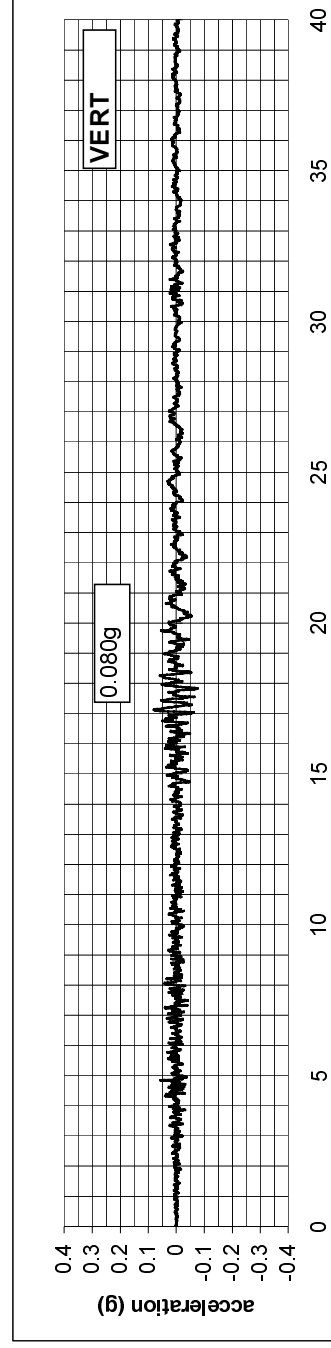
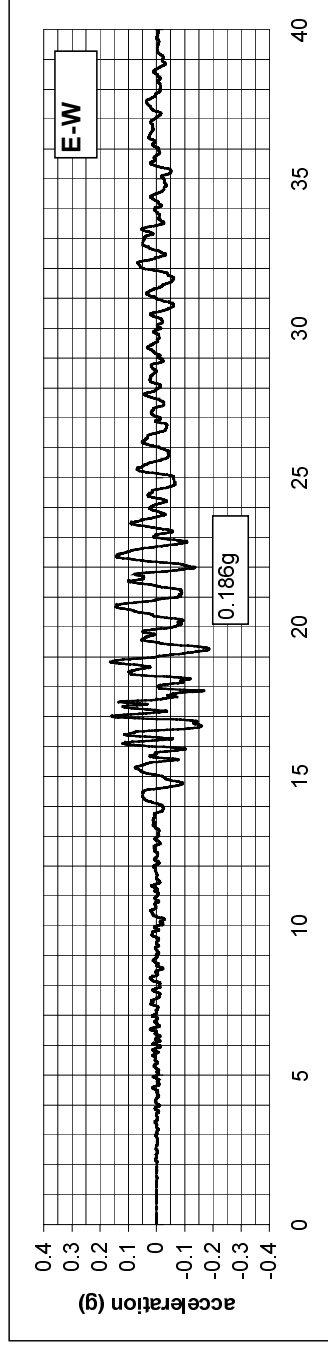
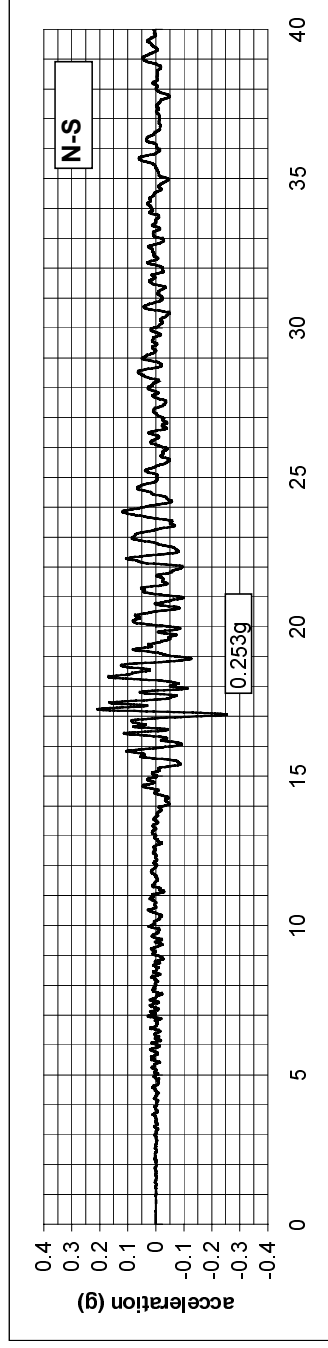
Event: Kocaeli, Turkey 17 August 1999
Station: Arcelik Factory, Gebze
Code: ARC

Ground Conditions: Unknown
Distance: 20 km



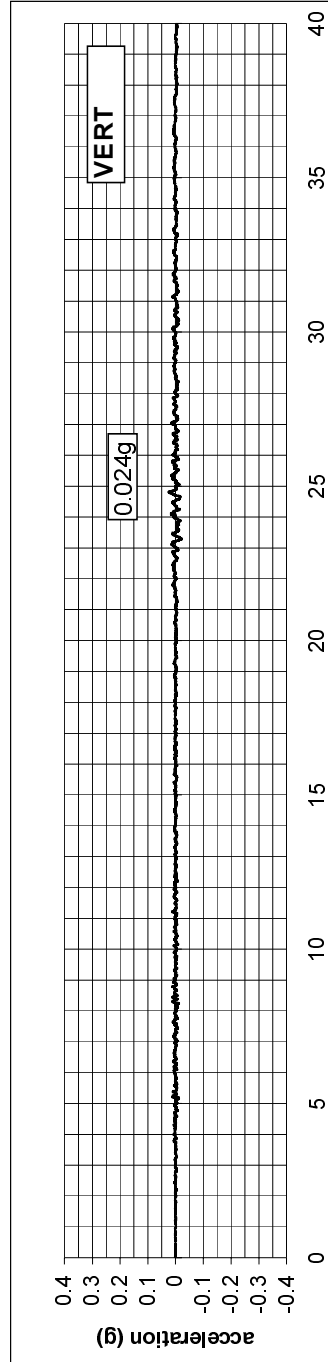
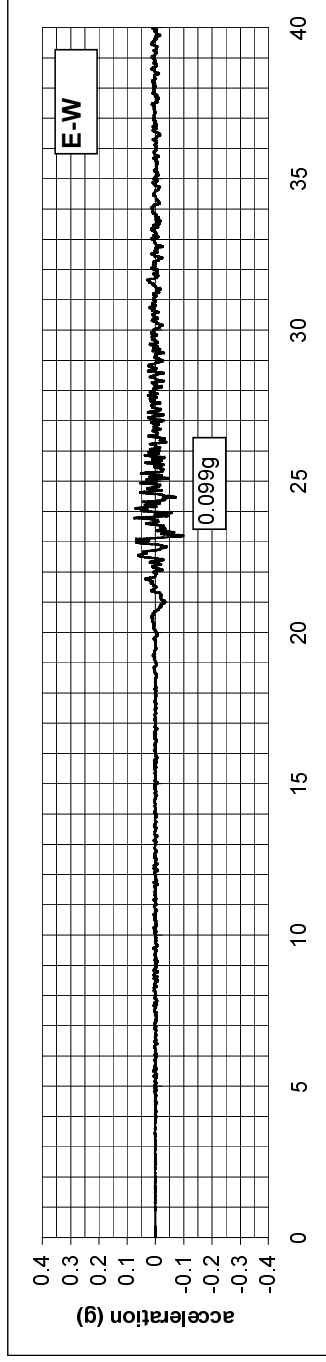
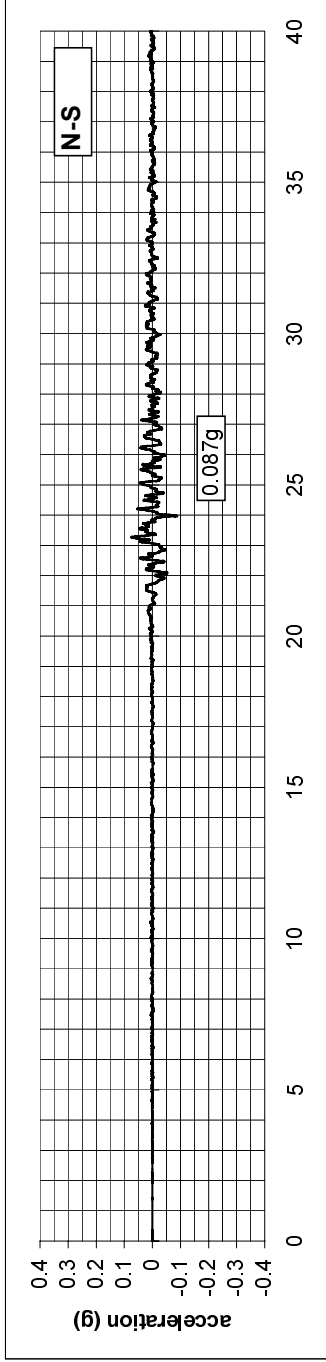
Event: Kocaeli, Turkey 17 August 1999
Station: Ambarlic Thermic Power plant
Code: ATS

Ground Conditions: Rock
Distance: 82 km



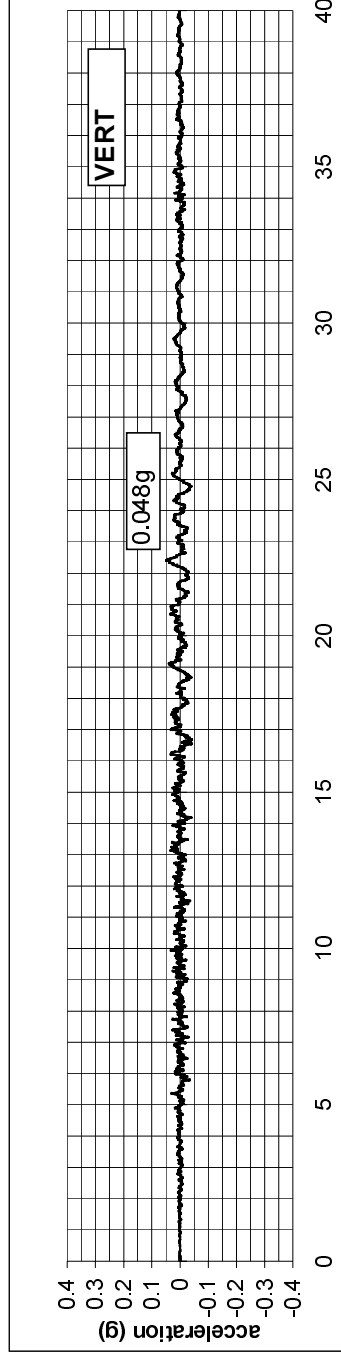
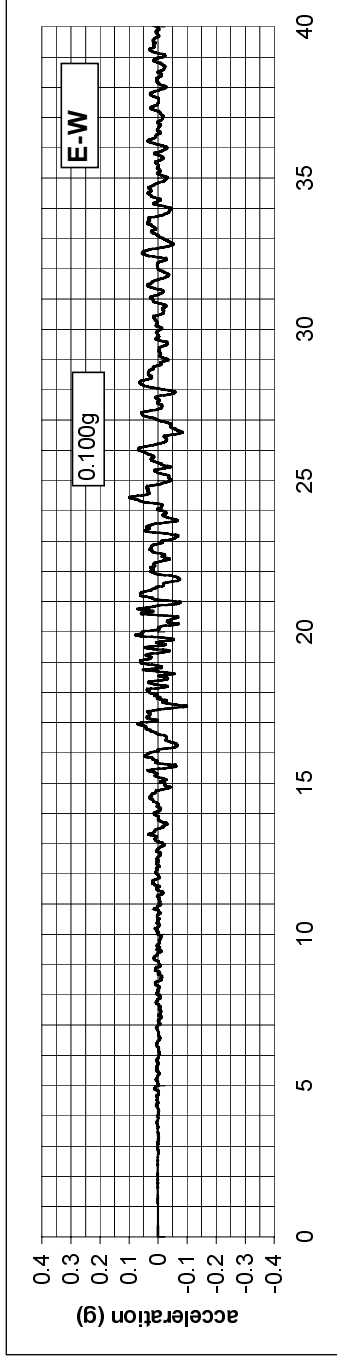
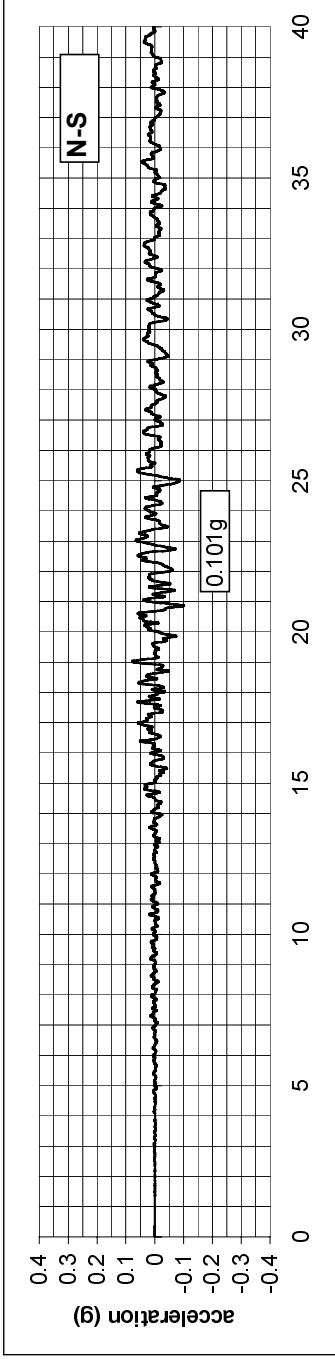
Event: Kocaeli, Turkey 17 August 1999
Station: Botas Gas Terminal?
Code: BTS (BOT)

Ground Conditions: Unknown
Distance: 141 km



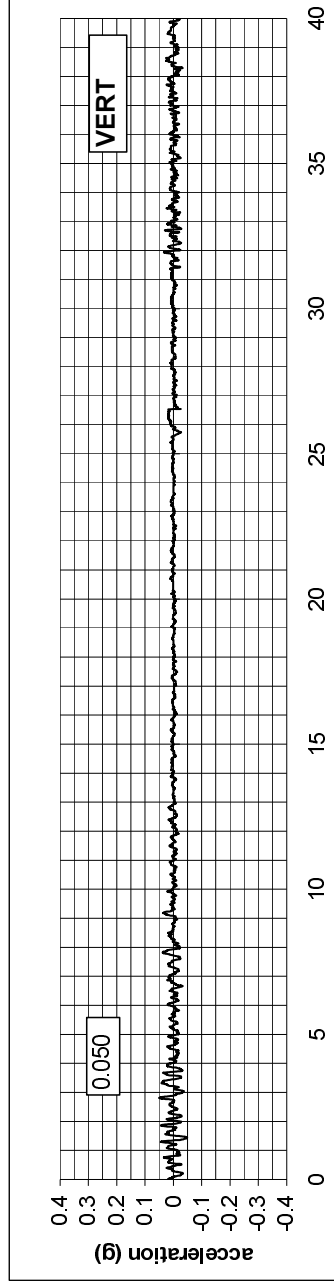
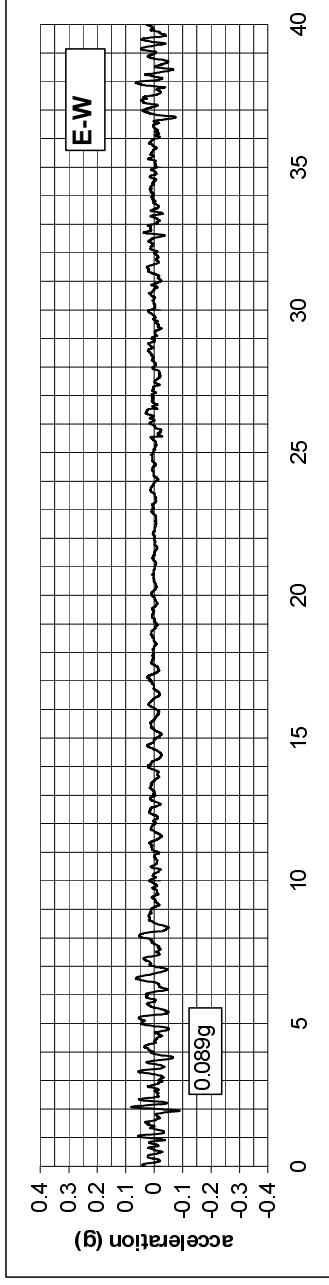
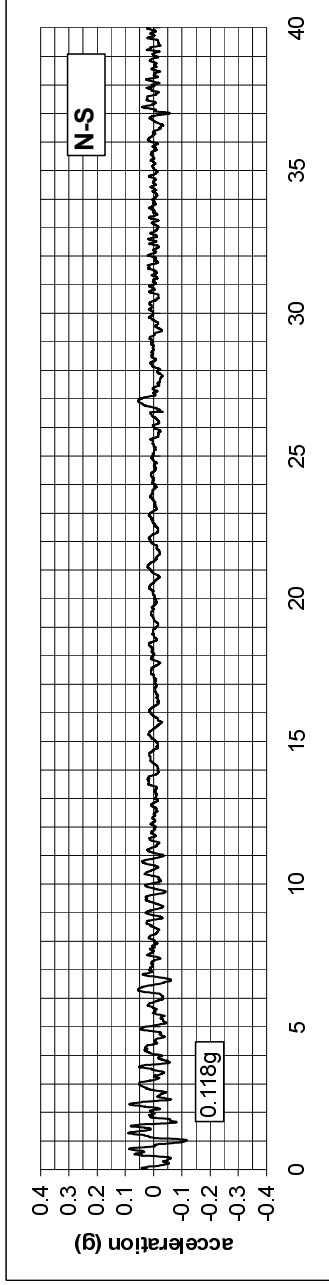
Event: Kocaeli, Turkey 17 August 1999
Station: Bursa Tofas Fabrikasi
Code: BUR

Ground Conditions: Unknown
Distance: 72 km



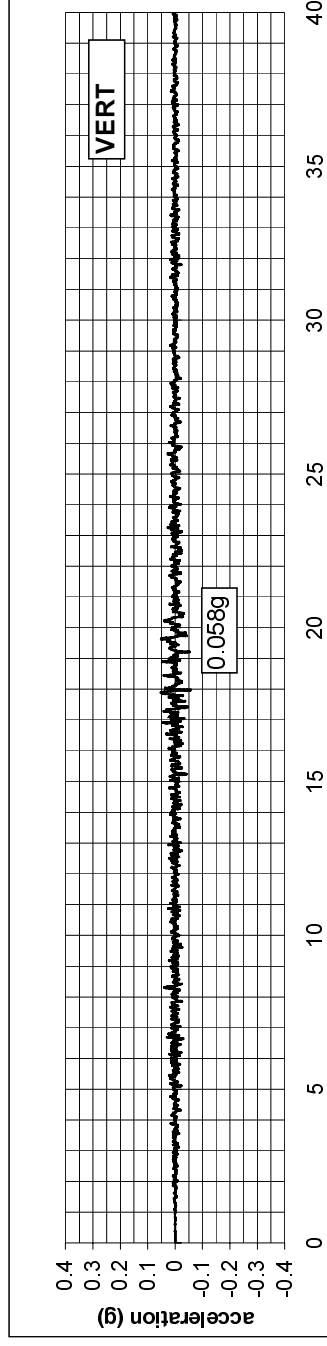
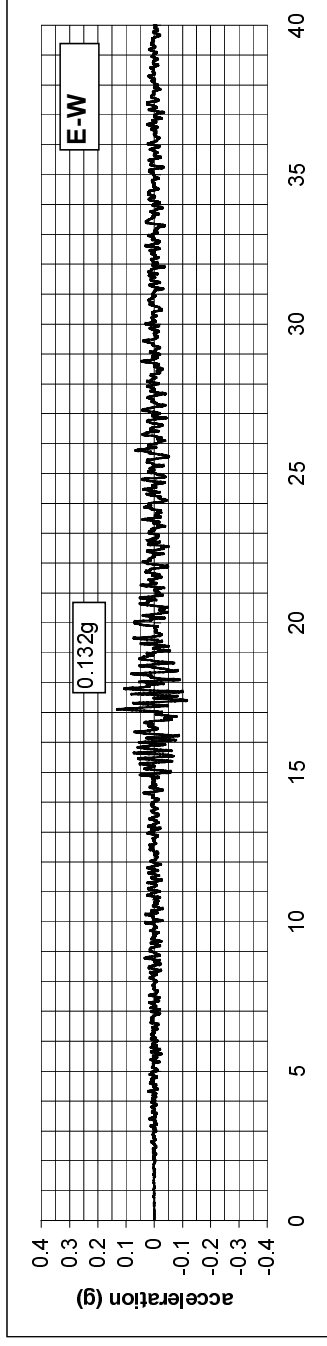
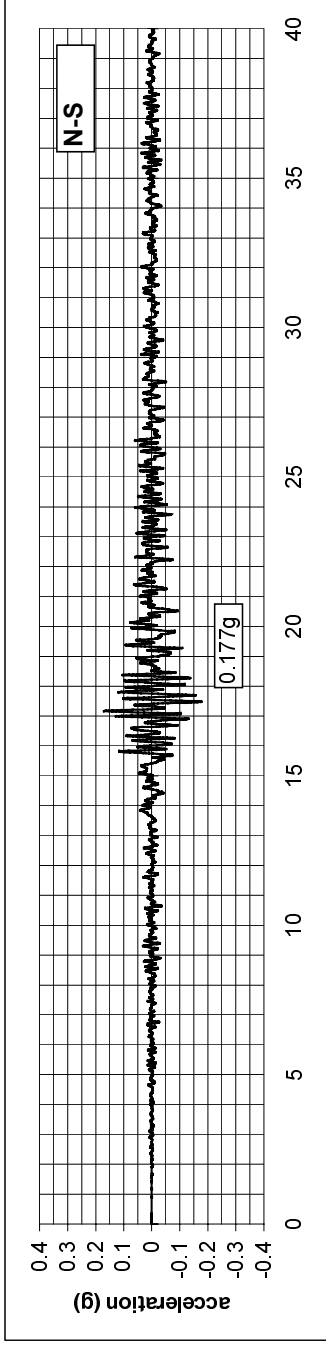
Event: Kocaeli, Turkey 17 August 1999
Station: Cekmece Nuclear Research Centre
Code: CEK

Ground Conditions: Unknown
Distance: 81 km



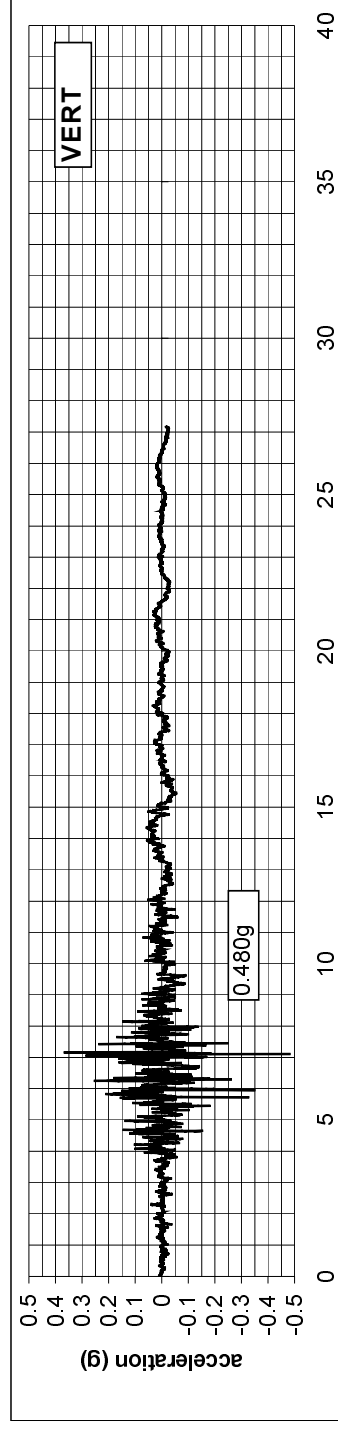
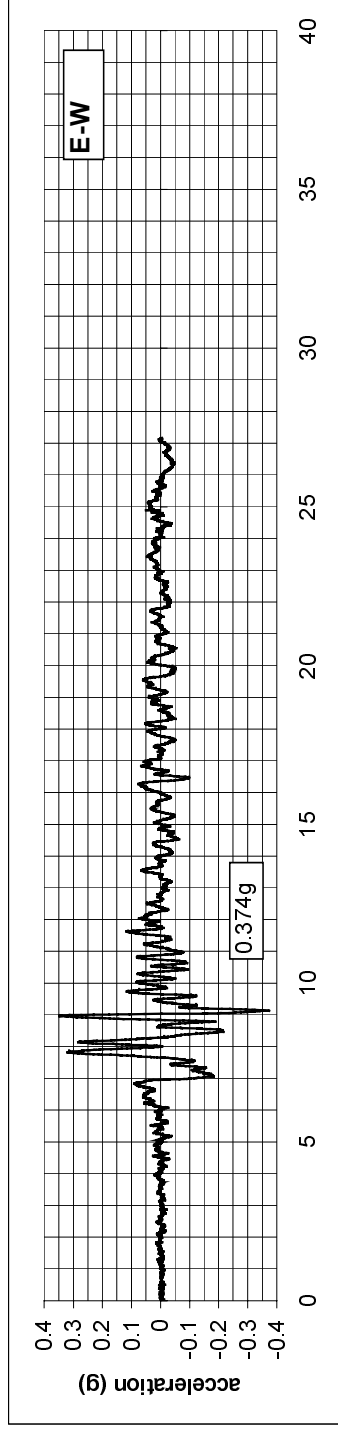
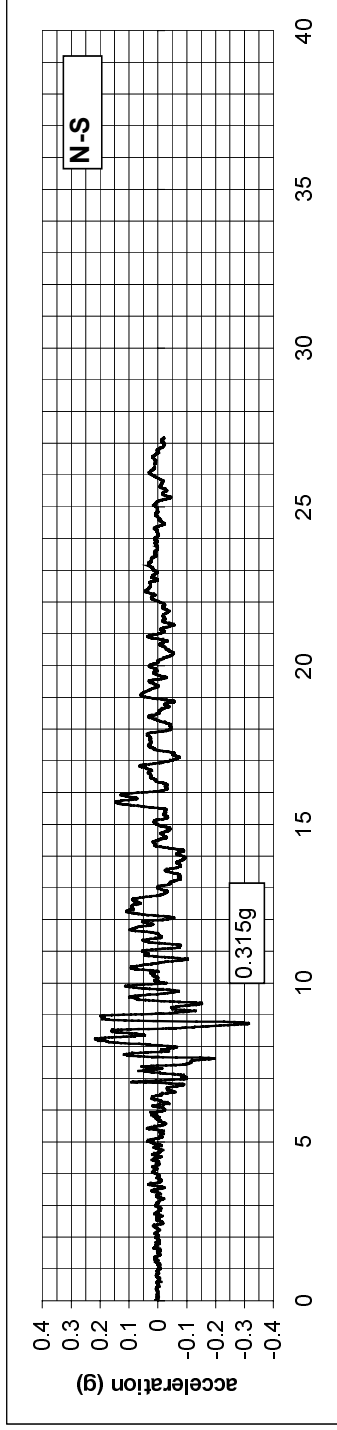
Event: Kocaeli, Turkey 17 August 1999
Station: Cekemece Nuclear Research Centre
Code: CNA

Ground Conditions: Unknown
Distance: 78 km



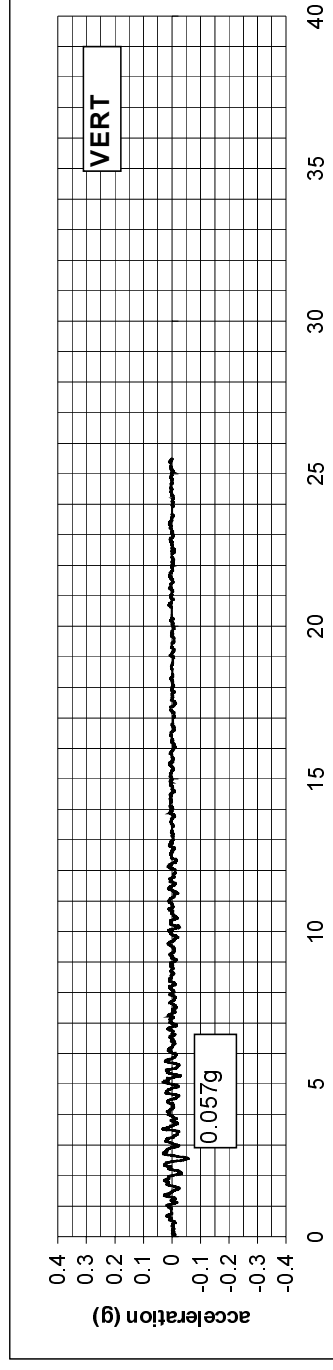
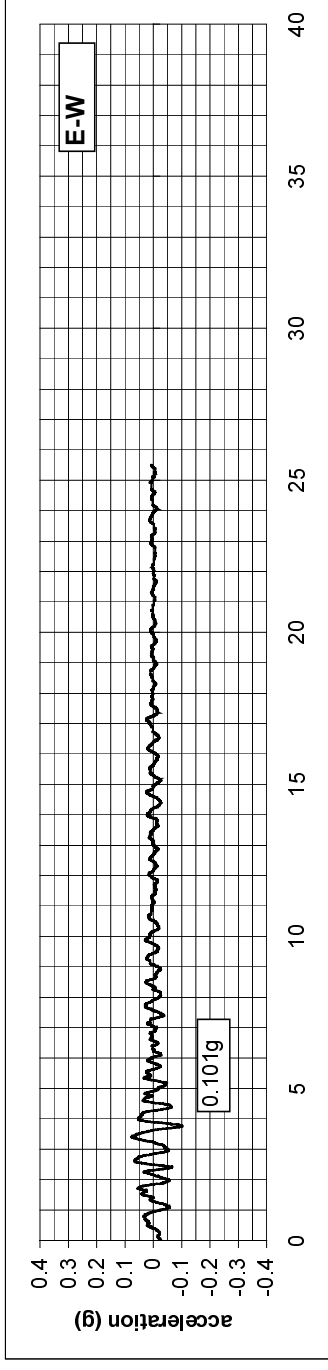
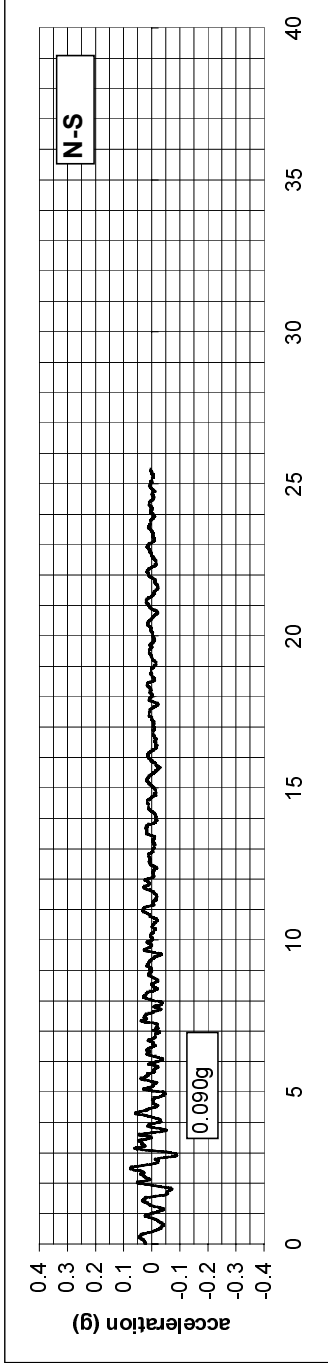
Event: Kocaeli, Turkey 17 August 1999
Station: Duzce Meterologi Istasyonu
Code: DZC

Ground Conditions: Soil
Distance: 14 km



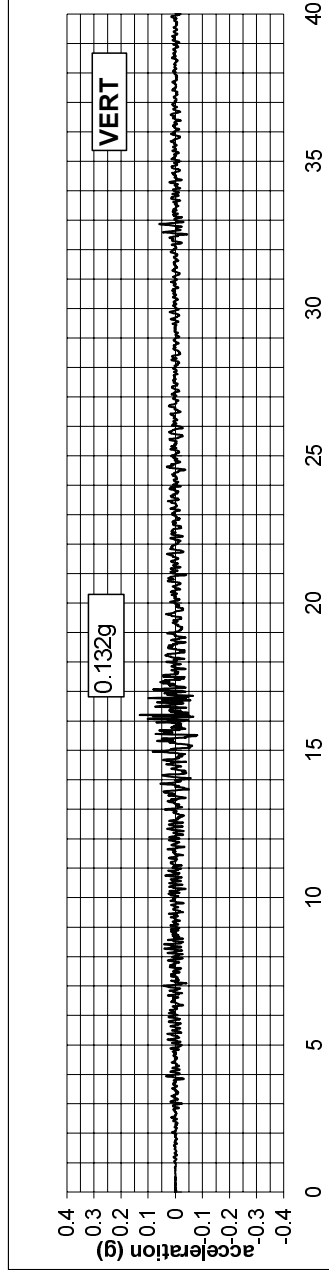
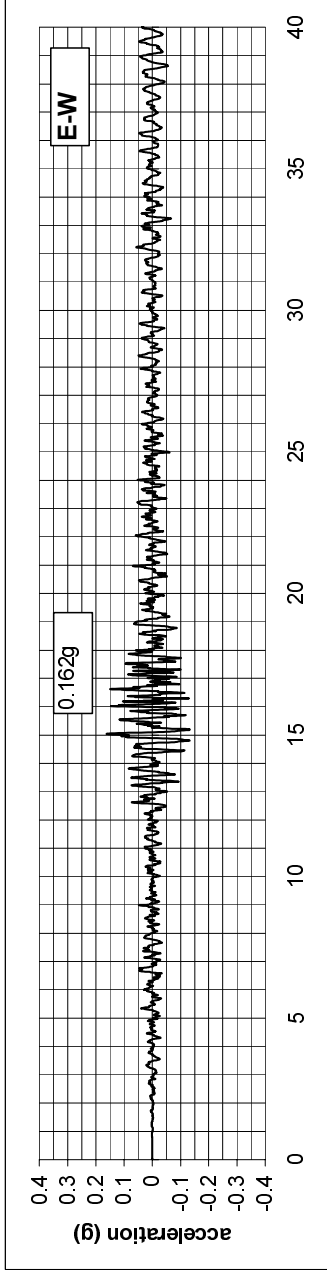
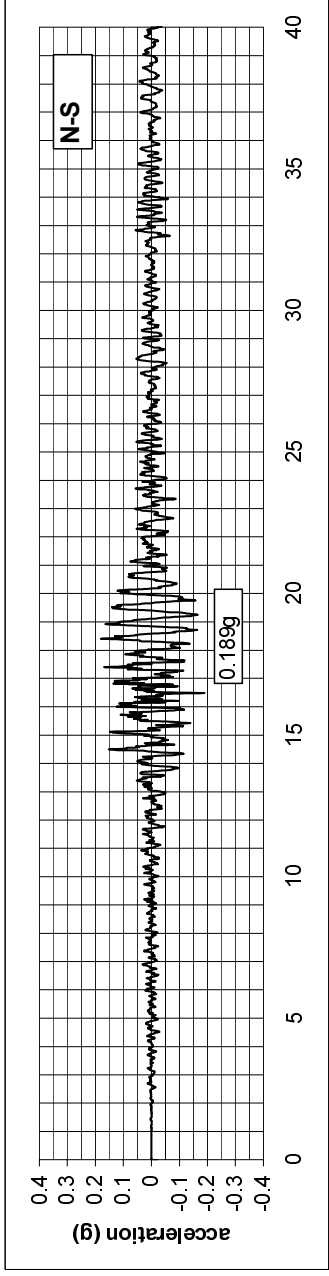
Event: Kocaeli, Turkey 17 August 1999
Station: Ereğli Kaymakamlık Binası
Code: ERG

Ground Conditions: Rock
Distance: 156 km



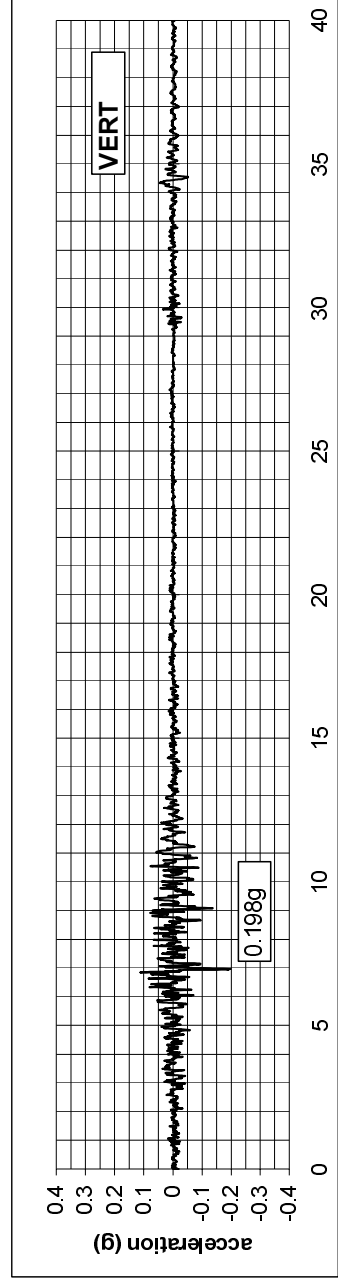
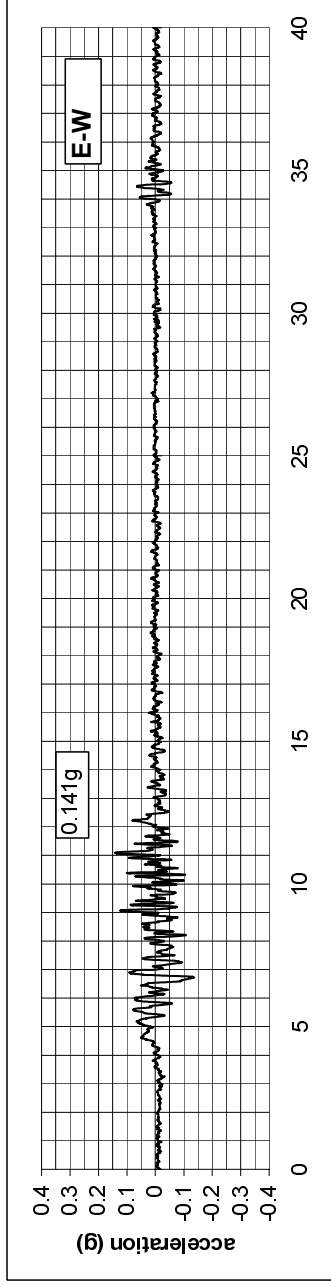
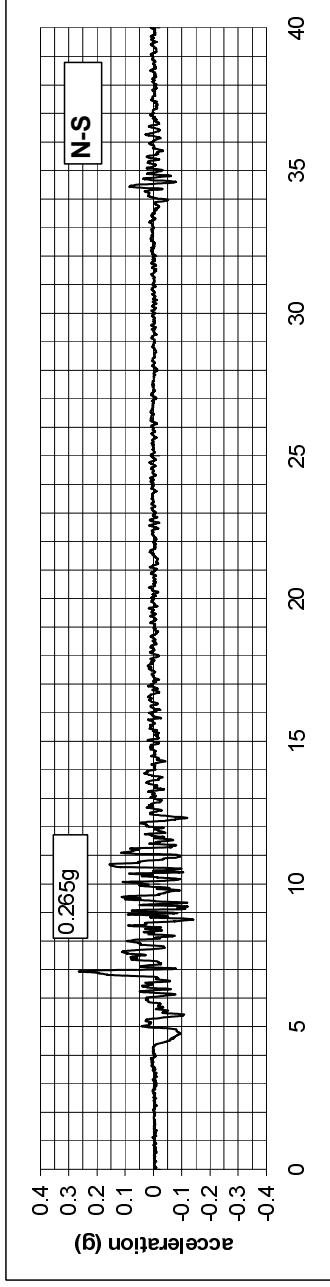
Event: Kocaeli, Turkey 17 August 1999
Station: Fatih Mosque Complex
Code: FAT

Ground Conditions: Unknown
Distance: 67 km



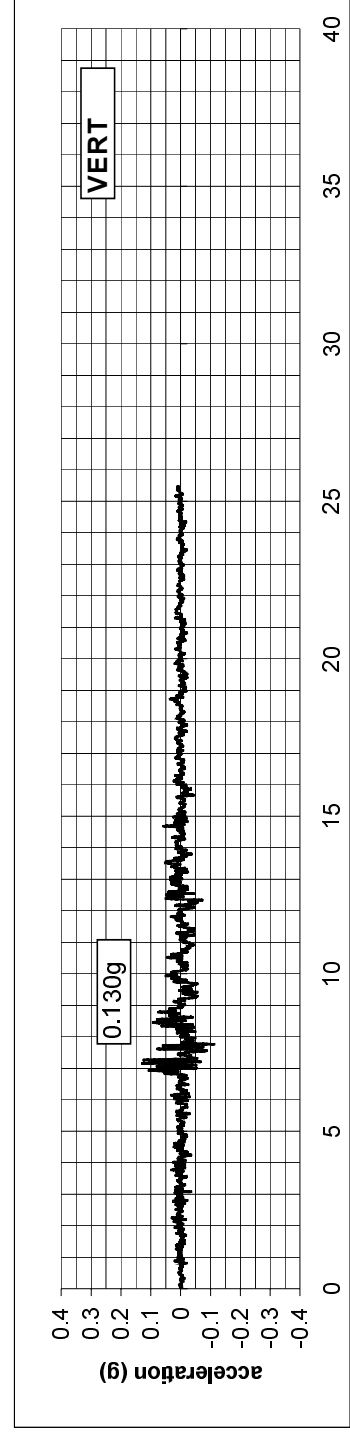
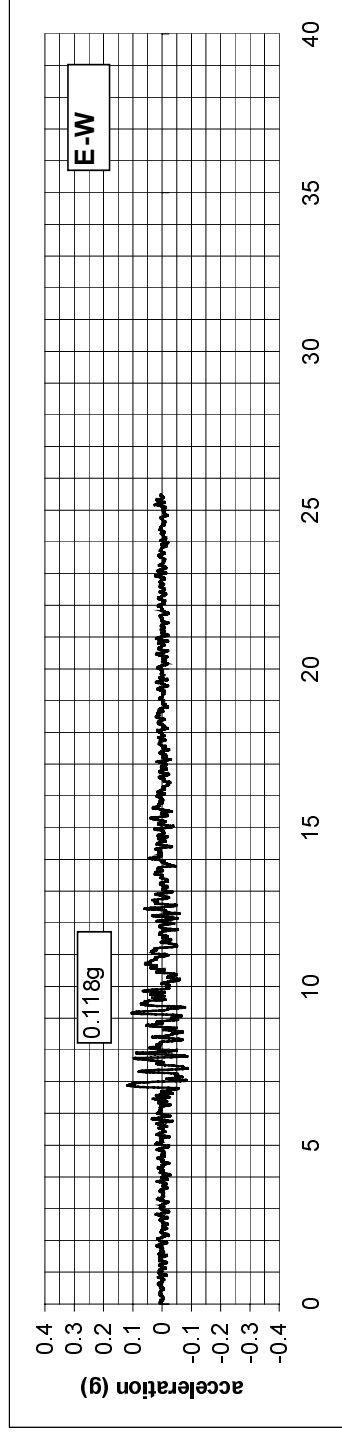
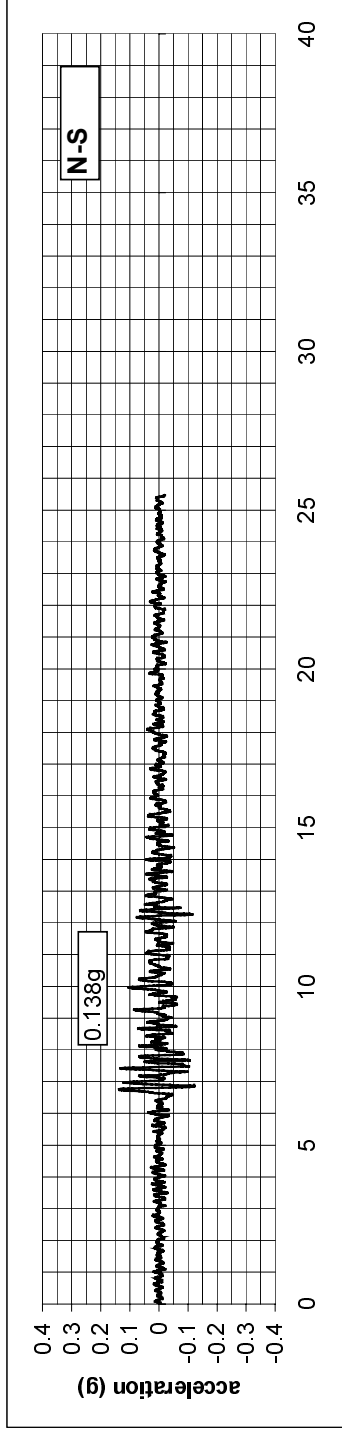
Event: Kocaeli, Turkey 17 August 1999
Station: Gebze Tubitak
Code: GBZ

Ground Conditions: Rock
Distance: 18 km



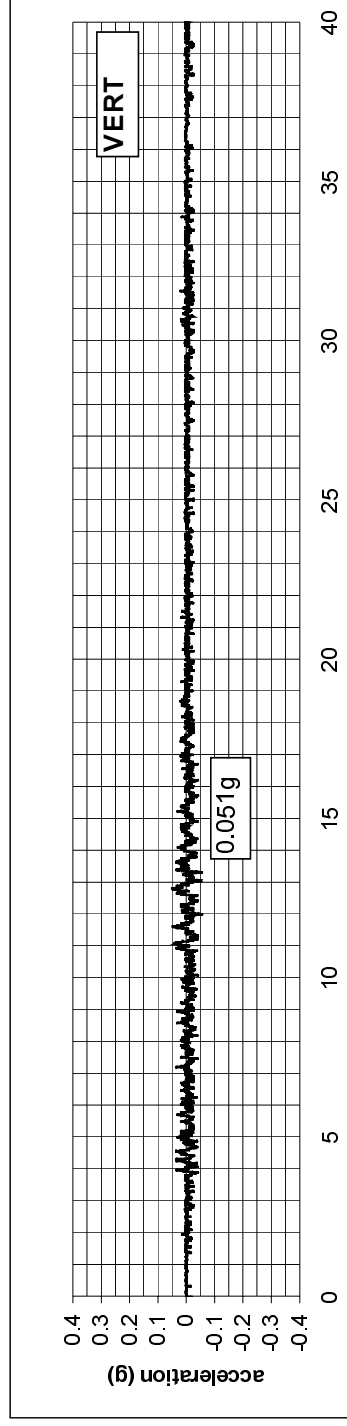
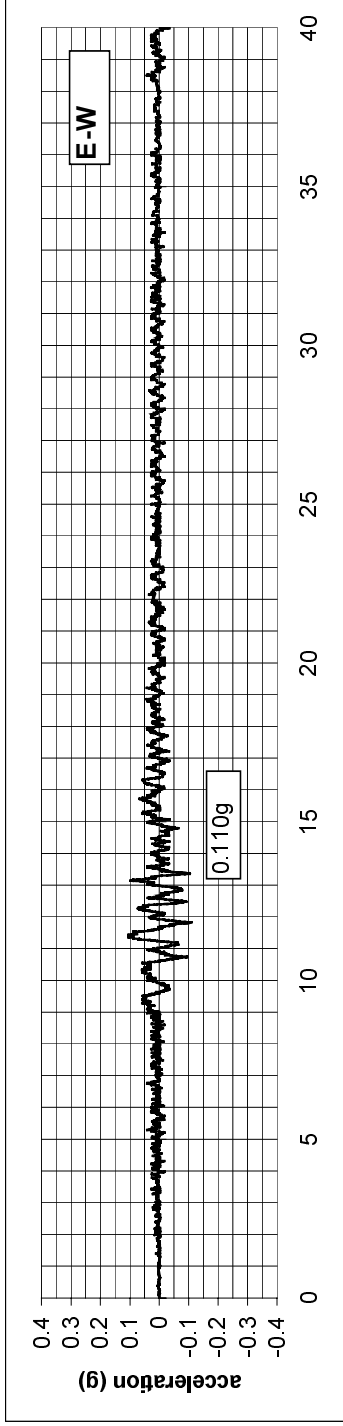
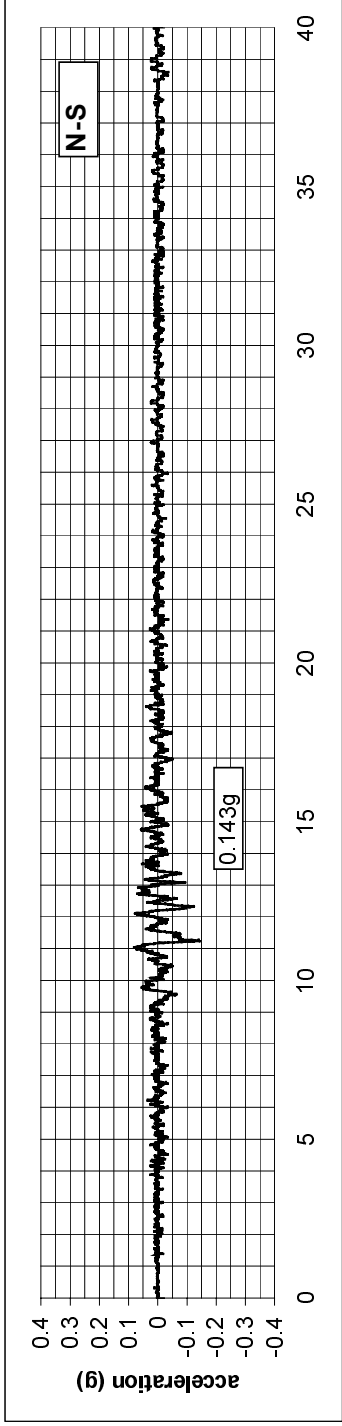
Event: Kocaeli, Turkey 17 August 1999
Station: Goynuk Devlet Hastanesi
Code: GYN

Ground Conditions: Rock
Distance: 37 km



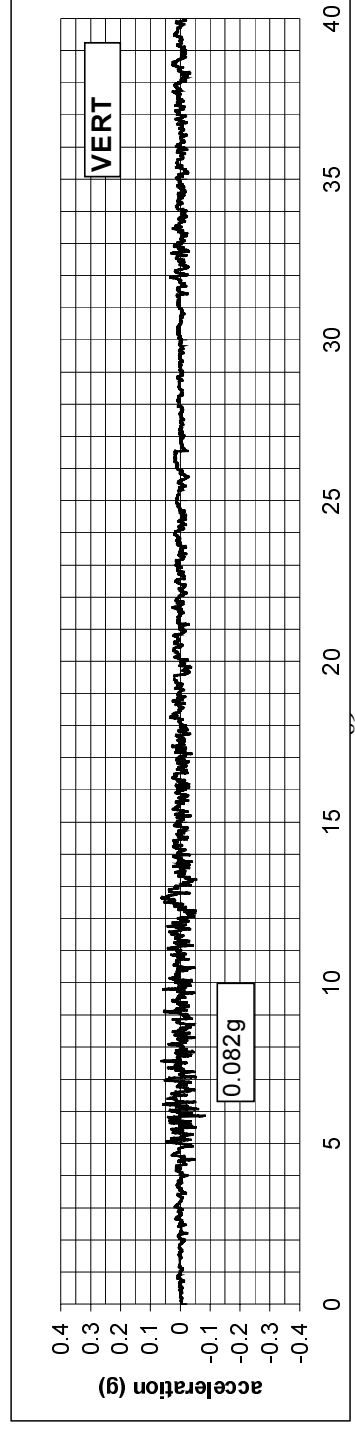
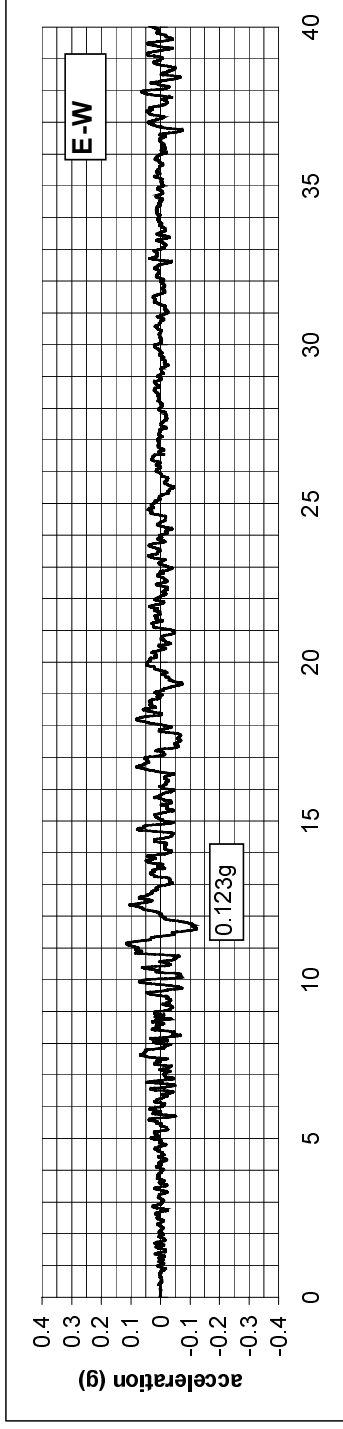
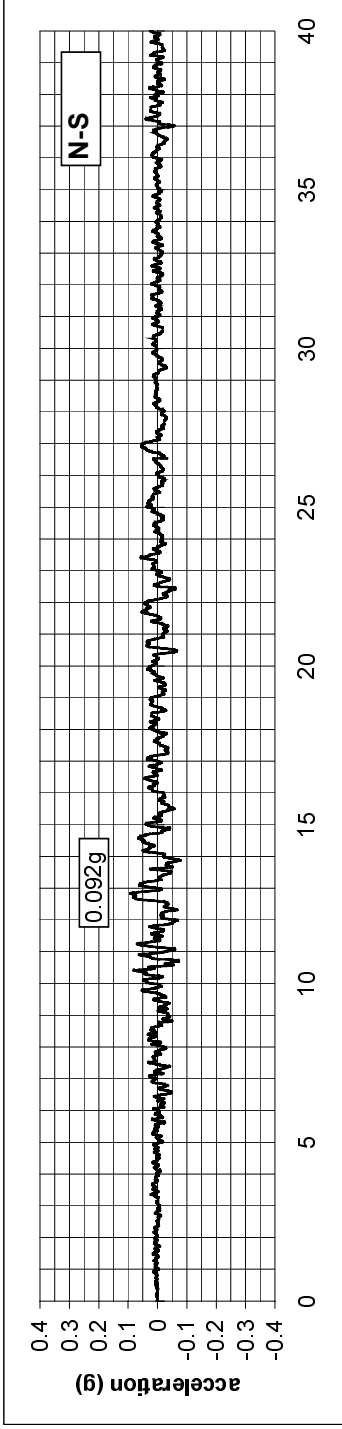
Event: Kocaeli, Turkey 17 August 1999
Station: Heybeliada Hospital
Code: HAS

Ground Conditions: Rock
Distance: 46 km



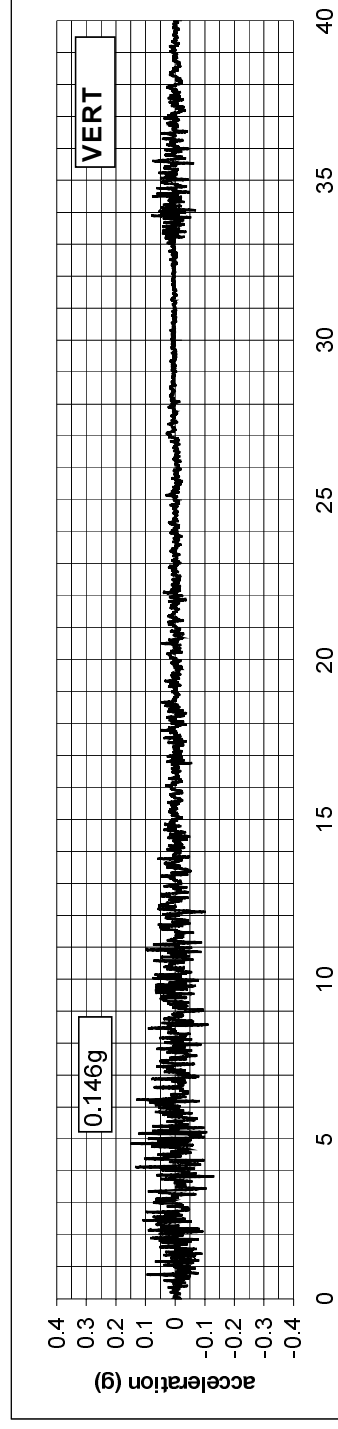
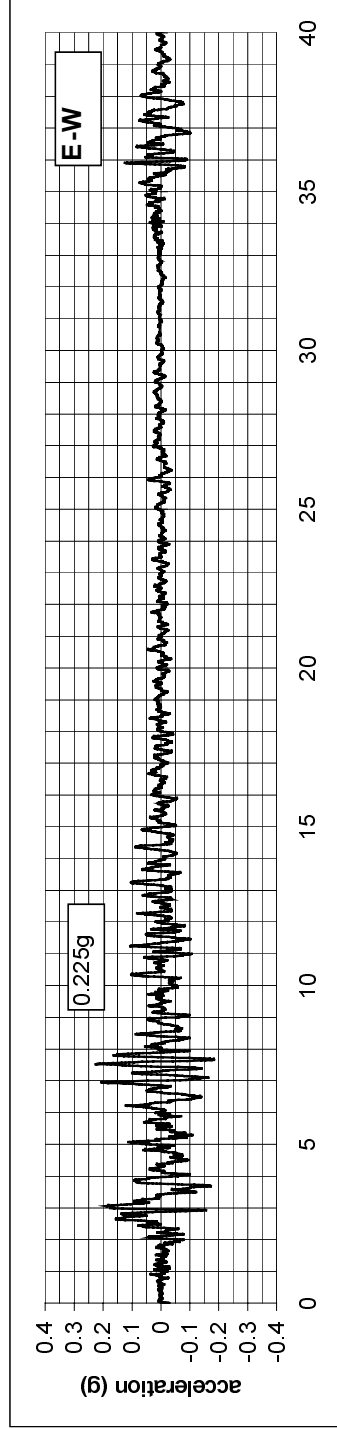
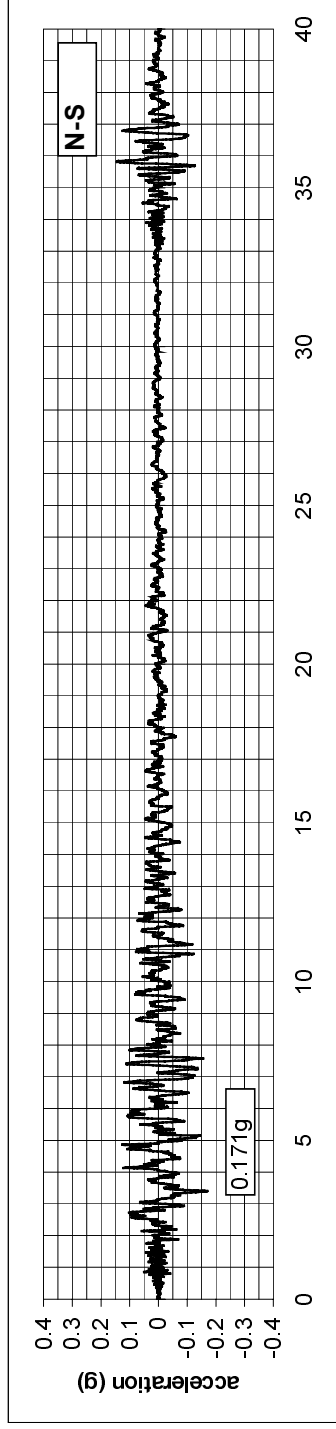
Event: Kocaeli, Turkey 17 August 1999
Station: Iznik Karayollari Sefligi
Code: IZN

Ground Conditions: Unknown
Distance: 32 km



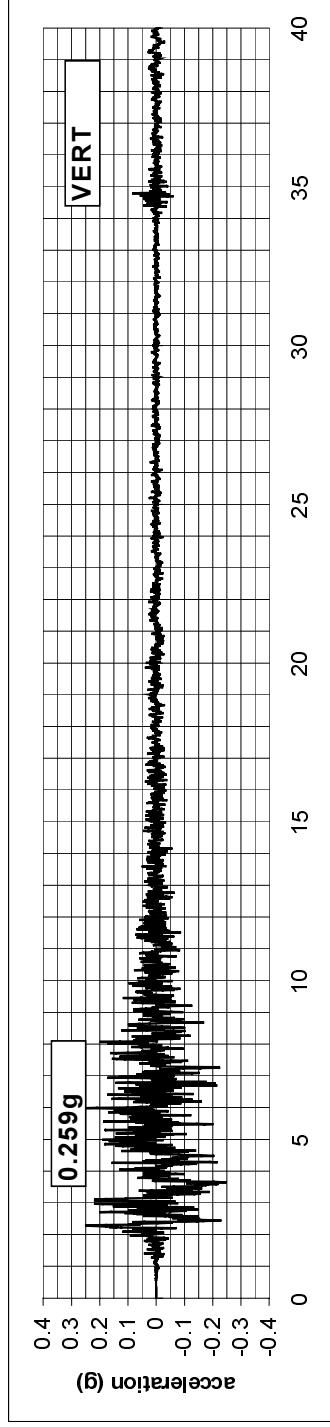
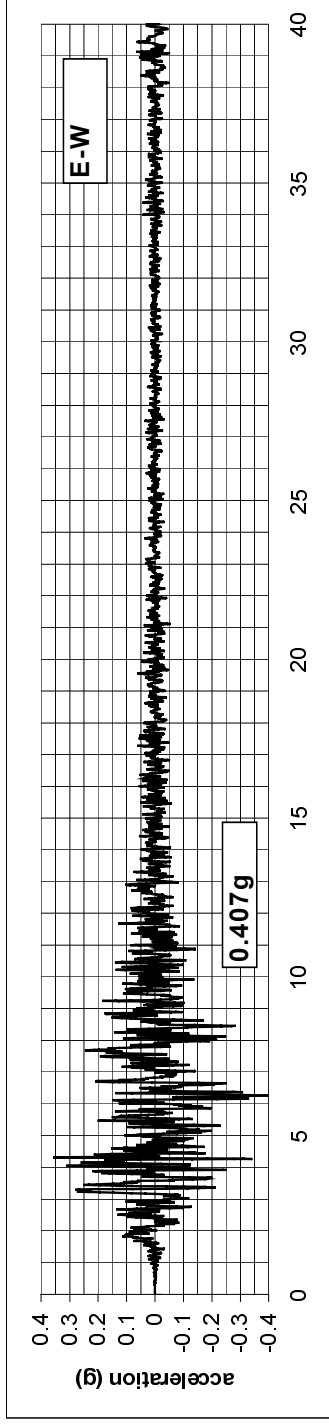
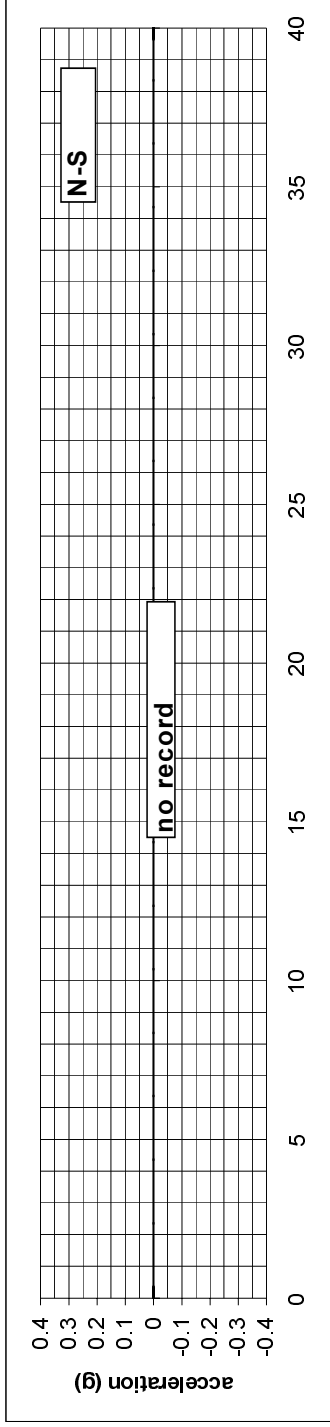
Event: Kocaeli, Turkey 17 August 1999
Station: Izmit Meteoroloji Istasyonu
Code: IZT

Ground Conditions: Rock
Distance: 7 km



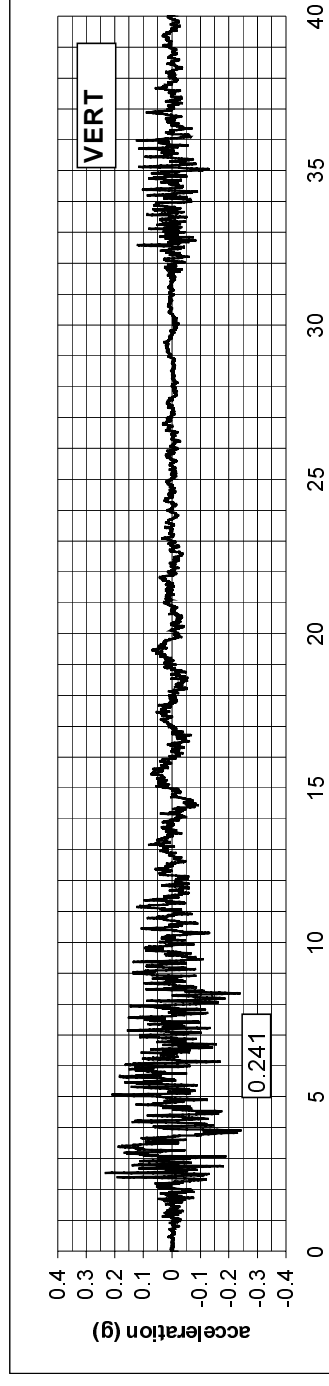
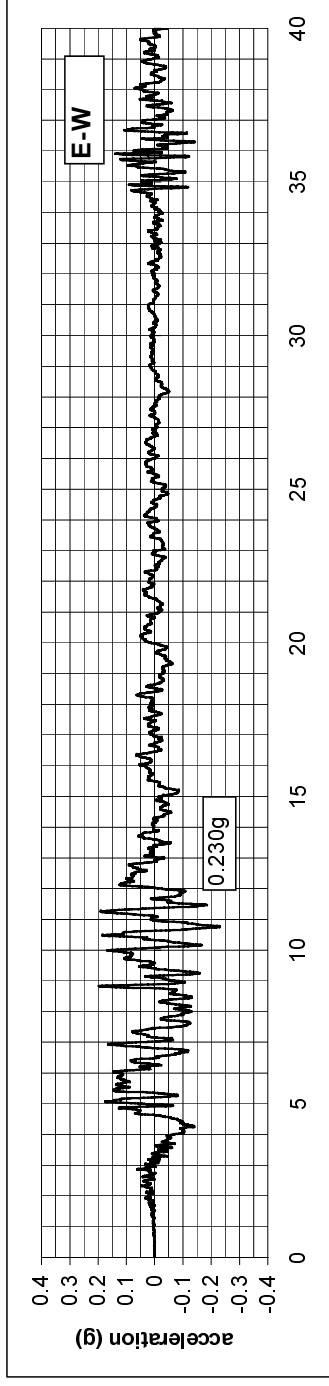
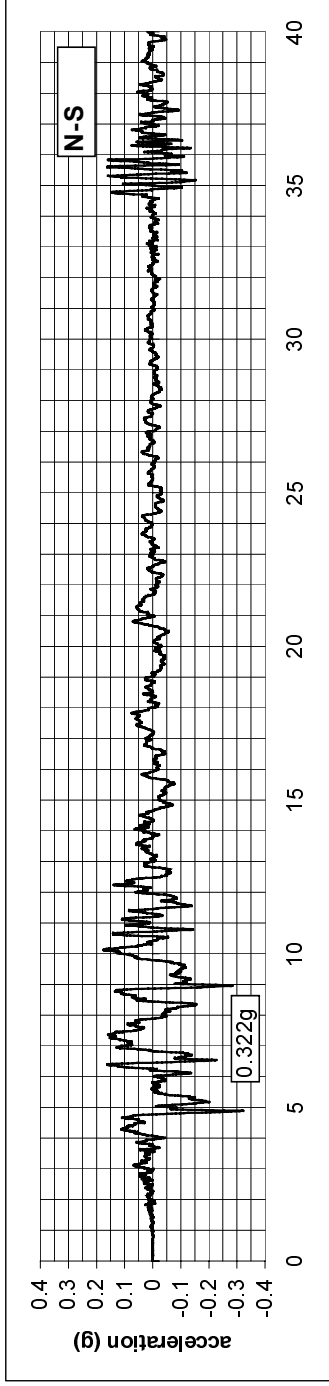
Event: Kocaeli, Turkey 17 August 1999
Station: Adapazari (Sakarya)
Code: SKR

Ground Conditions: Rock
Distance: 3 km



Event: Kocaeli, Turkey 17 August 1999
Station: Yarimca Petkim
Code: YPT

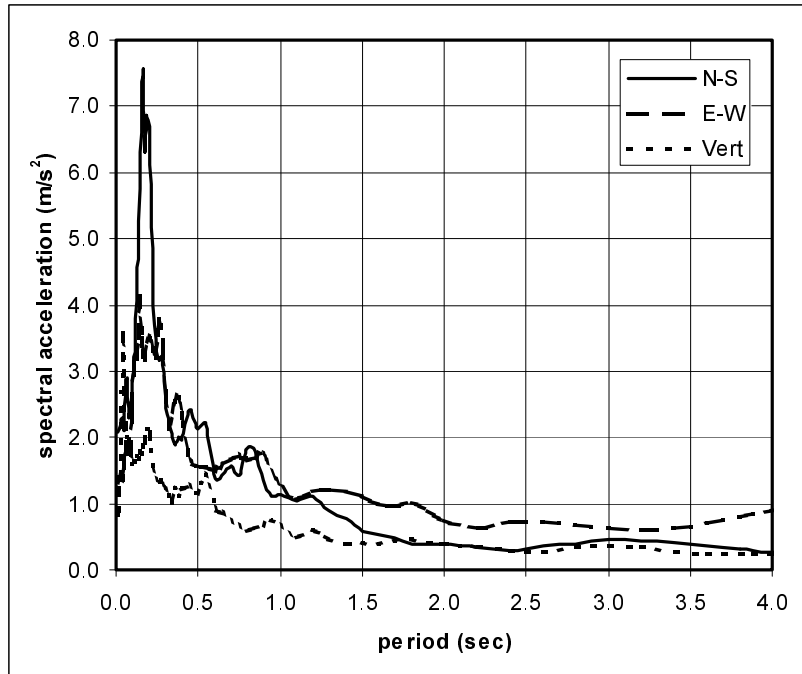
Ground Conditions: Soil
Distance: 4 km



Response spectra

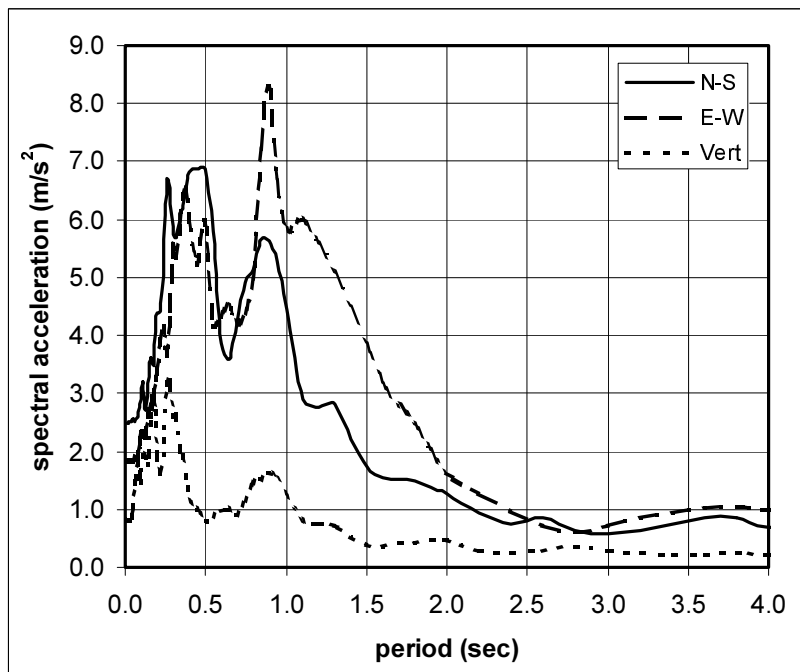
Event: Kocaeli, Turkey 17 August 1999
Station: Arcelik Factory, Gebze
Code: ARC

Ground Conditions: Unknown
Distance: 20 km



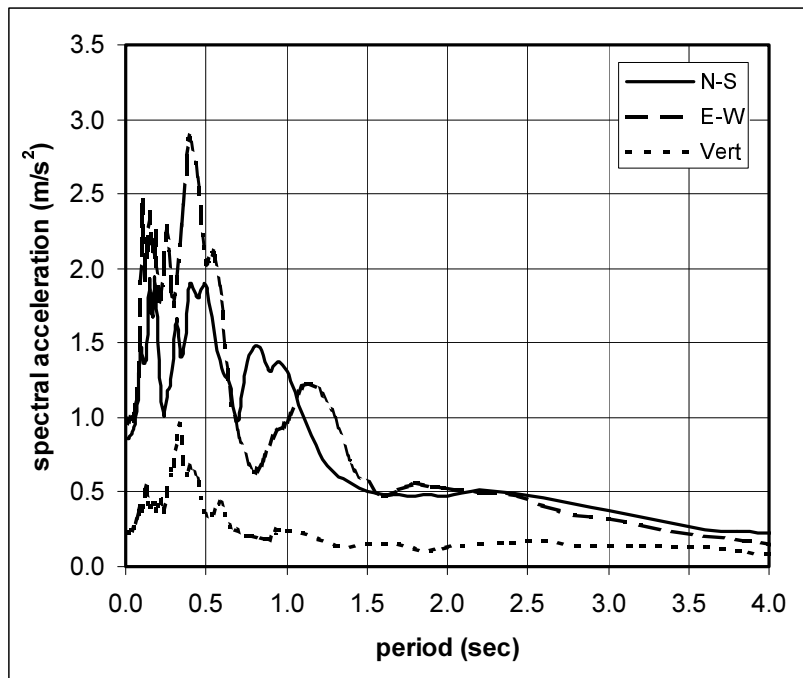
Event: Kocaeli, Turkey 17 August 1999
Station: Ambarlic Thermic Power Plant
Code: ATS

Ground Conditions: Rock
Distance: 82 km



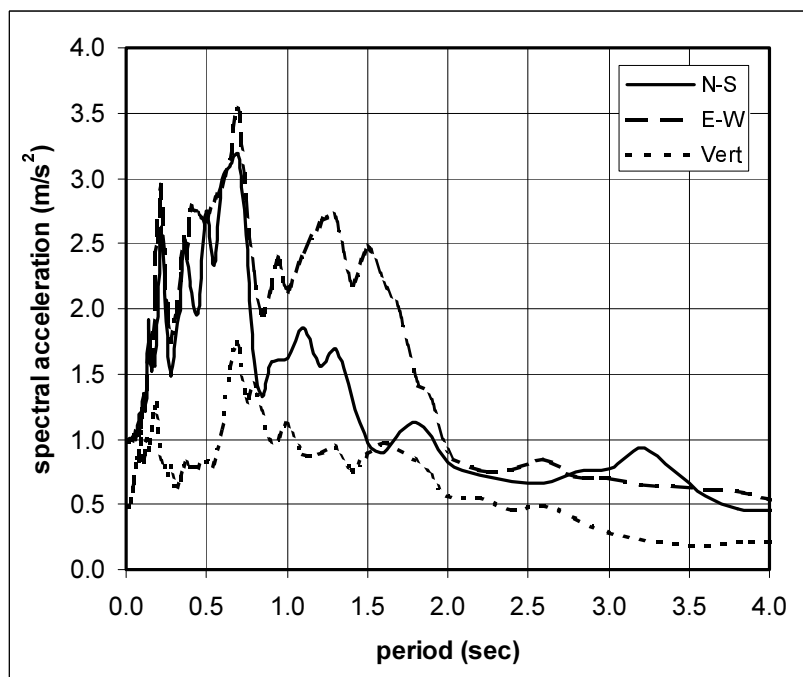
Event: Kocaeli, Turkey 17 August 1999
Station: Botas Gas Terminal?
Code: BTS

Ground Conditions: Unknown
Distance: 141 km



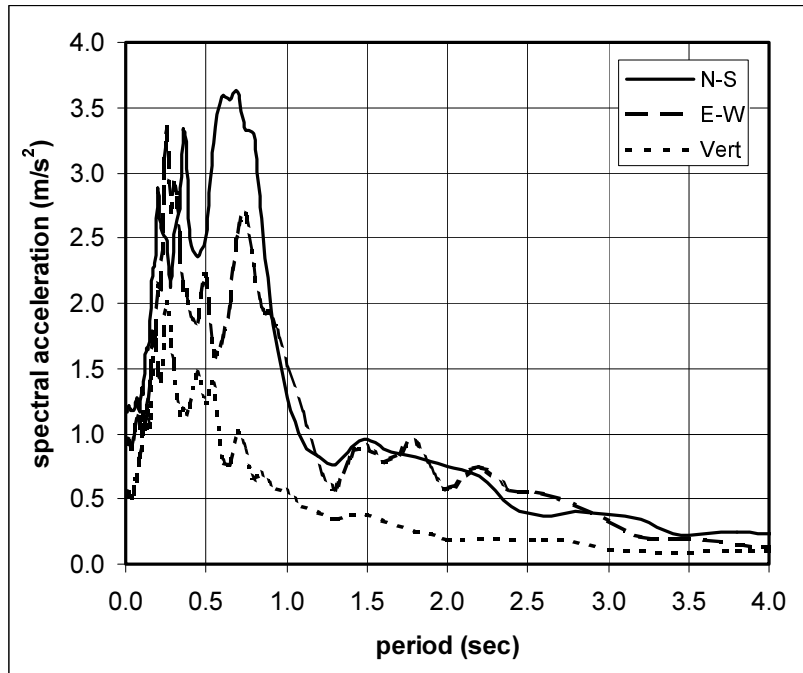
Event: Kocaeli, Turkey 17 August 1999
Station: Bursa Tofas Fabrikasi
Code: BUR

Ground Conditions: Unknown
Distance: 72 km



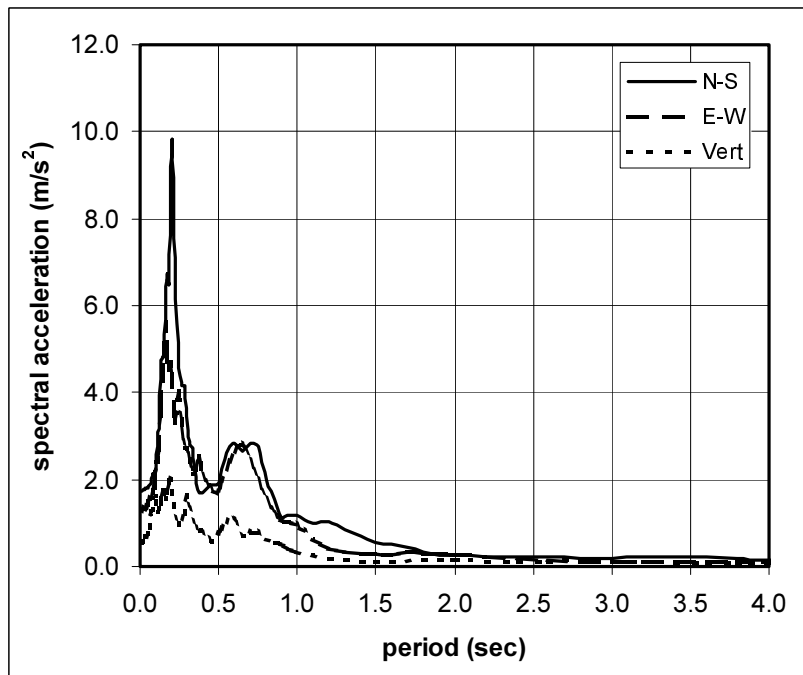
Event: Kocaeli, Turkey 17 August 1999
Station: CEKMECE Nuclear Research Centre
Code: CEK

Ground Conditions: Unknown
Distance: 81 km



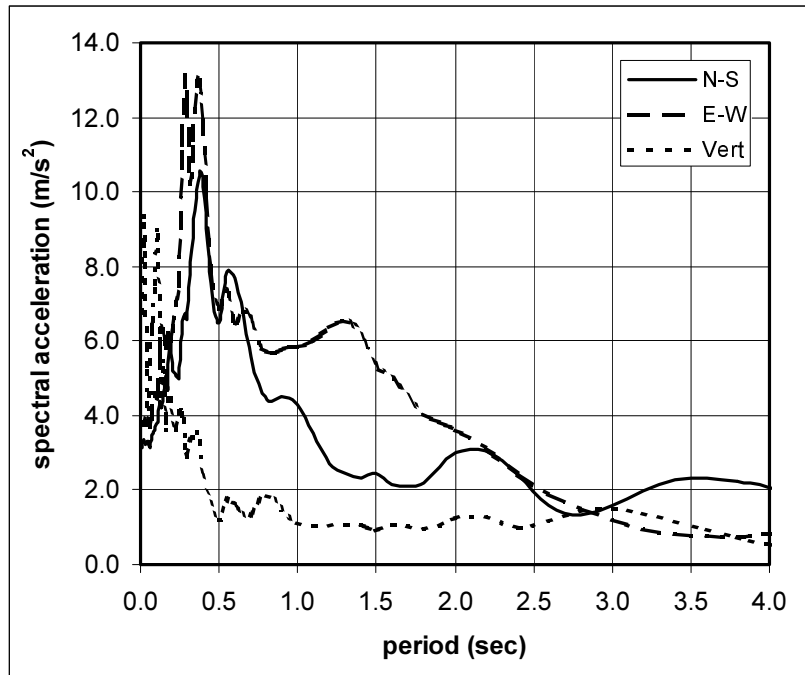
Event: Kocaeli, Turkey 17 August 1999
Station: CEKMECE Nuclear Research Centre
Code: CNA

Ground Conditions: Unknown
Distance: 78 km



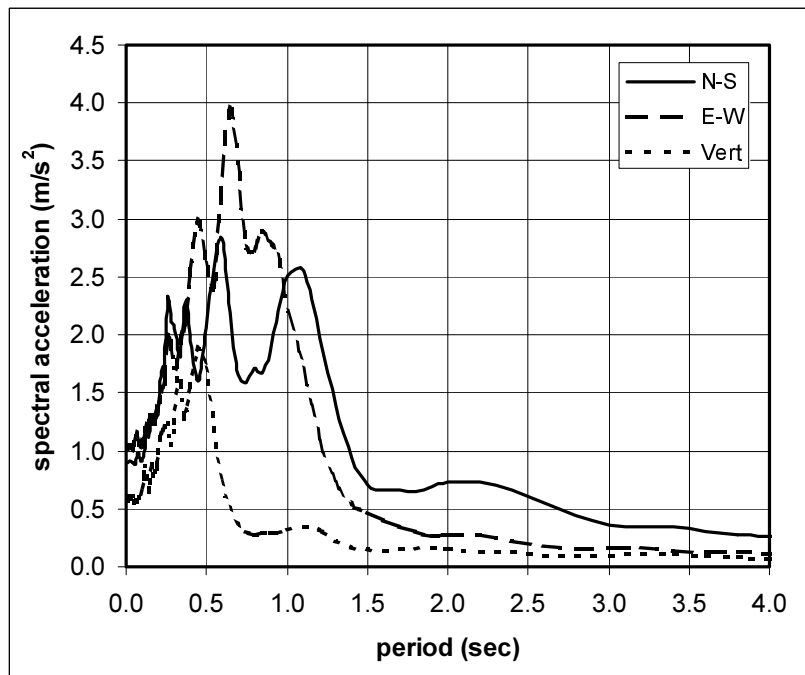
Event: Kocaeli, Turkey 17 August 1999
Station: Duzce Meteroloji Istasyonu
Code: DZC

Ground Conditions: Soil
Distance: 14 km



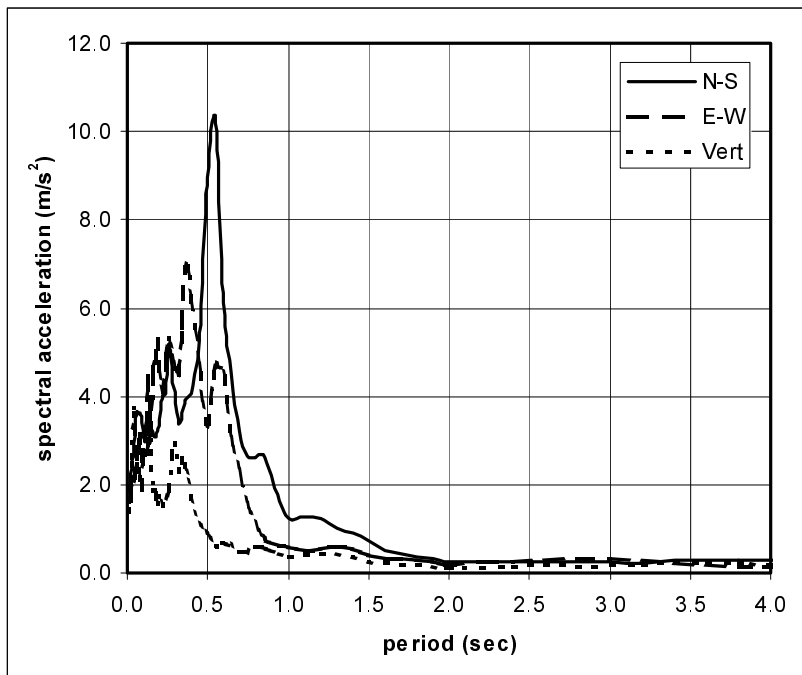
Event: Kocaeli, Turkey 17 August 1999
Station: Eregli Kaymakamlik Binasi
Code: ERG

Ground Conditions: Rock
Distance: 156 km



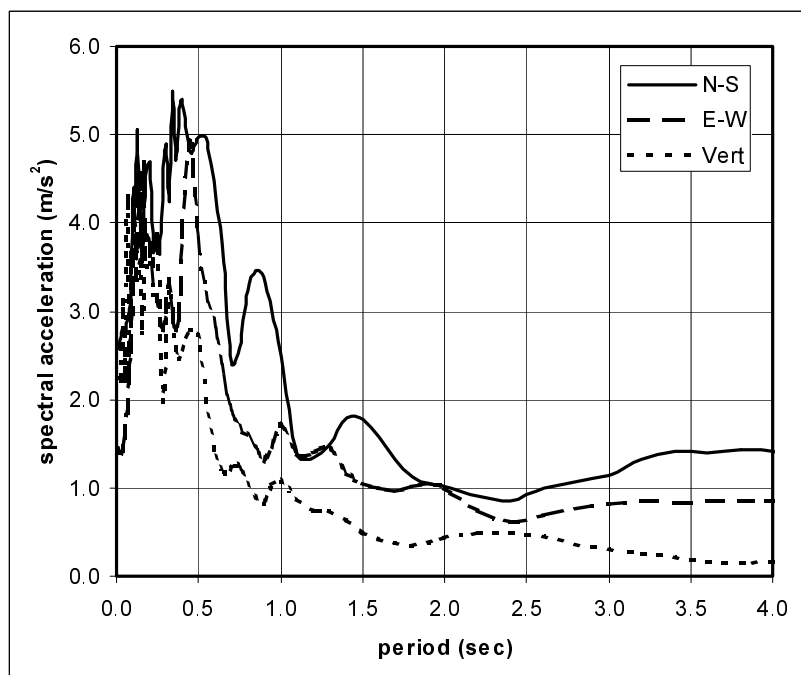
Event: Kocaeli, Turkey 17 August 1999
Station: Fatih Tomb
Code: FAT

Ground Conditions: Unknown
Distance: 67 km



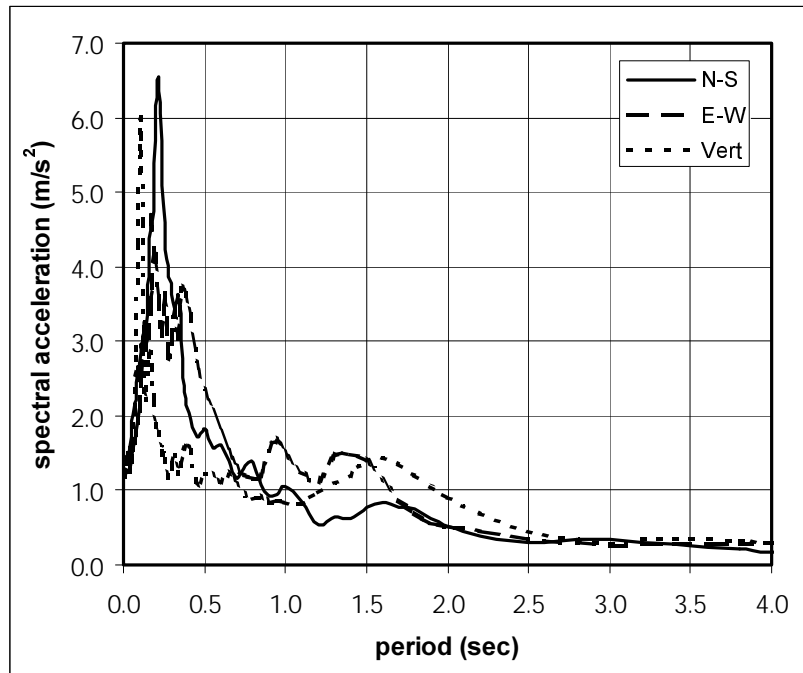
Event: Kocaeli, Turkey 17 August 1999
Station: Tubitak Marmara Arastirma Merkezi
Code: GBZ

Ground Conditions: Unknown
Distance: 18 km



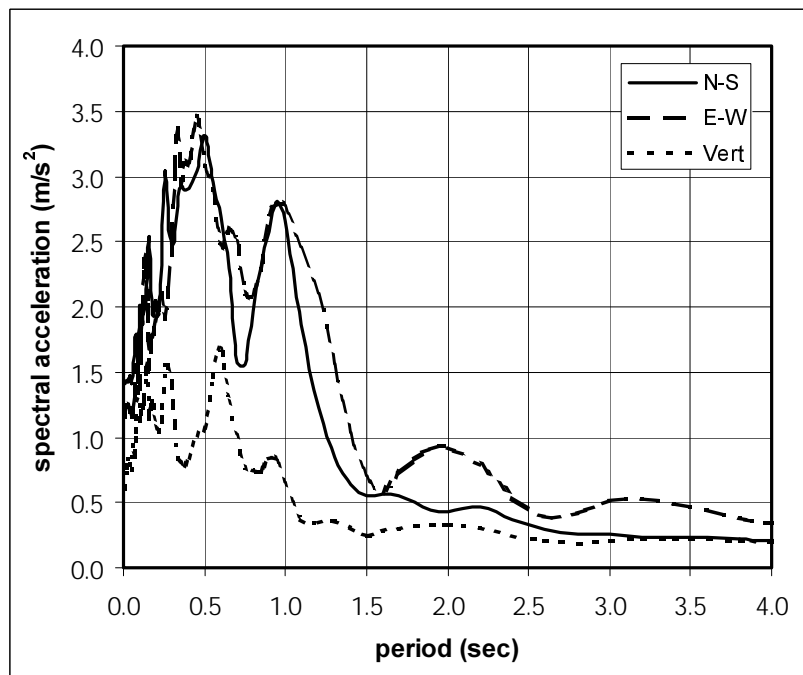
Event: Kocaeli, Turkey 17 August
Station: Goynuk Devlet Hastanesi
Code: GYN

Ground Conditions: Rock
Distance: 37 km



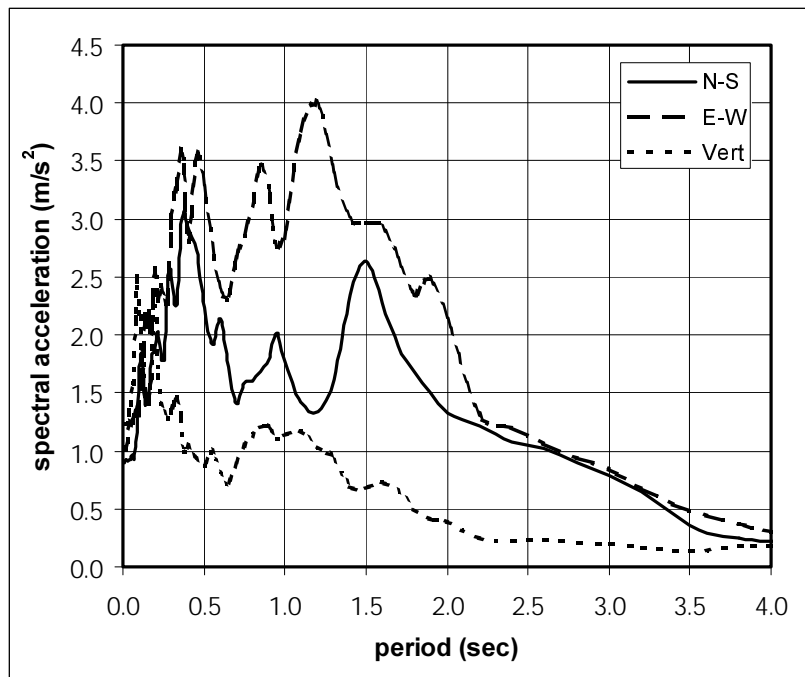
Event: Kocaeli, Turkey 17 August 1999
Station: Heybeliada Hospital
Code: HAS

Ground Conditions: Rock
Distance: 46 km



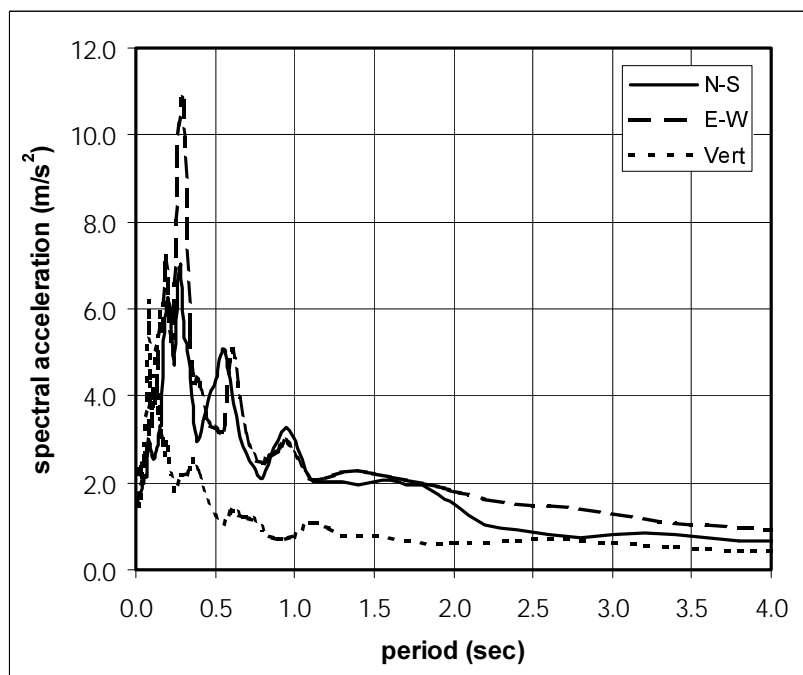
Event: Kocaeli, Turkey 17 August 1999
Station: Iznik Karayollari Sefligi
Code: IZN

Ground Conditions: Unknown
Distance: 32 km



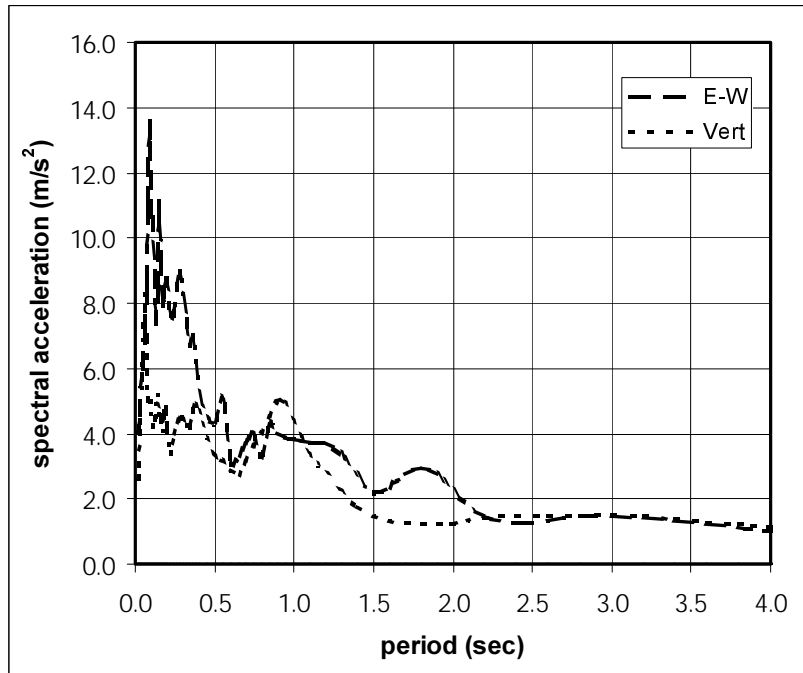
Event: Kocaeli, Turkey 17 August 1999
Station: Izmit Meteroloji Istasyonu
Code: IZT

Ground Conditions: Rock
Distance: 7 km



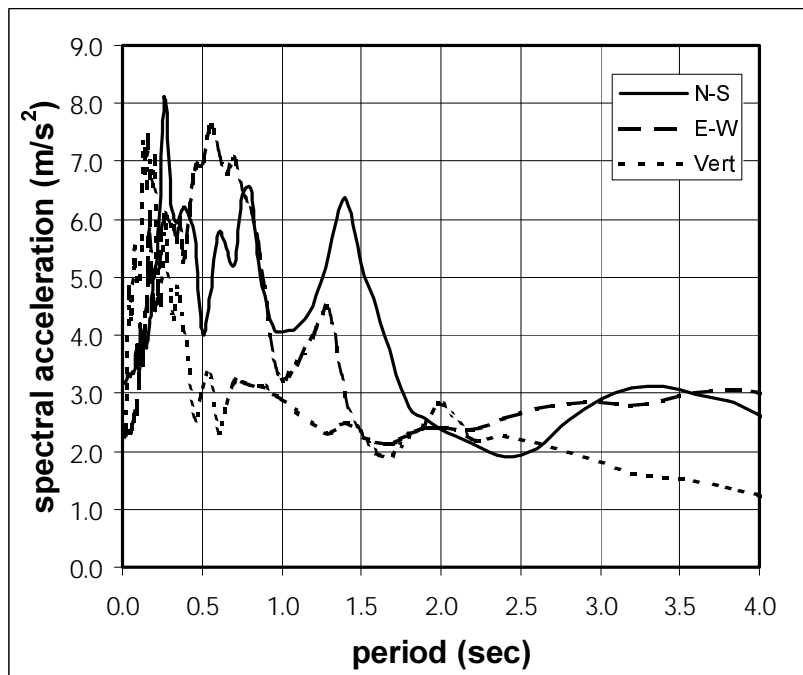
Event: Kocaeli, Turkey 17 August 1999
Station: Adapazari (Sakarya)
Code: SKR

Ground Conditions: Rock
Distance: 3 km



Event: Kocaeli, Turkey 17 August 1999
Station: Yarimca Petkim
Code: YPT

Ground Conditions: Soil
Distance: 4 km



4 Geological and Geotechnical Aspects

Matthew Free,
Ove Arup & Partners Hong Kong Ltd

Robert May,
Jacobs Gibb

Berrak Teymur,
Cambridge University

4.1 Introduction

The regional geology of the Izmit Bay area is presented on the 1:500,000 scale solid and superficial geology map of Turkey (Turkish Geological Survey, 1964). The relevant section of this map is reproduced in Figure 4.2, next page. A summary simplified version of the geology of the earthquake-affected area is presented in Figure 4.1 to highlight key features. The geology of Turkey is very complex due its location along the collision boundary between tectonic plates and subsequent active tectonic history. A description of the regional tectonics of Turkey is provided in Chapter 2.

This chapter provides first a brief review of the ground conditions in the visited areas of the region, which are relevant to the understanding of the seismic geotechnical effects observed. Then the detailed geotechnical observations carried out with reference to fault rupture, site response, liquefaction, and slope instability are discussed for each of the districts visited. Finally the response of geotechnical structures such as building foundations, retaining walls and earth embankments are presented. The regional distribution of the main geotechnical effects of the earthquake is illustrated in Figure 4.3.

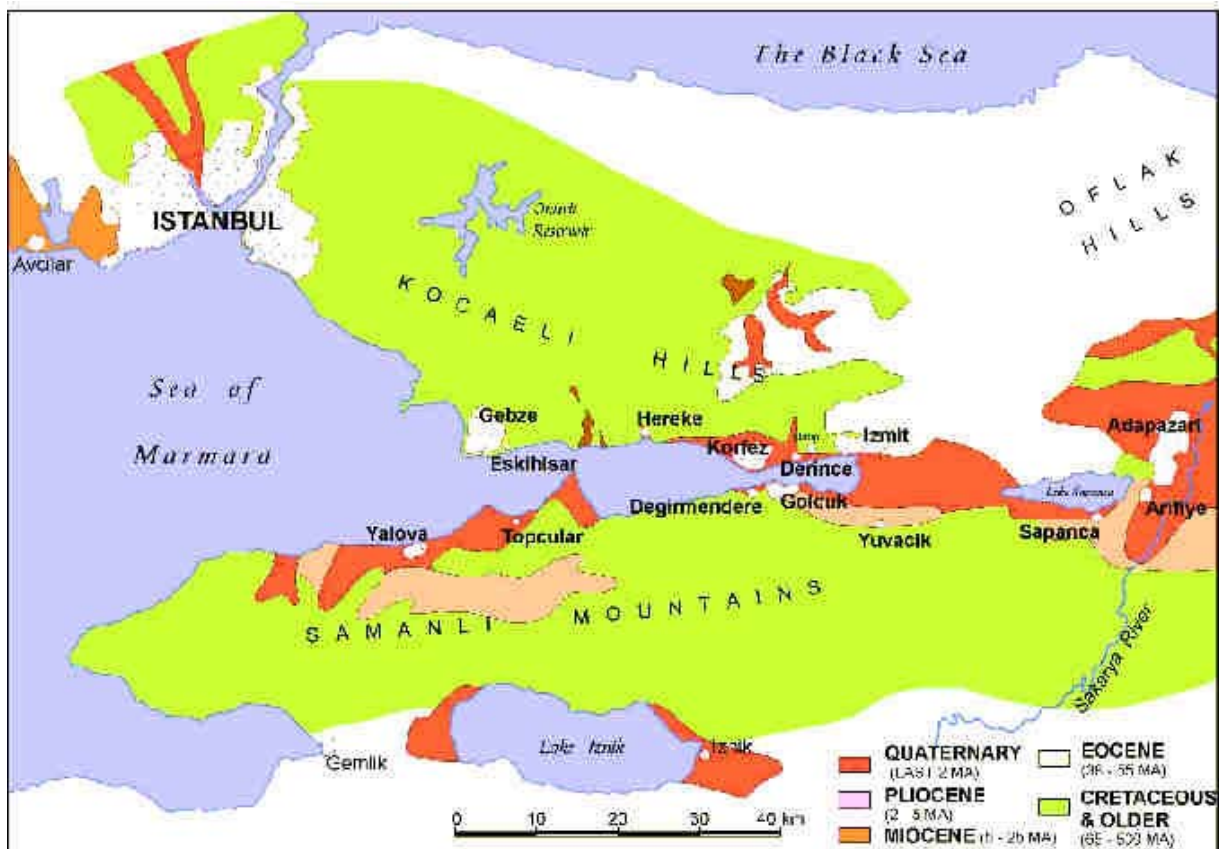


Figure 4.1: Simplified geological map of earthquake affected area

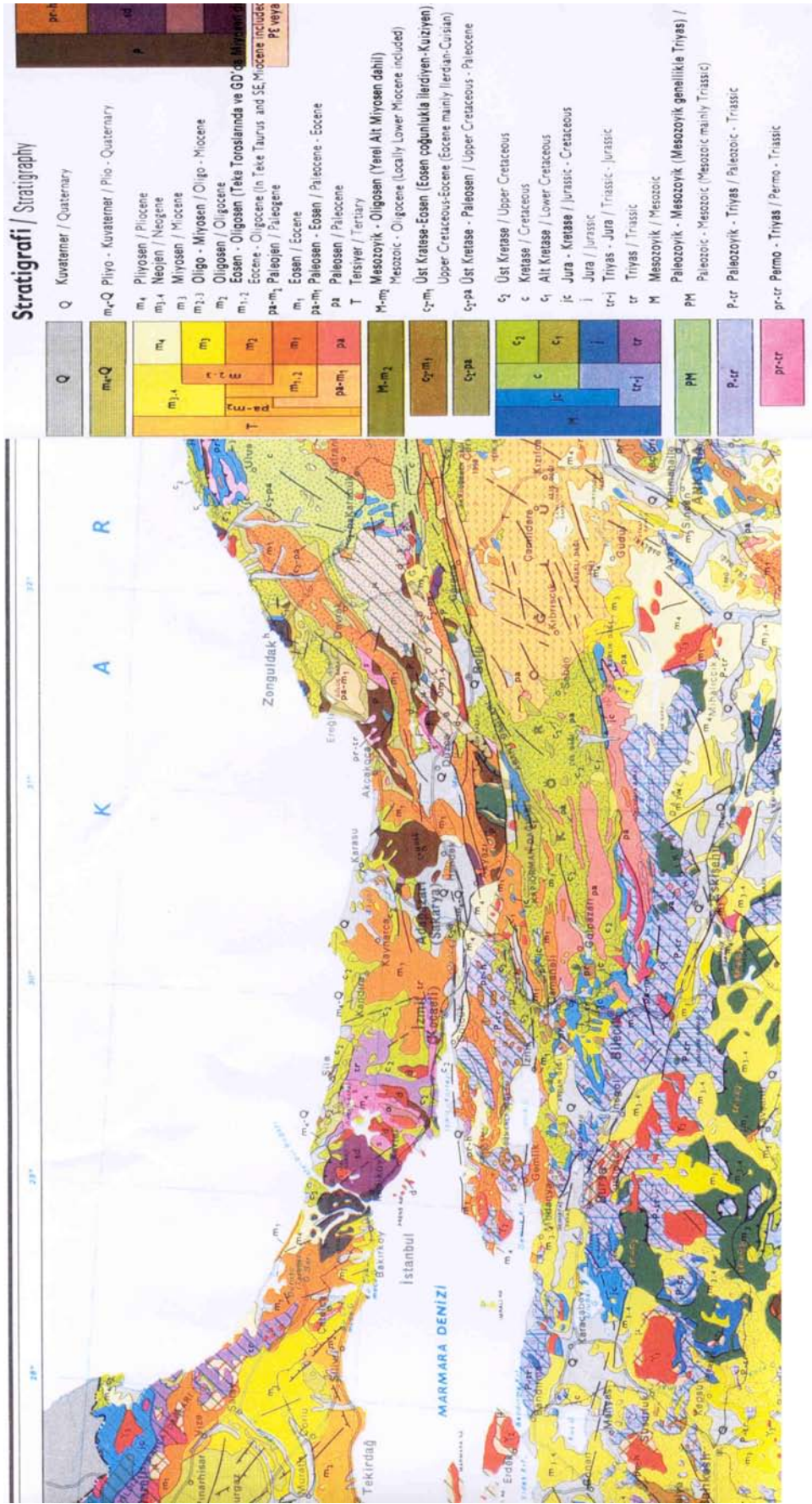


Figure 4.2: Extract from solid and superficial geology map of Turkey (Turkish Geological Survey 1964).



Figure 4.3: Location plan of earthquake affected area showing the location of geotechnical issues.

4.2 Local Ground Conditions

The ground conditions in selected areas visited by EEFIT are briefly described in the following sections.

4.2.1 Adapazari

Professor M. Erdik of Kandilli Observatory, Bogazici University, Turkey referred to Adapazari, as a mini Mexico City. The name Adapazari can be translated from Turkish as “Island Market”. It is understood that a large proportion of Adapazari City has been built on reclaimed land formed over a swamp. Adapazari is located on an alluvial plain, the Sakarya Plain, approximately 30 m above mean sea level. The topography of the city is typically flat lying with the Sakarya River meandering to the east of the city center. The northern portion of the city is located on a hilly ridge that rises to over 150 m above mean sea level. To the northeast of the city mountains rise to 500 m above mean sea level. To the South, the mountains east of Geyve rise to 1000m above mean sea level. The Sakarya Plain is located within a basin that extends from the Marmara Sea and Iznik Bay in the west to Hendek in the east (see Figure 4.1). The basin is interpreted to be a series of tectonic ‘pull-apart’ depressions formed by repeated strike-slip movement along the North Anatolian Fault Zone (Barka and Kadinsky-Cade, 1988). The plain is underlain by Quaternary Age alluvial deposits consisting of alternating layers of gravel, sand, silt and clay deposited by the Sakarya and Mudurnu rivers. The ground water level is typically very shallow and varies between 0.5 m to 3.0 m below ground level.

Figure 4.4 shows the locations of three boreholes carried out in central Adapazari City for the State Water Works Division. The boreholes are located on the southwest and north sides of the city centre within a 2 km radius from the City Hall i.e. within the area where the highest damage density was recorded. The geological logs for these three boreholes are also provided in Figure 4.4. The summary logs show that the alluvial deposits extend down to a depth greater than 116 m. The stratigraphy comprises an upper thin layer of topsoil underlain by 9 m to 18 m of sand and gravel, or silt and fine sand or clay. These layers are underlain by 67 m to 72 m of clay with lenses of silt, sand and gravel. At 83 m to 86 m below ground level a gravel layer 6 m to 14 m thick is encountered. Alternating layers of clay and gravel underlie this layer. In the boreholes at Site B Tuvasas and Site C the Office of Water Resources Housings, a layer of peat is encountered. Bedrock was not reached at the maximum drillhole depth of 116m below ground level.

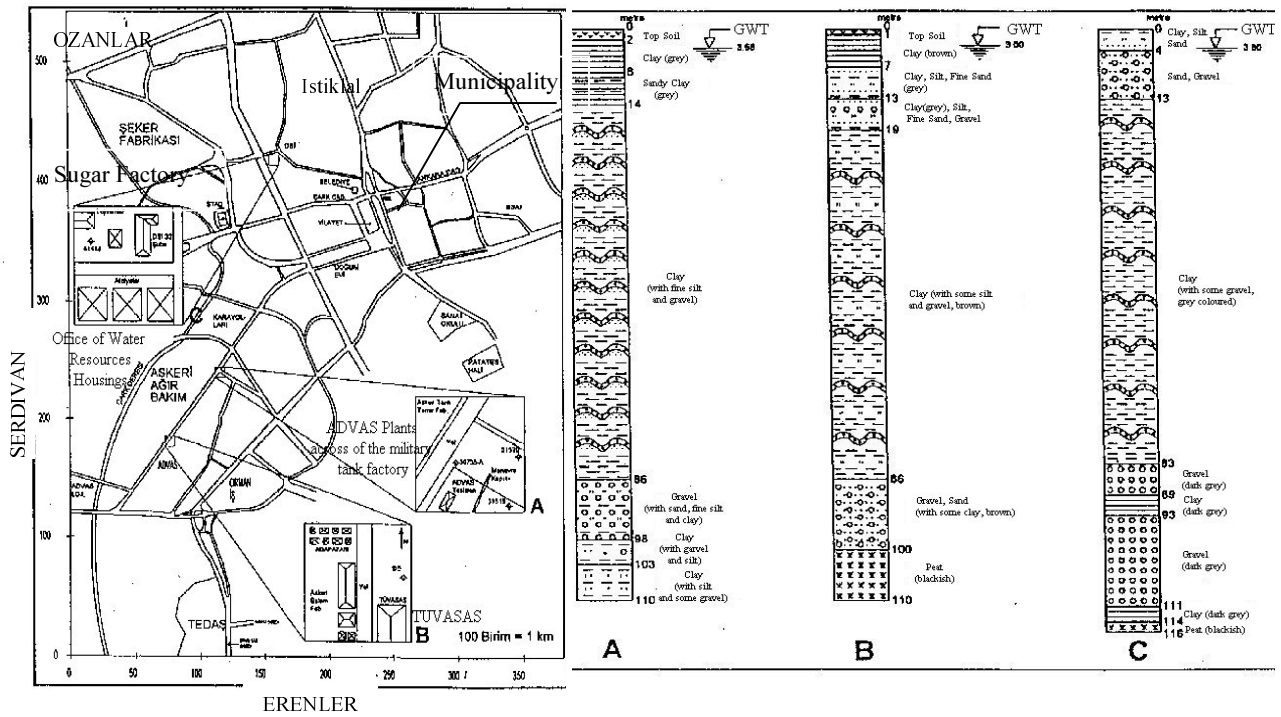


Fig. 4.4: Location plan for State Water Works Division boreholes in Adapazari City and summary of geological logs

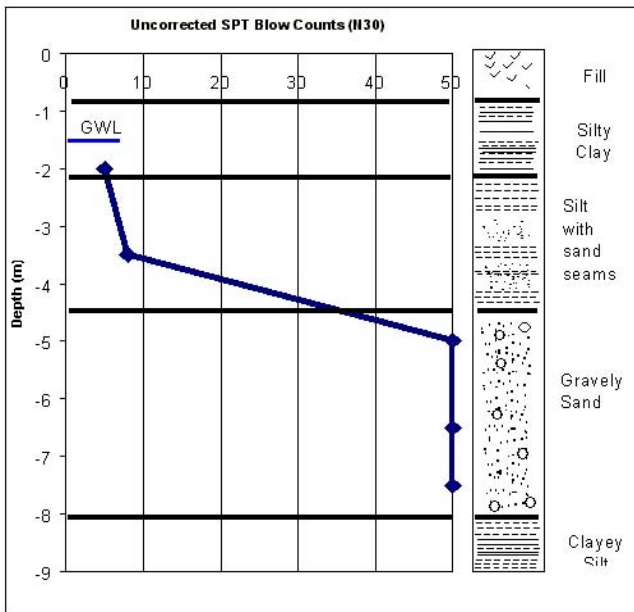


Figure 4.5: Summary geological log and uncorrected standard penetration test, N(30) profile for borehole 1-5, Cark Street, Adapazari City (from Erken 1999). N(30) refers to the number of blows for 30 cm, i.e. excluding the initial 15 cm seating blows.

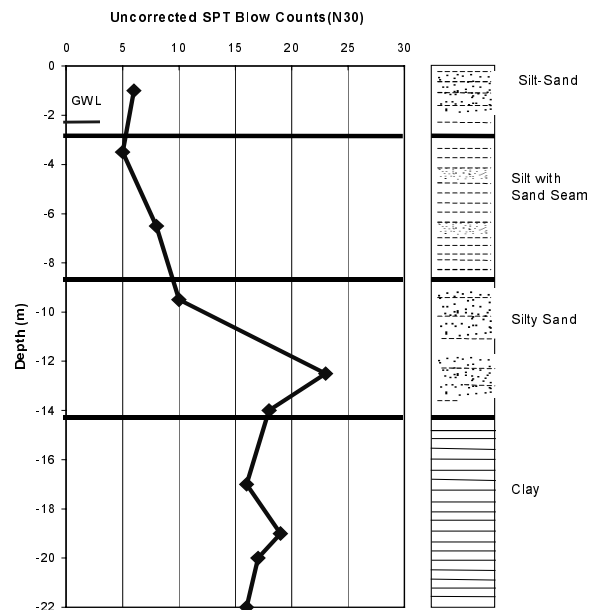


Figure 4.6: Summary geological log and uncorrected standard penetration test N(30) profile for borehole B6, Industrial Centre, Adapazari City (from Erken 1999).

Uncorrected Standard Penetration Test profiles together with summary logs for further three site investigation boreholes within Adapazari city centre where obtained from Erken (1999) and are shown in Figures 4.5, 4.6 and 4.7. Two boreholes, I-5 and I-19 are located in Cark Street a main road northwest of the City Hall and following the path of the Cark River. Borehole I-19 is understood to be located near to the Municipality Building. The location of the third borehole, B6 is unknown but it is described as having been drilled for the Industrial Centre Project. These logs indicate a surface layer of fill typically less than 2.5 m thick underlain by soft to firm clay/silt or silt or loose silt/sand or sand layers which are typically 3 m to 6 m thick. Layers of dense gravelly sand 3.5 m to 5.5 m thick may also be present at shallow depth.

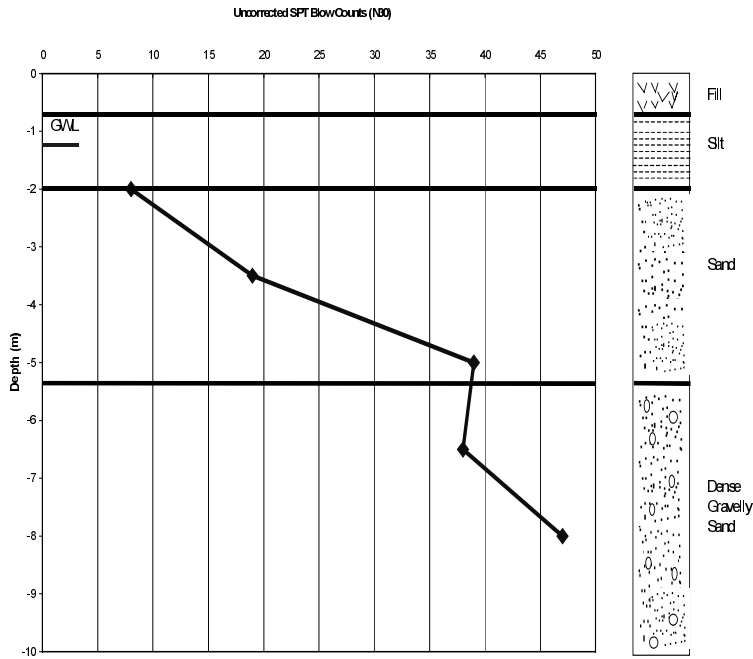


Figure 4.7: Summary geological log and uncorrected standard penetration test, N(30) profile for borehole 1-19, Cark Street, Adapazari City (from Erken 1999).

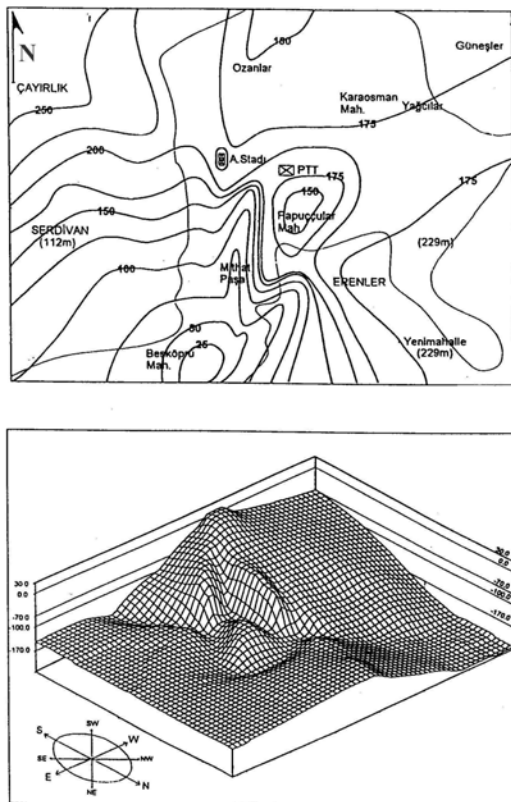


Figure 4.8: Contour plan and three-dimensional view (from NE to SW) of rockhead level beneath Adapazari City (Sakarya University Report, 1998).

Figure 4.8 shows a contoured plan and 3-dimensional view of the depth of rock beneath Adapazari City (Sakarya University Report, 1998). A maximum depth contour of 250 m is shown. In the Yenimahalle and Tabakhane districts the depth to rock is 229 m and in the Istiklal district the depth to rock is 212 m while near Serdivan the depth to rock is 112 m. Basement rocks in the region are Cretaceous Age mudstones and sandstones in the south and Paleozoic Age metamorphic rocks, understood to be gneiss, schist and marble, in the north. The basement rocks beneath Adapazari City itself are unknown.

4.2.2 Gölcük

Gölcük is located on the southern side of Izmit Bay near the eastern limit of the bay. The town is formed on a relatively narrow coastal plain. Levels taken pre-earthquake show the topography to rise from 1 m above mean sea level in the north to 10 m above mean sea level in the south. The main highway along the southern coast of Izmit Bay follows an elevated terrace level above Gölcük that appears to be approximately 5 m to 10 m above the coastal plain. The outskirts of the town sprawl onto the north facing hills that extend down to Izmit Bay.

The geological map (Turkish Geological Survey, 1964)(Figure 4.2) indicates that Quaternary age alluvial deposits and Pleistocene age sedimentary deposits underlie the coastal plain. The alluvial deposits form an alluvial fan delta that extends out into Izmit Bay. The hills above Gölcük are composed of metamorphic and volcanic rocks. The depth to rock beneath Gölcük is unknown but is estimated to be in the range of 50 m to 200 m. Geological logs from water wells in the area are understood to show in excess of 155 m of interbedded sands, gravels and clays.

Site investigation boreholes on the coastal plain reveal that the stratigraphy beneath the plain consists of alternating clay, silt, sand and gravel layers. A summary log and uncorrected Standard Penetration Test profile for a site investigation borehole near Gölcük (the exact location is unknown) is shown in Figure 4.9. The vertical and lateral extent of these layers is expected to be highly variable due to their formation in a geological environment consisting of meandering and braided alluvial channels within an alluvial fan delta.

The ground water level is very shallow and varies between 0.5 m to 2.0 m below ground level. The near surface stratigraphy exposed in a pile cap excavation at the Ford Otosan Plant located east of Gölcük town is shown in Plate 4.1, in Appendix 4A. The exposure consists of 1.2 m of gravelly sand fill overlying loose alluvial sand. The ground water is 2.0 m below ground level. Note that this observation was made post earthquake and measured subsidence in the area is approximately 2 m. The near surface stratigraphy exposed in a fault scarp near the Ford Otosan Plant is shown in Plate 4.2. The exposure shows approximately 1 m of gravel overlying fine to coarse sand with some gravel.

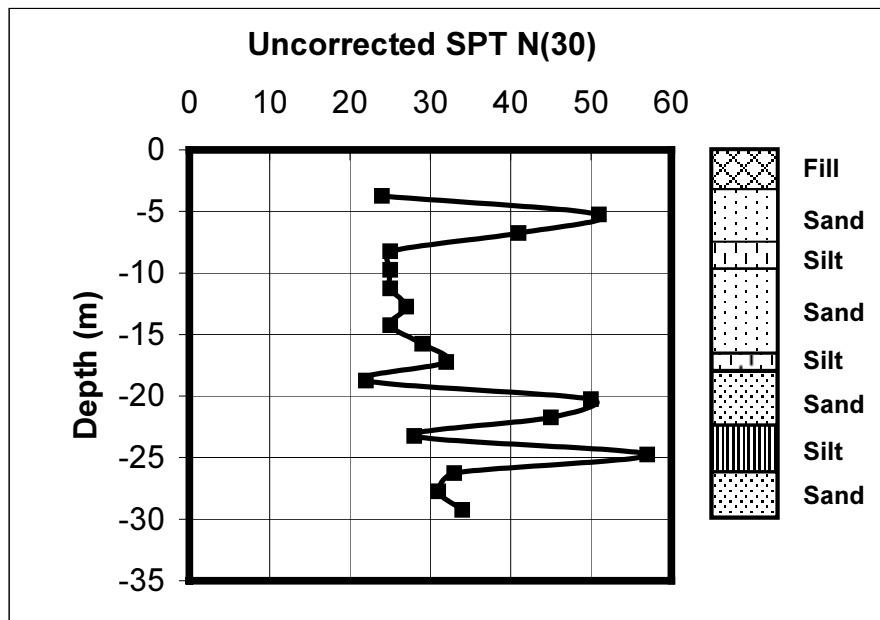


Figure 4.9: Summary geological log and uncorrected standard penetration test, N(30) profile for borehole in Gölcük area.

4.2.3 Izmit

Izmit is located on the northern and eastern side of Izmit Bay at the eastern limit of the bay. The old town is situated at the foot of the hills that rise to 250 m on the northern side of the bay. The new town, and a number of heavy industrial sites including the Tupras Refinery, is located on the narrow coastal plain that extends from Yarimca in the west to Izmit in the east. Older urban developments are located on a partially leveled triangular plateau that forms a blunt promontory projecting into the gulf. The topography of the coastal plain is flat and low lying with a gentle slope south to Izmit Bay. The hills behind the coastal plain rise steeply to the north. The geological map (Turkish Geological Survey, 1964) indicates that the coastal plain is underlain by Quaternary age deposits that are inferred to comprise alluvium and slope wash colluvium. The hills above the coastal plain are formed of Silurian and Devonian age greywacke and quartzite at their crest, dipping northward under Triassic and Cretaceous Age limestone, sandstone and marl and shale formations. Ozaydin and Inan (1984) describe Pliocene deposits underlying the oil storage tanks at the Tupras site on the coastal plain. These are described as consisting of stiff to hard clays and dense to very dense silty fine sand. Pleistocene deposits that are exposed along the coastal fringe contain dense sands and weakly cemented sandstone and stiff clays to very weak siltstone. The greater part of the plateau is formed of detrital aprons and fans ranging from pebbles and sands through to silt and marly clay layers. The combined thickness of the Quaternary deposits may exceed 100 m in this area with a further 50 m or more of Pleistocene soils.

A site investigation borehole carried out on the coastal plain at Izmit indicates that the stratigraphy beneath the plain consists of alternating clay, silt and sand and gravel layers. A layer of soft organic clay that extends to 29 m below ground level was encountered in the borehole. The exact location of the borehole is unknown but is described by Erken (1999) as being located on the Izmit Bay shoreline. The summary log and uncorrected Standard Penetration Test profile for the borehole is shown in Figure 4.10.

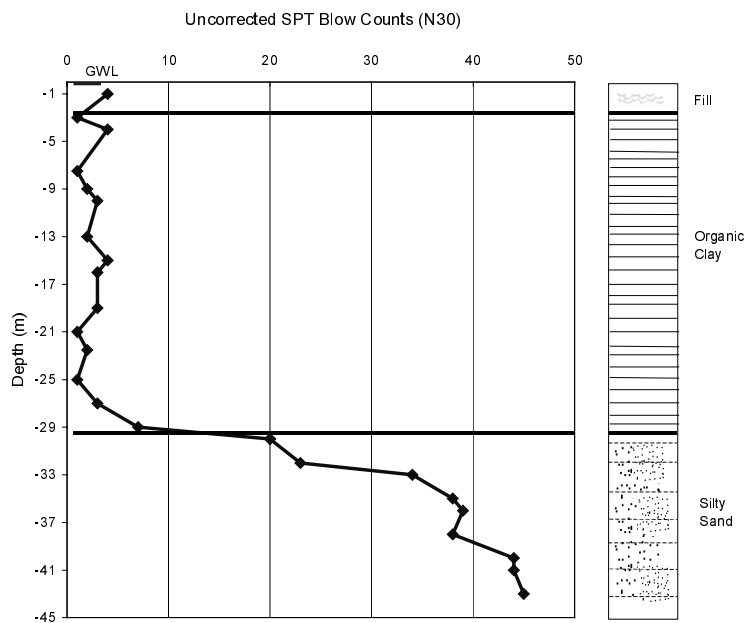


Figure 4.10: Summary geological log and uncorrected standard penetration test, N(30) profile for borehole S-5, Izmit (from Erken 1999)

4.2.4 Yalova

Yalova is located on an alluvial plain on the southern coast of Izmit Bay approximately 70 km west of Izmit City. The Arpa and Kuriliyoy Rivers flow through the plain from south to north.

The geological map (Turkish Geological Survey, 1964) (Figure 4.2) indicates that Quaternary age alluvial deposits and Pleistocene and Pliocene Age sedimentary deposits underlie the coastal plain. The Pleistocene and Pliocene Age sedimentary rocks also form a series of north-south oriented ridges that separate the alluvial valleys. The hills above Yalova to the south are composed of metamorphic and volcanic rocks. The depth to bedrock beneath Yalova is unknown but is expected to be in the range of 50 m to 100 m or more.

A summary log and uncorrected Standard Penetration Test profile for a site investigation borehole near Yalova is shown in Figure 4.11. The exact location of the borehole is unknown, but is described by Erken (1999) as being located at the Telecommunications Project site at Ciftlikkoy. The borehole reveals that the stratigraphy beneath the plain consists of alternating clay and sand layers. The vertical and lateral extent of these layers is expected to be highly variable due to their formation in a geological environment consisting of meandering and braided alluvial channels. The measured ground water level shown on the site investigation summary log is very shallow at 0.5 m below ground level. On the coastal plain, the ground water level is expected to be in the order of 0.5 m to 2.0 m below ground level and is not expected to show significant seasonal variation. On the hill slopes to the south of the town, the groundwater level is expected to be encountered at greater depth and can be expected to show significant seasonal variation.

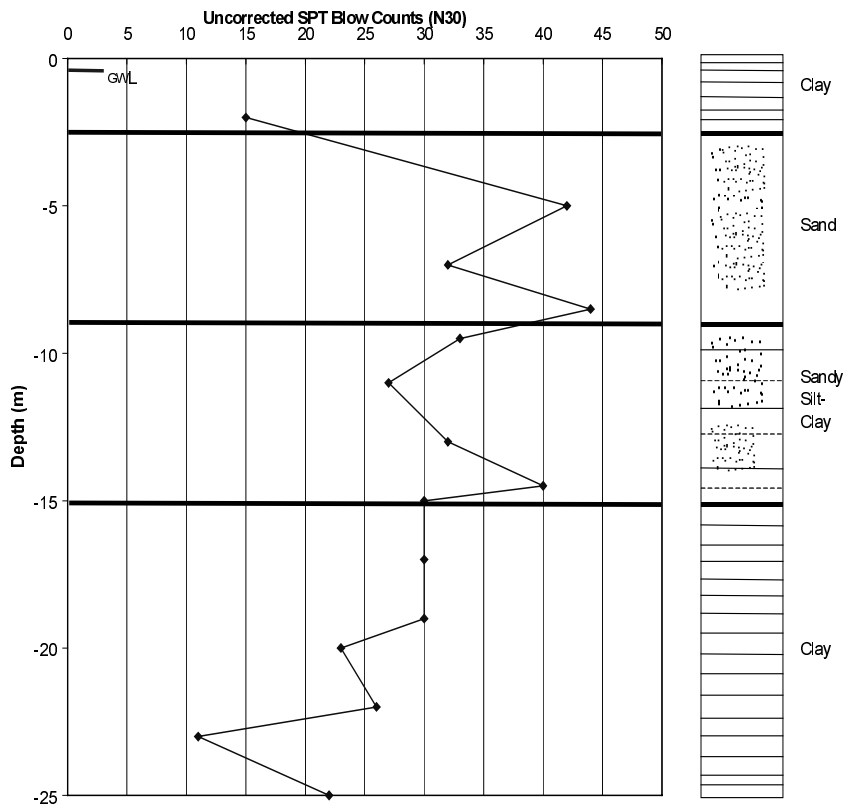


Figure 4.11: Summary geological log and uncorrected standard penetration test, N(30) profile for borehole SK1, Ciftlikkoy telecommunications project site, Yalova (from Erken 1999).

4.2.5 Düzce

Düzce is located within an alluvial basin approximately 200 m above sea level. The topography of the city is typically flat lying with the Asar River located to south of the city center. The basin is bounded on all sides by hills that rise to 500 m to 1800 m above sea level. The geological map (Turkish Geological Survey, 1964, Figure 4.2) indicates that Quaternary age alluvial deposits underlie the plain. The alluvial deposits comprise layers of gravel, sand, silt and clay that are understood to extend to greater than 70 m depth (Tabban, 1980). The ground water level is typically shallow and varies between 2 m to 7 m below ground level.

4.2.6 Avcilar

Over 1000 people were killed in the Istanbul greater metropolitan area due to collapse of buildings during the 17 August 1999 Kocaeli earthquake. The majority of fatalities and damage occurred in the suburb of Avcilar, approximately 20 km west of the Istanbul City centre. Avcilar is located on moderately steeply inclined east and south facing hillsides that face the Marmara Sea to the south and Kucuk Cekmece to the east. The geological map (Turkish Geological Survey, 1964, Figure 4.2) indicates that predominantly undifferentiated Pliocene age deposits underlie the Avcilar area.

Quaternary age deposits occur in the valleys near Bakirkoy and Buyuk Cekmece. Kopp et al. (1969) indicate that the area is underlain by unconsolidated sand and gravel of Pliocene Age and poorly lithified calcareous sand, marl and oolitic limestone of Upper Miocene Age. These deposits are in the order of 200m thickness (Kopp et al., 1969). An engineering geological map for the Istanbul region is provided in Figure 4.12. The engineering geological map indicates areas of potential slope instability as well as areas of different foundation conditions.

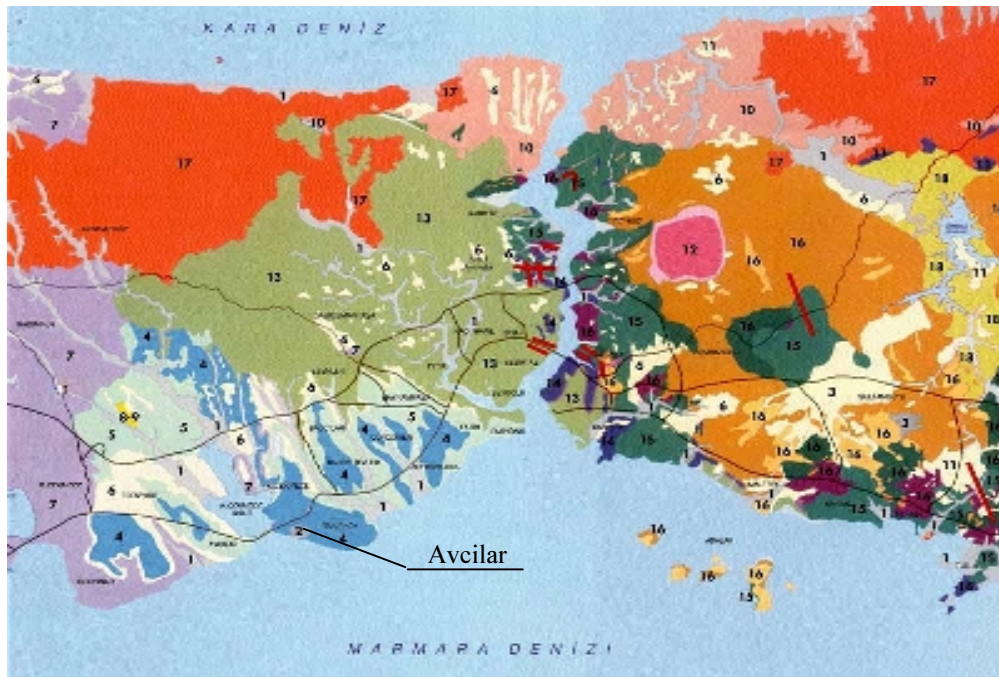


Figure 4.12: Engineering geological map of Istanbul City region. 1-3 stand for alluvial with low-loading capacities, 4 stands for alluvial deposit with good loading capacity with weak zones locally, 5 is for alluvial with low loading capacity with landslide probability with slopes. 6 is for high-loading capacity, 7 for low-loading capacity and 13 for rock (Municipality of Istanbul)

4.3 Fault Rupture

An important and unusual feature of the Kocaeli event is that the surface rupture of the fault passes directly through a heavily urbanised and industrialised area. The study of the area along the surface rupture zone provides a rare opportunity to investigate the response of man-made structures when a fault ruptures the ground directly beneath them or immediately adjacent to them. The surface rupture produced by the Kocaeli event is approximately 140km in length and consists of four main segments (see Figure 4.13):

- Gölcük segment;
- Izmit-Sapanca segment;
- Sapanca-Akyazi segment; and
- Düzce segment.

The fault zone is characterised by fractures with 0.5 m to 4.0 m of right lateral strike-slip offset across a narrow 0.5 m to 2 m deformation zone. Lateral or en echelon steps in the surface rupture are typically separated by 20 m to 70 m. In some areas the fault zone is broader with a series of two or more surface ruptures spread over a width of approximately 50 m to 200 m. In these areas the cumulative offset on each of the sub-parallel ruptures corresponds closely to the offset measured on the single main ruptures. A detailed assessment of the surface fault rupture is presented by Lettis et al. (2000) and the reader is directed to this work for further information.

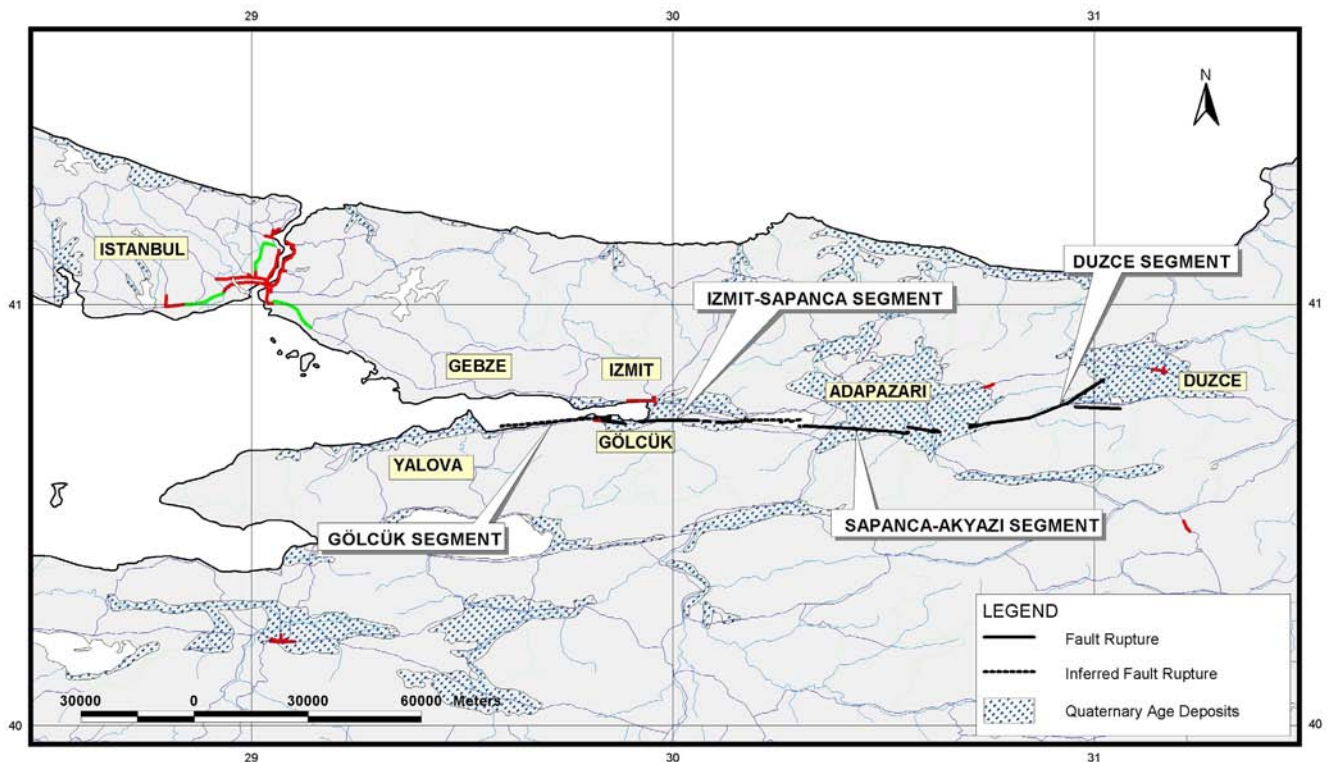


Figure 4.13: Map showing surface fault rupture during the Kocaeli earthquake. Location of fault rupture from Lettis et al. (2000). Location of Quaternary Age Deposits from Emre et al. (1998).

4.3.1 Gölçük segment

The fault zone of the Gölçük fault segment passes through the Gölçük Naval Base. The naval base is located on a blunt, north facing peninsula and the fault trace is offshore within Izmit Bay on the western and eastern sides of the peninsula. Damage to the naval base structures due to fault rupture was extensive. The rupture extended beneath a number of reinforced concrete frame office and accommodation structures leading to collapse of these structures. Interestingly the surface rupture broke around or side stepped a series of massive concrete bunkers without significant structural damage to the bunkers. The rupture extended offshore to the passing through the port facility of the naval base. The reinforced concrete deck of the port was offset by approximately 2m. No photographs were permitted at the naval base at time of the visit.

A down thrown pull-apart zone is located in the step over between the Gölçük and Izmit – Sapanca segments (refer to Figure 4.13). In the pull-apart zone the observed offset is predominantly associated with a northwest-southeast oriented normal fault. The northeastern side is down thrown by approximately 2 m to 2.5 m. This normal fault should be considered a secondary feature to the main predominantly strike-slip fault. The normal fault scarp is interpreted to start offshore within Izmit Bay as the coastline has been down thrown approximately 2 m. A substantial portion of the former shoreline is now inundated with seawater. Views of the Gölçük coastline are presented in Plates 4.3 and 4.4. At the location where the fault trace is interpreted to come in land to the southeast of the amusement park reconstruction works had destroyed the fault scarp trace. The fault scarp was first observed at the southern end of the Gölçük Football Stadium (see Plate 4.5). To the southeast, the scarp passes beneath the southwest corner of an indoor sports hall (see Plate 4.6). The building has been damaged locally but not catastrophically. The scarp can be followed through the eastern suburbs of Gölçük, where a number of residential buildings have been bisected and destroyed (see Plate 4.7). Buildings immediately adjacent to the fault rupture remain standing and are often only slightly to moderately damaged.

On the eastern side of Gölçük the fault zone passes to the south of the Ford Otosan Factory (see Figures 4.14a, b). Figure 4.14a shows an aerial photograph of this area with the fault alignment highlighted. The factory was under construction at the time of the earthquake and slight damage to a number of buildings could be observed. The normal fault scarp steps 20 m to 25 m to the right before the intersection with the western end of the body shop building of the factory. The deformation zone associated with this step passes through the south-western corner of the building causing

compression of the western wall and tilting of the columns (see Plates 4.8 and 4.9). Figure 4.14b shows the results of a survey carried out at the Ford Otosan Factory after the earthquake. The figure shows contours of vertical displacement in the vicinity of the factory. The vertical displacement was measured in the range 1.5m to 2.3m with the formation of a syncline that passed through the body shop building of the factory.

To the south-east of the Ford Otosan Factory the normal fault scarp passes through a non-built-up area and can be mapped for a further approximately 1 km.

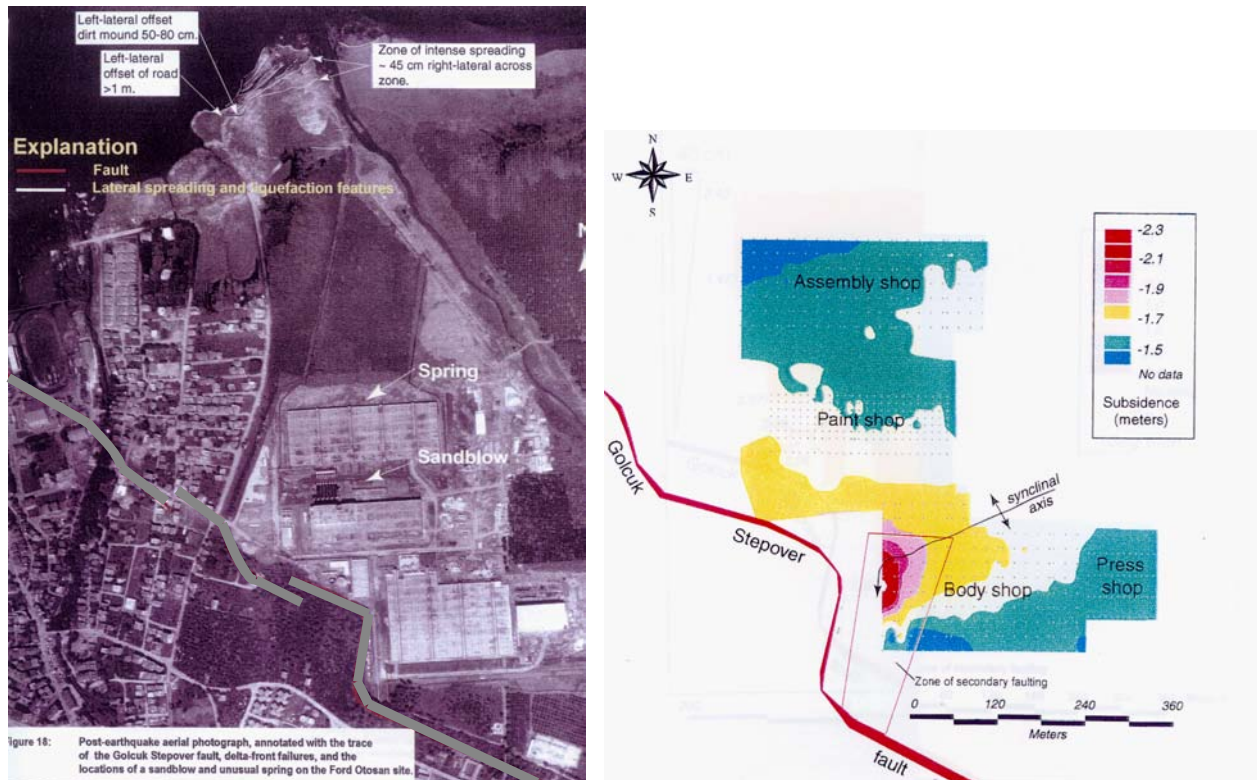


Figure 4.14a,b: (a)Aerial view of fault segment in vicinity of Ford Otosan Factory (from Sieh, Gonzales & Barka 1999). (b) Vertical displacement in the vicinity of the factory.

4.3.2 Izmit – Sapanca segment

The fault zone of the Izmit to Sapanca fault segment comes onshore at the southeastern corner of Izmit Bay near the town of Yuvacik. In this area the fault is almost purely right lateral strike slip with 2 m to 2.5 m of offset. In Yuvacik, the fault bisects a two-storey school building and the school collapsed as a consequence (see Plate 4.10). Adjacent to the school, at a distance of approximately 5 m from the fault rupture, a single storey reinforced concrete shop building is relatively undamaged. To the west of the school, the fault trace passes beneath a two-storey reinforced concrete residential structure that is under construction and this building is undamaged (see Plate 4.11). To the east of the school the fault trace passes within 20 m of a number of 2 to 3 storey reinforced concrete residential structures (see Plate 4.12). These buildings are slightly damaged. Between Izmit and Sapanca the fault rupture intersects the Istanbul to Ankara Highway and Railway. Damage to the highway pavement was extensive over a 20 km section south of Adapazari City. Significant visible damage to the railway was restricted to a single location where the fault offset the railway tracks. Damage to the highway and railway systems is described in detail in Chapter 7.

4.3.3 Sapanca – Akyarzi segment

Ten kilometers South of Adapazari City the fault rupture passes to the south of the Toyota Factory. The distance between the fault zone and the main buildings of the Toyota Factory was approximately 100 m to 200 m. The rupture zone in this area was approximately 50 m wide and comprised a series of irregular fractures with 0.1 m to 1.0 m of

offset and cumulative offset of greater than 2.5 m. The rupture caused extensive damage to the access road to the factory (see Plates 4.13 and 4.14) but no significant damage to the factory itself. A review of the EEFIT visit to the Toyota Factory is provided in Chapter 6.

4.3.4 Düzce segment

The easternmost extent of the August 17 rupture was the region surrounding Eften Lake near Duzce. In this region the offset on the fault reduced from 1.5m to approximately 0.2m and appeared to follow the range front on the northern side of the basin. At Eften Lake a step-over of approximately 2.5km occurred and the fault formed a series of shorter offset segments to the south of the lake. No displacement was observed east of Eften Lake.

4.4 Site Response

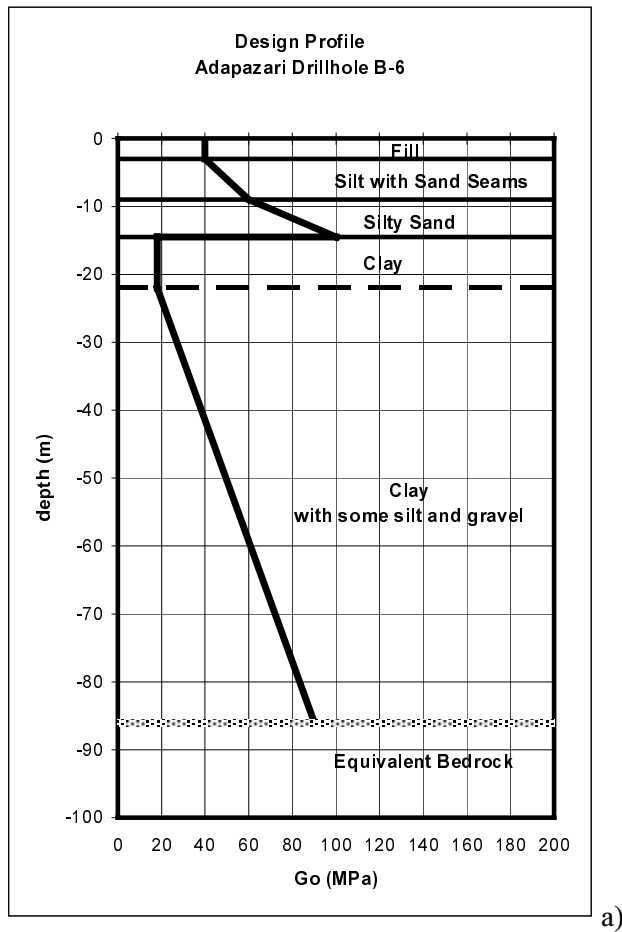
Earthquake ground motion can be substantially modified as the motion is transmitted up through the soil profile to the ground surface. This modification is known as site response and is a function of the soil profile geometry, the soil properties and the characteristics of the earthquake excitation. The magnitude of this modification varies with frequency. There are many documented earthquake case histories in which soil deposits have dramatically modified the earthquake ground motions such as Mexico City, 1985 (EEFIT, 1986) and Loma Prieta, 1989 (EEFIT, 1990). The distribution of geologically recent soil deposits in the earthquake-affected area, that are likely to have resulted in significant modification of the earthquake ground motion, is shown in Figure 4.13. Unfortunately, very few strong-motion recording instruments were located in the particular areas, where damage during the mainshock was most severe, so it is difficult to accurately determine the characteristics of the ground motion that will have contributed to the excessive damage. In order to investigate the likely site response, one-dimensional site response analyses have been carried out on a range of typical ground profiles in the earthquake-affected area that had been visited, namely Adapazari, Izmit, and Gölcük.

The ground profiles and soil parameters used for the analyses are presented in Figures 4.15a to 4.17a. The acceleration time history recorded at the Sakarya Station (SKR) north of Adapazari City has been used as the input earthquake motion for the one-dimensional site response analyses. The Sakarya station is located on stiff soil over rock (refer to Chapter 3). The results of the site response analyses are presented in terms of spectral ratio in Figures 4.15b to 4.17b. The spectral ratio is the ratio of the response spectra from the ground surface time history (i.e. the output from the 1-D analysis carried out using *Oasys* SIREN) and the response spectra from the rock level time history (i.e. the input for the 1-D analysis).

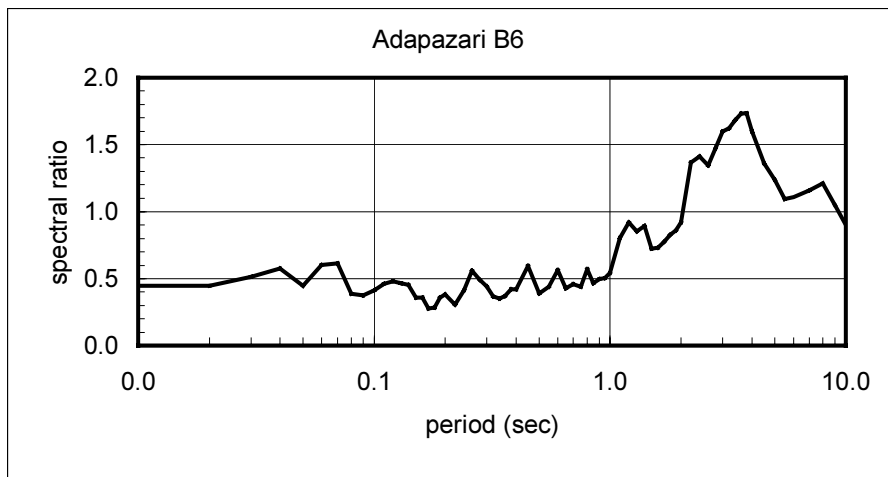
4.4.1 Adapazari

It has already been mentioned that Adapazari has been built on reclaimed land formed over a swamp. The ground conditions comprise a stiff crust of fill underlain by loose sands and silts or soft clays and silts (refer to Section 4.2.1). Ground shaking and subsequent damage to buildings was particularly severe in Adapazari City and this has been attributed to the amplification of the ground motions due to the local ground conditions. The site response analysis has been carried out on a ground profile assumed to be typical for the low-lying area of Adapazari. The northern part of the city is located on rock and is not represented by this analysis. The ground profile and soil parameters used for the analysis are presented in Figure 4.15a. The spectral ratio for the Adapazari site (see Figure 4.15b) indicates that the ground motion is strongly damped at higher frequency (short period) range and slightly to moderately amplified at low frequency (long period) range. This response can be attributed to the considerable thickness of weak soils present beneath Adapazari. It should be noted that the amplification shown at longer periods (>3 seconds) should be interpreted with caution as the accuracy of the input data and the consequent analysis is limited in this long period range.

The local site effects within the Adapazari Basin have also been examined by Beyen *et al.* (2000) using data from an aftershock network established in the city after the mainshock. Their results indicate a site amplification factor of about 10 (i.e. a spectral ratio of 10) in the period range 0.25 to 1.0 seconds. The large amplifications reported by Beyen *et al.* are for weak motion and will not necessarily be representative of the amplification likely to occur during strong shaking. These results are discussed in more detail in Section 3.6.3.



a)



b)

Figure 4.15: Adapazari ground profile for 1-D site response analysis.

4.4.2 Gölcük

The site response analysis has been carried out on a ground profile assumed to be typical for the low-lying coastal area of Gölcük. The ground profile and soil parameters used for the analysis are presented in Figure 4.16a. The spectral ratio for the Gölcük site (see Figure 4.16b) indicates that the ground motion is slightly amplified at high frequency range (0.03 to 0.07 second period) and slightly damped to unaffected at low frequency range (>0.07 second period).

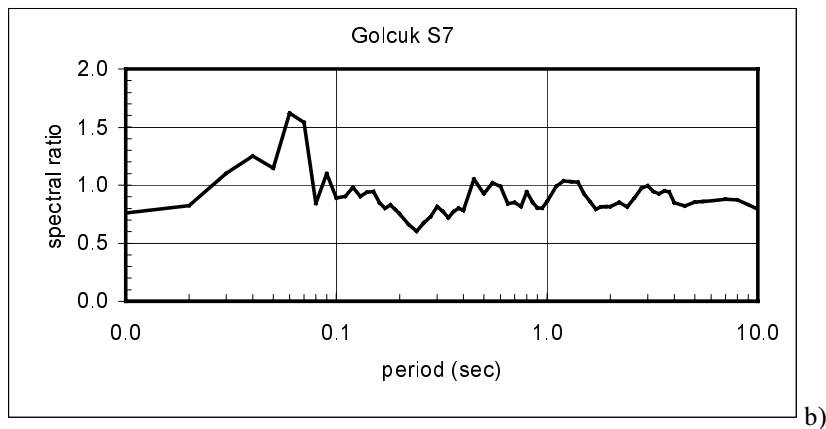
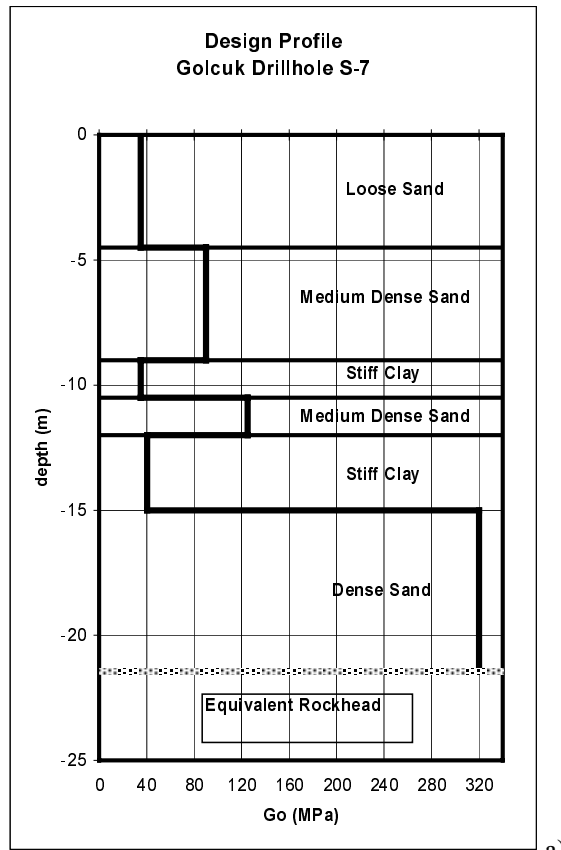
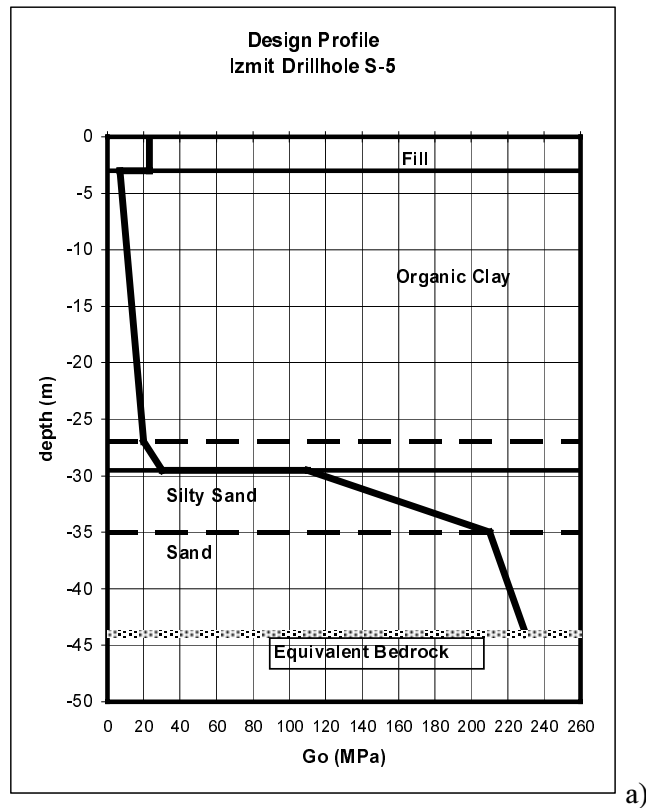


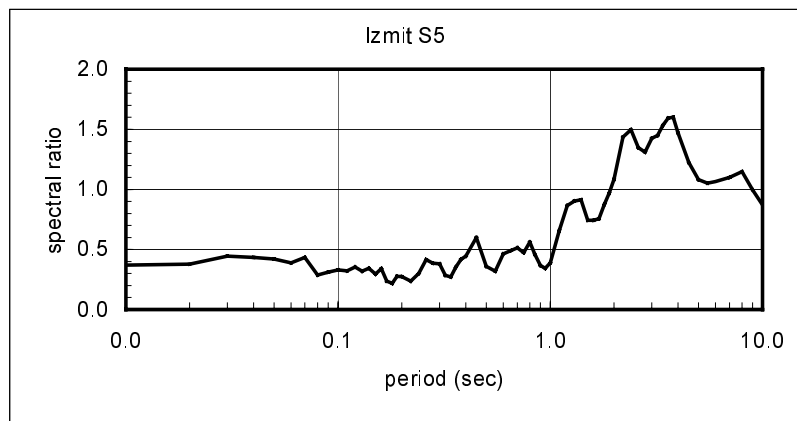
Figure 4.16: Gölcük ground profile for 1-D site response analysis and spectral ratio

4.4.3 Izmit

The site response analysis has been carried out on a ground profile assumed to be typical for the low-lying coastal area of Izmit. The old part of the city is located on rock and is not represented by this analysis. The ground profile and soil parameters used for the analysis are presented in Figure 4.17a. The spectral ratio for the Izmit site (see Figure 4.17b) indicates that the ground motion is damped at high frequency (short period) range and amplified at low frequency (long period) range in a very similar manner to that identified at Adapazari.



a)



b)

Figure 4.17: Izmit ground profile for 1-D site response analysis and spectral ratio

4.5 Liquefaction

Liquefaction is defined as the temporary loss of strength of a saturated soil due to cyclic loading and build-up of pore water pressure. Typically, saturated, poorly graded, loose granular deposits with a low fines content are most susceptible to liquefaction. Loose alluvium sands are present throughout the earthquake-affected area. In addition, the topography is often low lying and the ground water table is close to the surface.

The locations where liquefaction related phenomena such as sand vents and lateral spreads were observed are shown in Figure 4.3. At other locations direct evidence of liquefaction was not seen, but it is inferred from the geometry of failure, the ground conditions and the ground water conditions. Liquefaction phenomena have been reported in many other locations within the earthquake-affected area. The EEFIT team made observations of these phenomena in Adapazari, Sapanca, Gölcük and Izmit.

4.5.1 Adapazari

Extensive areas around Adapazari City are interpreted to have experienced liquefaction. The phenomena that support this interpretation are:

- sand venting and upwelling of sand over paved areas,
- ground settlement;
- differential settlement of buildings foundations and foundation failures; and
- ground fissures interpreted to be associated with ground oscillations.

The ground conditions beneath Adapazari City comprise up to 200m depth of generally soft to firm soils over rock. The majority of the soil column comprises clays with gravel, peat and sandy horizons. The upper metre of the profile is typically made ground. Below this there is typically 4 metres of very variable alluvial soils ranging from loose sand through silt to soft clay. Beneath these soils dense sandy gravel is frequently recorded with a thickness of 5 m or more. Sand venting and upwelling of sand over paved areas was observed in a number of areas (Plates 4.15). These phenomena were often associated with buildings where ground floor slabs had failed by bulging at the centre due to settlement of the strip footing around the perimeter of the building. The effects on building foundations are discussed separately in Section 4.7.

An assessment of the liquefaction potential of soils in three representative ground profiles beneath Adapazari City has been carried out using the methodology proposed by Seed and Idriss (1985). The ground conditions and ground profiles have been presented in Section 4.2.1. Figure 4.18 shows a plot of corrected standard penetration test blow count (N_{60}) versus cyclic stress ratio for the upper loose sand and silty sand layer. The results indicate that these layers are potentially liquefiable. Figures 4.19a to 4.19c are plots of corrected standard penetration test blow count (N_{60}) versus depth for the same three soil profiles beneath Adapazari City. Also shown on the plots are curves representing the boundary between liquefaction and non-liquefaction. It can be seen that liquefaction potential is limited to the upper sand and silty sand layer that is present at relatively shallow depth.

In locations where liquefaction has taken place, densification of the granular strata may have subsequently occurred. A method for estimating the amount of settlement following liquefaction has been proposed by Tokimatsu and Seed (1987). Based on this method the amount of settlement that would be expected from densification of a 5 m thick liquefiable layer is in the order of 50 mm to 150 mm. In many areas the amount of differential settlement of buildings was significantly greater than 150 mm (see Plate 4.16). The building settlement will also be a function of the bearing capacity of the soil in the liquefied state and, as such, the soil and building settlement will not necessarily correspond.

Where the ground surface is flat and no free face exists to allow lateral spreading, liquefaction at depth may allow the upper crust to oscillate in the form of ground waves. These oscillations are usually accompanied by ground fissures and fracturing of rigid structures such as pavements and pipelines. A number of these features were observed in Adapazari (see Plates 4.17a, b).

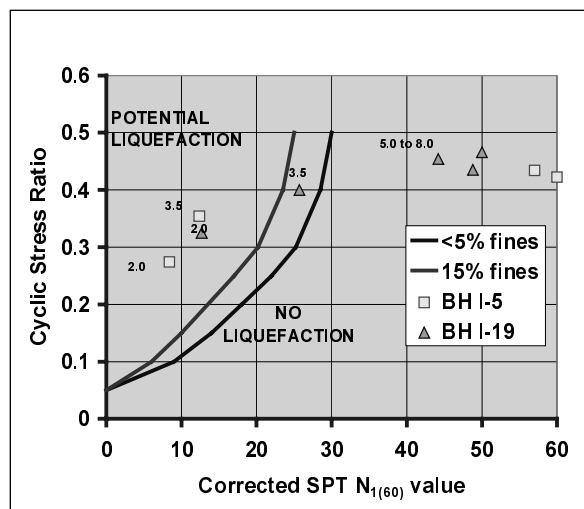


Figure 4.18: Liquefaction potential in Adapazari from SPT data. Depth below ground level (m) is shown beside each point. BH I-19 at 3.6 m is likely to be too silty to have liquefied.

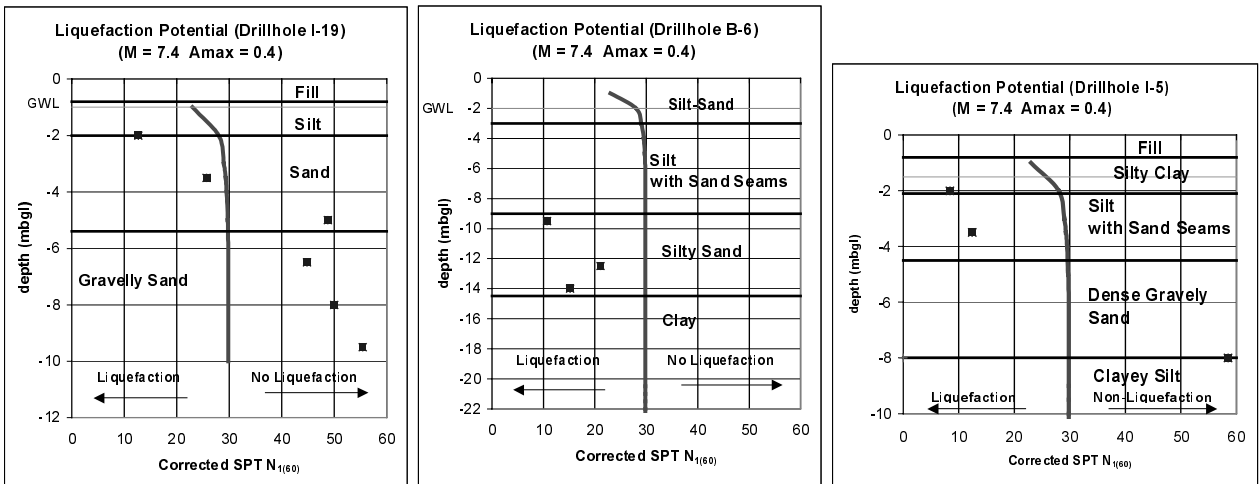


Fig 4.19 a, b, c: Liquefaction potential at Adapazari City for Drill holes I-19, B-6 and I-5. Note the limited depth of potential liquefaction for holes I-19 and I-5. For holes B-6 and I-5 correction for fine contents has been carried out.

4.5.2 Sapanca

During the earthquake an extensive area beneath and around the Hotel Sapanca, on the South Shore of the Sapanca lake, some 15 km south west of Adapazari, experienced liquefaction. This produced upwelling of sand over paved areas, differential settlement of the hotel, a large shallow angle slide with multiple scarps, and submergence of waterfront retaining structure (Figure 4.20). Scarps associated with the slide were observed at least 150 m inland from the former waterfront. The scarp in the vicinity of the hotel entrance is shown in Plate 4.18 and the submergence at the lake frontage of the hotel is shown in Plate 4.19.

Extensive areas of wet sand were noted overlying the access roadway and in the paved dining area at the shore. These areas contained ‘sand volcanoes’, indicating that the sand had been expelled with groundwater from the underlying stratum. Pumping of the sand underfoot readily reduced it to a liquefied state. Samples of the sand were obtained from the fissure at the site entrance at a depth of about 500 mm beneath the block paving. The sand from this location appeared similar to that expelled onto the paving except for the presence of gravel in the sand matrix beneath the roadway. Grading curves of the expelled sand (A) and the sand beneath the roadway (B) are shown in Figure 4.21. It is probable that grading B was produced by the gravel of the road sub-base sinking into the liquefied sand below.

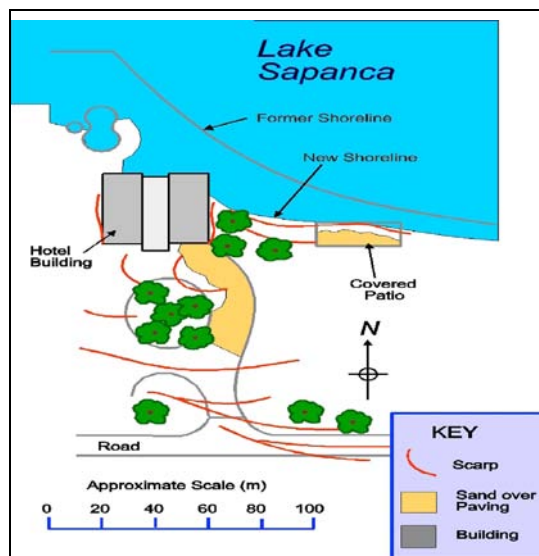


Figure 4.20: Sapanca Hotel layout plan

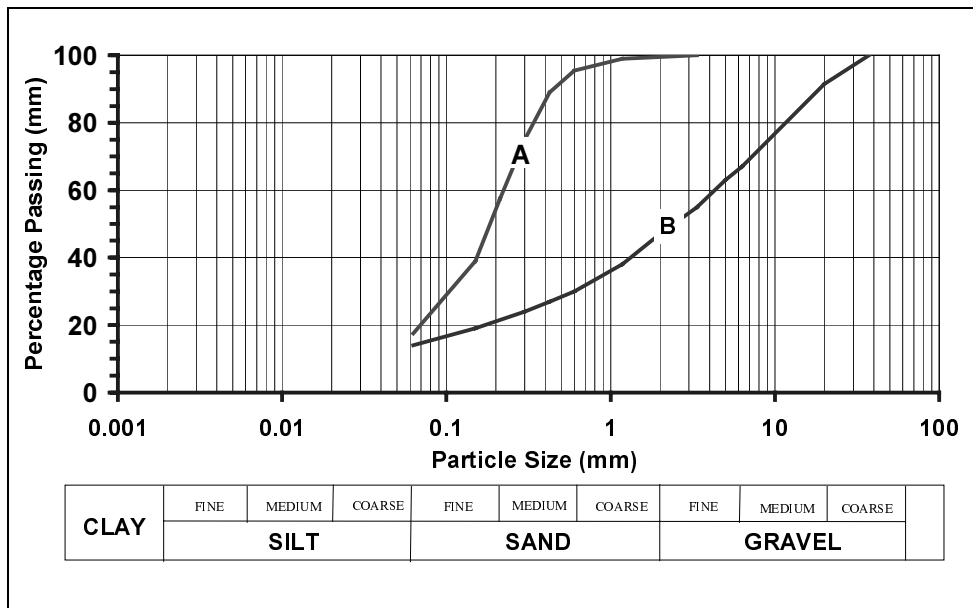


Figure 4.21: Grading Curves form Hotel Sapanca Site. (Courtesy Soil Mechanics Limited)

The Hotel Sapanca is located on the southern shore of Lake Sapanca. The hotel is approximately square in plan, measuring 40 m along each side and is 4 storeys high. The west and east wings appear to have been built on separate raft foundations. A full height glazed atrium runs through the centre of the structure. The hotel building did not collapse in the earthquake but it was an economic write-off. The vertical settlement induced by the slide submerged the northeast corner of the ground floor. The east wing of the building tilted and translated further than the west wing. This differential movement damaged the frame supporting the glazed roof of the atrium but collapse of the roof was avoided.

4.5.3 Gölcük

The waterfront at Gölcük along the southern coast of Izmit Bay is formed on alluvial fan and hill wash fan deposits overlain by recent reclamation fill. The ground conditions typically comprise alternating layers of silt, sand and gravel. Liquefaction of the sand layers in this area produced shallow angle slides with multiple scarps, submergence of the waterfront, upwelling of sand, and differential settlement.

Numerous shallow angle slides with multiple scarps were observed along the Gölcük waterfront, particularly along an approximately 3 km length of coastline north of the Ford Otosan site (see Figure 4.14). A large section of the Gölcük waterfront suffered 1.5 m to 2.5 m of subsidence interpreted to be fault related (refer to Section 4.3). In addition to this fault-related subsidence, which extends 1 km to 1.5 km inland, the coastline has subsided and been displaced locally due to the formation of lateral spreads.

Upwelling of sand onto paved areas was observed on the waterfront promenade at Gölcük. A sand vent was also reported to have occurred at the Ford Otosan site but this was not observed by EEFIT.

Differential settlement of the ground adjacent to the Ford Otosan site bodyshop building was estimated to be in the order of 0.75 m to 1 m over a distance of approximately 100 m (Plates 4.8 and 4.9).

4.5.4 Izmit

The water front at Izmit along the northern coast of Izmit Bay is the product of recent construction coinciding with the laying of the new trunk water main close to the former shoreline in 1997-8 (see Plate 4.20). In the earthquake the 60 m to 80 m wide strip of reclamation filled ground suffered liquefaction and lateral spreading (refer to Section 4.6.3). Details of the ground conditions are unknown. At the Izmit Steamer Port, the ground immediately behind the waterfront retaining structure settled by approximately 1 m as a result of the slide and post liquefaction densification

(Plates 4.21 and 4.22). A large number of tension cracks were observed in the ground surface and fine sand had vented onto the surface through the topsoil.

4.6 Earthquake Induced Slope Instability

Strong earthquakes often cause slope instability. The earthquake induced slope stability phenomena observed following the Kocaeli earthquake can be summarised into four main categories;

- rock falls,
- soil slumps,
- soil lateral spreads, and
- sub-aqueous landslides.

Many of the earthquake induced slope failures were related to liquefaction phenomena, but many others simply represent the failure of slopes that were interpreted to be only marginally stable under static conditions.

4.6.1 Rock falls

Minor rock falls of less than 5 m³ were observed in many locations where steep cuts in fractured rock masses had been formed. In particular, minor rockfalls were observed in road cuts between Gölcük and Karamusel on the south coast of Izmit Bay and inland on the road to Yuvacik Dam (see Plate 4.23). However, rock fall was not a significant phenomenon as the topography of the earthquake-affected region is generally low lying with relatively few significant rock slopes.

4.6.2 Soil slumps

Soil slumps, where sliding occurs on a basal shear surface and with a component of rotation, were observed in a number of locations. Soil slumps were particularly common along the steeply incised banks of the Sakarya River (see Plate 4.24). Significant soil slump features were also observed in the area south of Yalova particularly in the Pliocene to Pleistocene Age very weak mudstones.

4.6.3 Lateral spreads

Lateral spreads, where sliding occurs by translation on a basal zone of liquefied sand or silt or weakened sensitive clay, occurred in many locations. The distribution of sites at which lateral spreads were observed is illustrated in Figure 4.3. Such slides occurred on the lake coast at Sapanca and along the coast of Izmit Bay at Izmit, Gölcük and Degirmendere.

The lateral spread observed at Sapanca, and the associated damage to the Hotel Sapanca is described in Section 4.5 and illustrated in Figures 4.20 and Plates 4.18 and 4.19. The lateral spread occurred on a very low angle slope inclined 2° to 3° toward the lake and was associated with the formation of numerous tension gashes.

Significant areas of lateral spreading were observed along the southern coast of Izmit Bay. The lateral spread at the Izmit Steamer Port are described in Section 4.5 and illustrated in Plates 4.21 and 4.22. The lateral spread occurred on a slope inclined 2° to 3° toward Izmit Bay. The lateral spreading that occurred at Gölcük is described in Section 4.5 and illustrated in Plates 4.3 and 4.4. Lateral spreading was also observed at Degirmendere (see Plates 4.25 and 4.26).

4.6.4 Sub-aqueous landslides

At Gölcük and Degirmendere the lateral spreads appear to extend offshore and may include sub-aqueous landslides. Soon after the earthquake, fisherman reported changes in seabed levels and the occurrence of sub-aqueous ground movements. A large portion of the coastline of Gölcük has been submerged by 1.5 m to 2.5 m. The timing of the submergence and the lateral spreading is unclear.

4.7 Earthquake Effects on Building Foundations

Adapazari City suffered exceptionally widespread damage except in the southernmost districts of the city. As was the case at Gölcük and Yalova, the damage at Adapazari was principally to structures of 4 or 6 storeys. However, in contrast to other locations, many buildings in Adapazari City suffered foundation failures that resulted in settlements of up to a metre and significant tilting. Although Adapazari is a long established site, its structures are predominantly recent. Much of the older housing has been demolished in the last twenty years and rebuilt as 4 or 6 storey reinforced concrete frame structures on raft foundations. The older housing can still be found in some locations and is generally 2 storey and of brick or timber frame with brick infill construction. The older building stock suffered less damage unless unfortunate enough to be crushed in the collapse of one of their newer neighbours.

The foundation failures are a product of the particular ground conditions at Adapazari and the recent building boom. As discussed in Section 4.2.1, the ground conditions for most of the city comprise up to 200 m depth of generally soft to firm soils over rock. The majority of the soil column comprises clay with gravel, peat and sandy horizons. The upper metre of the profile is typically made ground reclamation fill. Below this there is typically 4 m of very variable alluvial soils ranging from loose sand through silt to soft clay. Beneath these soils dense sandy gravel is frequently recorded with a thickness of 5 metres or more.

Consideration of the ground conditions indicates that the foundation failures may have resulted from two main causes:

- liquefaction of the loose saturated sands, and
- bearing capacity failure in the soft silts and clays.

The results of an assessment of the liquefaction potential of soils beneath Adapazari City are described in Section 4.5. The assessment indicates that liquefaction of a 3 m to 5 m thick loose sand near surface layer may have occurred. When the soil is liquefied the residual undrained shear strength of the sand is greatly reduced. An estimate of the residual undrained shear strength can be made using the methodology proposed by Seed and Harder (1990). For sands with SPT N_{60} values of 8 to 10 the residual undrained shear strength is estimated to be in the order of 10 kN/m² to 20 kN/m². A five-storey reinforced concrete building might impose a foundation bearing pressure on its raft of approximately 75 kN/m². A simple bearing capacity assessment indicates that the liquefied material would have inadequate capacity to support the loads. Building foundation failures, interpreted to be caused by liquefaction, were observed throughout the city (see Plates 4.27 and 4.28). Failures were typically associated with unacceptably high differential settlement or bulging failure of the base slab.

In some cases, structures on clay soils also suffered foundation failure. The grading curve for a soil sampled from beneath a building that suffered a foundation failure is shown in Figure 4.22. The soil is a clayey silt with minor sand. The plastic and liquid limits for this sample were PL = 29 and LL = 62 and the undrained shear strength was manually assessed (the soil was easily penetrated by fist) to be less than 20 kN/m² (say 15 kN/m²). The damaged building is shown in Plate 4.29. The shear strength assessment suggests that some newer buildings in Adapazari may have unusually low static factors of safety against bearing capacity failure. As noted above, a five-storey reinforced concrete building might impose a foundation loading pressure on its raft of approximately 75 kN/m². The ultimate bearing capacity of the foundation may be only 10% to 20% above this value, i.e. a FoS of 1.1 to 1.2. It is normal for engineered structures on clay soils to have static factors of safety against failure of FoS = 3. This is principally to limit settlements to acceptable levels. Therefore, at Adapazari City it would be expected that settlement problems would be apparent for many of the taller buildings on raft foundations. Evidence of ongoing settlements prior to the earthquake was seen in the centre of the city where a number of buildings had steps down from pavement level to their ground floor entrances.

Earthquake loading imposes substantial horizontal and rotational forces on foundations. These forces reduce the ultimate vertical bearing capacity of the foundations. Combining the seismic foundation analysis of Shi and Richards (1995) with the seismic displacement analysis of Ambraynes and Menu (1988) indicates that settlements of up to about 800 mm could have occurred for rafts on clay soils.

Given the low bearing capacity of the soils and the magnitude of foundation movements that were observed at Adapazari, it is almost surprising that only a limited number of buildings overturned following expected patterns of failure. The reason may be attributed to the relatively shallow depth of liquefiable or yielding soil beneath the raft foundations. This may have prevented general circular failures from occurring in many cases. The development of higher tilts was observed in a number of buildings with narrow width foundation slabs (see Plates 4.27 to 4.29). The narrow width of the foundation slabs may have enabled rotational slip surfaces to form in the weak ground, unimpeded by any stronger soils a few metres further down.

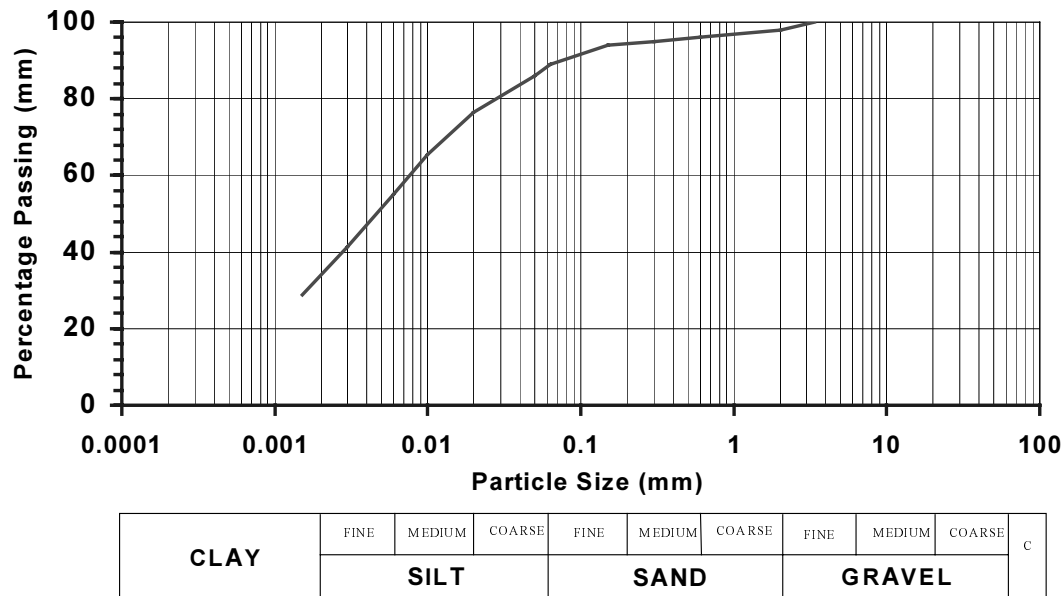


Figure 4.22: Particle size distribution for soil beneath tilted foundation slab at Adapazari

4.8 Earthquake Effects on Retaining Structures

The response of reinforced earth (or mechanically stabilised earth) slopes and walls to earthquake shaking is not well documented world-wide. The study by Tatsuoka *et al.* (1995) following the January 1995, Kobe Japan earthquake provides the most extensive resource of case study information.

Reinforced earth walls were used to retain the earth fill embankment for the northern approach to an over bridge crossing the E80 Trans-European Motorway at Arifiye. The earthquake severely tested these walls as the surface rupture of the main fault passed directly between the bridge abutments, within meters of the walls, leading to the catastrophic structural failure of the bridge span segments (refer to Chapter 7 for further details).

The 100 m long northern approach ramp to the bridge was constructed from reinforced earth and reached a height of 8 m above ground level at the abutment (Plate 4.30). Cruciform pre-cast panels attached to 40 mm wide galvanised steel ribbed soil reinforcing straps formed vertical faces to both sides of the ramp. A stream was channelled across the line of the earthworks through a 4 m wide reinforced concrete culvert 15 m north of the abutment.

In relation to ramp walls and embankments the following were observed:

- liquefaction of the foundation producing substantial settlement,
- distortion of the horizontal alignment due to ground strain, and
- differential excitation of the cope elements leading to pounding damage.

The soil beneath the ramp is silty sand with gravel and occasional cobbles and the groundwater table is approximately 1 m below ground surface. The earthquake appears to have caused liquefaction of the soil over a zone about 20 m wide to the north of the abutment, leading to settlement of about a 1 m at the base of the ramp. Settlements at roadway level were reduced to about 350 mm due to arching in the reinforced earth. Appreciable damage was caused to a vertical strip of panels on the eastern side of the ramp and panels at cope level on the western side were crushed. Although some fill escaped between damaged panels (Plate 4.31), none of the panels became detached from the soil reinforcing straps and the walls remained vertical.

Observations on the ramp indicate that it was originally constructed to a straight alignment from the abutment. However the post earthquake alignment is bent at a point about 20 metres north of the abutment, with the abutment

being displaced to the west by about 750 mm. It is considered that this may be due to ground distortion in the area close to the fault rupture. The effect of this distortion was to open gaps between panels on the eastern side of the ramp. Also on the eastern side of the ramp a horizontal gap of about 300 mm opened between adjacent sections of the concrete culvert.

Inspection of the reinforced concrete wall panels showed only minor effects from impact of the panels on one another during the earthquake. The effect on the cope units was rather more severe with spalling due to pounding on several units (see Plate 4.31 and 4.32). However this damage could readily be made good with in situ repairs.

Clearly the reinforced earth ramp should not have been built on potentially liquefiable soils without appropriate ground improvement or support measures. The consequence is that the southernmost 20 m section of the ramp will require rebuilding. However, in spite of this oversight, the reinforced earth behaved very well under severe imposed deformations and loadings. Had the adjacent bridge survived the earthquake, the approach structure would have provided adequate support for the road and would have maintained access for emergency services.

4.9 Earthquake Effects on Earth Embankments

Earth embankments are commonly used throughout the region for approach ramps for road over-bridges. A large number of these embankments suffered minor damage during the earthquake. The damage could be attributed to a number of causes:

- differential settlement of the embankment material,
- differential settlement of the foundation material,
- minor slope instability on the embankment slopes,
- differential lateral movement causing separation between the bridge abutment and the embankment, and
- horizontal distortion due to ground strain from the fault zone.

Damage to the reinforced earth embankment and retaining walls for the northern approach to an over bridge crossing the E80 Trans-European Motorway at Arifiye is described in Section 4.8 above. Damage to the embankment was primarily due to horizontal distortions caused by movement along the fault rupture zone, which passed beneath the embankment, and by settlement of the foundation material that is interpreted to have liquefied during the earthquake. Damage to the earth embankment on the approach road to the Toyota Factory, south of Adapazari City was also investigated. The embankment had settled by approximately 300 mm and separated from the bridge abutment (see Plate 4.33). The embankment had also suffered numerous small-scale soil slumps of 0.5 m³ to 1.5 m³.

The damage was most commonly manifested by bump-on and bump-off motorway bridge embankments in a 20 km stretch of road, 10 km west and east of the Adapazari region. Settlements ranging from 100 mm to 500 mm were observed (see Plate 4.34).

4.10 Gas Venting

The venting and flaring of natural gas is reported to have occurred following the 17 August 1999 earthquake in the area near Gölcük. Venting is reported to have occurred both on and offshore. Similar gas seeps were reported following the San Fernando earthquake in 1971 (Clifton et al. 1971) and by Field and Jennings (1987) following an earthquake in Northern California in November 1980.

The gas venting was particularly common from water wells where gas was found to bubble to the surface and could flare off when ignited (see Plate 4.35). Gas clouds or dense bubbling was also noted offshore near Gölcük.

4.11 References

- Ambraseys, N.N. and Menu, J.M. (1988) Earthquake-induced ground displacements. *Earthquake Engineering & Structural Dynamics* **16**, 985-1006.
- Barka, A. and Kadinsky-Cade, K. (1988). Strike-slip fault geometry in Turkey and its influence on earthquake activity. *Tectonics*, Vol. 7, No. 3, 663-684.
- Clifton, H.E., Greene, H.G., Moore, G.W. and Phillips, R.L. 1971. Methane seep off Malibu Point following the San Fernando earthquake. USGS Professional Paper, No. 733, 112-116.
- EEFIT (1986). The Mexican Earthquake of 19 September 1985, A Field Report by EEFIT, The Institution of Structural Engineers, London, UK.
- EEFIT (1990). The Loma Prieta, USA Earthquake of 17 October 1989, A Field Report by EEFIT, The Institution of Structural Engineers, London, UK.
- Erken, A. (1999). The effect of soil condition during Kocaeli earthquake, Istanbul Technical University, Istanbul, Turkey. (<http://193.140.203.8/earthqk/liq.htm>).
- Field, M.A. and Jennings, A.E. 1987. Seafloor gas seeps triggered by a northern California earthquake, *Marine Geology*, vol.77, 39-51.
- Kopp, K.O., N. Pavoni, and C. Schindler (1969). Geologie Thrakiens IV: Das Ergene-Becken. *Beih. Geol. Jahrb.*, Hanover, 76, 136p.
- Lettis, W., J. Bachhuber, A. Barka, R. Witter, and C. Brankman (2000). Surface fault rupture and segmentation during the Kocaeli earthquake (in press).
- Ozaydin I.K. and Inan S.Y.K. (1984), "Performance of large diameter oil tanks", International Conference on Case Histories in Geotechnical Engineering, University of Missouri.
- Safak, E., M. Erdik, K. Beyen, D.Carver, E. Cranswick, M. Celebi, E. Durukal, M. Erdik, T. Holzer, M. Meremonte, C. Mueller, O. Ozel, E. Safak, and S. Toprak (2000). Recorded mainshock and aftershock motions (in press).
- Sakarya University (1998). Adapazari City Centre-Geology and Geomorphology, Report No.1 Sakarya University and Adapazari Municipality, Izmit, Turkey, July 1998.
- Seed, H.B. and Harder, L.F. (1990). SPT-based analysis of cyclic pore pressure generation and undrained residual strength, in J.M. Duncan ed., Proceedings, H. Bolton Seed Memorial Symposium, University of California, Berkeley, 2, 351-376.
- Seed, H.B., Tokimatsu, K., Harder, L.F. and Chung, R.M. (1985). Influence of SPT procedures in soil liquefaction resistance evaluations, *Journal of Geotechnical Engineering*, 111, 2, 1425-1445.
- Shi, X. and Richards, R. Jr. (1995) Seismic bearing capacity with variable shear transfer. *Earthquake-Induced Movements and Seismic Remediation of Existing Foundations and Abutments*, Geotechnical Special Publication No. 55, 17-32, American Society of Civil Engineers.
- Sieh, K., Gonzales, T., Barka, A. (1999) Assessment of Seismic Fault Rupture, Ground Deformations and Submergence Hazards at the Ford Otosan Facility in Kocaeli, Turkey.
- Tatsuoka, F, Koseki, J. & Tateyama, M. (1995) Performance of erinforced soil strucutres during the 1995 Hyogo-ken Nanbu Earthquake.
- Tokimatsu, K. and H.B. Seed (1987). Evaluation of settlements in sand due to earthquake shaking, *Journal of Geotechnical Engineering, ASCE*, 113, 8, 861-878.
- Turkish Geological Survey (1989). Geological Map of Turkey Scale 1:2,000,000, General Directorate of Mineral Research and Exploration.

APPENDIX 4A



Plate 4.1 Ford Otosan, Gölcük Plant Press Shop under construction. View to west of pile cap excavation showing 1.2 m of reddish brown gravelly sand fill overlying loose alluvial sand. Evidence of jet grouting at site can also be seen. Foundations comprise four-pile groups with 600 to 700 mm diameter piles at 2000 mm centres. Main reinforcement is 10 number 16mm deformed steel bars and confining steel is 10 mm deformed steel. (photograph taken on 5 September 1999).



Plate 4.2 Near surface stratigraphy exposed in fault scarp in Gölcük near the Indoor Sports Hall showing a thin topsoil layer underlain by 0.5m of silty sand and 1m of sandy gravel (photograph taken 10 September 1999).



Plate 4.3 Coastal flooding associated with approximately 2m of vertical offset on Gölcük pull-apart zone normal fault. View is of submerged sea front promenade looking toward north-west (photograph taken on 10 September 1999).



Plate 4.4 Coastal flooding associated with approximately 2m of vertical offset on Gölcük pull-apart zone normal fault. View is of submerged sea front amusement park looking toward north (photograph taken on 10 September 1999).



Plate 4.5 Normal fault scarp adjacent to Gölcük Football Stadium. Stadium is on down thrown side with approximately 2m of vertical offset. EEFIT members are standing on back scarp tension cracks. View is toward south-east along fault alignment (photograph taken on 10 September 1999).



Plate 4.6 Normal fault scarp adjacent to Gölcük Football Stadium and passing beneath corner of Gölcük indoor sports hall. Sports hall wall has approximately 1.5m vertical and 1m lateral offset. View is toward south-east along fault alignment (photograph taken on 10 September 1999).



Plate 4.7 Normal fault scarp at Gölcük passes in front of three to five storey reinforced concrete frame buildings without causing collapse. At this location the fault, bearing 150° , formed a single scarp with 1.6m vertical offset (photograph taken on 10 September 1999).



Plate 4.8 Ford Otosan, Gölcük Plant Body Shop west wall. View from southwest corner looking north. Fissure in ground has formed along alignment of cement grout columns, which were installed across the site as ground improvement to increase bearing capacity and resist liquefaction susceptibility. Note differential settlement distortion of wall (photograph taken 5 September 1999).



Plate 4.9 Ford Otosan, Gölcük Plant Body Shop west wall. Failure and closure of door in west wall illustrates compression in north-south direction of approximately 400mm (photograph taken on 5 September 1999).



Plate 4.10 Fault rupture at Yuvacik bisected school building causing collapse. At this location the fault was divided into two ruptures oriented 285° with a central graben 5m to 8m wide. The main rupture had 1.5m right lateral offset and 0.7m vertical offset (photograph taken on 18 September 1999).



Plate 4.11 Fault rupture 'mole track' at Yuvacik passes beneath a three storey reinforced concrete frame building without causing collapse. At this location the fault was a single rupture oriented 285° with a 1.6m right lateral offset (photograph taken on 18 September 1999).



Plate 4.12 Fault rupture 'mole track' at Yuvacik passes in front of three-storey reinforced concrete frame buildings without causing collapse. At this location the fault formed two ruptures oriented 270° with a 1.6m right lateral offset on the main rupture and 0.9m right lateral offset on the secondary rupture (photograph taken on 18 September 1999).

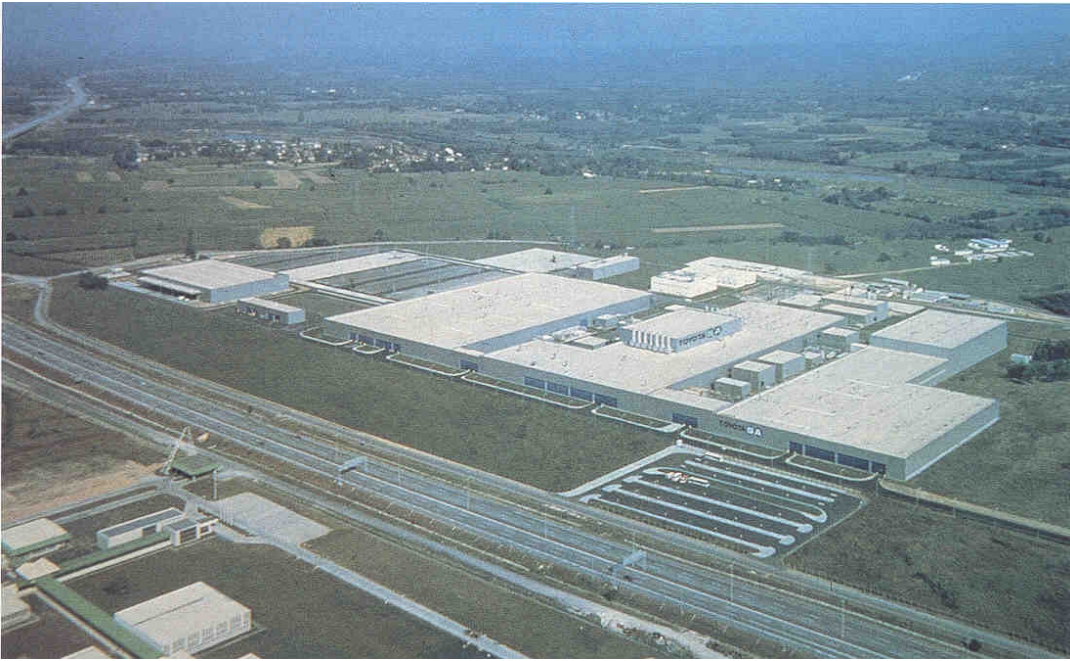


Plate 4.13 Oblique aerial view of Toyota Factory taken prior to earthquake. Highway is located on north side of factory and alignment is approximately east–west. The fault rupture passed to south of factory.



Plate 4.14 Fault rupture ‘mole track’ at entrance to Toyota Factory. Fault at this location formed broad 50m to 100m wide zone of deformation with series of sub-parallel ruptures (photograph taken on 8 September 1999).



Plate 4.15 Sand venting and 300mm differential settlement of pavement in central Adapazari interpreted to be associated with liquefaction (photograph taken on 6 September 1999).



Plate 4.16 Differential settlement of pavement and buildings in central Adapazari on Pamuklar Sokak interpreted to be associated with liquefaction. Distortion of pavement may also be attributed to uplift of services due to buoyancy of buried pipes (photograph taken on 6 September 1999).



(a) (b)
Plate 4.17 Compression ridges and fractures (a) and tension fissures (b) in the road pavement on Tasler Sokak in central Adapazari (photograph taken 8 September 1999).



Plate 4.18: At the Hotel Sapanca site, liquefaction of fine sand at depth is interpreted to have resulted in lateral spreading of the shoreline into Lake Sapanca. The failure scarp extended over 100 m back from former shoreline.



Plate 4.19: At the Hotel Sapanca site, the lateral spreading slide mass has moved toward the lake resulting in submergence of the lake front side of the hotel. The hotel is constructed on two independent raft foundations, however, only minor differential movement occurred between rafts.



Plate 4.20: Oblique aerial view of Izmit waterfront under construction in June 1998.



Plate 4.21 Ground settlement and low angle lateral spreading at Izmit Steamer Port. Note approximately 1m differential settlement between piled wharf structure and backfill. Also note tension cracks in foreground and slide toe uplift at centre left (photographs taken 11 September 1999).



Plate 4.22 Displaced waterfront structure with settled made ground behind at Izmit Steamer Port.



Plate 4.23 Minor rockfall debris observed on the road to Yuvacik Dam.



Plate 4.24 Soil slumping on banks of Sakarya River near Toyota Plant outside Adapazari (photograph taken on 8 September 1999).



Plate 4.25 Back scarp of low angle slide or lateral spread at Degimendere. Approximately 20m of waterfront promenade is understood to have failed (photograph taken on 10 September 1999).



Plate 4.26 Tension crack behind back scarp of low angle slide or lateral spread at Degimendere (photograph taken on 10 September 1999).



Plate 4.27 Bearing capacity failure of five storey building in Sedat Sokak in central Adapazari. Failure is interpreted to be due to liquefaction as building has settled into ground by 0.5m to 2m. Overturning has been arrested by neighbouring building (photograph taken 8 September 1999).



Plate 4.28 Bearing capacity failure and tilting of four and five storey buildings in Yenigun Mahallesi in central Adapazari (photograph taken on 6 September 1999).



Plate 4.29 Tilting building. Note separation of 1 m between arch and its springing on corner of structure.



Plate 4.30 Reinforced earth wall for E80 highway approach ramp at Arifiye. View toward the southwest. Culvert crosses the ramp beneath the nearer end of the damaged coping units. Vertical movement joints in the panels run up from the edges of the culvert.



Plate 4.31 Reinforced earth wall for E80 highway approach ramp at Arifiye. Damage to wall panels on the eastern side of the ramp. The ramp on the left side has settled with respect to that on the right. Opening of panel joints has been exacerbated by the horizontal distortion of the ramp about a 'hinge point' on the opposite side of the ramp.



Plate 4.32 Reinforced earth wall for E80 highway approach ramp at Arifiye. Pounding damage to cope units.



Plate 4.33 Differential settlement of approach embankment and damage to bridge abutment on access road to Toyota Factory outside Adapazari (photograph taken on 8 September 1999).



Plate 4.34 Differential settlement of earth embankment on-ramp and off-ramp to highway bridges formed bump-on and bump-off structures .



Plate 4.35 Gas vent and flare from drillhole casing at Ford Otosan Factory near Gölcük.

5 Performance of Buildings

Dina D'Ayala,
University of Bath

Paul Doyle,
Babtie Group

Robin Spence,
University of Cambridge

5.1 Introduction

The Kocaeli earthquake struck an extensive geographical area in which the population density, and hence urbanisation and construction of residential buildings, had had a steep increase in the last 20 years. Consequently, most of the building stock, as discussed in Chapter 1, is of relatively recent construction and up to 90 % of it has a structure formed by load bearing concrete frames. While buildings with steel structures represent a very small minority, other relatively common structural types are traditional masonry infill-timber frames and some traditional load-bearing masonry. These two typologies are rarely taller than two storey and they have comparatively fared well in the earthquake.

The seismic zonation of Turkey identifies the strip from the Marmara Sea to the Sapanca Lake as of highest risk, imposing the strictest code requirements, and hence most of the building stock should have been built to the 1975 Turkish Seismic Standards for building in zone 1. Some of the shortcomings of the 1975 Code, and of the quality of construction of moment resisting concrete frames in Turkey, had already become evident after the Erzincan earthquake of 1992, and the code reviewing process had been completed in 1997 with the publication of a new document, which has been enforced since the beginning of 1998. Consequently only a relatively small proportion of the building stock could have been designed according to the new standard. Moreover the width of Zone 1 (highest risk) along the Anatolian fault has been extended in the new Code to cover almost entirely also the previous Zone 2.

The major reason for the poor performance of residential buildings, which caused such a high number of casualties, should not however be considered a shortcoming of the code prescriptions as much as the general poor quality of materials and construction details, and in many cases the total lack of basic seismic provisions. Indeed the enforcement of the existing code remains a major obstacle for life safety.

The other concurrent cause of the widespread destruction has been identified in the poor soil condition on which many of the collapsed buildings were founded. Although not easily assessed, only a very small minority of buildings had pile foundations, while the majority with raft foundations, were usually set very superficially on soils prone to liquefaction and with comparatively low bearing capacity. The proportion of rigid body overturning of whole buildings was considerable, especially in Adapazari.

Most of the building stock throughout Turkey, and especially in the Istanbul metropolitan area, has similar characteristics, albeit with lower levels of hazard, according to the macrozonation map, and hence the implications in terms of possible devastation and casualties are only too evident. Henceforth, one of the most pressing issues, for the Turkey construction industry and the structural engineers, is how to estimate the realistic performance of these structures and devise possible strengthening measures.

Due to the high level of damage, most of the onsite inspection entailed examination of buildings externally, with limited internal survey where the conditions allowed it.

In the rest of this chapter a discussion on the 1975 and 1997 seismic codes is first presented. The following section 5.3 is based on the presence of many buildings under construction, which allowed investigation of the constructional process and materials used. It should however be noted that these cases were not necessarily representative of the past practice. An extensive collection of damage details, all too familiar, is presented with commentary in section 5.4, while a statistical and geographical analysis of the damage observed is reported in section 5.5.

5.2 Building Code Requirements

After the highly destructive 1939 M 7.9 Erzincan earthquake temporary seismic regulations for institutional buildings were issued in 1940, and the first Turkish Seismic Code was published in 1944 in the form of legal provisions, inspired by contemporary Italian seismic provisions. Successive revisions and updates followed in 1953, 1961, 1968, 1975, and 1997. In each period, the design philosophies and requirements were updated according to the current knowledge and in line with other seismic codes. The effect of ductility was first indirectly accounted for in the 1975 code. The 1997 code is similar to the Eurocode 8 1996 and the 1994 Uniform Building Code. In the following the two last updates, which were in force during the period of high urbanisation of the Marmara Sea Region, are outlined briefly with a discussion of the major differences.

5.2.1 The 1975 Seismic Code

The 1975 code is part of a publication of the Turkish Government Ministry of Reconstruction and Resettlement entitled *Specifications for Structures to be Built in Disaster Areas*, of which the seismic code represents part III and was produced by the Earthquake Research Institute (see M. Paz (ed.) 1994, chapter 34, for more details). This code gives provisions for regular structures, is based on static equivalent forces and allowable stress analysis. For structures that cannot be considered regular or are higher than 75 m a rigorous dynamic analysis is required. In this respect the code is not different from other European seismic codes of this generation. The typical levels of allowable stresses vary from 5 to 8 N/mm² for a 16 C class concrete, which is the class commonly used in Turkey, and 140 N/mm² for the mild steel. A 33% increase of allowable stress is permitted for load combinations including earthquakes.

As seen in chapter 1, the Turkish territory is divided in 5 seismic risk zones. The first, along the North Anatolian Fault and the Marmara Sea southern shores is of higher risk, while the fifth has risk zero. Istanbul is mostly in zone 2. This zonation applied also for the calculation of the design seismic coefficient of the 1975 code, although the description of the zones was based on the 1972 issue of the zoning map.

The equivalent seismic action is defined through the *seismic coefficient C* applied to the resultant gravitational loads at each storey of the structure. *C* is obtained as product of the seismic zone coefficient *C₀*, the structural coefficient *K* and the spectral coefficient *S*. A further coefficient of structural importance, *I* > 1, is applied to structures hosting governmental and emergency facilities, or buildings of high occupancy.

In table 1 the variability ranges are summarised for each coefficient.

Table 5.1. Range of values for the coefficient defining the seismic coefficient C of the 1975 Code

Coefficient	Range	Parameter
<i>C₀</i>	0.10 - 0.03	Seismic zones 1 to 4
<i>K</i>	0.60 – 1.60	Ductile behaviour, structural system
<i>S</i>	1 - 0.45	Type of soil and fundamental period of structure
<i>I</i>	1 –1.5	Importance and level of occupancy

The maximum value 1.6 for *K* is associated with steel frames, while for non-ductile moment resisting frames the maximum (i.e. least favourable) value of *K* is 1.5, and it is assigned when lightweight infill panel are present. This is the most common type of construction in the Turkish urban areas. However for ductile resisting frames (defined as “*frames designed and constructed with the potential capacity to sustain loads and dissipate energy in the inelastic range of deformation*”, and identified with steel or reinforced concrete frames), the *K* value can be as low as 0.60. Note that, unlike the *Q* factor in Eurocode 8 or *R* factor in UBC, the seismic force is obtained by multiplying by *K*, so the higher its value the lower the available ductility that is assumed.

For ordinary concrete buildings, therefore, (assuming *I* = 1) the maximum design seismic action can reach the value

$$\text{Max}(C) = C_0 S K I = 0.1 \times 1 \times 1.5 \times 1 = 0.15 \text{ g.} \quad (5.1)$$

However it should also be noted that *K* = 1 for “*all building framing systems not otherwise classified*”, so that the most likely value assumed in design for the seismic coefficient is 0.10 g.

The value in equation 5.1 can be compared with other contemporary codes of European and Mediterranean countries of comparable seismicity, which, for the same assumptions on building type, provide:

Greece	max (ϵ) = 0.16g	(1984)
Italy	max (K) = 0.12g - 0.156g	(1974-1986)
Algeria	max (C) = 0.168g	(1981-1988)
Romania	max (S) = 0.2 g	(1981)
Spain	max (S) = 0.173g	(1974) (Intensity IX)
Portugal	max (β) = 0.16g	(1983)

The formulation of the seismic coefficients are slightly different but, apart for the Portuguese Code, which makes explicit reference to ductility, all the others implicitly associate a factor of ~2.5 reduction of the spectral amplification due to plastic behaviour and dissipation capability of reinforced concrete frames. It shall be noted that, although the Turkish code assumes the lowest value of seismic coefficient, this is only slightly smaller than the Italian and the Greek requirements. All codes assume allowable stresses, the Greek one allows for a 20% increase of these.

The implicit assumption of ductility relies on the implementation of specific constructional details of the reinforcement and on the quality of the concrete. Only the Algerian codes specifically refers to the quality of construction and lists a number of parameters that defines such quality, which if not observed should yield to an increase of the seismic coefficient (corresponding to the value calculated above).

Essential ductility detailing were already included in the 1975 Code, for buildings in Zones 1 and 2; in particular these included strength of concrete, steel reinforcement ratios and details on anchorage, cross ties within joints and ties for mid-side longitudinal reinforcement.

Furthermore for buildings with a height to width ratio greater than 3, it is assumed that higher modal shapes are influential and the lateral shear force at each storey is reduced by an amount which varies from 3.6% to 15% of the calculated value, for increasing slenderness. For concrete frames this would typically occur for buildings with more than 10 storeys above ground. However the overturning moments at each storey should be calculated taking into account the effect of the reducing lateral force as applied to the upper storey.

5.2.2 The 1997 Seismic Code

After the destructive earthquake of Erzincan in 1992 a major revision of the seismic code was undertaken and a new version has been issued in September 1997, becoming operational from 1st January 1998 and amended in July 1998. A full English version of the code was available at the time of writing on the Internet website of Bogazici University¹, while a commentary to the new code is available at the Middle East Technical University website².

The general principles on which the Code is based are common to the Eurocode 8 and other international Standards of the second generation, i.e., essentially based on capacity design, to prevent structural and non- structural damage to buildings in low-intensity earthquake, to limit damage to repairable levels in medium intensity events and to prevent partial and overall collapse in high intensity events. The high intensity event or design earthquake is identified with a probability of being exceeded of 10% in 50 years, the actual intensity being measured in terms of peak ground acceleration and depending on the zoning.

The code is not only applicable to new built but also to buildings which undergo any modification or buildings which are to be repaired following previous earthquakes. Besides a national programme of assessment for hospitals and health facilities³, other public initiative to upgrade or strengthen existing buildings include the seismic rehabilitation of 108 reinforced concrete buildings in Ceyhan, damaged by the 27 June 1998 earthquake. (Gür, Sucuoglu, 2000).

The major innovation of the code is the explicit introduction of ductile design principles, which are specified for concrete structures, with indication of the necessary amount and distribution of longitudinal and shear reinforcement and anchorage details. It is also prescribed that in zones 1 and 2 all framed buildings and building of importance factor $I > 1$ shall be designed to high ductility standards. Buildings of nominal ductility are allowed in the other two zones, provided they do not exceed 25m height. Also, rather than defining a regular building, irregularity limits are stated and it is clearly indicated that soft or weak storeys should always be avoided, together with plan irregularities that lead to torsional effects. The height of the building in zones 1 and 2 is now limited to 25m for the application of the equivalent static method, i.e. to 7-8 storeys buildings.

The seismic coefficient is defined by equation 5.2 as the product of the effective ground acceleration coefficient, the spectrum coefficient and the importance factor, divided by the seismic load reduction factor, which is dependent on the structural behaviour factor R and the period:

$$C(T) = A_0 I S(T) / R_d(T) \quad (5.2)$$

where the range of variability of each factor is summarised in table 5.2.

Table 5.2. Range of values for the coefficient defining the seismic coefficient C of the 1997 Code

Coefficient	Range	Parameter
A_0	0.40 – 0.10	Seismic zone 1 to 4
R	4 to 8	Level of ductility: nominal or high for in situ r.c.
S(T)	2.5 -0.4	Type of soil and fundamental period of structure
I	1.5-1	Importance and level of occupancy

Choosing conditions equivalent to those adopted for the calculation of the maximum seismic coefficient for the 1975 Code yields

$$Max (C) = 0.40 \times 2.5 \times 1 / 4 = 0.25g \quad (5.3)$$

Therefore the basic seismic coefficient has been increased of 60% with respect to the previous code. However this has been calculated considering a ductility factor of 4, which is not permitted in zone 1, by the current code requirements. If the structural behaviour factor is taken as 8, then

$$Max (C) = 0.125g \quad (5.4)$$

which is indeed smaller than the seismic coefficient calculated with the 1975 Code. However this revised value is associated with the particular prescriptions and constructional details referred to above, which should ensure ductile behaviour. The conditions given by the 1997-8 code are considerably more stringent than the rules from the earlier codes for ensuring ductile behaviour.

While the 1997-8 code appears to have a stricter and more prescriptive approach to earthquake design, the above base shear calculations demonstrate that it relies heavily on the robustness and integrity of the building industry and the entire design-construction process. It indeed shifts the responsibility of delivering the seismic capacity of the structural system, from the design phase to the constructional phase of the process: the designer is required to choose certain values of the coefficients given the seismic zone, and is also required to provide specific distribution of reinforcement. However it is then the responsibility of the contractor and the local authority inspection system to guarantee and verify that the detailed measures have been implemented. Following the earthquake, enforcement of the code and quality control assurance were often blamed as the major causes of the poor seismic performance of the building stock as a whole, and hence the present situation begs the question of whether the new seismic design code is compatible with the present economic, social and legislative situation in Turkey.

5.2.3 Comparison of the design seismic spectra with the Kocaeli spectra

Following the release of the strong motion data in digital format, the group of researchers at Imperial College analysed some of the available accelerograms, to obtain inelastic response spectra. The results obtained by Elnashai et al. (2000), are presented in Figure 5.1 together with two envelope design spectra, obtained from the 1975 and the 1997 codes. The four numerical spectra presented are relative to the strong-motion recorded respectively in Yarimca, Adapazari, Izmit and Düzce.

Notwithstanding the above discussion on the structural behaviour requirement for buildings in zone 1, for the 1997 Code a structural behaviour factor $R=2$ was chosen for the comparison, as the numerical spectra for the different locations were obtained using a ductility factor $\mu=2$. This choice of the ductility factor is essential in the definition of the capacity of the structure, and it was mainly dictated by on site observation of the arrangement of the reinforcement in damaged column-beam joints. In the case of the 1975 code, however, as already mentioned, there is an implicit ductility factor of 2.5, already applied to the design spectrum curve, while the structural coefficient k has been set to 1.5 for the purpose of the comparison. Because the soil conditions at each site are largely unknown the design spectra have been plotted as envelope of the curves representative of all the possible site conditions provided by the two codes. It should be considered that the numerical spectra are obtained by an inelastic concrete model (three stiffness branches)

subjected to the recorded accelerograms, while the design spectra are based on an elastic model, and are uniformly scaled to include the effect of the chosen ductility factor (R or k).

Taking into account that the majority of existing buildings in the four locations considered would have been designed according to the 1975 code it appears evident that virtually none could have survived undamaged. Indeed, even removing the 2.5 implicit reduction factor, the maximum acceleration plateau of 0.375g would have been sufficient to absorb the seismic action for larger periods, but not in the range of fundamental period $T < 1$ second, typical of the concrete structures under discussion. If the energy equivalency criterion is considered it can easily be demonstrated that assuming a spectral acceleration of 0.6g as the maximum value that the structure should have withstood to remain elastic, in order to absorb the same amount of energy by dissipation, the same structure would have required a structural ductility $\mu=7.5$, i.e. been capable of sustaining lateral drift 7.5 times greater than the elastic limit, without loss of load-bearing capacity. This level of ductility would typically yield a storey drift of 4% of the storey height.

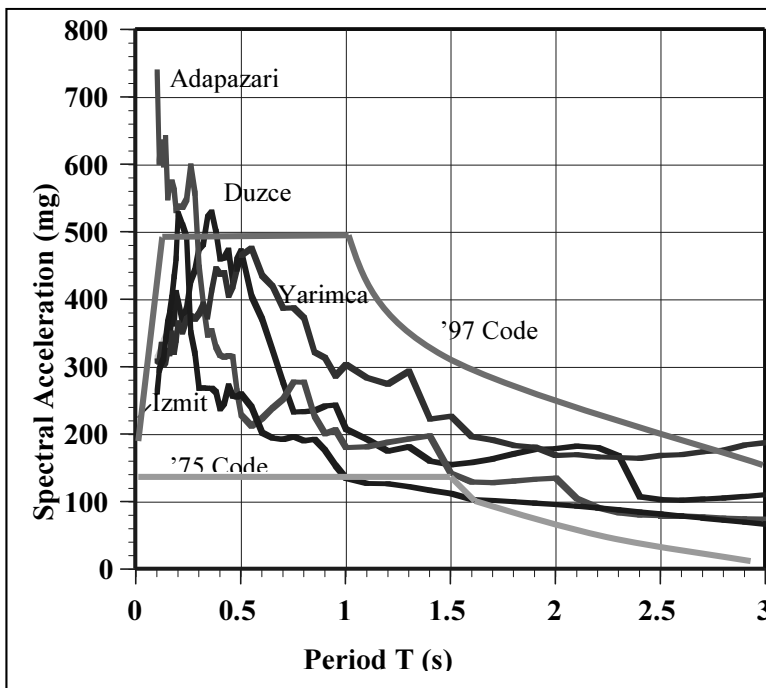


Figure 5.1: Comparison between inelastic spectra derived from strong-motion records and design spectra of the two codes.

Lateral displacement of this magnitude would not be permitted without adequate detailing of the plastic hinges and designing to withstand the substantial $P-\Delta$ effects that would be induced. In summary the analysis shows that the 1975 code under predicts demand on the capacity for a non-ductile frame with lightweight infill panels, both in terms of strength and ductility.

A different picture is presented by the design spectrum representative of the 1997 Code. In this case, having chosen a structural behaviour factor $R=2$, the spectrum obtained from the Yarimca record would be completely contained in the design spectrum, while Izmit and Düzce presents peaks just greater than the plateau value, for value of the natural period typical of 4 to 5 storeys buildings. However the record obtained from Adapazari presents very high values of acceleration for values of the period lower than 0.10 seconds, corresponding to reduced design acceleration in the design spectrum.

From this comparison, and assuming that the foundation and soil condition at the location of the instruments are representative of the soil condition in the nearby urban centres (which is known to be not the case in Adapazari, for instance), it should be expected that buildings in Yarimca designed according to the 1997 code with a reduction factor of 8, should have suffered relatively low level of damage, associated with a ductility demand of approximately 2, while buildings in Düzce and Izmit would have suffered more conspicuous structural damage, especially for building with fundamental period in the range 0.3 to 0.5, i.e. buildings with 3 to 6 storeys. The response to Adapazari record suggests that the reduction in design spectrum at low period is potentially unsafe when structures are founded on rock. These results are obviously only indicative and, while more rigorous analyses are needed to fully explain the observed structural behaviour on site, they can be compared with the damage surveys conducted in the immediate vicinity of the instruments and reported in chapter 3 and with the analysis of damage discussed in later sections of this chapter.

5.3 Performance of Residential Buildings

This section examines the manner in which domestic buildings performed during the earthquake. It looks at the performance of typical residential buildings in urban areas, examines typical collapse mechanisms, and briefly looks at foundation failures.

5.3.1 In situ reinforced concrete structures

The vast majority of residential buildings in the visited areas are what the Turkish refer to as *Beşkat*. *Beşkat* literally means five-storied, and it refers to the most typical number of storeys that this type of construction would have above ground. In more densely populated areas these buildings will have up to 8 storeys and typically each storey will have two to four apartments; usually each building is built with an independent structure but adjacent to the next one, with balconies on the principal façade, while in areas of lower density buildings are separated by small communal gardens and have balconies on each side of the construction. The actual number of floors varies typically between 3 and 8, however cases of 2 to 10 have also been observed.

The *Beşkat* are constructed in-situ from a reinforced concrete frame, with timber (older buildings) or concrete (more recent) floors and masonry infill. Buildings with coupled system r.c. moment resisting frame and r.c. shear walls represent a minority (introduced after the 1975 code), while buildings with shear walls system only are a rarity, however in some cases reinforced concrete [shaped lift shafts have been observed. The floor-to-floor height is typically 4 to 4.5 m for the ground floor, and 2.7 to 3 m for other floors. The roof construction is either made of light timber trusses and slates or (a minority) flat concrete slabs.

Many *Beşkats* have shops or similar commercial properties at the ground floor, especially on main thoroughfares, or simply a large entrance hall without partitions. This usually entails some modification of the structure in elevation, as infill walls are removed to create wider spaces at the ground level. Typical beam spans range from 2.5 to 6 m. Given the economic situation in Turkey many of these buildings are built in stages, one storey at a time when the owner can afford the cost of materials and workmanship. Meanwhile, “waiting” bars are left protruding from the top of the columns to provide continuity reinforcement for the columns of the following stage.



Figure 5.2: Typical r.c. frame building with protruding “waiting” bars

Masonry infill in older buildings is made out of solid fired clay bricks, (200x100x50 mm ca.) while in more recent construction is usually built up with extruded, multi cell, hollow clay tiles, of dimensions 250x200x80 mm ca. with a 4-6mm thick walls. They appear to be fired to a high temperature, giving a very strong but brittle material. The voids are usually laid horizontally, with little or no mortar in the vertical joints. Some buildings had the voids vertical, in which case mortar surrounds the block. In areas such as cantilevers, a very lightweight foamed block is used. A similar type of block is also used to lighten the floor slab construction. This type of construction is very common in most part of south Europe as it allows construction of relatively light-weight double leaf cladding with good sound and thermal insulation capacity. A minority of buildings have aerated lightweight concrete block (known as Ytong).



Figure 5.3: Typical medium-high density urban block in Yalova. Notice the failure of the corner building



Figure 5.4: Aerated concrete block (Ytong) infill panels

The reinforced concrete frames, especially in older buildings, often have columns all oriented with their greater cross sectional dimension, and hence stiffness, in one direction, creating weaker frames in the orthogonal direction. In some cases beams are only laid in one direction while connection between parallel frames relies upon the concrete slab forming the floor. However in many pancake collapse there was little or no evidence of continuity of reinforcement and proper anchorage length between the slab and the columns. In cases of filler block joist slabs, which are rather common, the typical thickness is up to 300 mm, resulting in very stiff floors but also substantial concentration of mass, attracting

higher lateral forces, and effectively constituting a weak column-strong beam connection.

In ordinary buildings up to 30 years old, the reinforcement is made of smooth mild steel bars, with typical yield strength of 240 N/mm^2 according to a study by Bayülke(1983). High strength steel (ST-III) with yield strength of 420 N/mm^2 is used sporadically or in governmental buildings. In more recent buildings deformed or ribbed rebars were also observed as longitudinal reinforcement in columns. While the smooth mild steel bars could have worked satisfactorily if they had proper anchorage lengths and sufficiently closely spaced links, especially at beam-column joint location, this was observed to be the exception, rather than the norm. In fact many have been the observed cases in which columns of two successive floors lay adjacent after the earthquake with the reinforcement bars strained but not severed, having lost any contact with the concrete mass of the lower column. (see Figures 5.5a and 5.5b).



Figure 5.5a: Slender column, lack of bonding and absence of stirrups



Figure 5.5b: behaviour of smooth mild steel reinforcement

The inherent seismic vulnerability of this type of construction had been repeatedly observed since the 1967 Adapazari earthquake. Notwithstanding the continuous publication of enhanced seismic codes, however, poor workmanship, questionable ethics and practice in both design and construction, as well as a lack of qualified controlling authority, are still referred to as the major causes of the amazing level of destruction observed in the 1999 earthquake. Indeed it would appear that the building stock in this part of Turkey has become increasingly vulnerable in the last 30 years.

It has regularly been reported in studies of previous earthquake damage in Turkey that an important contributory factor to the high level of damage in reinforced concrete buildings is poor concrete strength (Bayülke, 1983, EEFIT, 1993, Bogaziçi University, 1992, Wenk, et al 1998). As a part of this study a small sample of structural concrete taken from a principal structural column of a collapsed building (Figure 5.6) was retrieved and returned to the UK for testing. The tests were performed at Sandberg's laboratory. The sample was not of sufficient size for compressive strength testing to be carried out. However a descriptive study, supplemented by tests for cement and chloride content and sample grading were possible. The grading curve together with a typical UK structural concrete grading curve for comparison are shown in Figure 5.7.

The testing laboratory's comments are: " The concrete was unusual for a structural concrete in that the aggregate was much finer than normal. Indeed the material appears to resemble a render. There are numerous voids in the sample suggesting that the strength would not be very great".



Figure 5.6: The collapsed building in Gölçük from which the sample was taken.

At 11.6% by weight the cement content was also below what would be expected for use in an important structural member. However the chloride content was low, suggesting that if (as seems likely from the grading) the aggregate is an unmodified sea-sand, it has been effectively washed. This one small sample is not necessarily representative of the structural concrete used in the area, but it confirms earlier findings as well as more recent comments by Cagatay and Haktanir (1999) that, in the 1999 Kocaeli earthquake “concrete quality of collapsed and damaged buildings was far below the minimum C20 class (20 N/mm² crushing strength) required in the specification for structures in earthquake areas”. Poor compaction and inappropriate grading are two of the principal reasons for this given by these authors. Direct observation revealed that in other cases an excess of non hydrated cement was to be found around aggregate.

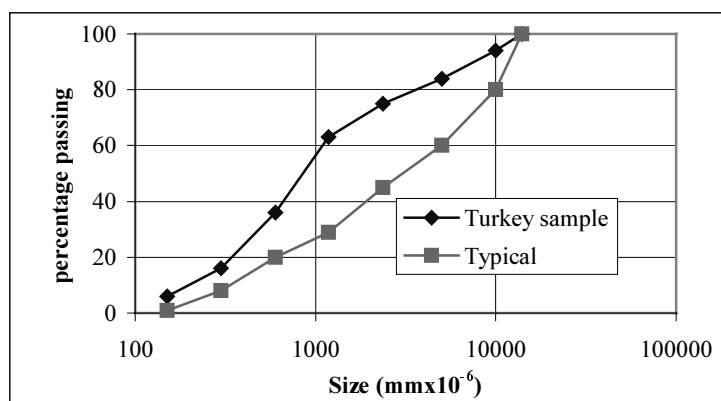


Figure 5.7: Grading of concrete sample

5.3.2 Timber infilled frames

The timber infilled frame, called *Himis*, is made of a space truss timber frame, similar to the Portuguese cajola, and infilled with either clay or adobe brick. In most cases they are plastered, in some cases the infill is left exposed. By

contrast in the *Bagdadi* type, the frame is covered by a wooden lath cladding system and the space between the laths filled with a variety of material depending essentially on availability and quality of workmanship. The framing elements might be either logs or sawn planks, of roughly 100x100 and 50x100 mm cross section for the vertical and diagonal elements, respectively, and the geometry of the frame system might vary quite considerably. The floor structure is also made of timber joist and planks and the plan shape is usually square. Average height is two storeys, rarely up to 3. Further details on this type of structures can be found in Bayülke (1983), who established values of 0.3 and 0.4 seconds for the first natural period for timber structures of 2 and 3 storeys, respectively. While up to 30 years ago the most common type of residential single or double dwelling in this part of the country, they have been extensively demolished and replaced by higher density concrete buildings in most urban areas (see chapter 1). The surviving examples are often in a poor state of maintenance and their dynamic performance might be adversely affected. A specific vulnerability is identifiable in the very shallow, unconnected foundations, and it has been observed in areas of liquefaction and subsidence that a lateral mechanism forms with hinges at the foot of the columns (see Figure 5.10 and Figure 5.11). When founded on more competent soils these buildings usually performed well.



Figure 5.8: Himis timber house standing next to failed r.c. building



Figure 5.9: Bagdadi timber house (photo B. Teymur)



Figure 5.10: Damage to Himis house caused by soil failure

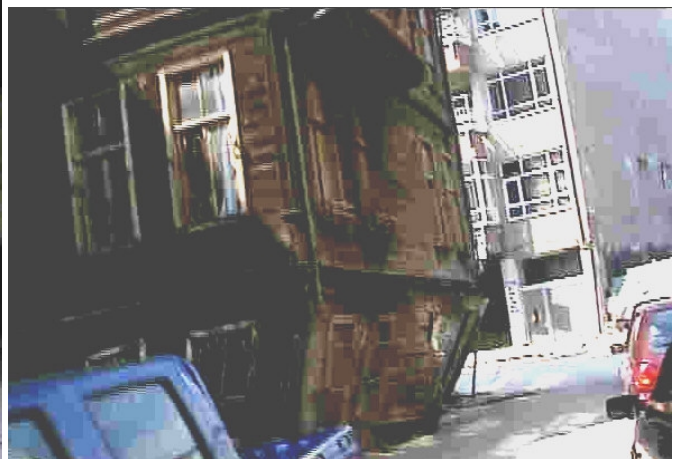


Figure 5.11: Hinge column failure of Bagdadi house in Adapazari

5.3.3 Load bearing Masonry

Masonry structures whether of brick (*tugla*) or stone (*tas*) are rather rare in the earthquake epicentral area. Traditionally they are built of solid bricks and timber floors, but more recently these have been replaced by concrete slab floors. It is reported that before 1992 it was also common practice to build load bearing masonry with hollow bricks, however no evidence of this was reported in the surveyed area.



Figure 5.12: Adapazari. XIX century restored 3 storey masonry building survived undamaged in an area of numerous collapses, while another similar building suffered damage level D3, with diagonal cracks around the openings.

5.4 Typical Collapse Modes in Concrete Buildings

5.4.1 Introduction

Residential buildings were particularly badly hit in this earthquake, with very large numbers of buildings collapsing, being rendered unusable, or badly damaged. While the specific damage was often influenced by factors related to the peculiarities of each building, a general pattern can be identified in the collapse modes, which are here listed in order of decreasing destruction:

- Multi-storey or '*pancake*' collapse
- Soft storey collapse
- Foundation failure associated with subsidence or liquefaction.
- Upper stories failures, roof failures.
- Shear cracks of in-fill masonry
- Shear / bending failure of column to beam connections

Official statistics record 77,927 heavily damaged or destroyed residential and commercial units, and to 76,768 seriously damaged units. A proportion of the severe damage was a result of site effects, from proximity to the fault; to the extensive damage caused by the coastal slump in Golcuk; and to the widespread soil liquefaction in Adapazari. The geotechnical implications of these phenomena have been discussed in chapter 4. From a structural point of view, it should be noted that more stringent urban planning control should have prevented construction in some of these areas or should have required deep foundation on piles. Indeed, the complete overturning as rigid bodies of some of the buildings in Adapazari proved that a raft foundation with continuous beams is not sufficient to withstand the soil failure effects. On the other hand, a minority of buildings that survived unscathed were indeed founded on piles. The buildings that suffered rigid overturning were usually of relatively small foot print plan and slender in aspect (Figure 5.13).

While foundation failures were usually localised along certain roads and streets, generally the other types of failure occurred in a relatively random way, which makes it difficult to ascribe to a particular structural or constructional characteristic or class of buildings. However some general trends are identified from the statistical analysis of the damage surveys discussed in section 5 of this chapter.

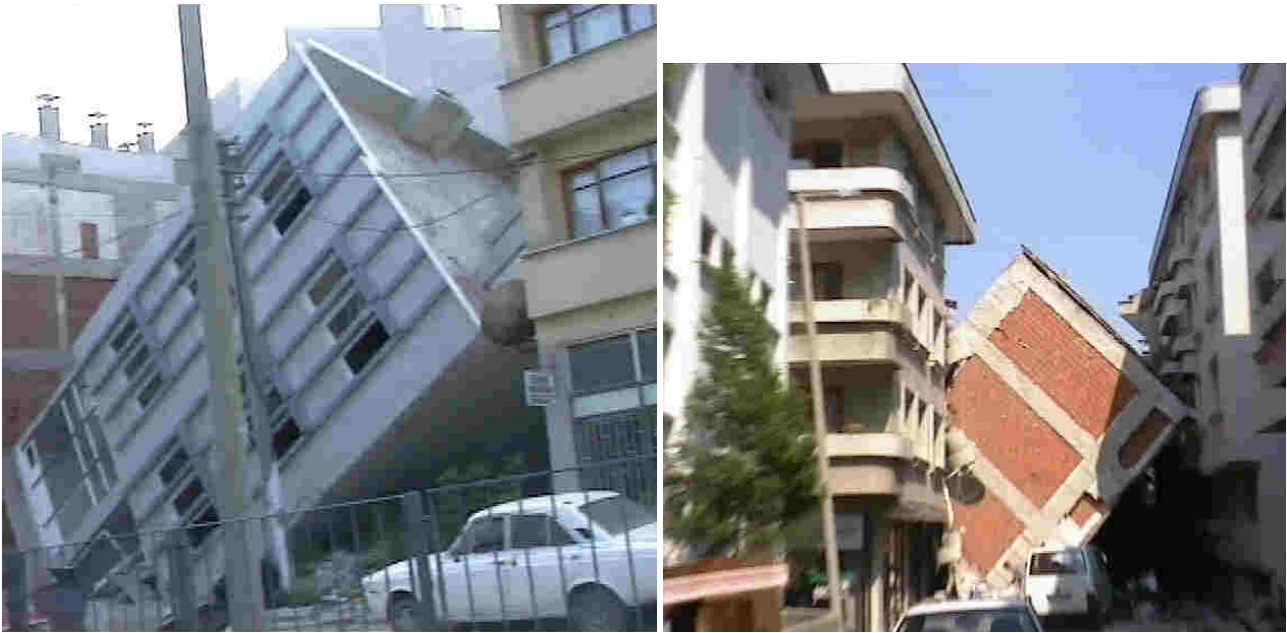


Figure 5.32 Two overturned building in Tigcilar, the worst district of Adapazari affected by liquefaction

In general it can be said that where soil conditions were poor most buildings sank, but the upper structures was not damaged. In some cases, observed in Adapazari, where liquefaction was accompanied by soil bearing failure, buildings of competent structure overturned as rigid bodies. Elsewhere buildings with inherent fragility suffered damage to the lower storeys. In cases in which the soil appeared to be competent, if there was an inherent weak axis in the columns layout, failure would occur at the lower storey with a mechanism forming in the plane of the weak axis, otherwise a pancake mechanism would develop. In all cases these buildings presented a weak-column-strong beam configuration. Although some areas in Adapazari and Golcuk had a 100% destruction rate, there were also cases of buildings with moderate damage standing next to completely destroyed ones. Moderate damage usually consisted of failure of the lightweight roof structure or shear cracks in the infill lightweight masonry.

Further detail and examples of each failure mode are given in the following sections.

5.4.2 Pancake Collapses

Pancake collapses are associated with formation of hinges in columns at some storey, usually the ground that then spreads to other levels. This type of failure is usually caused by substantial lateral displacement, and seismic input characterised by relatively low frequencies. This is illustrated by Figure 5.14a) and b). Case a) is located in Pabuccular Cad. in Adapazari: every column has collapsed with a lateral drift of the floors. Little damage had occurred to the floor slabs. Case b) is in Nato Cad. in Adapazari, where it can be assumed that the pounding from the adjacent stiffer building on the left, might have been a cofactor in the total collapse of this building. It has been said that many of the corner buildings failed because of pounding in two orthogonal directions from adjacent buildings. It should be noted that the building to the left failed by soft storey failure in the plane normal to the road. This is the weakest plane of the frames.

Further dramatic pancake type of collapses are illustrated in figures 5.15a) and b). In both these case the lateral drift of the buildings at collapse may be seen.

A slightly different mechanism was observed in buildings with very thin slabs (about 5 to 7 cm). Both photographs in Figures 5.16 a) and b) show the same building in Yuvacik. The whole building had been thrown sideways, as the columns on one side collapsed. In figure 5.16a), the horizontal members at the top of the photograph are the columns, with the beams vertical. Figure 5.16b) shows the floor and roof slabs overlapping with substantial in plane failure.



Figure 5.14a: Pancake collapse.



Figure 5.14b: Slender building with column oriented in the direction orthogonal to failure plane. Lack of reinforcement continuity



Figure 5.15a



Figure 5.15b: Site with three buildings collapsed and one standing



Figure 5.16a: Overturning of the frame with loss of infill



Figure 5.16b: slab damage to the same building of Figure 5.16a

5.4.3 Lower Storey Collapse

Ground and first floor collapse resulted to be the most common type of collapse. In many cases the ground floor contained shops and was un-occupied at the time of the earthquake (3 am). As a result, casualties and fatalities were lower than would have been expected from the number of collapses. In many cases the ground floor was weaker than other floors as many of the partition walls had been removed, for commercial purpose, and often the floor to ceiling height was greater than for other floors. Very common were also compound mechanisms where two or more lower floors collapsed. These failures are illustrated by Figures 5.17, 5.18, and 5.19.



Figure 5.17: Buildings in Cark Cad., Adapazari for which the lower 2 storeys columns had collapsed.



Figure 5.18a: Collapse of the lower 2 storeys

Figure 5.18b: Close up of the columns of 2 storey with the strained mild steel



Figure 5.19 a: Lower storey collapse of a 4 storey building and failure of infill panels

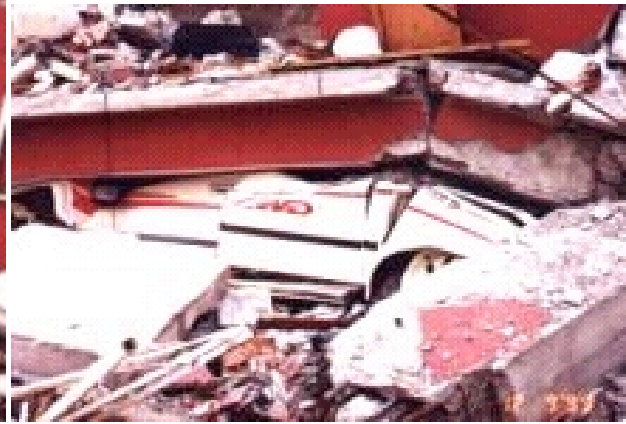


Figure 5.19 b: bottom right detail of fig 5.19a), showing failure of the beam

In Figure 5.18a, b, two stories had collapsed, and in so doing had slid into the street. Figure 5.18b shows the columns of the first and second floor standing next to each other with the reinforcement bars having become highly plastic and pulled out of the column.

Of particular concern in many building that had collapsed was the practice of arranging all the elements such that their stiffer axis was in one direction, with only nominal stiffness in the other. Typically, all the columns were long and narrow, often being no wider than the width of the masonry, with a depth of up to 1m. A typical building may have had 6 to 10 columns orientated from front to back, with only one or two orientated in the transverse direction, frequently in the rear wall. Whilst this provides an arrangement where the space utilised by columns is minimised, it is not compatible with providing equivalent seismic strength in both directions. Figures 5.20a, b, and c all relate to the same building, in Adapazari, and illustrate graphically the consequences of not having enough capacity in both directions.



Figure 5.20 a, b: General view and detail of failed building in Milli Egemenlik Cad., in Adapazari

The building, less than three years old, had been built to high specification (uPVC windows, plaster mouldings on the ceiling, etc.). The mechanism of failure appeared to be failure of the ground floor columns about the minor axis. Closer examination of the building revealed that the columns were mainly orientated in the same direction. At the far end (relative to the photos), the building had a semi-circular plan, with the columns being on radial lines, and hence their main axis gradually rotated until they were at 90 deg to the main axis of the building. Beside these there appeared to be few elements contributing to longitudinal stability. The high stiffness of the columns at the semi-circular end of the building meant that they attracted high loads, and consequently collapsed. Figure 5.20b shows the column detail at the near end of the building, whilst Figure 5.20c shows the semi-circular end of the building. Here the column has failed about the major axis, and then punched through the slab.



Figure 5.20c: The gravity loads are now carried by the surviving infill panels

Figures 5.21 and 5.22 are taken from two estates of “holiday” flats on the south coast of the Marmara Sea, not far from Yalova. Although they are called holiday flats, retired people occupy a considerable number on a permanent basis. Every block of flats in the two estates had lost its ground floor, with some of the blocks having suffered a pancake type of collapse. In each case the columns had been unable to carry the seismic loads. The flats above the first floor were relatively undamaged. It was ascertained from residents that many of the ground floors were occupied by shops, restaurants, and similar.



Figure 5.21a



Figure 5.21b

For one of these blocks of flats, at the Aydin resort to the east of Yalova, a site investigation was in progress during the visit from the EEFIT team. A single borehole had been undertaken to a depth of approximately 22m. This showed that the ground conditions consisted of medium dense sand and gravels approximately 5m thick, with soft clay below. This clay had an N value as low as 3 in some cases. The bottom of this soft clay had not been reached at the time of the EEFIT inspection.

The upper layer of good materials is quite capable of carrying the loads imposed from a five story block of flats, with correct design of the foundations. Indeed, for this type of speculative development it is likely that site investigation had been limited to trial pits and the presence of the soft clay layer was not appreciated. This layer would have almost certainly caused considerable amplification of the earthquake motion, and as a result the loads would have been increased, leading to collapse of the highly stressed lower floor columns.



Figure 5.22a



Figure 5.22b

5.4.4 Foundation and soil failure

Many foundation failures were noted in Adapazari, associated with large vertical and sideways movement. These were caused by liquefaction, or alternatively by the loss of bearing capacity of foundation on apparently competent strata, which overlaid softer material. The latter may have been punched through under the additional loads imposed by the earthquake. The four photographs below illustrate ground behaviour in one road in Adapazari, Pabuccular Cd. In Figure 5.23a, the building has largely remained intact, but has settled by approximately 600 mm. Figure 5.23b again shows building settlement, this time of the order of 300mm with a sideways movement of similar magnitude. Apart from this, the building appeared to be largely undamaged.



Figure 5.23a: 7 storey hotel building with raft foundation



Figure 5.23b: Soil failure. The building is undamaged

Sand was apparent over a considerable extent of the pavement in this road. This is illustrated in Figures 5.24a and b. This may be indicative of liquefaction, or it may be sand that had been used as a bedding material below the paving. The following photographs (Figures 5.25a) and b)) show typical damage at Degirmendere, on the south shore of the Marmara sea, where the subsided area extended about 250m along shores and about 70 m inland, photographed from the opposite shore.



Figure 5.24a



Figure 5.24b



Figure 5.25a



Figure 5.25b

5.4.5 Upper floor collapse

Whilst many of the collapses were instigated by the failure of the ground floor columns, in some buildings the ground storey remained intact, but upper storeys failed. Figure 5.26a, which was taken in Degirmendere, shows all the floors except the ground floor collapsed. In Figure 5.26b, which is from the holiday flats discussed above, the ground floor had collapsed, as had the upper two floors. In both cases it is notable that the collapse had occurred in a corner. In the first case it can be noted that at ground floor there is a shear wall which might have resulted in a substantial change in stiffness between this and the upper floors, while in the second case, the corner had less infill panels than the rest of the building. Another very common form of damage was the collapse of the roof, which is very often made of a light thrusting timber structure with a mantle of insulation and tiles. Two occurrences are shown in Figures. 5.27a and b.



Figure 5.26a



Figure 5.26b



Figure 5.27a: Roof failure in a light damaged building in Adapazari



Figure 5.27b: Roof failure in a 8- storey building in Izmit

5.4.6 Masonry infill failures

In many cases the performance of the masonry infill was critical in ensuring the survival of surveyed buildings. Although masonry walls are not included in the seismic design, in practice they act in shear to carry some of the lateral load. In order for the building to collapse, it is necessary for both the walls and the frame to fail. In practice, the masonry walling being more rigid than the concrete structure, cannot withstand the same level of lateral displacement without experiencing tensile cracking. This however does not prevent its capacity to carry gravity loads as a diagonal compression struts forms between the tensile diagonal cracks. If the shaking has many reversals, and there is substantial failure in the adjacent column the infill walls will eventually fail by crushing of the compression strut at the toe. Two conditions are essential for the effective coupling of the two systems; the masonry walls should be tied to the concrete structure so as to prevent out of plane failure, and they should be competent in withstanding relatively high compression.

As mentioned in Section 5.3 essentially three different types of brick/block are used for infill. In all cases observed during the EEFIT mission, the masonry walls were not tied into the concrete, but just mortared up to the columns. That notwithstanding, in relatively few cases had the brick panels failed out of plane, despite the absence of ties. This is likely due to the fact that the hollow extruded clay blocks have little mass relative to their depth, and consequently are well suited for resisting out of plane loads. In many of the badly damaged buildings, diagonal shear cracks had formed in the masonry walls indicating their role in redistributing lateral loads. While in the majority of cases only one diagonal crack is present, associated with substantial lateral displacement and damage to the r.c. structure at ground floor, in few cases of lighter shaking and perhaps stiffer and more competent frames typical x cracking is visible (Figure 5.28b).



Figure 5.28a: Composite diagonal and out of plane failure of infill



Figure 5.28b: X cracks in the lateral wall between opening

5.4.7 Bending failure and shear failure

It has already been mentioned that many of the concrete frames examined had a heavy slab sitting on stiff beams. A typical consequence of this arrangement is the extensive damage of the supporting columns. In Figure 5.29, which depicts a typical case of soft storey, hinges have formed at top and bottom of most columns of the ground floor, while there is hardly any damage in the beams framing into them or in the upper structure. This building might have been saved from collapse by the fact that some of the columns are oriented with their principal axis in orthogonal directions. Note also that not all columns have beams framing into them in the 2 orthogonal directions. A very brittle type of failure is produced by the occurrence of high shear action in the upper portion of the column. This is shown in Figure 5.30 in which a diagonal shear crack in the column is clearly visible. The longitudinal reinforcement has yielded, there is no evidence of shear links in the immediate vicinity of the joint and complete failure of the column has only been prevented by the presence of the infill wall. In the case of Figure 5.31 the collapse is almost complete.



Figure 5.29: Hinges forming at bottom and top of columns.



Figure 5.30: Shear failure in column



Figure 5.31: Shear failure of ground floor column

5.4.8 Summary

Given the high level of destruction witnessed as a result of the Kocaeli Earthquake, it was not possible to determine conclusively the failure mechanisms associated with most collapsed buildings, of which often only a pile of rubble was left. However some general conclusions can be drawn on likely failure mechanisms, and from these lessons learned for the future re-building programme. It is considered that many of the failures can be attributed to the following causes, in order of importance:

- Magnitude of the earthquake
- Poor foundation soil leading to liquefaction and/or bearing failures
- The general arrangement of the buildings, in particular their unequal distribution of stiffness (and strength in elevation. While some buildings had irregular plans, these were not the majority.
- Inappropriate design practice, including elements not having adequate strength and ductility; and the columns being weaker than the connecting beams.
- Poor detailing resulting in connections having insufficient ductility. More care was also needed to ensure that items such as links are adequate and that sufficient anchorage is provided.
- Poor construction practice resulting in items such as dry joints, and poor quality concrete.

At the time of the earthquake, considerable comment was made in the press and on television about the poor quality of construction. Whilst this did not help, it was probably only a secondary issue. The primary cause of failure in most building can be summarised as being a summation of incorrect detailing and construction.

The primary lesson to be learned from this earthquake is that if Turkey is to continue using similar types of buildings (and economics will almost certainly dictate that it will) it must ensure that:

- Competent professionals carry out designs.
- Appropriate site supervision is carried out to ensure that the buildings are constructed as designed.
- An adequate site investigation is available to ensure that any soil-structure effects are accounted for.
- More training in earthquake design is provided.
- Construction practice is improved by better training.

It is appreciated that many of the above recommendations could considerably increase the cost of future buildings. The challenge will be to ensure that these are implemented by means such that they are affordable. Costs can be reduced by having a number of standard designs; by pooling information such as site investigation; and having only part time site supervision. Some of these suggestions can only be carried out by a more involved role of the local authority in controlling future building projects.

5.1 Geographical and statistical analysis of damage

Official surveys on level and distribution of damage, reveals that in the major urban centres affected, Izmit, Golcuk, Adapazari and Yalova, the buildings with little or no damage amount to approximately one half or more than the entire population (see Figure 5.32. Note that the cumulative histograms do not include undamaged buildings). Also, from the preliminary maps of damage drawn on the basis of aerial surveys, it was evident that the worst affected areas were localised in clusters (see Figure 5.33a and b). Indeed during the subsequent visit, it appeared that in some streets no buildings had collapsed, whilst in others, one or two buildings only had been damaged. In the areas where the worst damage had occurred, however, whole streets were affected with few if any buildings surviving.

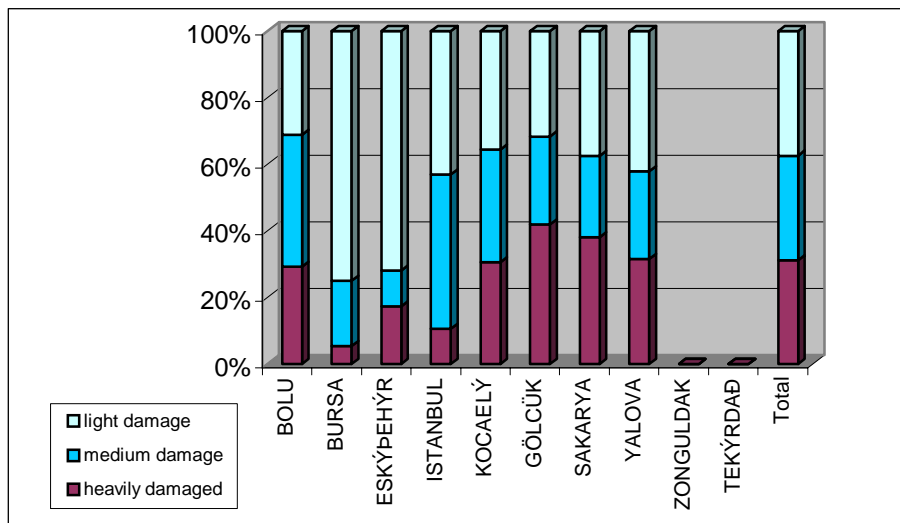


Figure 5.32: Official distribution of damage by municipality at 30-06-2000.

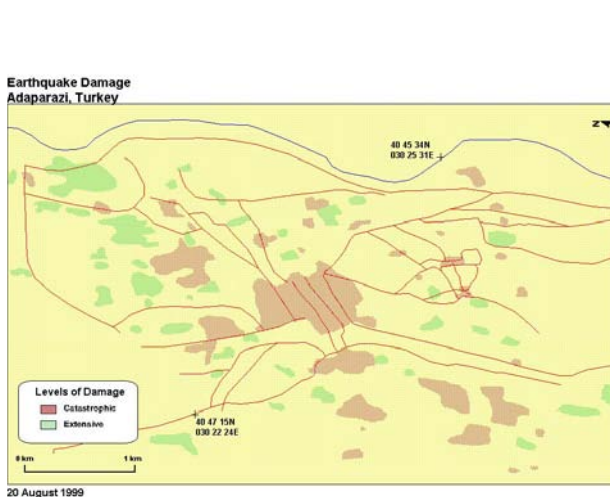


Figure 5.33a: Damage survey of Adapazari based on aerial photography (North is left)



Figure 5.33b: Damage survey of Yalova based on aerial photography (Bogazici University 20-08-99)

This is more clearly shown by reference to Adapazari where the photographs in Figures 5.34 to 5.38 were taken within 1km of each other (all within the red patch at the centre of the map in Figure 5.33). The photographs illustrate the southern and north part of Nato Caddesi, running North-South on the west side of the centre; the eastern end of Bahcivan Sokak (north of the Belediye); and the northern portion of Izmit Caddesi where entire blocks of houses were destroyed. Also damage was highly concentrated at the western end of Milli Egemenlik Cad., and Fabrika Cad., two main roads running west from the centre and two blocks apart (the two parallel roads at the centre of the red patch in the map of Figure 5.33).



Figure 5.34a: Nato Cad. south showing relatively little damage



Figure 5.34b: Nato Cad. north showing numerous soft storey collapses



Figure 5.35: Bahcivan Sokak, showing some damage, but the majority of buildings surviving



Figure 5.36a, b: Izmit Caddesi, where few buildings survived. Most of the damaged buildings were 5 stories with shops.



Figure 5.37a, b: Milli Egemenlik Cad. Damage was localised along the northern end of the road



Figure 5.38a: Fabrika Cad. westward of the tobacco factory



Figure 5.38b: Fabrika Cad. eastward of the factory

The EEFIT team conducted three damage surveys in Adapazari, Gölcük and Yalova. In Adapazari about 300 buildings were surveyed, in Gölcük 200 and in Yalova about 80. Given the short time available information was collected from the street on type of structure, estimated age of construction, position in the block and number of storeys, level of damage and type of damage and for each building a reference picture was taken. The results for Adapazari are shown in the following tables. Six types of structural system were identified, brick masonry, reinforced concrete frames with 3 different types of infill or coupled with shearwalls, and timber.

The distribution of number of storeys identifies a majority of buildings with 4 and 5 storeys (beşkats). It is worth noting that the data is not complete for the whole sample, as some of the buildings surveyed have been taken from pictures. The apparent geographical scatter within the city centre is due to the necessity of surveying a reasonably representative area in a short time, so that undamaged buildings were not recorded, except the minority that appears immediately adjacent to damaged ones in reference pictures. Damage level for each building was assessed according to the six-point scale (D0-D5) of the European Macroseismic Scale (EMS, 1998) The data on type and level of damage is shown in Figures 5.40 and 5.41.

As the data on type of damage show quite unequivocally a major proportion of the damage was caused by failure of the soil. This is distributed in clusters along some of the surveyed streets, especially in the region east of the centre. However this was not always associated with complete collapse of the structure. In fact overturning due to soil failure have only been recorded in a minority of cases, however in the same region where the soil bearing failure was quite dramatic.

The major cause of collapse was by far to be identified with the presence of soft storey either at ground floor or first floor level, identified in 27% of cases, while pancake collapse, usually triggered when a more even distribution of stiffness in elevation is present, was counted only in 13% of surveyed buildings. It might be of interest to notice that this type of collapse occurred in clusters, and usually not in conjunction with soil failure, although in some cases this was difficult to identify. Structures on more competent soil and without soft storeys (mainly due to the presence of shops at ground floor level) performed better, with shear cracking and some time out-of-plane collapse of the infill masonry, especially in case of hollow bricks.

Of the data shown in Figures. 5.40 and 5.41 three correlations are of interest, the distribution of number of storeys with structural type, the correlation between damage level and number of storeys and the correlation between damage type and damage level.

The correlation between type of structure and damage type and level is less significant as the majority of the samples is made out of reinforced concrete structures. Significant statistics on the behaviour of the infill is also made insignificant by the small proportion of buildings for which the type of infill was identified.

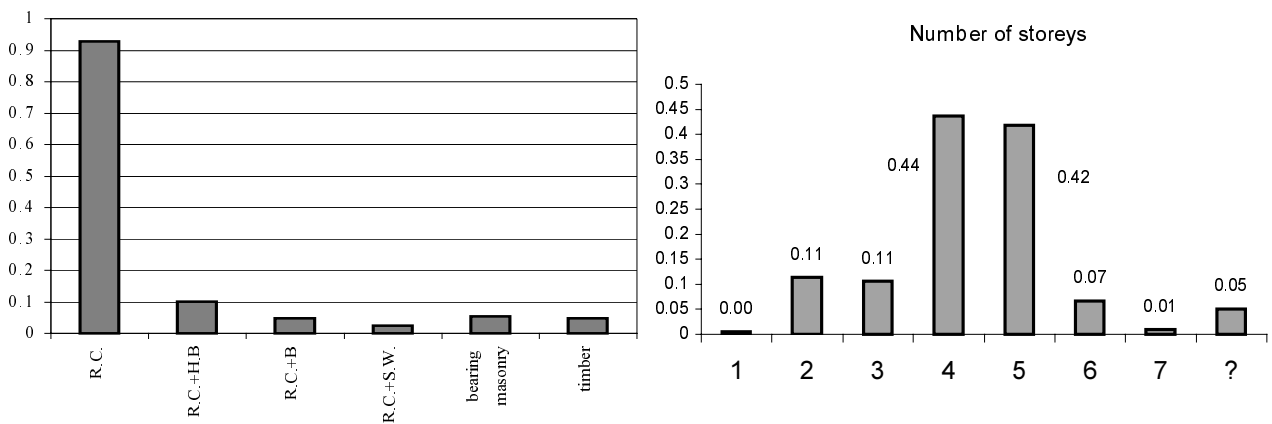
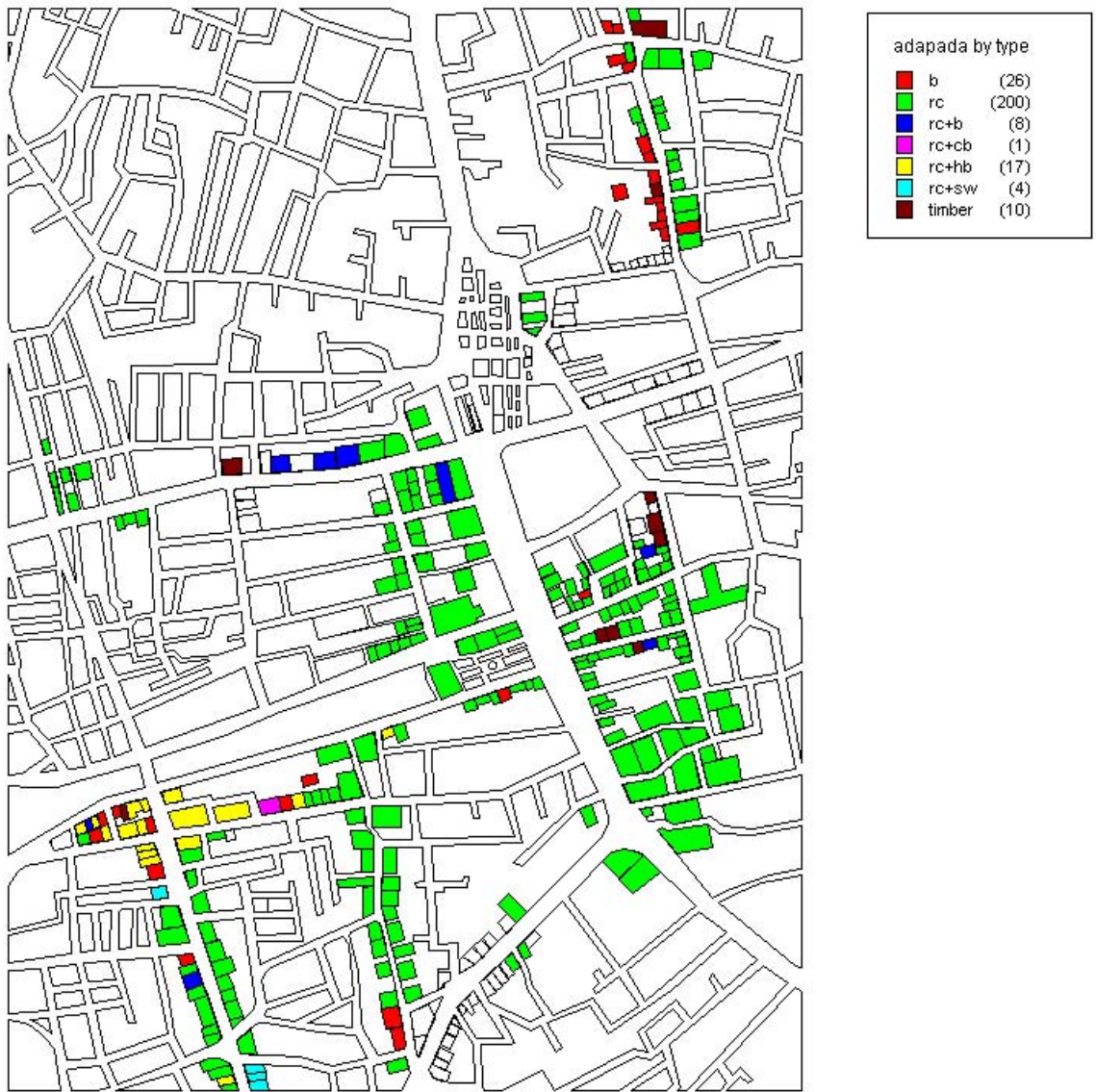


Figure 5. 39: Distribution of types of buildings and number of storeys in Adapazari centre.

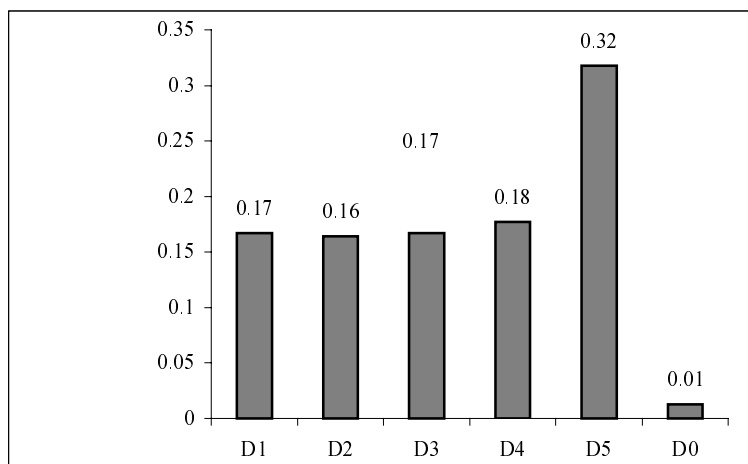
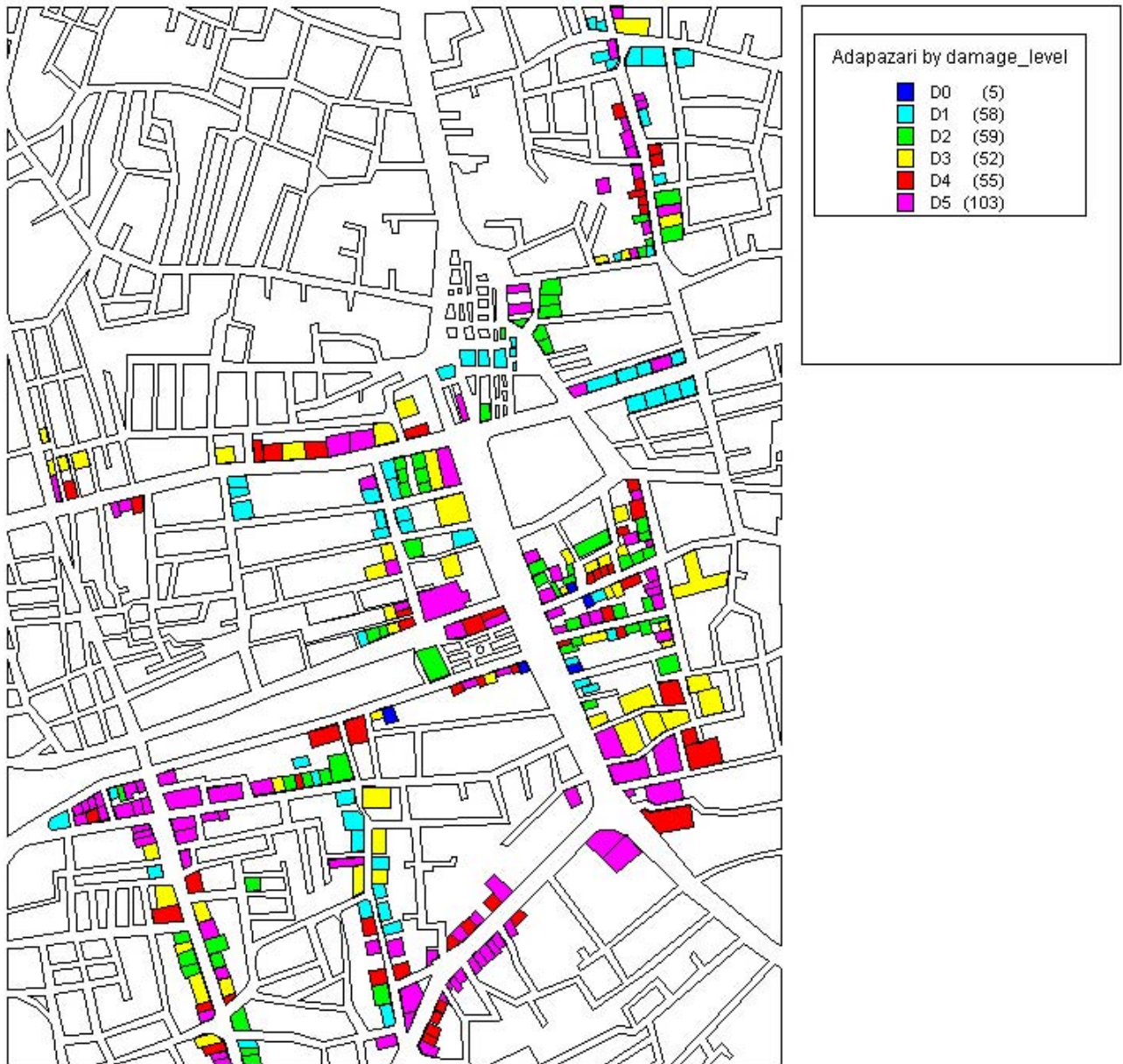


Figure 5.40: EMS 98 damage level distribution and mapping

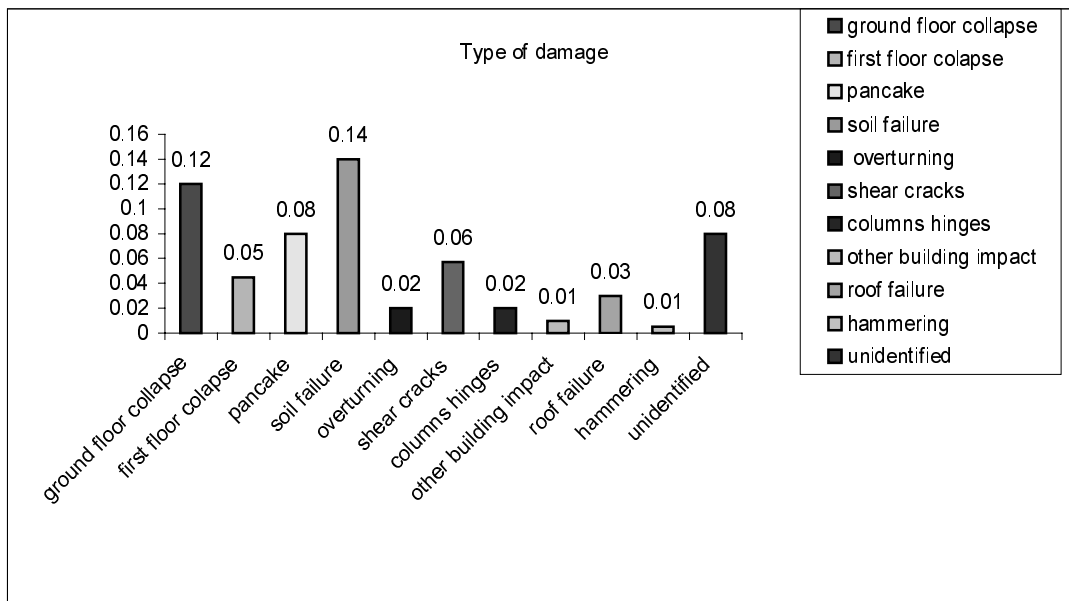
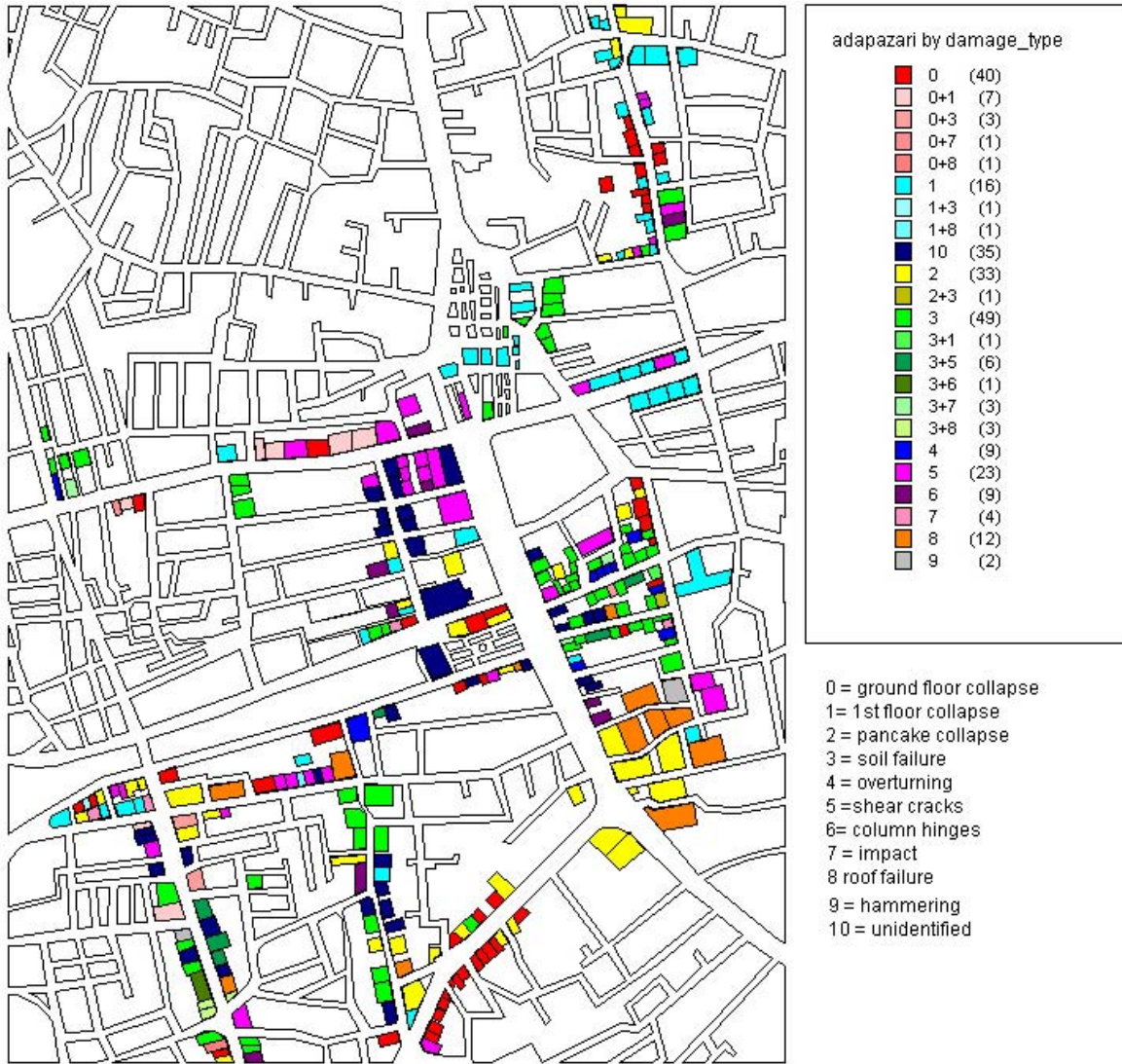


Figure 5.41: Distribution of damage by type

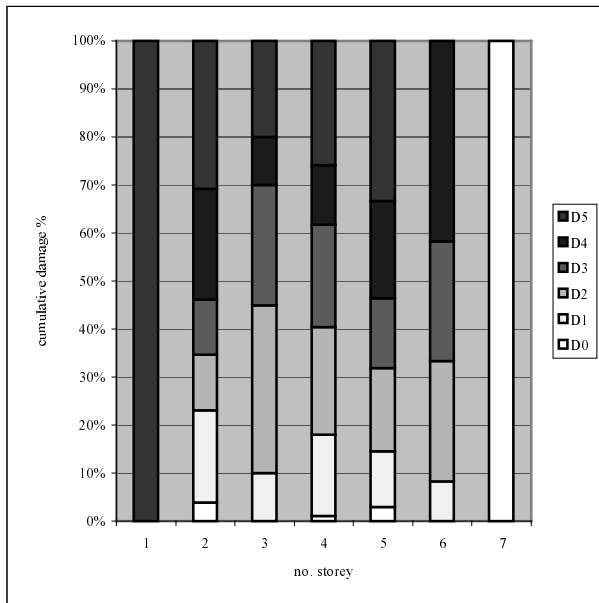


Figure 5.42: Distribution of damage level by number of storeys.

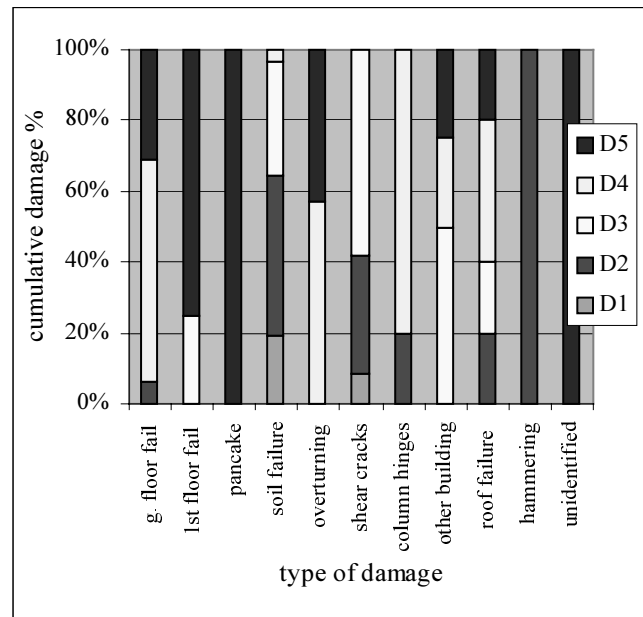


Figure 5.43: Distribution of damage level by damage types

These results have important implications both for estimations of earthquake risk for r.c. buildings in Turkey, and also for macroseismic intensity assignment. If the intensity assignment is based on the assumption that the low rise buildings are of vulnerability class B, the intensity at this location was clearly VIII (“many buildings of vulnerability class C suffer damage grade 2, a few grade 3”). If however the r.c. frame buildings are assumed to be of vulnerability class C (“frame without earthquake-resistant design”), then intensity IX is more appropriate (“many buildings of vulnerability class C suffer damage grade 3; a few grade 4”). This compares with intensity assignments for Izmit of EMS=8.5 made by the Italian GNDT group, and EMS=IX made by the Turkish Ministry of Disaster Affairs (see Chapter 3).

Finally, with reference to a possible correlation with strong motion parameter, it is worth remembering that in Adapazari there was only one instrument located on competent rock at some 5 Km from the town centre. A damage survey conducted in the vicinity of the instruments shows a substantial difference not only in damage distribution, as there was no incidence of complete collapse but also a substantial difference in damage types, confirming the important role played by the foundation soil.

5.6 Damage survey in Izmit

A small building damage survey in the town of Izmit was conducted by Robin Spence (Cambridge University) in conjunction with G. Zuccaro of Naples University and CAR Progetti (Italy) and F. Papa of the Italian National Seismic Service (SSN) on 23 and 24 September 1999. Its purpose was to identify differences in performance between different building types; accordingly an area was chosen for survey where there was a mixture of building types and a range of damage levels, but few collapsed buildings. The buildings were also a mixture of residential buildings and commercial buildings. The survey area consisted of two adjacent streets at the eastern end of Izmit: Erdogan Sokak and Mehmet Alipasa Sokak (Figure 5.44) and the adjoining streets. In total 110 buildings were surveyed, and information was collected for each building on:

- number of stories
- vertical structure type (r.c. frame, brick, stone or block masonry)
- upper floors structure type (r.c. slab or timber)
- roof structure type (timber or r.c.)
- existence of infill walls
- existence of soft storey
- damage typology



Figure 5.44: Mehmet Alipasa Sokak, part of the survey area

Table 5.3. Distribution of the sample by vertical structure and numbers of stories (%)

No of stories	1	2	3	4	5	6	7
RC	3.8	6.3	16.3	29	25	12.5	7.5
Masonry	7.7	42.3	23	23	3.8	0	0

This note gives a brief overview of the damage distribution; a more detailed analysis and study of damage typologies will be published in due course. By vertical structure, there were 81 reinforced concrete buildings in the sample, 26 masonry buildings and 3 of other or unidentified types; the distribution by numbers of stories among the two principal structure types was as shown in Table 5.3.

Of the reinforced concrete buildings only 7 (8.6%) had infill walls contributing to the structural frame, and no less than 43 (53%) were judged to have soft stories. Damage level for each building was assessed according to the six point scale (D0-D5) of the European Macroseismic Scale (EMS, 1998) Table 5.4 shows the distribution by damage level among the r.c. and masonry buildings. In the last column, it is worth observing that the number of seriously damaged buildings was more than twice as high for the r.c. buildings as for the masonry buildings. If the building sample is subdivided purely by storey height, the difference in performance is even more remarkable, Table 5.5.

The differences between the performance of the taller buildings and the low-rise buildings is very striking. Over 30% of the taller buildings were seriously damaged or collapsed (more than 40% of those, the majority, with soft storeys), while only 7.5% of the low-rise buildings suffered the same levels of damage.

In conclusion, the survey showed that the performance of r.c. buildings of 4 storeys or more was extremely poor, and worse than previous expectations based on past damage surveys elsewhere in Turkey (Coburn and Spence 1992). The survey took place in an urban area where there was no strong motion instrument nearby, so correlation with ground motion parameters was not possible.

Table 5.4 Damage distribution by vertical structure type (%)

Damage level	D0	D1	D2	D3	D4	D5	D3 or more
RC	6.1	38.3	29.6	16.0	4.9	4.9	25.8
Masonry	15.4	30.8	42.3	11.5	0	0	11.5

Table 5.5. Damage distribution by number of storeys

Damage level	D0	D1	D2	D3	D4	D5	D3 or more
Less than 4 floors	12.5	55	25	0	2.5	5	7.5
4 or more floors	5.9	25.3	37.3	23.8	4.4	3.0	31.2

5.7 Conclusions

The most common type of residential building in this part of Turkey is without doubt the reinforced concrete frame of 4 or 5 floors with a minority of taller buildings. This has proved to be the most vulnerable type of construction present, with a high proportion of partial and total collapses in all major urban centres along the Marmara Sea coast. A high proportion of these buildings was built in the last 25 years and should have been designed according to the 1975 Turkish Seismic code. This code assumed an implicit ductile capacity of the frame and the maximum ordinate of the design spectrum is about 4 times smaller than the peak acceleration obtained by processing the recorded strong motion with a non linear oscillator by El-Nashai et al.(2000). This outlines the high level of reliance that the code put in the appropriate detailing of reinforcement, in order to deliver the needed ductility. Unfortunately, upon inspection, resulted evident that in many cases the constructional knowledge associated with this was lacking and that provisions for lap splicing, cut-off, amount and distribution of ties and stirrups and formation of hooks, had not been put into practice. Moreover the quality of the concrete was usually rather poor contributing to the overall brittle behaviour of most structural columns.

The majority of these buildings have infill panels made with different types of brick, that could theoretically enhance the overall seismic behaviour by working in parallel with the main structure. However a great majority of the most recent built have masonry infill made of very brittle lightweight extruded tiles laid with the holes horizontally so that they are not competent to resist neither shear or the compression associated with the vertical loading, once the main structures have failed.

The most common form of failure was the soft storey collapse of the first one or two storeys brought about by the use of rigid beams and heavy slabs and the fact that most columns in a building will be oriented with their major inertia axis all parallel, creating a weak plane in the orthogonal direction. In areas of higher shaking the proportion of multi -storey or pancake collapse were preponderant, especially for buildings with regular elevation.

The soil- structure interaction played a crucial role, especially in Adapazari and on the south shore line, where entire blocks were affected by soil liquefaction and bearing failure and subsidence. A number of spectacular rigid overturning of buildings was recorded, the structure of the building being virtually unaffected.

The limited damage surveys carried out, and the evidence of the earthquake, all point towards the high level of vulnerability of the urban environment of this part of Turkey. This coupled with the location in the highest hazard region of Turkey provide clear evidence and support, not only for the high level of live and economic losses experienced in the Kocaeli earthquake, but also toward the substantial risk to which the population will still be exposed in future events. This risk had been already highlighted by the destructive events of the last decade in Erzincan, Dinar and Ceyhan, and evidently the promulgation of a new seismic code is not sufficient to reduce the vulnerability. It should not be overlooked that many of the buildings still standing and apparently with light damage, will have developed hidden weaknesses, and strategies and sufficient practical knowledge to carry out effective strengthening intervention

are of limited availability. It is essential to promote a substantial campaign of social and political awareness of this risk and a complete reform of the engineering training and practice, and of the law enforcement system.

5.8 References

- Aydinoglu M.N. et al., (1998), Specification for Structures to be Built in Disaster Areas: Part III-Earthquake Disaster Prevention, Ministry of Public Works and Settlement, Republic of Turkey.
- Bayülke N, (1983). *Building types in Bolu, West Turkey and their probable earthquake damage*.in A comprehensive study on earthquake disaster in Turkey in view of seismic risk reduction, Hokkaido University, Sapporo 1983 pp. 211-236
- Bogaziçi University Report (1992). *March 13, 1992 ($M_S = 6.8$) Erzincan Earthquake: A preliminary reconnaissance report*. May 1992
- Cagatay I.H, Haktanir, T. (1999). “ Malpractices in Concrete Applications and Disadvantages of using sea sand as Concrete Aggregate in Reinforced Concrete Structures in Earthquake-Prone Areas of Turkey”. *Proceedings, International Conference on the Kocaeli earthquake*, Istanbul Technical University, December 1999
- Coburn and A., Spence R. (1992). *Earthquake Protection*, John Wiley and Sons
- EEFIT (1993). *The Erzincan, Turkey Earthquake of 13 March 1992*. A Field Report by EEFIT. Institution of Structural Engineers, London, April 1993
- Elnashai, A S, Antoniou S. (ed) 2000. *Implications of recent earthquakes on seismic risk*. Imperial College Press, London, 2000
- G. Grunthal, (ed) 1998. *European Macroseismic Scale 1998, Conseil de L'Europe*, Luxembourg 1998
- Gur, T. Sucuoglu, H., (2000) *Seismic rehabilitation of 108 R/C buildings in Ceyhan after the 27 June 1998 Adana-Ceyhan earthquake*. Report no: METU/EERC 2000-01, Middle East Technical University, Earthquake Engineering Research Centre.
- Paz M. (ed.) 1994. *International handbook of Earthquake Engineering*, Chapman and Hall New York 1994.
- Wenk, T et al (1998). *The Adana-Ceyhan earthquake of June 27 1998*. Swiss Society for Earthquake Engineering and Structural Dynamics

Acknowledgements

EEFIT thank Dr John Pickering of Messrs Sandbergs for agreeing to undertake the concrete testing free of charge

¹ Website, <http://www.koeri.boun.edu.tr/earthqk/FINEND-999.pdf>

² Website, <http://www.metu.edu.tr/home/wwwdmc/code.html>

³ Personal communication Owen and Partners, Istanbul

6 Industrial and Commercial Sites

Alan Stewart,
Babtie Group

Paul Doyle,
Babtie Group

Dina D'Ayala,
University of Bath

6.1 Introduction

The motorway corridor between Istanbul and Izmit is the most heavily industrialised area in Turkey, with particular concentrations of industry between Korfez and Izmit along the north shore of Izmit bay. The earthquake area contains large numbers of single storey concrete portal frame factory units hosting light industrial activity, petrochemical plants around Izmit, two car plants, tyre factories, paper factories, cement plants and numerous other industrial facilities. It has been estimated that two thirds of Turkey's industrial output is generated in this area, and the industrial losses are reported to be around 2 billion USD (Kandilli), or 1% of GDP.

This chapter presents a damage survey of an industrial estate southwest of Adapazari, on which more information is contained in the Appendix 6A, then case studies of petrochemical plants, the Castrol Plant in Korfez, and the Petkim plant in Yarimca; two case studies of car plants, the Toyota SA Car Plant close to Adapazari, and the Ford Otosan car plant under construction near Golcuk; finally the performance of a car park in Adapazari is discussed together with few other commercial buildings.

6.2 Damage Survey of Industrial Estate

Structural steel is significantly more expensive than reinforced concrete in Turkey, with concrete construction regarded as simple, widely understood technology. A great many structures, which would be constructed of steel in Western Europe, are therefore built of concrete in Turkey. A typical light industrial unit is formed of precast concrete ridged portals with masonry infill wall panels, the roofs generally consisting of concrete purlins with profiled metal decking. The structures are not well tied together and such units have not performed well, with failure often caused by excitation of the heavy rafter/purlin arrangement. In contrast the few examples of steel truss roofs on concrete columns emerged relatively undamaged. Examples were examined at Korfez, Izmit and Adapazari. The failures allowed close examination of reinforcement and connection details, which local engineers regard as fairly typical.

An industrial park has been developed in the last ten years to the south west of Adapazari, about 5 km from the fault, with a large number of factories arranged along a single road approximately 2km long.

These factories are mainly single storey (apart from office accommodation) constructed from portal frames in either steel or concrete. Most of them were substantial buildings having floor areas in the range 1500 m² to 5000 m². The bulk of the factories had been constructed in pre-cast concrete, with some of them being only partly completed. Work on the latter appeared to have been stopped for some time, with cladding only partly completed. However some of the heavily damaged factories had been in use until the earthquake. Approximately two thirds of this estate was surveyed and a record made of 28 factories in terms of structural type, approximate dimensions, level and type of damage. The complete damage survey is contained in the Appendix 6A to this chapter.

Construction details of the precast concrete frames are fairly standard throughout. The foundations are universally large pads containing sockets into which the precast column is concreted to provide a moment connection (Figure 6.1). The column heads are either then corbelled to take the rafter ends, or there is a half joint at about 1/3 span in the rafter. The connections are either single or twin bolts sleeved through holes in the rafters, hence the columns act as vertical cantilevers with the rafter/column connections as pins. In multiple bay portals, the rafters are frequently continuous over internal columns, resting directly on the column heads and held by two bolts projecting from the column through the rafter.



Figure 6.1



Figure 6.2



Figure 6.3

Hence, three principal frame types can be identified:

- Type 1: a cantilever column, with a corbel connection and a single vertical dowel at the eaves. This type of frame is illustrated in Figure 6.2 and Figures 6.4a to 6.4c
- Type 2: similar to type 1 but with a more enclosed joint using two bolts. Figure 6.5a shows some of the heavier rafters and Figure 6.5b shows a typical failed connection of this type.
- Type 3: half joints in rafters, shown in Figure 6.3, generally with connections to internal columns as shown in Figure 6.6a. Figure 6.6b shows the typical failure pattern.



Figure 6.4a: Typical failure of main columns



Figure 6.4b: Failure of main columns with part built external cladding



Figure 6.4c: Detail of failed connection at base of columns. Note the ruptured longitudinal bars



Figure 6.5a: Failure of rafters: note about 1.5m depth at apex giving a very heavy roof



Figure 6.5b: Detail of connection



Figure 6.6a: Detail of connection between top of column and rafter continuous over



Figure 6.6b: Typical failure pattern



Figure 6.7



Figure 6.8



Figure 6.9



Figure 6.10

Although both the 1975 and 1997 seismic codes have requirements dealing with precast industrial buildings, it appears that, under construction, these structure lack sufficient lateral stability. Indeed the masonry infill panels

and the roof decking would have an essential role in providing bracing, however an inherent weakness is shown by the failing of the precast frame themselves in shear, prying or pull out of the bolts, (Figure 6.7) or in some cases by minor axis bending of the columns (Figure 6.8). Similarly, the purlins are poorly connected, typically by a projecting wire twisted round a loop protruding from the rafter (Figure 6.9). Figure 6.10 shows a general view of one of the failed buildings.

Where the structures have been completed the unreinforced masonry infill panels provide transverse restraint and lateral bracing to the column, although sometimes failing out of plane due to a lack of connection to the columns. Major damage still resulted from relative movement between the columns and rafters or failure of the gable wall (Figure 6.11) which is often poorly connected at roof level. Only in one building was roof bracing observed and this was significantly undersized for the seismic loads which occurred.



Figure 6.11

The results of the damage survey carried out in Adapazari are summarised in Table 6.1 below and in the diagram in Figure 6.12 which analyses the level of damage with respect to the 5 types of structures described.

Table 6.1: Level of damage by structural type for the building of the industrial estate in Adapazari

Structure type	Level of damage	Number of warehouses
Precast concrete	Collapsed	13
	Badly damaged needing demolition	2
	Survived	3
Steel frame including galvanised cold formed	Survived	6
Reinforced in situ concrete	Survived	2

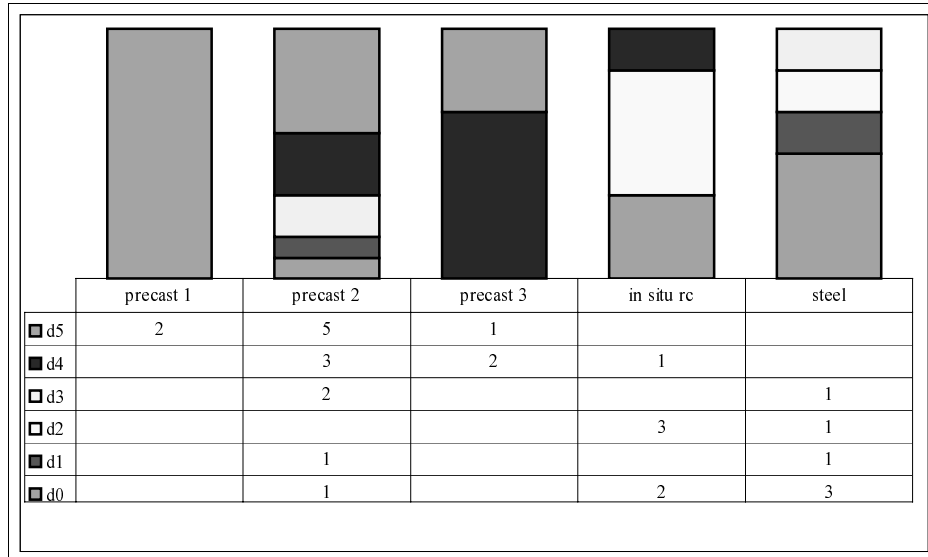


Figure 6.12: Histogram of damage by structural type of the industrial estate in Adapazari

Elsewhere in the region further pre cast concrete buildings were seen to have collapsed, although many had survived. In all cases where a pre cast building had failed, failure was initiated at the joints, where insufficient capacity and/or ductility had been provided. Examples of failures for both in situ concrete and steel frames, are shown in Figures 6.13a to 6.13c.



Figure 6.13a Failure of in-situ concrete and steel roof trussed factory near Yuvacik



Figure 6.13b: Failure of RC factory south Marmara Sea area



Figure 6.13c: Failure of steel frame on top of RC concrete framed building near Izmit

Examples were also observed of failure of cladding, which although not totally disruptive, nevertheless has a major impact. Even if the structure survived the plant inside may move, or be disrupted. This is illustrated in Figures 6.14a to 6.14c.



Figure 6.14a: Failure of cladding – factory near Korfez



Figure 6.14.b: Failure of cladding – factory near Korfez. The EOT crane in this building needed to be replaced post earthquake.



Figure 6.14c: Movement of plant inside factory near Adapazari. This 10t press moved approx 1m in the earthquake. As shown by rust marks

6.3 Petrochemical Plants

Although there is a major concentration of petrochemical plants in the area, most of those approached refused access. However, Castrol and Petkim agreed to an inspection of their plants and it proved possible to gain a general impression of several others from outside the fence.

6.3.1 Castrol Plant

The Castrol plant at Izmit was examined in the company of Mr Aksoy, the plant manager. The plant employs 100 staff and suffered three weeks of lost production. Castrol estimate the cost of repair at 1 million USD, with lost production accounting for a further 4 million USD.

The plant comprises large oil storage tanks, pipe work, process plant, a warehouse for storage of the product and two administration blocks. The buildings are generally concrete framed, with the exception of a steel framed warehouse, and the plant was not seismically designed. Water and electricity both failed during the earthquake, but the grid electrical supplies were restored within a few hours. The plant has no back up electrical supply of its own.



Figure 6.15

Both concrete framed office blocks showed limited cracking (Figure 6.15). However, the warehouse, which contains integral racking, was supported by emergency bracing at the time of the visit (Figure 6.16). The racking is a proprietary system in which there is little longitudinal restraint, and joint rotation (Figure 6.17) caused many of the bolts connecting the shelving to the uprights to shear, resulting in the racking system leaning over at an angle of approximately 15 degrees. The entire building was out of plumb as a result, with racking of the cladding evident on the elevations (Figures 6.18a and b). At the time of the visit, temporary diagonal bracing to the racking system had been added, as well as inclined props. Plans were being made to empty the warehouse, and to move the stock to a temporary off site warehouse. It was considered that it would be too dangerous to use forklift trucks (due to the possibility of accidentally hitting the racking and thereby destabilising it), so the warehouse would be emptied by hand using conveyor belts installed on temporary scaffolding. The cost of emptying the warehouse and rebuilding was estimated to cost of the order of 1 million USD. However, this would allow approximately 4 million USD of stock to be recovered.



Figure 6.16

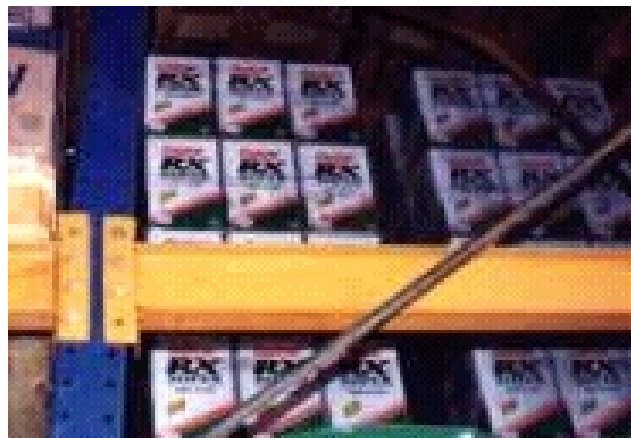


Figure 6.17



Figure 6.18a



Figure 6.18b

The oil storage tanks are 10m diameter by 15m high and were full to within 0.5m of the top at the time of the earthquake. Settlement of around 30mm was noted at each tank (Figure 6.19) but the draw off pipework remained intact and no leaks occurred. There was no “elephant’s foot” buckling of the tanks.



Figure 6.19

The pipework around the site was generally poorly restrained, but there was no evidence of damage despite the gross movements which may have occurred, and the plant manager had noted no leaks. The majority of the factory was undamaged, and production was able to continue. Details from the Castrol factory are given below in Figures 6.20a to c. Details of the failed warehouse are given below in Figures 6.21a to c.



Fig 6.20a: Main processing area. Steel frame, and process plant undamaged



Fig 6.20b: Precast concrete warehouse - undamaged



Fig 6.20c: Near failure of connection for canopy roof connecting two buildings



Fig 6.21a: Tilt of warehouse when compared to adjacent loading bay



Fig 6.21b: Buckling of bracing to racking system. Diagonal from bottom left to top right is new bracing installed post earthquake



Fig 6.21c: Racking tilted over. Note new props in top right corner

6.3.2 Petkim

The Petkim petrochemical facility at Korfez is one of the largest state-owned facilities in the country and is a major supplier to other companies. Petkim suffered extensive damage to its port, collapse of wooden cooling towers (Figure 6.22) and severe damage to concrete cooling towers. One of the building housing the company offices and one of the strong motion instrument also experience moderate damage.

A number of other gas firms are located in the immediate vicinity, with numerous spherical LPG storage tanks surrounding the area, but no major structural damage was observed or reported at these plants.



Figure 6.22: Collapsed Wooden Cooling Towers at Petkim

6.3.3 Tupras Refinery

The team were refused entry to the Tupras refinery, which supplies approximately 1/3 of Turkey's oil. However, the damage which occurred was widely reported at the time and has been confirmed by other teams which did gain entry. Several tanks and a cooling tower burned out of control for three days when naphtha spilled from a floating roof tank and ignited; the water supply to the refinery being lost. A second fire started in a crude unit, when a 100 m. high reinforced concrete heater stack collapsed, demolishing equipment and pipework.

6.4 Car Plants

6.4.1 Toyota Sa

The Toyota Sa plant was built in 1992/93 to then current seismic Japanese code requirements. The plant began operation in 1994 and was producing 50 cars a day prior to the earthquake. The fault rupture passes through the grounds of the plant, although it appears that the owners had not previously appreciated that the fault was quite so close.

However, the plant is constructed on poor ground and it was realised that the fault was not too far distant. Therefore the need for a rigorous seismic design was recognised when the plant was initially planned. Although this significantly increased the construction cost to 80 million USD, the plant was virtually undamaged and was due to restart production at the time of the visit.

The site ground conditions consist of 12m of soft ground on gravel, with the water table at 3m depth. The building structure and major plant items are carried on a total of 3800 number 400mm square concrete piles end bearing in the gravel at about 14m depth. The steel columns are cast into sockets in the pile caps, generally on a 10m x 10m grid (except for the paint shop where a 20m x 10m grid was adopted). They are orientated with the webs of alternate columns rotated through 90 degrees to equalise stiffness. No bracing is used, with the columns acting as part of a moment frame between the ground and roof structure, which is a deep 3D space truss. The floor is not piled but is simply a ground slab, although the top metre of soil was reworked to improve bearing resistance. At one location there was 25mm vertical displacement of the floor slab relative to the adjacent pile cap but otherwise the slab performed well with only local spalling of the movement joints. A general view of the assembly shop is given in Figure 6.23a, with details of the roof in Figure 6.23b.

Some auxiliary buildings make use of concrete columns, generally with a steel roof.



Figure 6.23a: General view of the main assembly shop

Figure 6.23b: The truss roof structure



Figure 6.24: Services run in the roof

The earthquake caused no damage to the structure of the main factory, but columns supporting the roof of an ancillary transformer building exhibited some cracking. In one place some cladding was shaken off. Much of the larger machinery is set into floor pits and the plant manager reported some opening of the movement joints in the pits.

Within the factory, there was only minor damage to the plant items. Some of the control panels, which had not been bolted down, tipped over and the paint shop fans, which were floating on springs, bounced off the springs but were reinstated without difficulty. One of the press machines moved about 100mm. Lagging to pipe work showed some fretting where structural movement had occurred (Figure 6.24).

The electrical supplies to the site failed during the earthquake but were operational again the same day. The supply is taken direct from the 154 kV national grid rather than from the local 33kV grid, which would be more usual. The latter was badly affected and some local areas were without electricity for a week. The primary and back up 25 MVA transformers for the electrical supply suffered some damage. The primary unit translated on its

rails but remained operational (Figure 6.25a and b); the 60 tonne back up unit came off the rails and was removed for inspection although subsequently reported to be still functional.

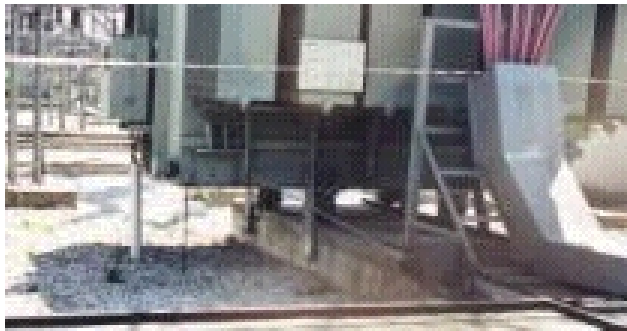


Figure 6.25a



Figure 6.25b

The gas supply system has an automatic shut off which activated, but the main tanks were undamaged (Figure 6.26). The water distribution system in the site ruptured in many places (Figure 6.27) and was being replaced by plastic pipe at the time of the visit. Within the plant, the only reported damage was cracking at a few valves and elbows.



Figure 6.26

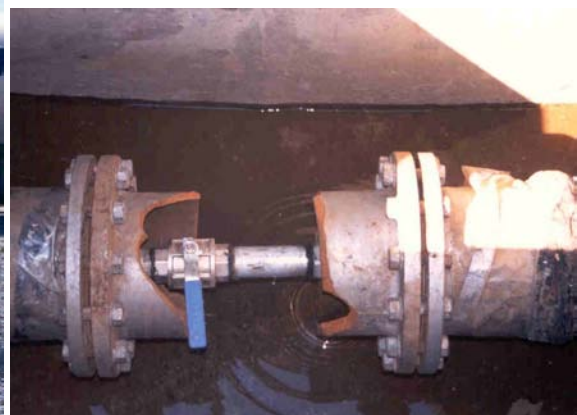


Figure 6.27

Electroplating of the car bodies is carried out in an above ground tank approximately 10m x 3m x 3m. Sloshing of the container solution was reported to have caused the loss of 14 tonnes of electrolyte.

The access road was badly damaged by vertical and horizontal movement at the fault (Figure 6.28, 6.29) but the damage was not inhibiting vehicle access for repairs.

At the time of the earthquake, the plant was shut down for annual maintenance, for which the assembly lines were cleared, and this helped to minimise consequential losses from movement of part completed cars. In fact, only four cars suffered significant damage. At the time of the visit, 7 September 1999, it was expected that production would re-commence in about a week. Thus the plant would have been out of action for 4 weeks following the earthquake. This shut was mainly as a result of the need for post earthquake inspection, as well as repair of the minor damage that had occurred, such as toppling of switch panels.

The plant has 420 shift workers and 130 staff. Because of the shut down many of the employees were away from the area at the time of the earthquake and as a result only two were killed. However, most of the employees had suffered in the earthquake, with many having lost their houses. Toyota SA were supporting a total of 266 people, by providing temporary accommodation.

We would like to acknowledge the help given by Unlow Usel, the plant General Manger, in providing information on which the above is based.



Figure 6.28



Figure 6.29

6.4.2 Ford Otosan

The Ford Otosan plant at Golcuk was under construction, but near completion, at the time of the earthquake. The superstructure had been erected but little of the ground slab had been constructed. The plant was apparently designed against earthquakes, but nevertheless suffered significant damage.

In a number of cases concrete columns had fractured (Figure 6.30a), and the body shop had suffered permanent sway deformation (Figure 6.30b). Ground improvement had been carried out prior to construction, consisting of grout columns intended to improve bearing capacity and resist the effects of liquefaction. However, this had not been entirely successful. Figure 6.30c shows a ground fissure following one line of grout columns, and differential settlement is evident in the adjacent west wall of the body shop. More details of the survey carried out at this plant are included as commentary to plates in Appendix 6B



Figure 6.30a: Column Damage in Bodyshop



Figure 6.30b: Bodyshop west wall showing distortion of columns. Roof has kept its shape and pipe work from roof clearly shows horizontal displacement.



Figure 6.30c: Fissure in ground formed along alignment of cement grout columns.

6.5 Performance of Commercial Buildings

Although many commercial buildings performed well in the earthquake, there were a number of examples of building which had suffered in the earthquake. These are discussed further below.

6.5.1 Car park in Adapazari (Katli Otopark)

This was a major structure located on Hal Cad. in Adapazari, consisting of a market at ground floor with car parking above, and is shown in Figures 6.31 a to c. It measured of the order of 100m x 50m, and was one of the main car parks for Adapazari. It had five storeys, and was divided into a number of independent sections by longitudinal and transverse movement joints. The building was constructed as an in-situ reinforced concrete moment frame, with waffle slab floors. The ramps may have also assisted in providing additional lateral load capacity.



Figure 6.31a



Figure 6.31b



Figure 6.31c

The lower floors had collapsed, leaving half of the building standing. The collapsed section of the building was on the Hal Cad. frontage, with the split between the collapsed and standing sections of the building occurring on the longitudinal movement joints.

Although only half of the building had collapsed, the remainder of the building was in such a bad condition that collapse was imminent.

This portion of the building did, however, illustrate how the failure had occurred. Failure had occurred by plastic hinges forming in the concrete columns, with buckling of reinforcement as the concrete failed. This is illustrated in Figures 6.32a and b. The columns were highly reinforced with a significant number of ties. These details would suggest that the building had been seismically designed. However, all the columns measured approximately 1000mm x 500mm, and were aligned in the same direction to facilitate parking. Failure had occurred about the

minor axis. It was also apparent that the building had undergone significant torsions, as the damage became progressively worse nearer the outside. Near the ramps the columns were less heavily damaged



Figure 6.32a



Figure 6.32b

6.5.2 Office block in Adapazari (Milli Egemenlik Co)

This five storey office building had suffered failure of the ground floor in a “classic “ soft storey failure. The lowest columns had failed, causing the building to topple sideways, but there appeared to be relatively little damage to the upper floors (see Figures 6.33 a to b).



Fig 6.33a



Figure 6.33b

6.5.3 Stores on South Coast

There were two stores on the south coast of the Marmara Sea, between Yuvacik and Golcuk, which although still standing had been badly affected by the earthquake. Figs 6.34a to d illustrate the first, which was a furniture store. Of particular note is that although the reinforced concrete frame is largely intact, the floor level for one of the end bays had dropped by about half a metre. It was also apparent that what failures there had been occurred in the beams, rather than in the columns.



Figure 6.34a



Figure 6.34b



Figure 6.34c

There was extensive damage to the external cladding, exposing the structure. On a subsequent visit to this store, the owner had hired access equipment and was removing the stock, so limiting the economic damage. However future trading from the building would be impossible, with demolition the only option.






Figure 6.34d











Figure 6.35




The second store showed even less structural damage Figure 6.35. However, it had entirely lost its glass façade. Again, the main structure had performed adequately, but the building was not usable.

APPENDIX 6A: DAMAGE TO INDUSTRIAL ESTATE NEAR ADAPAZARI

Construction	Estimated size		Cladding	Condition	
	Length	Width			
5 storey in situ RC frame	20m	40m	Masonry	Ok	
3 bay pre-cast concrete portal frame type 1	72m	84m	Part completed masonry walls. No roof cladding.	Collapsed	
2 bay cold formed steel tied portal	30m	55m	Steel wall and roof panels + masonry dado wall	Ok	
3 bay pre-cast concrete portal frame type 2	54m	60m	Part built. No cladding	Collapsed	
2 bay pre-cast portal frame type 3 with two storey office building in first two bays	36m	72m	Part built masonry walls. Cladding on roof	Collapsed	
3 bay pre-cast concrete portal frame type 2	42m	54m	No cladding	Collapsed - failed by twisting of central columns. Outer frame still standing	

Steel portal frame with side bracing. One bay in-situ concrete to first floor with steel above	54m	24m	No cladding	Ok	
2 bay in situ concrete frame for walls. Steel truss roof	72m	24m	Masonry infill for walls. No cladding on roof.	Slight buckle on bracing	
2 bay steel portal frame, with longitudinal tension only "X" bracing (very light)	72m	60m	Masonry infill walls. Light weight cladding on roof	Bracing failed in one bay. Bracing considerably stretched in others.	
3 bay portal frame. Outer bays in-situ concrete to first floor. Columns above and roof in cold formed steel.	78m	30m	Masonry walls, with asbestos cement type roof	Minor damage to masonry walls	
3 bay pre-cast concrete portal frame type 2. In use	60m	54m	Masonry walls half height with glazing above. No roof - removed.	Collapsed roof. Walls standing	
3 bay pre-cast concrete portal. frame type 2. In use as textile factory	72m	72m	Masonry walls. Light weight cladding on roof	Collapsed	

2 bay pre-cast concrete portal frame type 2. In use as electrical goods factory	130m	40m	Masonry walls. Roof cladding removed from site.	Purlins / drain channels failed. Main frame still standing but very badly damaged	
Two storeys office annexe to above, in-situ concrete	30m	30m	Masonry walls. Roof unknown	Ok	
3 bay pre-cast concrete portal frame type 1	72m	72m	PC panels for roof. No walls	Collapsed. Very badly broken.	
2 bay pre-cast concrete portal frame type 2. In use as textile factory	66m	36m	Masonry walls with lightweight cladding for roof	Roof collapsed. Walls OK	
2 bay pre-cast concrete portal frame type 2	36m	48m	No cladding	Collapsed	
2 bay steel frame. No purlins or bracing.	180m	36m	No cladding	Ok	
2 bay steel portal frame with bracing	48m	36m	No cladding	Ok	
2 bay pre-cast concrete portal frame type 3. In use	36m	36m	Masonry walls with lightweight cladding for roof	Roof collapsed. Walls standing	
2 bay pre-cast concrete portal frame type 2	36m	36m	No cladding	Collapsed	
2 bay steel portal with in situ concrete service building	60m	36m	Masonry walls with lightweight cladding for roof	Ok	
2 bay pre-cast concrete portal frame type 2	66m	36m	Masonry walls with lightweight cladding for roof	Roof OK. Still standing but very badly damaged	
2 bay pre-cast concrete portal frame type 2	48m	36m	Masonry walls with lightweight cladding for roof	Collapsed	

2 bay pre-cast concrete portal frame type 2	48m	36m	Masonry walls with lightweight cladding for roof	□	
2 bay pre cast concrete portal frame type 2. In situ concrete frame service building occupying half of one bay	36m	84m	Masonry walls with lightweight cladding for roof	Minor damage to masonry walls and windows to service building	
Single bay portal frame type 2 (modified) with lean to bays on either side of portal frame. Office block in last two bays	32m	84m	Masonry walls with lightweight cladding for roof	Bay between service building and main building collapsed. Minor cracks to remainder of frame. Halving joint failure in service building.	
3 bay pre cast concrete portal frame type unknown. Service building at one end. Building in use	54m	84m	Masonry walls. Roof no longer present	Roof collapsed. Walls still standing	

Note: Condition 'OK' indicates no visible damage, although it was not possible to carry out a detailed internal inspection in all cases.

APPENDIX 6B: PHOTOGRAPHICAL SURVEY OF DAMAGE TO FORD OTOSAN, GÖLCÜK.



Plate 6.1: Ford Otosan Plant, Golcuk. Press Shop under construction. View to west of pile cap excavation showing 4 pile group of 600 to 700 mm diameter piles at 2000 mm centres. Main reinforcement is 10 number 16mm deformed steel bars. Confining steel is 10 mm deformed steel with unknown pitch (5 September 1999).



Plate 6.2: Ford Otosan Plant, Golcuk. Body Shop. Overturned electronic equipment. The plant was not operational at the time of the earthquake. Ground beams and floor slab were not complete in this area. Equipment was standing on aggregate layer. Note that columns and roof appear to be in good condition for most buildings (5 September 1999).



Plate 6.3: Ford Otosan Plant, Golcuk. Body Shop. On closer inspection a large number of columns were damaged at the base (5 September 1999).



Plate 6.4: Ford Otosan Plant, Golcuk. Body Shop. Separation of construction joints in floor slab of building. Sliding occurred along plastic sheeting layer beneath concrete without tearing sheeting (5 September 1999).

Plate 6.5: Ford Otosan Plant, Golcuk. Body Shop west wall. Failure and closure of door in west wall illustrates compression in north-south direction of 400mm (5 September 1999).

7 Infrastructures and marine facilities

Paul Greening,
Department of Civil Engineering, University of Bristol

Dale Vince,
Jacobs Gibb

7.1 Introduction

As the previous chapters have outlined, the Koçaeli earthquake is characterised by enormous human casualties and economic losses. Due to the proximity of the Koçaeli earthquake to the gulf of Izmit, a large number of waterfront structures were subjected to seismic loading. The extent to which waterfront structures in the area were damaged during the earthquake varied widely, ranging from no damage through to total failure. Devastating damage to large amounts of housing stock and to a lesser extent industrial and port facilities stands in contrast with limited damage caused to civil engineering structures. Media images of a collapsed highway bridge appeared to infer similar damage whereas in fact the damage to this bridge was the exception rather than the rule. The present chapter discusses the performance of the highways network, the dams and port facilities during the earthquake.

7.2 Performance of Terrestrial Infrastructures

The substantial economic and social growth of northern Turkey, presented in Chapter 1 was conveyed by, but it also stimulated, improvements in the highways and water supply networks. Examples include the E80 “Trans-Europe” route currently under development, and the newly completed Yuvacik dam and water treatment works, which was constructed to improve the water supply to the industrial and residential areas surrounding Izmit. The map of the earthquake-affected area set out in Figure 7.1 shows principal civil engineering structures and those investigated by the EEFIT mission.

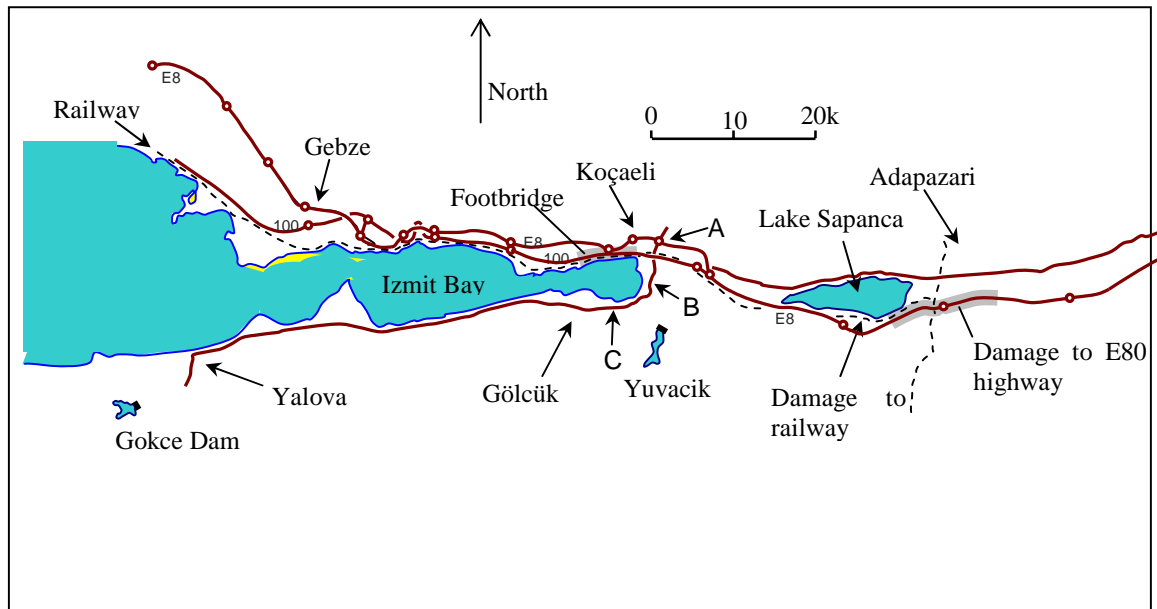


Figure 7.1: Layout of Transport Links and Civil Engineering Structures in Earthquake Area

The extent of the fault rupture is also shown. Hills rising to both north and south of Izmit bay house numerous small dams including the newly completed Yuvacik dam. The topography of the area results in east-west corridors both north and south of the bay carrying major road and rail links between Istanbul and the Turkish Capital Ankara. The EEFIT team was able to visit two dams and several bridges during the course of the mission. The following sections set out the results of inspections as well as referring to some other reported damage to highway structures.

7.2.1 Damage to Bridges and Highways

Images of the collapsed highway bridge close to Arifiye, south of Adapazari filled television screens in the immediate aftermath of the earthquake – Figure 7.2. Ten people perished in a bus crushed by one of the deck units. Figure 7.3 shows a photo of the collapse taken shortly after the earthquake. Compressive damage to the E80 is seen in the foreground of Figure 7.4. The fault rupture was found (EERI, 1999) to pass directly beneath the highway crossing resulting in large differential movement of the bridge piers. The extent of the movement was such that the bridge deck units could no longer span between their supports.



Figure 7.2: Collapse of Highway Bridge From News Footage



Figure 7.3: Collapsed bridge on E80 highway (photo: N.Apaydin)



Figure 7.4: Fault rupture crossing the E80 highway (photo H.Aydin)

The collapsed sections were cleared in a matter of days allowing the E80 to re-open. By the time of the EEFIT mission, the bare bridge piers provided the only evidence of the collapse. At the time of the visit, only one lane of the E80 was in use while repairs to the other carriageway resulting from the rupture were repaired (Figure 7.5).



Figure 7.5: Road repair resulting from fault rupture

The collapsed bridge was in the main area of damage to the E80 highway marked on Figure 7.1. An adjacent structure was inspected by the EEFIT team. The bridge was close to the Toyota plant referred to in chapter 6 and in an area which had experienced considerable surface disruption. Figures 7.6 and 7.7 show clear disturbance to the bridge abutment and resulting damage to the bridge itself; this type of damage along with evidence of tilting of piers was typical of the relatively minor damage to bridges in the region.



Figures 7.6, 7.7: Movement of overpass abutment and of road bridge abutment close to fault rupture

In the same area damage to road bridges crossing the Sakarya river has been reported (EERI 1999). The bridges consist of large hollow pre-stressed concrete sections in eight spans. Damage to shear keys at the end of each section was reported. Figures 7.8 and 7.9 show damage to the bridge seating and bearing pads. The bridge carrying the west-bound section of the E80 was closed for repairs following the earthquake.



Figures 7.8, 7.9: Spalling and damage to bearing pad at seat of bridge deck (photo: N.Apaydin, H.Aydin)



Figure 7.10: General view of viaduct in Izmit



Figure 7. 11: Column detail

A raised viaduct carrying the junction of highways 100 and 130 in the east of Kocaeli (shown as A on Figure 7.1) was inspected closely (Figure 7.10). While the structure did not show any immediate signs of damage, it was close to the epicentre of the earthquake and was adjacent to structures which had suffered very severe damage. A more

detailed inspection revealed evidence of some cracking and shifting of abutments which would require minor repair. Some evidence of movement of the bridge decks during the tremor was apparent but restraints at the top of the supporting columns (Figure 7.11) had clearly not allowed the decks to stray from their bearings.

A road bridge carrying highway 130 over a river running into the eastern end of Izmit bay was inspected (marked B on Figure 7.1) and is shown in Figure 7.12. As with the previous example, the bridge was very close to both the fault rupture and the epicentre of the earthquake itself. In addition the immediate area consisted of soft alluvial deposits which themselves had been affected by the earthquake. As with other bridges, there was evidence of damage at the interface between abutments and bridge units, in this case the concrete supports appeared to have suffered pounding from the steel deck unit (Figure 7.13). In common with other engineered bridges, settlement of the surrounding ground (slumping of the alluvial deposits adjacent to the bridge can be seen in Figure 7.12) had resulted in the bridge standing proud of the adjacent road surface. Remedial works had been implemented, creating an asphalt ramp bringing the highway up onto the bridge structure. This repair was a very common sight throughout the earthquake affected area.



Figure 7.12 River Crossing South of Izmit



Figure 7.13 Pounding Damage to Supports

A similar situation was encountered on a river crossing of the same highway to the east of Gölçük (marked C on Figure 7.1). This location was directly adjacent to a concrete batching facility that had been largely destroyed and it appeared that police were enforcing a limit on weight of traffic on the bridge. Two large viaducts on the E80 close to Izmit have been reported (EERI 1999) to have suffered no damage in the earthquake. The EERI report also suggests that the viaduct close to Düzce was fitted with energy dissipation devices that had been successful in preventing damage.

The EEFIT team inspected several footbridges in the Izmit area. A typical example is shown in Figure 7.14. A number of similarly designed bridges provide access from Izmit town over the E80 and railway to the coast. None of the bridges was closed but some damage was clearly evident (Figure 7.15). Several structures had been affected by differential settlement of piers, sinking of ground down and into the bay was an obvious feature. The column-heads of the bridges had clearly been designed to restrain the decks in the event of horizontal excitations. This approach had clearly worked at the expense of some damage to the restraints as shown in Figure 7.16.



Figure 7.14: Footbridge in Izmit



Figure 7.15: Detail of damage to the access staircase



Figure 7.16: Typical Footbridge Column Head Detail

7.2.2 Dams and water supply

Of 472 operation dams in Turkey, 48 lay within the area affected by the earthquake. The Turkish authorities were quick to announce via the website of the Turkish commission on large dams (TRCOLD, 2000) that none had suffered any damage. Two of the dams closest to areas of damage to residential and commercial buildings were visited by the EEFIT team. These were the recently completed Yuvaçık dam, located within approximately 5km of the epicentre and the Gokçe dam located around 55km to the west, close to the town of Yalova, both being shown on Figure 7.1.

The Gokçe rockfill dam is one of 15 currently supplied by the new Yuvaçık dam. This embankment dam is around 10 years old and was found to have suffered no obvious damage during the earthquake. The dam is 50m high but the water level at the time of the earthquake was found to be very low. The dam employed a concrete spillway with steel radial gates controlling water overflow (Figure 7.17). The intake/valve structure was of monolithic construction and showed no visible signs of damage (Figure 7.18). The pumping facilities at the dam were however reportedly without power for two days following the earthquake.



Figure 7.17: Gokce Dam: Radial Gate Structure



Figure 7.18: Gokce Dam: Intake Structure

The fortunes of the dam were in contrast with those of the nearby town of Yalova, which had suffered large amounts of damage. It is currently believed that the level of damage in Yalova itself was due to poor ground conditions. Structures in villages on the hillsides close to the dam were observed to have suffered negligible damage.

The Yuvaçık Dam (Figure 7.19) is located close to the epicentre of the earthquake and around 7km from the fault rupture. Seismic design criteria were included at the design stage and with the result that very little damage occurred. A full programme of damage assessment and remedial works to the dam and its water distribution network is in hand at the time of writing.

The Yuvaçık Dam is one of the world's biggest recent water supply projects. It was realised by a consortium of Thames Water, Izmit Municipality, Gama Industry, Guris Construction, Mitsui Co. and Sumitomo Corporation. Thames Water will operate the dam for 15 years, after which its operation will be transferred to Izmit Municipality. The dam was conceived for water storage and subsequent treatment to provide a potable supply. A by-pass is provided to allow emergency supplies of raw water to be drawn off the reservoir for industrial supply. The throughput of treated water is 142Mm³ per year.

The dam is an embankment dam with gravel shoulders and clay core, was first impounded in June 1998 and brought into service in January 1999. The dam height is 108m with a live storage capacity of 55Mm³. At the time of the earthquake, the retained depth of water was approximately 93m. It has been reported that a seiche was induced in the dam with a height of approximately 2.5m.

The dam was designed with a 1.5m excess height to allow for settlement over its lifetime. Seismic design of the dam was carried out to the Turkish State Hydraulics Institute (DSI) standards; a horizontal peak ground acceleration of 0.15g was used for the dam, with a lower acceleration used for design of the structures.



Figure 7.19: Yuvacik Dam

No seismic measuring instruments were in place on the dam, a network of survey points (Figure 7.20) had been monitored both before and after the earthquake. Prior to the earthquake, monitoring of the earthfill embankment over the previous year had measured settlement of 25mm. Following the earthquake, a maximum settlement of the earthfill embankment was measured as approximately 130mm. This equates to a volumetric strain amplitude of about 1.2%, which agrees well with that calculated using the Tokimatsu and Seed (1988) approach to shakedown settlement.

Very little evidence of the earthquake could be seen at the dam site, the only sign of the event being a minor rockfall from the valley sidewalls adjacent to the dam crest (Figure 7.21).

Mechanical and electrical works at the dam were designed to DSI standards. A visual inspection after the earthquake indicated that only relatively minor damage had occurred to civil and mechanical plant at the Water Treatment Plant. The output from the plant was disrupted for a short time only whilst a shut-down was implemented to carry out damage inspections. Testing of the M&E equipment is being carried out as an ongoing programme, for example testing of the radial gates will be carried out when the retained water level falls below spillway cill level.

The water distribution pipeline runs along the north coast of Izmit bay as far as Gebze, and along the southern shore as far as Gölçük. This region coincides very well with the extent of structural damage to residential and industrial buildings to the west of the epicentre. The distribution network comprises approximately 103km of steel pipeline with diameters between 2.2m and 1.2m, and 45km of ductile iron pipeline with diameters between 900mm and 250mm. The whole of the pipeline is buried in excavated trenches in the top few metres of ground. Two major pumping stations and four minor pumping stations were provided.



Figure 7.20 Survey Point on Yuvacik Dam Crest



Figure 7.21 Small Rockfall Adjacent to it

Water supply via the two major pump stations on the pipeline was temporarily interrupted due to low suction pressure at the upstream pump station. Supplies were restored following extensive checks on the controls and instrumentation systems.

The main damage to the water distribution network occurred to pipeline that is buried in the vicinity of the fault. As a result of large scale disruption of the ground in the vicinity of the surface rupture, these pipelines were subject to large relative displacements. Deflection of the 2.2m diameter treated water main caused a leak at a location where it crossed the fault line. Damage also occurred to a number of ductile iron branches, resulting in leakage.

Figure 7.22 shows a length of pipeline that crosses the surface rupture. It is clear that the pipe has suffered significant shear deformation, a close-up view being shown in Figure 7.23. It is currently postulated by the site engineers that concentrated shear at the point of ground rupture caused movement of the pipe within its backfilled trench, resulting in axial extension, strain hardening and axial compression. The pipeline generally withstood these gross deformations, but in the most severe cases, leaks resulted.

Large scale damage to concrete pipes forming the water distribution system have been reported. The shortfall in water supplies was made up of chlorinated tanker supplies direct from Yuvacik and lorry loads of bottled water.



Figure 7.22: Damaged run of pipeline in a region of high ground disturbance



Figure 7.23: Local distortion of pipe due to displacement imposed by ground movement

7.3 Comments

It is apparent that engineered structures many of which would have been designed to the recent codes fared very well in the earthquake. This contrasts very starkly with the devastation caused to residential dwellings.

A certain amount of damage to the main highway E80 and related structures has been reported. The damages have very largely been as a result of proximity to the large displacements at the fault rupture thus one might argue that damage was unavoidable. Remedial work was carried out speedily allowing the main highway to open a matter of days after the earthquake.

The earthquake provided an early test of the recently constructed water supply system. A large repair bill will need to be faced resulting from the disruption caused to the large water supply mains caused by severe ground movements. The centre-piece Yuvacik dam and water treatment works fared very well during and in the immediate aftermath of the earthquake.

7.4 Performance of Waterfront Structures

Figure 7.24 shows the locations of various waterfront structures in the gulf of Izmit. The majority of the industrial waterfront facilities and container berths in the area are situated on the North coast of the Gulf of Izmit between Istanbul and Izmit. There are also numerous small jetties along the North coast and a roll on-roll off ferry terminal at Eskihisar, 60km East of Istanbul. The South coast of the gulf has roll on – roll off ferry terminals at Yalova and Topcular in the West, with Gölçük naval base at the eastern end of the gulf. The EEFIT mission visited a number of facilities along the coast carrying out inspection both from ground and from sea. In the following a discussion of the observed damage is presented of quay and jetties according to structural types.

7.4.1 Quay structures

7.4.1.1 Sheet and Tubular Piled Walls

Sheet pile quay walls on both shores of the gulf suffered significant damage. The most common mode of failure involved large lateral seaward movement of the cope beam, accompanied by settlement and washing out of the fill behind the wall.

This type of failure occurred at Gölçük naval base, resulting in the collapse of concrete ground slabs up to 20 metres behind the tied sheet pile wall (Figure 7.25). Settlement of the fill had resulted in the fill level dropping by approximately 2 metres. Services running in precast trenches behind the cope were severely disrupted.

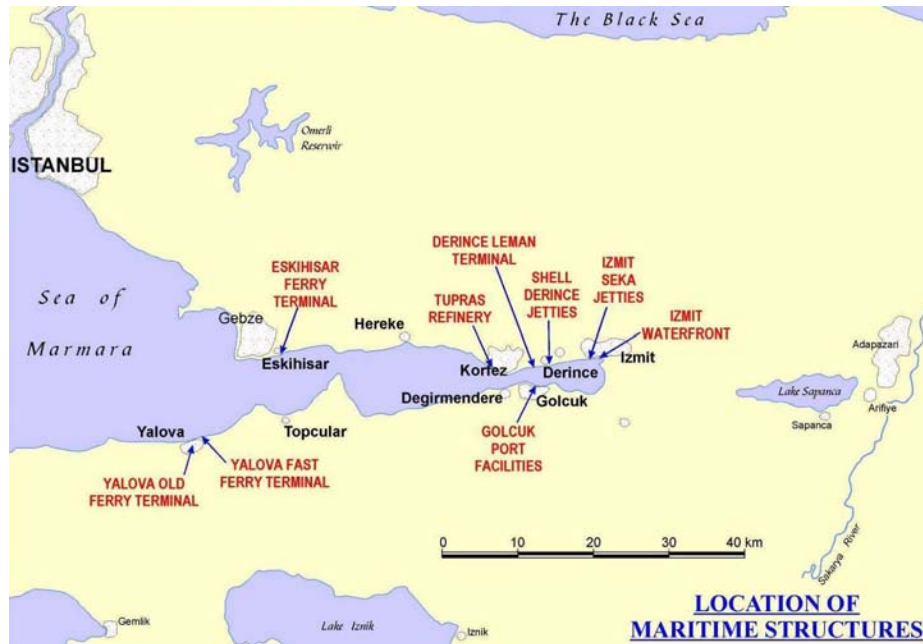


Figure 7.24: Location of maritime structures



Figure 7.25

The seaward movement of the wall in some locations was in the order of 1 metre; however, the lateral movement was restrained at 50 metre intervals by the presence of piled jetties running perpendicular to the quay. The extent of lateral wall movement suggests liquefaction of the retained fill, which caused movement of the deadman anchors.

The ferry terminal at Eskişehir consists of an original quay - part gravity wall, part sheet pile wall - which has subsequently been extended seawards by a piled suspended deck structure. A single ground-bearing slab had collapsed about two weeks after the earthquake immediately behind the line of the original quay wall. Closer

inspection revealed that the collapse had occurred at the junction between the gravity wall and sheet pile wall. Damage to the top of the gravity wall indicated that during the seismic event, the sheet pile structure had pounded against the gravity structure. This movement resulted in a permanent gap of 200 mm between the two structures. This allowed water to penetrate the wall and wash out the fill behind, leaving no support for the overlying deck slab (Figure 7.26). The fill underneath adjacent deck slabs had undergone relatively minor settlement of 50 mm. No significant seaward movement of the sheet pile wall was apparent, suggesting that the performance of any anchors present was adequate.



Figure 7.26

7.4.1.2 Gravity Walls

The Derince Leman industrial facility to the west of Izmit has a number of container berths. The oldest quay, a sheet pile wall with concrete deck, suffered the most damage. The wall had moved outwards allowing the fill behind the wall to settle approximately 1 metre (Figure 7.27.) A steel framed warehouse 20 metres back from the wall had remained structurally intact despite considerable settlement (Figure 7.27). The only damage inflicted on the building was due to a rail mounted cargo crane that serviced the quay tipping over and striking the corner of the warehouse. The adjacent quay was in the final stages of construction and its form of construction appeared to be a tubular piled wall. This quay also suffered settlements and cracking of the deck, but on a scale small enough for the quay to be serviceable when construction is completed.



Figure 7.27

At Eskihisar ferry terminal, gravity walls experienced only slight outward movement and settlement; the main damage was due to the aforementioned pounding by the adjacent sheet pile wall. A small promenade approximately 15 kilometres west of Izmit failed due to the outward movement of a gravity retaining wall and subsequent settlement of the fill behind the wall.

7.4.1.3 Piled Deck and Revetments

Quay structures consisting of a reinforced concrete deck supported on vertical steel piles performed significantly better in the earthquake than other types of construction. The fast ferry terminal at Yalova, constructed in 1997, was one of the few waterfront structures in the area to suffer minimal damage. The 1.5 metre thick concrete deck of the ferry berth is supported by steel tubular piles and sits above a rock revetment. (Figure 7.28) The stability of the revetment - and in particular its liquefaction resistance - are critical to the adequate performance of this type of quay.



Figure 7.28



Figure 7.29

The Derince Leman industrial facility had in addition to the previously mentioned quays, a container berth of steel tubular piled deck construction (Figure 7.29). This quay appeared to have suffered no damage during the earthquake.

7.4.2 Jetty structures

7.4.2.1 All Reinforced Concrete Construction

Considerable damage was caused to four reinforced concrete jetties along the North coast of the gulf to the West of Izmit. A jetty that had served as a cargo berth for the Seka paper factory in Izmit failed by crushing of the concrete pile heads at the landward end (Figure 7.30.) This failure allowed the deck to rotate severely (Figure 7.31) The seaward end of the jetty, which is supported by two rows of piles (rather than the single row at the landward end), survived despite the severe loss of concrete at the pile heads.



Figure 7.30



Figure 7.31

A concrete jetty 50 metres to the west of the cargo jetty had suffered the collapse of two of its spans. The deck was supported on slender concrete columns which were supported by concrete pile caps. The failures occurred in the columns, allowing the deck to drop 500 mm (Figure 7.32.). Approximately 4 kilometres further west at the Shell refinery in Korfez, two reinforced concrete jetties had suffered total collapse. Failure had again occurred at the pile heads. The east jetty had completely sunk leaving only a sheared pile head as evidence of its existence (Figure 7.33.) The western jetty was only partially visible. The remaining parts of the jetties showed signs of pounding along the jetty axis prior to failure. It appears that the failures may have involved shallow angle sub marine landslides.



Figure 7.32



Figure 7.33

7.4.2.2 *Steel Pile/Concrete Deck*

In general, jetties with a concrete deck supported by steel piles fared better during the earthquake than the concrete piled equivalent. At Gölçük naval base, a steel pile/concrete deck jetty suffered an unusual failure, possibly attributable to the presence of the fault directly beneath the structure. The jetty, approximately 80 metres long, was constructed in two separate sections. The seaward section had moved 3 metres northwards and 3 metres eastwards, with no change in vertical level (Figure 7.34.) The eastward component of the movement is consistent with the direction of the tectonic plate movement. An identical jetty situated 100 metres to the west showed no signs of damage or movement.



Figure 7.34



Figure 7.35

In Izmit, a steel piled jetty suffered no damage despite the 300 mm seaward movement of an adjacent promenade (Figure 7.35) and a drop in the ground level behind the jetty of 1.5 metres. On the north coast of the gulf to the west of Izmit, four steel piled concrete jetties were observed at various industrial facilities; all four structures appeared to be undamaged. The mooring jetty at the Yalova fast ferry port was also undamaged (Figure 7.36.)



Figure 7.36

7.5 Conclusions

It is clear that, in general, waterfront structures consisting of a concrete deck supported by tubular steel piles performed significantly better under seismic loading than other types of structure. Although some failures could be attributed to the age, lack of maintenance or the poor construction quality of the structure, the sheet pile wall failure at Golcuk naval base showed that even modern structures with excellent construction quality are vulnerable if the design concept is inappropriate to the situation. Retaining walls, if not carefully designed, are prone to lateral displacements caused by liquefaction of the retained fill and increased active earth pressures that arise during a seismic event. This was borne out by the poor performance of retaining walls throughout the area. The mode of failure of these walls suggests inadequate design of the anchor blocks and/or poor compaction of the fill seaward of the anchor block leading to insufficient passive earth pressures.

Another problem area appears to be at the junction between two different types of quay structure. Not only is differential settlement a problem, but the different stiffnesses of, for example, a sheet pile wall and a gravity wall cause each structure to move out of phase under forced oscillation. This can lead to one structure pounding against the other and should be an area of concern when designing, for example, an extension to an existing quay. This pounding damage was also seen at construction joints between structures of the same type.

Whilst this section has focused on the influence of structural type on seismic performance, the influence of ground conditions, and in particular the potential for liquefaction, is critical and must not be overlooked during the design stage.

7.6 References

EERI Special Earthquake Report. The Izmit (Kocaeli), Turkey Earthquake of August 17, 1999. <http://www.eeri.org/Reconn/Turkey0899/Turkey0899.html>

Turkish commission on large dams. <http://www.icold.org.tr/>